Glyco-engineering and glyco-analytics of therapeutic proteins secreted from Chinese hamster ovary cells

By

Qiong Wang

A dissertation submitted to Johns Hopkins University in conformity with the requirements for the degree of Doctor of Philosophy

Baltimore, Maryland

May 2019

Abstract

Chinese hamster ovary (CHO) cells represent the predominant platform in biopharmaceutical industry for the production of recombinant biotherapeutic proteins, especially glycoproteins. This dissertation focuses on comprehensive glyco-analytics and glyco-engineering of recombinant proteins secreted from CHO cells.

For advanced glyco-analytics, an intact glycopeptide analysis method was performed to simultaneously analyze the site-specific N- and O-glycan profiles of the recombinant EPO-Fc protein secreted from the CHO-GS stable cell line and compared the effects of two commercial culture media, EX-CELL (EX) and immediate Advantage (IA) media, on the site-specific glycosylation profile of the target protein.

For glyco-engineering in CHO cells, a novel chemical analog (1,3,4-O-Bu_3ManNAc) was investigated on the sialic acid content of cellular proteins and a model recombinant glycoprotein, erythropoietin (EPO). Addition of 200-300 μM 1,3,4-O-Bu_3ManNAc resulted in >40% increase in final sialic acid content of recombinant EPO, while feeding of ManNAc at almost 100 times higher concentration of 20 mM concentration produced a less profound change in EPO sialylation. Further, supplementation with 1,3,4-O-Bu_3ManNAc for two stable CHO cell lines, expressing human EPO or IgG, enhanced protein expression for both products with negligible impact on cell growth, viability, glucose utilization, and lactate accumulation. In contrast, sodium butyrate treatment resulted in a ~20 % decrease in maximal viable cell density and ~30 % decrease in cell viability. In addition, the beneficial impact of 1,3,4-O-Bu_3ManNAc on EPO glycan quality, while evident in wild-type CHO cells, is particularly pronounced in glycoengineered CHO cells with stable overexpression of β-1,4- and β-1,6-N-acetylglucosaminyltransferases (GnTIV and GnTV) and α-2,6-sialyltransferase (ST6) enzymes responsible for N-glycan antennarity and sialylation.

Moreover, the two critical human genes-β-1,4-galactotransferase 1 (B4GALT1) and β-1,3-N-

acetylglucosaminyltransferase (B3GNT2)-for the initiation and elongation of poly-LacNAc on N-glycans in CHO cells were also investigated. The overexpression of B3GNT2 in EPO-expressing CHO cells did not increase the LacNAc content on recombinant EPO protein, but also resulted in nearly 100% elimination of sialylation on recombinant EPO and overall glyco-conjugates in CHO cells.

Advisors: Dr. Kevin J. Yarema, Dr. Hui Zhang and Dr. Michael J. Betenbaugh

Preface

This dissertation consists of 6 chapters and is focused on the glycoengineering in CHO cells to produce recombinant proteins with optimized glycan structures and advanced mass spectrometry-based glycosylation analysis methodology.

Chapter 1 provides an introduction of the glycosylaiton pathways in mammalian cells, and compared the CHO glycosylation with human glycosylation. CHO cells is currently the predominant production platform in biopharmaceutical manufacturing. The glycan patterns on recombinant proteins secreted from CHO cells is compatible to humans. This work has been published in Biotechnology & Bioengineering [1], Emerging Topics in Life Sciences [2], Glyco-Engineering [3] and Heterologous Protein Production in CHO Cells [4]. Permission for use was granted by John Wiley and Sons (license number 4577911163772) and by Springer Nature (license number 4577920069010 and 4577920279468).

Chapter 2 describes an advanced glycosylation analysis using an intact glycopeptide analysis method to simultaneously analyze the site-specific N- and O-glycan profiles of the recombinant EPO-Fc protein secreted from a CHO-GS stable cell line.

Chapter 3 introduces 1,3,4-O-Bu_3ManNAc analog as a novel sugar analog can simultaneously increase both the productivity and sialylation of recombinant proteins in CHO cells. This work has been published in Biotechnology & Bioengineering and Biotechnology Journal [5] [6] [7]. Permission for use was granted by John Wiley and Sons (license number 4577920746464, 4577920855810 and 4577920941689).

Chapter 4 explores the ability of B3GNT2 and B4GALT1 for LacNAc initiation and elongation on recombinant EPO in CHO cells.

Chapter 5 introduce a protocol of using CRISPR/Cas9 gene editing method for modulating antibody fucosylation in CHO cells. This work has been published in Recombinant Protein Expression in Mammalian Cells. Permission for use was granted by Springer Nature (license

number 4578571144913).

Chapter 6 concludes the dissertation and discusses future work.

Acknowledgement

I want to thank my family and friends for their continuous love, help and support. I am so fortunate to have a very supportive network of family for giving me the opportunities and experiences that have made me who I am. These include my parents, Min Xu and Jianguo Wang, my uncles and aunts, my cousins and niece, my grandparents, and many friends.

I was also grateful for having three great advisors, Dr. Michael J. Betenbaugh and Dr. Hui Zhang and Dr. Kevin Yarema. From their constant guidance and mentoring, I have grown a lot both as a scientific researcher and as a better person during these last six years.

My colleagues at Pathology department, Biomedical Engineering department and Chemical and Biomolecular Engineering department at John's Hopkins University provided me with instruction, guidance, advice, and direction; it was wonderful both professionally and personally to work with them. I would especially like to thank Dr. Bojiao Yin, Dr. Ganglong Yang, Dr. Weiming Yang, Dr. Andrew Chung for their help with protocols, experimental design and troubleshooting, and conceptual understanding.

Additionally, I would like to acknowledge the following collaborators for their valuable input throughout the years. Dr Rahul Bhattacharya, Dr. Christopher T. Saeui at the Biomedical Engineering department for their technical help and advice for 1,3,4-O-Bu_3ManNAc analog synthesis and analysis work. Dr. Liqun Chen, Dr. David J Clark, Dr. Yingwei Hu, Ms. Minghui Ao and Dr. Hoti Uddin and Dr. Ryan Cho at the Pathology department for their technical help and advice with glycan and glycopeptide mass spectrometry analysis. Dr. Tingting Li, Dr. Geng Yu, Dr. Joseph Priola, Dr. Kelly Heffner, Dr. Jimmy Kirsch, Chien-ting Li and former and current Betenbaugh lab members at Chemical and Biomolecular Engineering department for their continuous help and support. I also want to thank the members of my dissertation committee: Dr. Kevin Yarema, Dr. Hui Zhang, Dr. Michael J. Betenbaugh, Dr. Marc Ostermeier and Dr. Yuan Chuan Lee for generously offering their time, support, guidance and good will throughout the preparation and review of this document.

Without the funding from the National science foundation (NSF) and the the Maryland Innovation Initiative grant and Department of Chemical and Biomolecular Engineering at Johns Hopkins University, this research would not have been possible.

Table of Contents

List of Tables

List of Figures

Supplemental figures:

Chapter 1 Glyco-engineering strategies in mammalian cells

1.1 Summary

Chinese hamster ovary (CHO) cells represent the predominant platform in biopharmaceutical industry for the production of recombinant biotherapeutic proteins, especially glycoproteins. These glycoproteins include oligosaccharide or glycan attachments that represent one of the principal components dictating product quality. Especially important are the N-glycan attachments present on many recombinant glycoproteins of commercial interest. Furthermore, altering the glycan composition can be used to modulate the production quality of a recombinant biotherapeutic from CHO and other mammalian hosts. This chapter as a review first describes the glycosylation network in mammalian cells and compares the glycosylation patterns between CHO and human cells, which provided as an introduction to the dissertation. Next genetic strategies used in CHO cells to modulate the sialylation patterns through overexpression of sialyltransfereases and other glycosyltransferases are summarized. In addition, other approaches to alter sialylation including manipulation of sialic acid biosynthetic pathways and inhibition of sialidases are described. Finally, this chapter also covers other strategies such as the glycosylation site insertion and manipulation of glycan heterogeneity to produce desired glycoforms for diverse biotechnology.

1.2 Glycosylation in mammalian cells

Glycosylation is a critical post-translational modification found on most of these biotherapeutics. What is unique about glycosylation compared to other post-translational processing events is the structural variety and functional diversity present, in which the glycosylation can vary widely even for a single protein and also from organism to organism. Glycosylation characteristics can play a major role in modulating a protein's stability, folding, targeting/trafficking, immunogenicity, biological activity, and especially circulatory half-life [8]. Oligosaccharides are attached cotranslationally through glycosidic linkages on specific asparagine (N-linked) or serine/threonine (O-linked) residues. While N-glycans are the most common modification on biotherapeutics including monoclonal antibodies and will be the focus of the current review, several therapeutic glycoproteins such as erythropoietin (EPO) and etanercept (Enbrel) also include O-glycan modifications[9]. N-glycans are linked to the Asn of the Asn-X-Ser/Thr consensus sequence in which X denotes any amino acid except proline [10]. A consensus sequence for O-linked glycosylation has yet to be identified [8]. Given its non-template driven nature, heterogeneity of glycosylation arises both from variations in glycosylation site occupancy and in the diversity of final glycan structures attached to glycoproteins emerging from the cellular secretory compartments. As a result of the stochastic nature of interactions between enzymes and oligosaccharide substrates and the variety of enzymes that can act on any one glycan substrate, a wide range of different glycans are generated for most proteins as these proteins traverse through the endoplasmic reticulum (ER) and various Golgi compartments [11] [12].

In particular, the N-linked glycosylation pathway in mammalian cells involves a highly complex and interconnected reaction network catalyzed by glycosidases and glycosyltransferases contained within different compartments of ER and Golgi apparatus, depicted in the schematic of Figure 1-1. The biosynthesis of mammalian N-glycans initiates at the cytoplasmic face of the ER membrane with the assembly of GlcNAc-P from UDP-GlcNAc to the dolichol phosphate (Dol-P) lipid carrier to generate dolichol pyrophosphate N-acetylglucosamine (Dol-P-P-GlcNAc) [13]. Then fourteen monosaccharides are sequentially added to Dol-P-P-GlcNAc to form an oligosaccharide precursor ($Glc_3Man_9GlcNAc_2$)

[13]. Next, oligosaccharyltransferase (OST) selects Asn-X-Ser/Thr sequons in a nascent polypeptide and proceeds with an *en bloc* transfer of $Glc_3Man_9GlcNAc_2$ to the side chain amide of asparagine and releasing Dol-P-P in the process [14]. The glucose residues on the precursor are sequentially trimmed by the ER α-glucosidase I and II to form monoglucosylated glycan, which is a key intermediate in the ER lectin chaperones calnexin/calreticulin-associated glycoprotein folding control cycle [15]. Once correctly folded, the precursor is trimmed by ER α-mannosidase I to yield $Man_8GlcNAc_2$-protein before exiting the ER. After translocation into the cis-Golgi, the $Man_8GlcNAc_2$ glycoform is further trimmed by Golgi α-mannosidases I to give $Man_5GlcNAc_2$, a key intermediate along the pathway to form hybrid and complex N-glycans and sometimes found as a final glycan product.

As shown in Figure 1-1, biosynthesis of hybrid and complex N-glycans begins in the medial-Golgi by the action of an N-acetylglucosaminyltransferase (GnT-1 or Mgat1), which adds a GlcNAc to $Man_5GlcNAc_2$ [13]. Then the majority of N-glycans are trimmed by Golgi α-mannosidase II removing two mannoses from $GlcNAcMan_5GlcNAc_2$ to yield $GlcNAcMan_3GlcNAc_2$. Hybrid N-glycans result when a structure such as $GlcNAcMan_5GlcNAc_2$ undergoes no further extensions and two terminal Man residues remain exposed. In addition, another GlcNac can be added to the innermost Man group by the enzyme β1,4-N-acetylglucosaminyltransferase III (GnT-III or Mgat3) in the medal Golgi, resulting in bisecting GlcNAc structures which can also alter the capacity for other downstream enzymes to act on the glycan structure.

Then the enzyme β-1,2-N-acetylglucosaminyltransferase II (GnT-II or Mgat2) adds a second GlcNAc to the $GlcNAcMan_3GlcNAc_2$ structure to generate the glycan product $GlcNAc_2Man_3GlcNAc_2$, which is the precursor for all multiantennary complex N-glycans. Tri-and tetra-antennary branches can be achieved by adding GlcNAc at α(1,3)-mannose site by N-acetylglucosaminyltransferase IV (GnT-IV or Mgat 4) and at α(1,6)-mannose site by N-acetylglucosaminyltransferase V (GnT-V or Mgat 5) . Additional modification of complex and hybrid N-glycans can occur in the trans-Golgi and include the addition of core α(1,6)-fucose to the GlcNAc adjacent to Asn at the N-glycan sites by α-(1,6)-fucosyltransferase and the branch elongation by the

addition of a β-linked galactose residue to GlcNAc to produce Galβ1-4GlcNAc, or poly-acetyl-lactosamine (poly-LacNAc) sequences. Finally, these terminal GlcNAc residues can serve as acceptors for a range of galactosyltransferases followed by sialyltransferases and fucosyltransferases, leading to even more complex structures [13].

1.3 Glycosylation differences between human cells and CHO cells

Chinese hamster ovary (CHO) cells are widely used in many commercial and clinical biopharmaceuticals due to their capacity to produce glycoforms which are, with exceptions, accepted by the human immune system [16, 17]. Alternative mammalian cell lines also used in the production of biopharmaceuticals include baby hamster kidney (BHK21), murine myeloma and hybridoma cell lines (NS0 and Sp2/0), and, to a lesser extent, human host cell lines such as human embryonic kidney (HEK293) and human retinal cells (PER.C6)[17-19].

Especially, two non-human glycans—terminal Galα1,3-Gal residues (alpha-Gal) and N-glycolylneuraminic acid (Neu5Gc) epitope—exist in non-human mammalian cells and could elicit adverse immunogenic reactions in humans [20] [17]. Mouse cells have an α1,3-galactosyltransferase enzyme that produces glycans containing the alpha-Gal linkage [21]. The second potential immunogenic epitope Neu5Gc is common in all non-primate mammalian cells [17] due to the presence of the enzyme, N-acetylneuraminic acid hydroxylase, which coverts CMP-Neu5Ac to CMP-Neu5Gc in all mammals other than old-world primates [22]. Furthermore the presence of a circulating polyclonal anti-Neu5Gc antibody response have been detected in humans [17] [20]. In contrast to the alpha-Gal epitope, Neu5Gc can even be taken up from the media as a metabolite by all mammalian cells, including human cells, and then metabolically incorporated onto cell surface glycoconjugates, While all mammalian cells have the potential for immunogenic epitopes, mouse myeloma cells (NS0 and Sp2/0) tend to express higher levels of both of these epitopes compared to hamster (CHO and BHK), making recombinant products form murine cells a higher likelihood for being immunogenic in humans, This potential immunogenicity can especially be a concern when the therapeutic glycoproteins are administered repeatedly in large doses for

chronic diseases [22] [23] [24].

Even without these two non-human immunogenic epitopes, the glycosylation patterns of proteins expressed in CHO and human cell lines can be different [25]. CHO cells typically do not express N-acetylglucosaminyltransferase III (GnT-III) and thus lack bisecting GlcNAc residues in their glycoforms, which can impact antibody efficiency [26]. Human cells can produce the glycans with GnT III and antibodies produced in mouse myeloma cells contain a fraction of glycans with bisecting GlcNAc residues [27].

1.4 Glyco-engineering strategies in mammalian cells

The numerous applications of recombinant monoclonal antibody (rMAb) therapeutics ranging from diagnosis to treatment of major diseases including cancers, autoimmune disease and inflammatory disorders have continuously expanded, in step with technological improvements and innovations in the development and production of rMAbs [28]. To date, the majority of recombinant glycoproteins in production from the most widely used mammalian cell lines such as Chinese hamster ovary (CHO), Murine myeloma (NS0) and mouse myeloma (Sp2/0) are recombinant monoclonal antibodies, including chimeric, humanized or human immunoglobulin Gs (IgGs) [27]. Many biotherapeutics such as growth factors, cytokines, hormones, and enzymes are glycoproteins. The glycosylation of biotherapeutics has been identified as a critical quality attribute [29] because each biotherapeutic requires defining glycosylation to maintain consistent characteristics such as solubility, thermal stability, protease resistance [30], aggregation, serum half-life [31], immunogenicity and efficacy [32].

1.4.1 Non-immunoprotein sialylation

Among the numerous sugar moieties found in glycans, the terminal sialic acid (Neu5Ac) is considered particularly important for the lifespan of glycosylated proteins. As an electro-negatively charged acidic 9-carbon monosaccharide, sialic acid is α-glycosidically linked on the C3- or the C6-hydroxyl group of the terminal galactose in humans, through the action of a2,3-sialyltransferases (ST3) or the a2,6-sialyltransferase-1 (ST6) [33] [34] [35]. Terminal sialic acid residues can alter protein properties

including biological activity and in vivo circulatory half-life [35]. Serving as a biological mask, the distal sialic acid can shield Gal residues that when exposed prompt a fast removal of the protein from blood circulation due to endocytosis-mediated uptake by asialoglycoprotein receptors on the hepatocytes [36] [37] [35]. Therefore, in mammalian cells, it is generally desirable to maximize the distal sialic acid content of a glycoprotein in order to ensure its quality and consistency as an effective therapeutic [38].

However, the sialic acids of glycoproteins expressed in mammalian cells are incomplete, which is affected by two opposing cellular processes. The first process consists of two steps-- the biosynthesis of sialic aid and its addition to glycans from a cytidine monophospho-sialic acid (CMP-SA) substrate catalyzed by sialyltransferase and the second process is the extracellular removal of sialic acid by sialidase cleavage [39] [35]. Both of these pathways are targets for genetic engineering. Hence here we mainly discuss the genetic manipulation in sialylation process, and divide it into three parts--- genetic engineering in sialylation pathways, overexpression of N-acetylglucosaminyltransferase (GnT) genes, inhibition of sialidase activity, which has also been summarized in Table 1-1.

1. Genetic engineering in sialylation pathways

Genetic engineering of sialyltransferase enzymes is probably the most straightforward method to alter sialylation content in terms of modifying the oligosaccharide biosynthesis reaction networks. Sialyltransferases are ultimately responsible for introducing a Neu5Ac residue to the penultimate galactose residue.

Six β-galactoside a2,3-sialyltransferases (ST3GAL1-6) and two β-galactoside a2,6-sialyltransferases (ST6GAL 1-2) are responsible for forming these terminal sialic acids in mammalian cells. Human glycoproteins bear sialic acid residues in both α2,3- and α2,6-linkages, whereas only α2,3-terminal sialic acids are found in glycoproteins from CHO and BHK cells. Earlier report from our group revealed that three genes from the a2,3-sialyltransferase family (ST3GAL3, ST3GAL4 and ST3GAL6) are responsible for a2,3-sialylation in CHO cells using siRNA knockdown approaches, among which ST3GAL4 plays the critical role in determine glycoprotein a2,3-sialylation [40]. Besides, ST6GAL l is the sole member of the ST6GAL family that can synthesize the terminal NeuAc α2,6-Gal glycoconjugates [41] .

In the past, the overexpression of heterologous α2,6-sialyltransferase with or without recombinant α2,3-sialyltransferase serves to introduce linkages similar to those found in human cells and has long been adapted to elevate the amounts of sialic acid on recombinant proteins [35]. Since the first introduction of ST6GAL1 in CHO cells in 1989 [42], rat or human ST6GAL1-expressing CHO and BHK cells were successively generated and tested for various therapeutic glycoproteins production [43] [44]. Expressing rat ST6GAL1 in recombinant human tissue plasminogen activator (tPA) CHO expressing cell line has significantly increased the a2,6 sialylation level [43]. A similar protocol was applied to modify recombinant human interferon-ɤ (IFN-ɤ) and the tissue-inhibitor of metalloproteinases-1 in CHO and human erythropoietin (EPO) in BHK-21A cells. Especially, analysis of the IFN-ɤ showed >40 % content of α2,6-linked sialic acid with improved pharmacokinetics in clearance studies when compared to wild-type IFN-ɤ produced by CHO cells[14]. In all cases, the total content of sialic acid did not rise drastically and the ratio of a2,6- to a2,3-linked sialic acid never exceeded 50%. It was concluded that the recombinant ST6GAL1 enzyme poorly competes with the endogenous ST3 enzymes (ST3GAL3, ST3GAL4 and ST3GAL6) for the same donor and acceptors[23].

Meanwhile, the step prior to sialylation for N-glycans typically involves the addition of galactose onto the branched N-glycan chains (Figure 1-1) and insufficient or inconsistent galactosylation would result in unsatisfactory sialylation level. Thus, co-overexpressing both the human β1,4-galactosyltransferase (β1,4-GalT) and α2,3-sialyltransferase (a2,3-ST) would result in synthesis of glycoprotein products with a greater and consistent proportion of fully sialylated N-glycans [24, 35]. The resulting oligosaccharides showed greater homogeneity compared with control cell lines, in which ≥90 % of available branches were capped with sialic acid [24]. Compared to α2,3-ST expression alone, co-expression of β1,4-GalT and α2,3-ST in CHO producing EPO cell line achieved higher sialic acid content and more trisialyated glycans [45].

Except for sialyltransferases, the availability of nucleotide sugar substrates and the transport of them to the Golgi could also determine the extent of protein glycosylation [18]. The biosynthesis of sialic acid in mammalian cells takes place in the cytosol, finished in the nucleus and transported to the Golgi (Figure

1-2). Especially, in eukaryotes, uridine diphosphate (UDP)-GlcNAc is initially epimerized to *N*-acetyl mannosamine (ManNAc) by UDP-GlcNAc 2-epimerase (GNE), and ManNAc is phosphorylated to ManNAc-6-phosphate by ManNAc kinase (MNK). These two enzymes are integrated into a single bifunctional enzyme (encoded by GNE) [46] [47] [48]. As a rate-limiting enzyme, GNE is regulated by feedback inhibition of the level of cytoplasmic free CMP-Neu5Ac. A genetic disease called "sialuria" arises from the absence of feedback regulation of this enzyme, leading to excessive synthesis of free sialic acid, which is accumulated in cytoplasm and secreted into urine.

This sialic acid pathway enlightens researchers new approaches to increase the sialylation of therapeutic proteins. As a direct precursor of sialic acid, N-acetylmannosamine (ManNAc) supplementation has long been studied for its effect on sialylation. Numerous reports demonstrated that ManNAc supplementation can significantly increase CMP-sialic acid in the intracellular pool up to 12-fold ,but only improve protein sialylation to a very limited extent about 10%-20% sialylation increase [49] [50] [33]. A similar issue exists with the overexpression of CMP-SAS and sialuria-mutated GNE/MNK in the biosynthesis pathway, which cannot further increase sialylation [48] [51] [52] . All these approaches could easily increase the intracellular pool of CMP-sialic acid levels, but the next step-transporting CMP-sialic acid to the Golgi is hampered by the inefficiency of CMP-sialic aid transporter (CMP-SAT) on the Golgi membrane, thereby causing the reduced availability of CMP-sialic acid substrate for sialylation. Nik Wong et al overexpressed CMP-SAT alone n CHO IFN-ɤ cell line and resulted in 4%-16% increase in site sialylation of IFN-ɤ[3] . Therefore, combinatorial engineering have been adapted in many groups by improving sialic acid content in the intracellular pool and the availability in the Golgi. Yeon Tae Jeong et al overexpressed a2,3-ST, CMP-SAS and CMP-SAT in CHO recombinant EPO cell line, and a corresponding increase in the sialylation was observed compared to the co-expression of of a2,3-ST and CMP-SAS [52]. Son YD et al introduced sialuria-mutated rat GNE/MNK, Chinese hamster CMP-SAT and human α2,3-sialyltransferase (α2,3-ST) simultaneously into recombinant human EPO-producing CHO cells and found the sialic acid content of rhEPO produced from engineered cells was 43% higher than that of control cells. Ratio of tetra-sialylated glycan of rhEPO

produced from engineered cells was increased ~32%, and ratios of asialo- and mono-sialylated glycans were decreased ~50%, compared with control [48].

1. Overexpression of *N*-acetylglucosaminyltransferase (GnT) genes

Overexpresson of branching genes would increase sialylation acceptor sites. For human proteins, bi-, tri-, and tetra-antennary structures are produced with complex-type N-glycans consisting predominantly of the disaccharide Galβ1,4-GlcNAc capped by a terminal sialic acid. As illustrated in Figure 1-1, tri- and tetra-antennary complex N-glycans are controlled by UDP-N-acetylglucosamine:α-1,3-D-mannoside β-1,4-N-acetylglucosaminyltransferase (GnT-IV or MGAT4) and UDP-N-acetylglucosamine:α-1,6-D-mannoside β-1,6-N-acetylglucosaminyltransferase (GnT-V or MGAT5). These branched structures are associated with various biological functions, including cellular proliferation, cell surface signaling [26], cancer metastasis and regulation of T-cell activation [53] and also affect therapeutic proteins' clearance rate by the glomeruli of the kidneys [54]. Nonetheless, in CHO cells, only a small percentage of glycoproteins contains the GlcNAcβ1-6 branch, the GnT-V product [55]. Thus, more extensive modifications for glycoform distribution are expected if genetic modulations are introduced in the branching pathway of N-oligosaccharide biosynthesis, thereby potentially increasing the number of sialylation acceptor sites.

In order to tailor the multi-antennary glycoforms of recombinant proteins, overexpression of GnT IV and V were used in CHO cells producing human IFN-ɤ and EPO cell lines [55] [40] . In both cases, tri- and tetra-antennary sugar chains have dramatically increased, representing ≥ 50% of the total sugar chains and almost all N-glycans were in tri- or tetra-antennary glycoforms[40]. At the same time, an increase in poly-N-acetyllactosamine (Galβ1-4GlcNAcβ1-3) was also observed [55]. However, the increase in sialic acid content didn't keep up with the increase of available sialylation acceptor sites because of incomplete sialylation. In further studies, mouse ST3 and/or rat ST6 were introduced in CHO IFN-ɤ cell line stably transfected with GnT V, reaching 61.2% in a2,3- and a2,6-linked sialic acid content. And the coordinated overexpression of GnT IV, GnT V and ST6GAL1 genes in CHO EPO cell line enhanced sialic acid content approximately 45% compared to control CHO EPO expressing cells.

More recently, an emerging approach to enhance sialylation is to restore GnT I function in CHO GnT I-deficient mutants. The GnT I-deficient mutants are generated either through the lectin *Ricinus communis agglutinin I* (RCA-I) selection or by genetic modulations. Treating the CHO cells with the cytotoxic lectin *Ricinus communis agglutinin I* (RCA-I) was supposed to select mutants with defects in the N-glycosylation pathway upstream of galactose addition because it was reported to be specific for terminal β1,4-linked galactose [56]. Unexpectedly, genetic analysis of RCA-I-resistant CHO mutants showed they are all the same type of mutants with different genetic mutations in the GnT I gene [57], similar to Stanley's Lec1 mutant. A plausible explanation is that RCA-I is not specific for terminal β1,4-linked galactose but possibly binds many glycan structures except for $Man_5GlcNAc_2$ [58]. Without functional GnT I, the cells fail to transfer N-acetylglucosamine to $Man_5GlcNAc_2$ glycan (Figure 1-1). Surprisingly, the restoration of functional GnT I in these mutants led to an increase in the sialylation of recombinant proteins both in transient expression as well as in stably transfected clones [57]. While the molecular mechanism for this phenomenon remains unknown. Recombinant EPO produced in this RCA-1 mutant line enhanced 30% sialylation compared with the control EPO producing CHO clone cultured under the same conditions. Moreover, HPAEC-PAD and MALDI-TOF MS analyses showed that EPO produced by the GnT I-restored CHO-GnT I-deficient cells contained higher content of tri- and tetra-antennary glycans.

2. Inhibition of sialidase activity

Any attempt to maximize sialic acid content of therapeutic protein should also consider the sialidase activity because glycoprotein is subject to desialylation and degradation during prolonged cell culture [59] [35]. Sialidase (neuraminidases, N-acylneuraminosyl glycohydrolases, EC 3.2.1.18) are exoglycosidases catalyzing the hydrolytic removal of sialic acid from sialoglycoconjugates (glycoproteins, polysaccharides, gangliosides) [60].Then the asialoglycoprotein product would be rapidly cleared from the plasma by asialoglycoprotein receptors in the liver. There are four sialidases (Neu 1-4) identified in human, mouse, rat and CHO cells and their activity has been localized on different subcellular level: Neu1 is located in the lysosome, Neu2 is a cytosolic protein, Neu3 is located in the

plasma membrane and Neu4 is a second lysosomal sialidase. These sialidases can be crucial to various biological such as growth control and differentiation, tumorigenesis, T cell activation and immune cell interactions, neuronal differentiation and genetic defects [61] [60]. The functions of these sialidases vary in part due to different substrate specificities and subcellular locations [35] . Therefore, in mammalian cells, it is often desirable to lower the cellular sialidase activity to ensure protein product quality and consistency as an effective therapeutic.

In mammalian cell culture, the extracelluar sialidase originates from the cytosol of the CHO cells, and is released to the cell culture supernatant as a result of cell lysis [62]. The generic technique would be to genetically inhibit sialidases' activity in CHO cells before they are released to the culture medium. When gene expression of CHO Neu2 was knocked down to 40% by homologous recombination or RNA interference (RNAi), the sialic acid content of the recombinant glycoprotein was improved but only when cells were in the death phase [59] [63]. In another study, CHO cells overexpressing recombinant human interferon gamma (IFN-ɤ) were treated using short interfering RNA (siRNA) and short-hairpin RNA (shRNA) to reduce expression of the Neu1 and Neu3 sialidase genes [38]. By knocking down expression of Neu3, a 98 % reduction in sialidase function in CHO cells was achieved. Correspondingly, the sialic acid content on recombinant IFN-ɤ was found to be increased 33 % and 26 %, respectively, with samples from the cell stationary phase and death phase as compared to corresponding controls [38]. Interestingly, Neu2 is a cytosolic protein, Neu3 is located in the plasma membrane, when using the same siRNA technique to knock down both genes individually, Neu3 knockdown almost silenced sialidase activity, while Neu2 knockdown only reduced sialidase activity to 40%. Unlike Neu2 knock down effects that acted exclusively on the death phase, protein sialylation was enhanced in the whole cell process after knocking down Neu3 expression, suggesting different mechanisms of protein sialylation regulation by Neu2 and Neu3 [35].

In addition to silence the genes for sialidases, novel approaches have been focused on inhibiting the enzymatic activity of sialidase. Bcl-x_L, an antiapoptotic protein that inhibits the release of proapoptotic molecules from mitochondria, is well-documented for its role on extending culture longevity by

suppressing apoptotic cell death and resulting in improved glycoprotein production [64] [65] [66]. While overexpression of Bcl-x_L also can enhance the sialylation of glycoprotein produced in CHO cell lines by reducing cell lysis and delaying the extracellular accumulation of sialidase activity during prolonged cell culture [67]. Likewise, the investigation of anti-apoptotic components of silkworm hemolymoh revealed *Bombyx mori* 30Kc19 gene expression can also enhance recombinant protein production and sialylation in CHO [68] [69]. Stable expression of the 30Kc19 gene in a CHO cell line producing recombinant human EPO would increase the EPO production and sialylation by 102.6% and 87.1%, respectively [69]. Moreover, with the introduction of 30Kc19 gene the host suspension cells produced recombinant Human EPO with more complex glycan structures and a larger content of sialic acid and fucose. For increased productivity, 30Kc19 protein suppresses the loss of mitochondrial membrane potential and consequently improves the generation of intracellular ATP and inhibit CHO cell apoptosis[69]. For enhanced glycosylation, except for delaying cell lysis and release of sialisase into culture media, the 30Kc19 protein is somehow able to maintain the activity of glycotransferases involved in the glycosylation process.

1.4.2 Antibody sialylation

For many therapeutic glycoproteins, the terminal sialic acids on glycans can have a clear and critical role for a protein's circulatory lifespan and efficacy. Serving as a biological mask, the distal sialic acid can shield Gal residues that when exposed prompt the rapid removal of the protein from blood circulation due to endocytosis-mediated uptake by asialoglycoprotein receptors on hepatocytes [36] [37] [35]. Therefore, in mammalian cells, it is often highly desirable to maximize the terminal sialic acid content of non-antibody glycoproteins in order to ensure their quality and half-life as an effective therapeutic. Even for antibodies, the sialic acid can act to alter the properties of the resulting protein[70]. The half-life of many antibodies is regulated through antibody Fc CH3 domain binding to the neonatal FcR (FcRn) and is believed to be independent of the Fc sugar moiety [71]. However, IgG Fc sialylation has emerged as an important topic of intense study in recent years. Researchers have observed that increasing IgG Fc α2,6 sialylation enhances the anti-inflammatory activity of intravenous immunoglobulin [72] and sialylation

enhancement deteriorates CDC activity[73]; while decreasing Fc sialylation can facilitate FcγR receptor binding onto natural killer (NK) cells followed by an increase in ADCC activity[74] [75], and lower affinity binding to insoluble or cell-surface antigens, but not affect the antibody binding to soluble antigens[76]. The mechanisms of antibody ADCC and CDC activity have been illustrated in Figure 1-3.

1. Increase antibody α2,6 sialylation for promoting anti-inflammatory activity.

Intravenous immunoglobulin (IVIg) predominantly consists of pooled polyclonal IgG from thousands of donors and has been used therapeutically to treat inflammatory diseases at high doses [77] [78]. The sialylation on the glycan of the Fc portion of IVIg has been reported to exhibit superior anti-inflammatory efficacies over desialylated IVIg and deglycosylated IVIg [72]. Both desialylated IVIg and deglycosylated IVIg abrogated the anti-inflammatory effect in vivo [72]. The demand for high doses (1-2g/kg bodyweight) of unfractionated IVIg is due to a generally low concentration of sialylated IgG in human plasma. In a mice model of arthritis, equivalent levels of anti-inflammatory activity were exhibited when using 1g/kg IVIg and 0.1g/kg sialic acid-enriched IVIg, indicating a 10-fold enhancement with the addition of terminal sialic acids [72, 79]. Several independent *in vivo* models further confirmed this theory that the terminal sialylation of Fc glycans is essential to elicit a sufficient anti-inflammatory activity for IVIg [80] [81]. In addition, the presence of α2,6-linked sialic acid residues, rather than α2,3-sialic acids, plays a critical role in inducing IVIg-elicited anti-inflammatory activity [79] [82] [76].

The major issue in using IVIg to treat auto-immune diseases is the inconsistent therapeutic efficacy and potency at high-dose administration and the lack of sialylated products for clinical use [83]. Lectin chromatography using *sambucus nigra agglutinin* (SNA) was considered for enriching sialylated IgG glycovariants in the IVIg preparation, due to this lectin's binding specificity to α2,6 sialic acids. One analysis of fractions obtained by lectin chromatography revealed that SNA preferentially binds to glycans of Fab, which contains 46.2% sialylated N-glycans accounting for 15-25% of serum IgG [84] [85] [86] [87] [88] and an easier accessibility than Fc glycans to bind to SNA lectin [89]. Moreover, experiments with a monoclonal antibody from a human cell line and IVIg Fc fragments indicated that at least two sialic acids in the Fc region of an antibody are required for lectin binding [89] [85]. Such glycoforms

contain either two monosialylated glycans (S1-S1 glycoform) or a disialyated glycan (S2-S0 glycoform), which represents 1% or less of the total human IgG [90] [89] [85].

These restrictions have stimulated researchers and engineers to generate therapeutic alternatives that could leverage the broad mechanisms of action of IVIg while improving therapeutic consistency and potency in a scalable and controllable antibody production process. Washburn et al proposed a controlled and scalable process to produce fully hyper-sialylated IVIg (S2-S2 glycoform) by treating native IVIg with in vitro β1,4-galactosyltransferase and α2,6-sialyltransferase [83]. The *in vivo* characterization of this drug candidate revealed consistent and enhanced anti-inflammatory activity up to 10-fold higher than native IVIg across different animal models [83]. A mass spectrometric quantification revealed that the IVIg preparation consist primarily of the IgG1 isotype[89]. Furthermore, a completely α2,6-sialylated recombinant IgG1 greatly enhanced potency at a much reduced dose of 0.03g/kg bodyweight compared to 1-2g/kg bodyweight for native IVIg [79].

In terms of increasing antibody sialylation in cells, the sialylation of the antibody is controlled primarily by the interaction of local IgG structure with the carbohydrate and the accessibility of the sialyltransferase to sialylate the N-glycan on the polypeptide[91]. Overexpression of α2,6 sialyltansferase (α2,6-ST) in a recombinant IgG-producing CHO cell line has been examined for increasing the sialylation content of recombinant IgG[92] [93]. For example, transfection of rat α2,6 sialyltransferase increased the sialylation content in a CHO IgG3 expressing cell line [92] .The recent report on genomic sequence of the CHO-K1 cell line revealed that ST6GAL1 gene is retained in CHO genome, but its expression is severely suppressed and regulated [94]. The introduction of an endogenous CHO ST6GAL1 gene into the CHO cell line can serve to enhance the α2,6 sialylation level of recombinant proteins in CHO[95]. Most attempts to overexpress ST6GAL1 in CHO revealed that this approach could only moderately enhance α2,6-sialylated glycans, and the mixture of α2,6 and α2,3 sialylation existed in the final glycoforms[96] [93]. Meanwhile, co-overexpression of β1,4-GalT and α2,6-ST was implemented to achieve a glycoprofile dominated by α2,6-sialylation for recombinant antibody production[74]. More recently, our group disrupted two α2,3 sialyltransferases (ST3GAL4 and ST3GAL6) and combined this cell line

variant with α2,6 sialyltransferase overexpression in pursuit of an exclusive α2,6 sialylated CHO cell line [97]. Antibody produced in our α2,3 sialyltransferase knockout-α2,6 sialyltransferase overexpressing cells contains solely α2,6 sialylation [97].

Amino acid substitution of specific residues in the CH2 domain of the IgG molecule provides an alternate route to modulate IgG sialylation level in independent of the sialyltransferase overexpression approach discussed above. Replacing Phe^{241}, Phe^{243}, Val^{264}, Asp^{265} or Arg^{301} with alanine in each case on an IgG3 antibody can increase sialylation and galactosylation. In particular, 73% of oligosaccharide chains were monosialylated or disialylated in F243A mutant and around 40% of oligosaccharide chains were sialylated in F241A and V264A mutants relative to compared to wild-type IgG3 with negligible levels (4% sialylation) prior to the mutations
[91] [98]. To an even lesser extent, D265A and R301A mutants increased IgG3 sialylation about 30% and 16% individually [91] [98]. Crystallographic analysis and nuclear magnetic resonance (NMR) analysis revealed that the F241A and F243A replacement caused localized destabilization of the protein-glycan interface in the CH2 domain, indicating a greater degree of conformational flexibility and mobility compared to native Fc [98] [99] [100], enabling the carbohydrate to obtain increased access to glycosyltransferases [101].

Taking together, the combination of IgG protein mutations with sialyltransferase overexpression can further maximize the sialylation content on antibody Fc region. In one study, the F243A replacement resulted in 53% α2,3 sialylation of either one or both branches of the N-glycans of a recombinant IgG3 produced in CHO, and following transfection of rat ST6GAL1 into this line, 60% of IgG-Fc-linked glycans were S1 or S2 sialylated with a mixture of α2,3 and α2,6 sialic acids [92]. Our group investigated single and multiple amino acid substitutions of the Fc region with sialyltransferases knock-in and knock-out strategy to alter the sialylation pattern on IgGs expressed from CHO cells. Four single amino acid mutations (F241A, F243A, V262E and V264E) as well as combining all mutations in IgG expressing CHO cells resulted increased α 2,3 sialylation and combining all the 4 mutations resulted in the highest levels of α2,3 sialylation in unmodified CHO K1 cells. Engineering CHO cells containing dual knockouts

of the ST3GAL4 and ST3GAL6 encoding α2,3 sialyltransferase together with overexpression of α2,6 sialyltransferase (ST6Gal1) resulted in the exclusively α 2,6 sialylated antibodies. One clonal isolate contained over 60% disialylated glycans (G2FS2) and approximately 80% glycans sialylated on one or both branches. These studies demonstrated a new strategy in antibody glycan design incorporating genome and protein engineerings in order to control and tailor specific glycan profiles.

2. Antibody Fc sialylation may affect ADCC and CDC activities

Distinct from the anti-inflammatory activity, the sialylation of IgG Fc region can also affect other properties of antibody, such as ADCC and CDC activities. So far, the influence of antibody sialylation on ADCC activity has yet been settled and distinctive results exit. For example, expression of exogenous sialidase A gene in mammalian cells resulted in the expression of soluble enzyme that was capable of removing sialic acid from antibodies secreted into the medium. ADCC assay showed that the two IgG1 antibodies expressed in sialidase A-transfected cells had greater than 10-fold improved potency compared to the control mock-transfected IgG1s [75]. Using zinc-finger nucleases to inactive CMP-sialic acid transporter gene resulted in a mutant CHO cell line lacking functional CMP-sialic acid transporter and the removal of sialic acid from IgG1 reported ADCC enhancement [102] . In contrary, several recent investigations revealed that Fc sialylation doesn't impact the *in vitro* FcγRI and IIIa receptor binding and ADCC activity of IgG1, whether it is mono- or di-sialylated glycans[73, 103]. However, mono-sialyalted IgG1 showed a slight binding improvement to FcγRIIa than bi-sialylated IgG1[103, 104]. Regarding to CDC activity, the presence of terminal sialic acid deteriorate IgG1 C1q binding and reduced C3b deposition on the cell surface [73].

Antibody sialylation clearly promote anti-imflammoary actitiy in a α2,6 sialylation manner, but the mechanisms of antibody sialylation on other effector functions, such as ADCC, has rarely been studied and further explorations are necessary to elucidate the role of Fc sialylation on antibodies.

1.4.3 Antibody defucosylation

Numerous studies have shown that the core-fucose residue of the CH2-associated N-linked

oligosaccharides plays a critical role in regulating the magnitude of antibody effector function ADCC [105] [106] [107] [108] [109]. Compared to the fucosylated antibodies from wild-type CHO cells, defucosylated antibodies exhibited 100-fold higher ADCC *in vitro* [110]. The core fucose is bound through a α-1,6 linkage to the innermost GlcNAc residue on an N-oligosaccharide (Figure 1-3C), which could hinder Fc binding to Fc receptors of lymphocytes[108]. It has been demonstrated that the antibody ADCC enhancement due to fucose elimination is attributed to a subtle conformational change in a limited region of IgG1-Fc, resulting in higher Fc binding to gamma receptor IIIa (Fc FcɣRIIIa) on NK cells[109, 111] [112]. Compared to amino acid mutations in the antibody Fc region, enhanced binding affinity for FcɣRIIIa of fucose-negative antibody alone is sufficient to induce maximal ADCC [113] .

Moreover, antibodies with Fc regions containing nonfucosylated N-glycans exhibit dramatically enhanced ADCC without any detectable change in CDC or antigen binding capability [108] [114]. The lack of fucose is primarily responsible for controlling binding to FcɣRIIIa receptor and in the recruitment of mononuclear cells (primarily NK cells) as effector cells for ADCC[105, 110, 115]. However, studies on polymorphonuclear cells (PMNs) found that highly-fucosylated antibodies were preferentially more effective in triggering PMN, which mediated tumor cell lysis via FcɣRII[110]. Thus, the impact of Fc fucosylation on ADCC still needs further exploration and may be critically dependent on the specific effector cell type recruited. Given that the majority of monoclonal antibodies on the market are targeted to mediate cytotoxicity of NK effector cells, we will focus on the defucosylation of antibodies here.

1. Inactivation of α1,6 fucosyltransferase---Disruption of FUT8 gene

Inactivation of the α1,6 fucosyltransferase has been extensively studied and still represents the most efficient cellular modification preventing the addition of fucose to the core of the complex N-glycan . In mammals, the FUT8 gene encodes α-1,6 fucosyltransferase in the medial Golgi cisternae that catalyze the transfer of fucose residues from GDP-fucose to the innermost GlcNAc of the tri-mannosyl core structure via the α1,6 linkage[116]. In order to generate non-fucosylated antibodies, disruption of the FUT8 gene has been investigated via various approaches as discussed below [117] [108] [118] [119].

Traditionally, numerous methods such as antisense cDNA, shRNA or transgenic overexpression

were used to reduce or remove fucosylation [120]. The introduction of small interfering RNAs (siRNAs) against the FUT8 gene reduced FUT8 mRNA expression to 20% in CHO/DG44 cells and combined with *Lens culinaris agglutinin* (LCA) selection yielded 60% antibody defucosylation with over 100-fold higher ADCC [117]. Disrupting both FUT8 alleles in CHO/DG44 cell line by sequential homologous recombination produced completely defucosylated recombinant antibodies. Chimeric anti-CD20 IgG1 produced from FUT8-/- CHO cells showed the same level of antigen-binding activity and CDC as the FUT8+/+-produced [108]. However, the time-consuming homologous recombination strategies either cannot produce completely nonfucosylated antibodies or the complete knockout of FUT8 is reversible and the difficulty of recapitulating the knockout in protein-production cell lines has prevented the widespread adoption of homologous recombination FUT8-/- cells as hosts for antibody production [121] [120] [108]. To improve the efficiency of disrupting FUT8 gene, technologies such as zinc-finger nucleases (ZFNs) and transcription activator-like effector nucleases (TALENs) were developed and reported [121] [122]. Using zinc-finger nucleases (ZFNs) to disrupt the FUT8 gene in a region encoding the catalytic core of the enzyme produced FUT8-/- CHO cells in 3 weeks at a frequency of 5% in the absence of any selection, and these lines produced antibodies completely lacking core fucosylation but having an otherwise normal glycosylation pattern without adverse phenotypic effects [121]. Separately, Cristea et al. demonstrated knockout of FUT8 gene via simultaneous TALE nuclease-mediate integration of an antibody cassette [122]. Composed of sequence-specific DNA-binding domains connected to a nonspecific DNA nuclease, ZFNs and TALENs enable a broad range of genetic modulations by inducing DNA double-strand breaks that stimulate error-prone nonhomologous end joining (NHEJ) or homology-directed repair (HDR) at specific genomic locations [123] [124]. Thus, NHEJ can be harnessed to mediate functional disruptions of target genes, as indels occurring in a coding region could lead to frameshift mutations and protein function loss [125] [126].

More recently, distinct from the protein-based ZFNs and TALENs, the CRISPR (clustered regularly interspaced short palindromic repeat)/Cas9 (CRISPR-associated protein 9) system, derived from the microbial adaptive immune system [127], has emerged as a potentially facile and efficient alternative for

inducing targeted genetic alterations [124], , and applied to diverse species such as plants, animals, bacteria, and yeast [128], as well as in CHO cells [129] [126] . Instead of protein-DNA binding in ZFN and TALEN systems, the CRISPR system required only Cas9 nuclease and single guide RNA (gRNA) binding to targeted DNA sequence[130], giving it several advantages including ease of customization, higher targeting efficiency, and multiplexed genome editing capability [131]. Sun et al. reported functional FUT8 disruptive clones (FUT8-/-) in CHO cells using CRISPR/Cas9 were obtained within 3 weeks at indel frequencies ranging from 9 to 25%, which was enhanced to 52% with LCA selection and the derived FUT8-/- clone had the ability to produce defucosylated therapeutic mAb with no detrimental effects on cell growth, viability or product quality [126]. Moreover, Grav et al. employed CRISPR/Cas 9-targeted FUT8, BAK and BAX triple knockouts simultaneously and created a cell line producing afucoylated antibody with improved protein productivity [132].

2. Overexpression of GnT-III

A different and complementary approach to improve an antibody's biological activity would be to overexpress β-1,4-N-acetylglucosaminyltransferase III (GnT-III) enzyme to produce antibodies enriched in bisecting oligosaccharides. GnT-III is a Golgi-localized enzyme that catalyzes the addition of an N-acetylglucosamine (GlcNAc) residue on to a bisecting position of the N-linked oligosaccharide, as depicted in Figure 1-1 [133]. Overexpression of the GnT-III gene in a CHO cell line expressing an anti-neuroblastoma IgG1 resulted in enhanced ADCC activity because bisecting GlcNAc inhibits fucosylation and further elongation of the N-glycan structures [134]. Thus, GnT-III overexpression leads to an increase in non-fucosylated and hybrid oligosaccharides content, which further enhance binding affinity for FcγRs [135] [136]. Overexpression of the GnT-III in a CHO cell line producing anti CD-20 antibody resulted in a 20-fold lower antibody dosage in order to achieve the same ADCC effect induced by the antibody produced from the parental CHO cell line [137]. Furthermore, by fusing the catalytic domain of GnT-III to the localization domain (cytoplasmic, transmembrane, and stem region) of other Golgi-resident enzymes of the N-glycosylation pathway in HEK293-EBNA cells, a chimeric GnT-III was expressed that can compete even more efficiently against the endogenous core a1,6-fucosyltransferase, yielding

principally bisected non-fucosylated hybrid-rich glycans [135]. Golgi alpha-mannosidase II (Man II) yields the GlcNAc2Man3GlcNAc1 precursor for all biantennary, complex N-glycans as illustrated in Figure 1-1. Co-expressing both GnT-III and Man II led to a higher proportion of bisected non-fucosylated complex-rich glycans [135]. While both glycovariants featured strongly increased ADCC activity compared to the wild-type antibody, the hybrid-rich antibody showed reduced CDC compared to complex-rich or wild-type counterparts [136] [138]. It is worth noting that the effect of bisecting GlcNAc of the IgG1 on enhancing ADCC is modest when compared to that of defucosylated IgG1, therefore, the lack of fucosylation appears to play the critical role in the enhancement of ADCC[137] [134] [106].

3. Inhibiting the supply of nucleotide sugar substrate for fucosylation

An alternative approach for producing fucose-negative antibodies is to knockout enzymes responsible for biosynthesis of GDP-fucose, the donor for fucosyltransferase in the Golgi apparatus. The advantage of this approach is that it targets all fucosyltransferases, not just FUT8 [120]. In mammalian cells, GDP-fucose is synthesized by two distinct pathways as illustrated in Figure 1-4. The *de novo* pathway is characterized by the conversion of GDP-mannose to GDP-4-keto-6-deoxymannose by GDP-mannose 4,6-dehydratase (GMD). This keto intermediate is then converted to GDP-fucose by GDP-4-keto-6-deoxymannose-3,5-epimerase-4-reductase (GMER, or FX protein). The *salvage* pathway directly utilizes fucose that is transported into the cytosol from an extracellular origin or fucose that is liberated from catabolism of fucosylated glycans in the lysosome and then transported into the cytosol [139]. The *salvage* pathway is enabled by fucokinase and GDP-fucose pyrophosphorylase (GFPP) [139]. Subsequently, GDP-fucose synthesized by these two pathways is transported into the lumen of the Golgi apparatus by GDP-fucose transporter (GFT) [140].

Reduction-of-function analyses using siRNA revealed three key genes involved in oligosaccharide fucosylation, including α1,6-fucosyltransferase (FUT8), GDP-mannose 4,6-dehydratase (GMD), and GDP-fucose transporter (GFT). Single-gene knockdown of the individual targets was insufficient to completely defucosylate the products in antibody-producing cell lines [141]. For GFT, introduction of a CHO GFT siRNA expression plasmid into a human antithrombin III (AT-III)-producing cell line showed

approximately 75% reduction of Golgi GDP-fucose, resulting in 10-40% defucosylation in AT-III [140]. Similarly, Kanda et al. reported expression levels of GFT mRNA could be reduced more than 90% in GFT siRNA-expressing antibody-producing CHO cells, but only a 20-40% reduction of the recombinant IgG Fc oligosaccharide fucosylation was observed [142]. In all, a positive relation between the Fc oligosaccharide fucosylation and the mRNA expression for both GMD and FUT8, but not for the GDP-fucose transporter, was observed suggesting that GMD and FUT8 are independent bottlenecks for α1,6 fucosylation [142] .

Alternatively, a mutant of the Pro- CHO 5 cell, Lec 13, has been isolated using *lens culinaris agglutinin* (LCA) selection, with a loss of GMD activity resulting in only 10% of fucose residing on the glycan chain compared to the parental cell line [143]. But Lec13 is unsuitable for the serum-free fed-batch production of fucose-negative antibody because the remaining GMD activity in Lec13 accumulates intracellular GDP-fucose via the *de novo* pathway and gradually increases the ratio of fucosylated products with extended culture [144]. Alternatively, a GMD knockout in CHO/DG44 cells was devoid of intracellular GDP-fucose and to produce completely non-fucosylated antibodies, but the fucosylation could be recovered through the *salvage* pathway upon the addition of *L*-fucose into the culture medium [142]. Alternatively, a double knockdown of FUT8 and GMD using a short hairpin siRNA tandem expression vector could rapidly convert antibody-producing CHO cells to fully non-fucosylated antibody producers in serum-free fed-batch culture [141].

Thus, a consideration of fucosylated and non-fucosylated antibody levels is important in order to control the product's quality and efficacy, especially around ADCC, as required by regulatory authorities [145]. While a commonly used strategy in CHO host cells to generate defucosylated antibody is to knock out the FUT8 gene, which can result in completely afucosyalted antibodies, this approach may predicate parallel cell line development of both the afucosylated and unmodified host cell lines. Furthermore, large-scale clone screening to obtain primarily unmodified and FUT8-KO clones with highly similar product quality attributes, excepting the presence of fucose residues in the unmodified clones, will be useful in ensuring that any advantage observed on ADCC can be attributed specifically to afucosylation [145]. To

circumvent these issues, other approaches have been explored and developed to evaluate the importance of fucosylation without knocking out or down the FUT8 gene. Given the nature of fucosylation mechanism in CHO (Figure 1-4), cells with an inhibition of the *de novo* pathway depend on the *salvage* pathway to synthesize GDP-fucose which requires L-fucose feeding to the cell culture media. Thus, once the de novo pathway is blocked, L-fucose can added as a switch to changing antibody glycan profiles from the afucosylated to fucosylated glycan variants without affecting other product quality features

The use of small interfering RNAs (siRNA) have knocked down the expression of FUT8, GDP-mannose 4,6-dehydratase (GMD) and GDP-fucose transporter (GFT) in the fucosylation pathway and reduced antibody fucosylation content[117, 141]. However, it may cause unpredictable off-target effects that are impractical to implement at the manufacturing level. Likewise, overexpression of the prokaryotic GDP-6-deoxy-D-lyxo-4-hexulose reductase (RMD) enzyme [146] could share similar drawbacks. RMD enzyme converts GDP-mannose to GDP-6-deoxy-d-lyxo-4-hexulose and reduces the GDP-6-keto-6-deoxy-mannose synthesis in the *de novo* pathway [146]. Also, as mentioned above, the expression of GnTIII overexpression can generate glycan species that are not commonly present on antibodies and may not be desirable for product quality consistency [145]. Addition of chemical inhibitors such as 2-deoxy-2-fluoro-L-fucose [147] add expense and have off-target activities that may risk increasing product heterogeneity.

Furthermore, The utilization of a GMD KO host for expression of fully afucosylated antibodies has been suggested [142], but the specific productivity reported for the GMD knocked out cell line was not very high [142]. Alternatively, FX protein (or called GMER) knock out clones via CRISPR approach can express antibodies with comparable productivity as parental host with a desired ratio of primarily fucosylated to afucosylated glycans when L-fucose is titrated into the production media in order to achieve intended levels of FcγRIII-binding and ADCC for an antibody [145]. Thus, there are a variety of different cell engineering and media modification strategies that can be applied to alter the fucosylation status and potential ADCC efficacy of antibody biotherapeutics. Choosing which one to use will depend on the effectiveness and practical implementation of the technique as well as a consideration of other

factors including biomanufacturing compatibility and availability based on intellectual patent considerations.

1.4.4 High-mannose glycan generation

Aside from complex and hybrid N-glycan types, high mannose glycans ($Man_{5-9}GlcNAc_2$) are characterized by terminal mannose sugars of five to nine residues attached to the $GlcNAc_2$ core [148]. They are typically non-natural glycoforms, accounting for below 5% of the recombinant therapeutic antibody glycoprofile, but they can have a major impact on *in vivo* therapeutic activity--- enhancing ADCC , decreasing CDC and increasing clearance rate [149] [150] [151, 152]. In addition, high-mannose glycans have been widely applied to generate minimally glycosylated glycoproteins for X-ray crystallography [153].

Golgi N-acetylglycosaminyltransferase I (GnT-I, also called Mgat1) is a type II transmembrane enzyme that plays a key role in the biosynthesis of N-linked glycans [154]. As shown in Figure 1-1, it specifically transfers GlcNAc from UDP-GlcNAc onto the α 1,3 branch of the oligomannose core to initiate hybrid and subsequently complex N-linked carbohydrate synthesis in the medial Golgi [154]. Thus, methods for increasing high mannose levels focus on inhibiting glycosylation in or before the medial-Golgi, mainly by knocking down or knocking out the GnT-I gene.

For high mannose glycans, one of the most widely used and numerously studied cell lines is the Lec1 CHO mutant cell line [155]. Owing to a defect in GnT-I, Lec1 cells synthesize only oligomannose-type N-glcyans [156] [154, 157]. Over the years, two discrepancies have emerged concerning about the Lec 1 cells, one concerns the unpredictable high mannose oligosaccharide (Man5-Man9) distribution in Lec 1 cells[158] [112] [152], while another focuses on the presence or absence of core α1,6 fucosylaiton in theLec 1 cell line [159] [152] [160], which prohibits its extensive application in industry. Recently, new high mannose cell line alternative to Lec 1 have been established using genetic techniques in order to study the role of GnT-I in glycosylation. Sealover et al. reported the use of zinc-finger nuclease (ZFN) genome editing technology to disrupt GnT-I gene in CHO, generating cell lines that produce recombinant

proteins predominantly bearing Man5 glycans [161]. They successfully generated 5 clones out of 90 (5.6%) containing deletions in the GnT-I gene without lectin enrichment, and all five GnT-I-deficient cell lines demonstrated similar growth and productivity characteristics to the wild-type CHO-K1 host cell line [161]. Alternatively, Lee et al. demonstrated efficient targeted gene integration into site-specific loci in CHO through CRISPR/Cas9 genome editing together with a compatible donor plasmid harboring short-homology arms, the gene of interest (GOI), and a fluorescent marker gene as an indicator of random integration[162]. By applying CRISPR/Cas9 and homology-directed DNA repair (HDR) mediated targeted integration, the GnT-I locus was completely disrupted in most target clonal cells (20 out of 25 clones), which showed a relative GnT-I copy number of close to 0 compared with that of 1 in GnT-I in CHO-S wild type cells[162].

1.4.5 Obtaining Homogeneous Glycan Patterns

Another issue with N-glycans of recombinant antibody is the generation of heterogeneous glycoforms, which can present challenges in protein purification, product consistency and lot-to-lot reproducibility, resulting in variable therapeutic efficacy. For example, this diversity can adversely affect drug potency and pharmacokinetics [163] [164]. However, N-glycans are often crucial for protein folding, so these difficulties cannot be overcome by removing N-glycosylation sites [165]. Heterogeneity is attributed to the lack of 100% enzymatic efficacy of each step in mammalian N-glycan biosynthesis and the completion of different enzymes for same substrates [165].

To solve this issue, Meuris et al. introduced a new strategy (GlycoDelete) of shortcutting N-glycosylation to simple and homogenous glycoproteins expressed in HEK293S cells, as shown in Figure 1-5[165]. Briefly, the authors inactivated N-acetylglucosaminyltransferase I (GnT-I) to produce high-mannose glycans. Then they overexpressed an endo-N-acetylglucsoaminidase (Endo T) targeted to the trans-Golgi, followed by *Concanavalin A* (ConA) lectin selection. With the following actions galactosyltransferases (GalT) and sialyltransferses (SialT) in the Golgi, GlycoDelete cells produce proteins with the Gal-GlcNAc disaccharide or its α-2,3-sialylated trisaccharide derivative and some of the monsaccharide

intermediate [165] . To assess the potential of these GlycoDelete glycans and their influence on therapeutic proteins, human GM-CSF (hGM-CSF) and an anti-CD20 antibody were produced in HEK293s and HEK293sGlycoDelete cells [165]. For hGM-CSF the presence of altered glycan obtained using the GlycoDelete cells had no detectable effect on the activity of the protein generated by these cells. On the other hand GlycoDelete anti-CD20 exhibited a significantly reduced FcγR affinity and an increased circulation time in mice compared to HEK293s produced anti-CD20 [165] [166].

Finally, in order to provide homogenous glycoforms, Zhang et al. conducted a comprehensive Zinc-finger nuclease knockout screen of 19 glycosyltransferase genes and identified the key genes that control decisive steps in N-glycosylation in CHO [167]. The authors stacked knockouts of GnT-IV-A/GnT-IV-B/GnT-V to produce almost homogenous biantennary N-glycans [167]. Subsequently, the introduction of ST6Gal-I in CHO ST3Gal4/6 knockout cells produced a normal range of N-glycans with only a2,6-sialylation, and when combined with a GnT-IV-A/GnT-IV-B/GnT-V knockout, homogenous biantennary N-glycans capped by a2,6-sialylation were generated [167].

1.5 Summary and Conclusions

This chapter has highlighted the role of glycosylation as a critical quality attribute in biotherapeutic production, and more importantly how these glycans can be manipulated in CHO expression system through cell engineering, as summarized in Table 1-1. Mammalian cell lines such as CHO can produce valuable recombinant proteins that can be accepted by human as therapeutics. However, subtle differences between glycosylation in human and other mammals exist and understanding these differences requires knowledge of the physiological characteristics of each cell type. Moreover, these differences can help to direct efforts towards glycan re-engineering in order to make a greater variety of glycan moieties in CHO cells. Efforts to exert control over protein glycosylation in CHO cells have been demonstrated through several success stories such as the maximization of terminal sialylation to extend therapeutic circulatory half-life. Furthermore, the implementation of a new set of valuable tools and technologies, such as the application of genomics, proteomics, glycomics and other ‘omics tools has enabled users to obtain an even better

understanding of the glycosylation pathways present in mammals and how they differ ever so subtly across species. The advent of advanced technologies such as CRISPR Cas9, TALE nucleases,RNA interference tools as well as the combination of next-generation of sequencing with systems biotechnology enable specific changes in cell glycosylation processing. These tools and knowledge bases will enable cell engineers to make even more highly refined and targeted modifications to the processing capability of these cells in order to meet the requirements of highly efficient bioprocesses in the future.

Figures and Tables

Figure 1-1. Schematic of N-glycosylation biosynthesis pathway in CHO cells

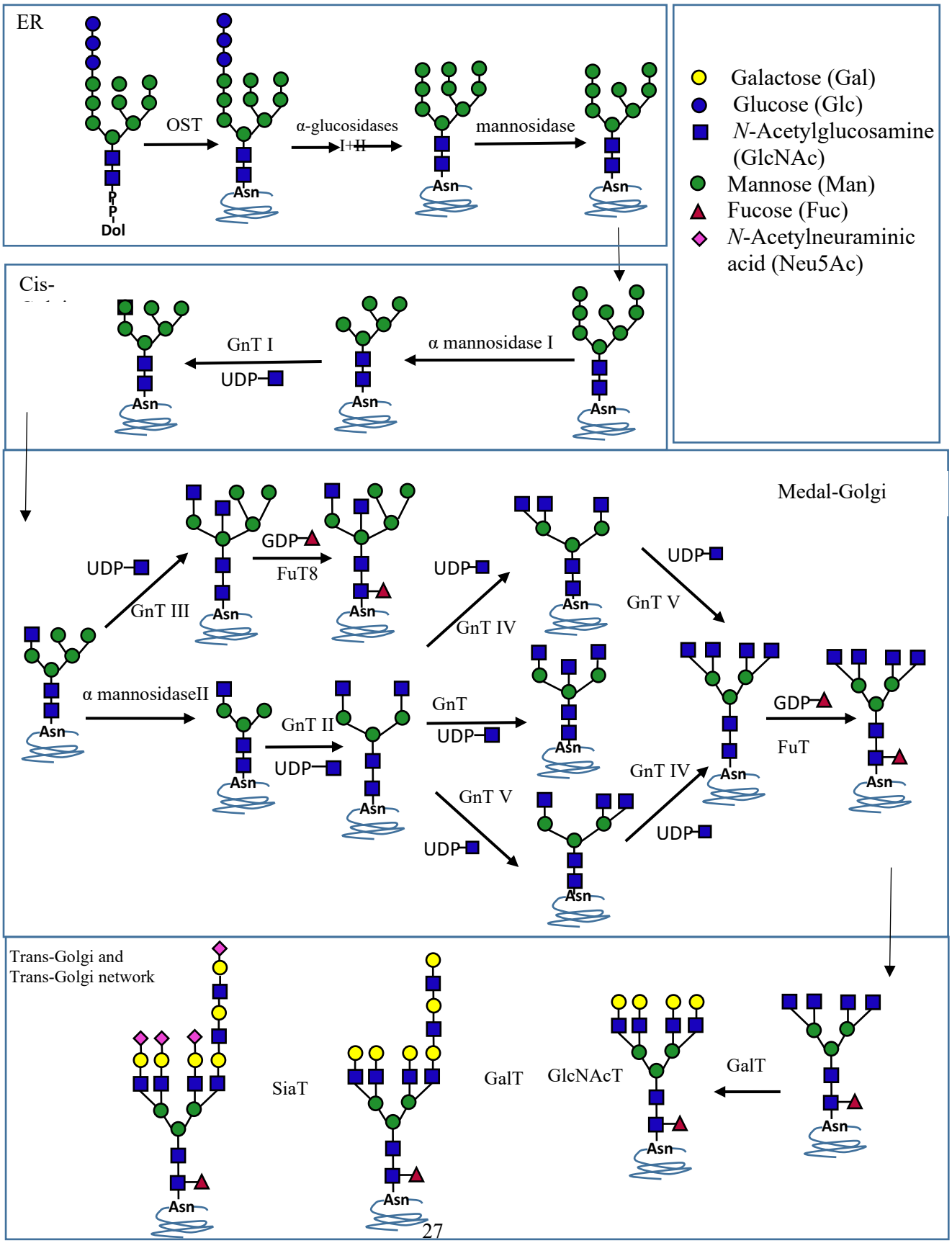

Figure 1-2. Schematic representation of sialic acid biosynthesis pathway in mammalian cells.

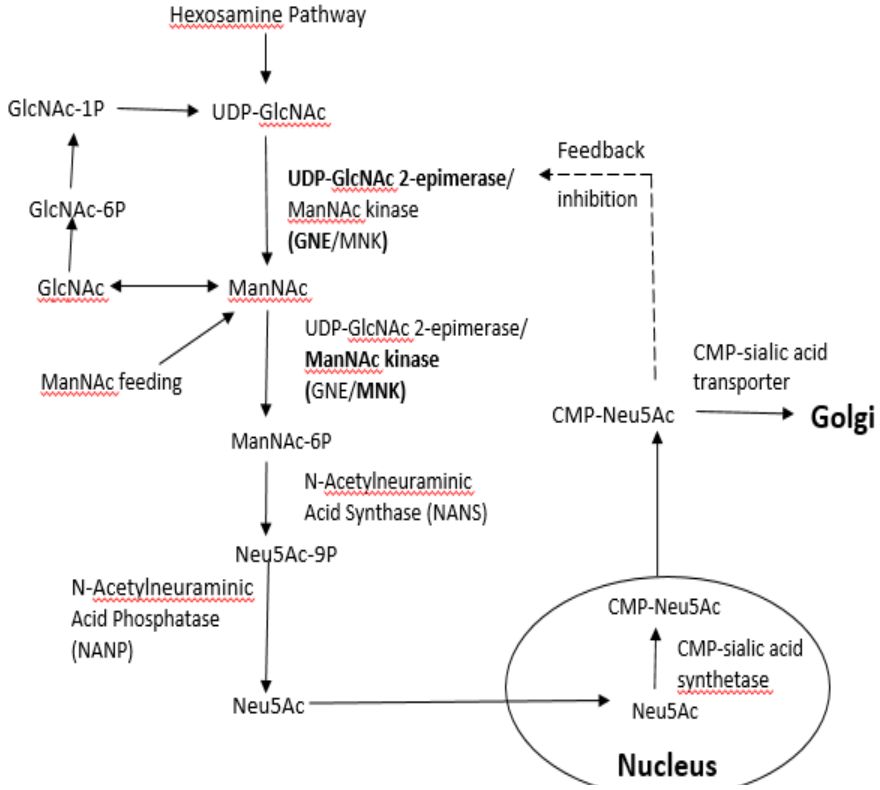

Figure 1-3. The Fc glycans on IgG affects antibody effector functions. Figure 1-3A,Human IgG1 structure with glycans attached at Asn297 N-glycosylation site in the CH2 of the Fc region. C: constant domain; V: variable domain; H: heavy chain; L: light chain; S-S: disulfide bond; Fab: Fragment antigen binding domain; Fc: Fragment crystallizable domain. Fc regions which binds effector molecules and cells. Figure 1-3B, the schematic diagram of antibody-dependent cellular cytotoxicity (ADCC) and complement-dependent cytotoxicity (CDC) mechanisms in immunology. Figure 1-3C, the representative glycan structures identified on antibody Fc region

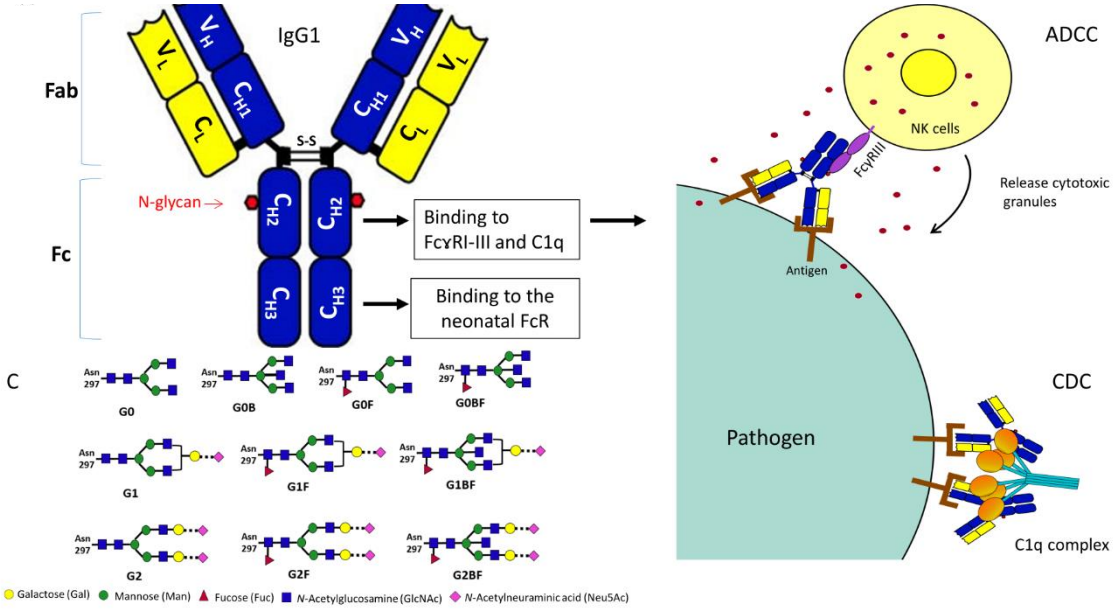

Figure 1-4. The pathways of oligosaccharide fucosylation in mammalian cell lines. GMD: GDP-mannose 4,6-dehydratase; GFPP: GDP-fucose pyrophospohorylase; FX protein/GMER: GDP-4-keto-6-deoxymannose-3,5-epimerase-4-reductase.

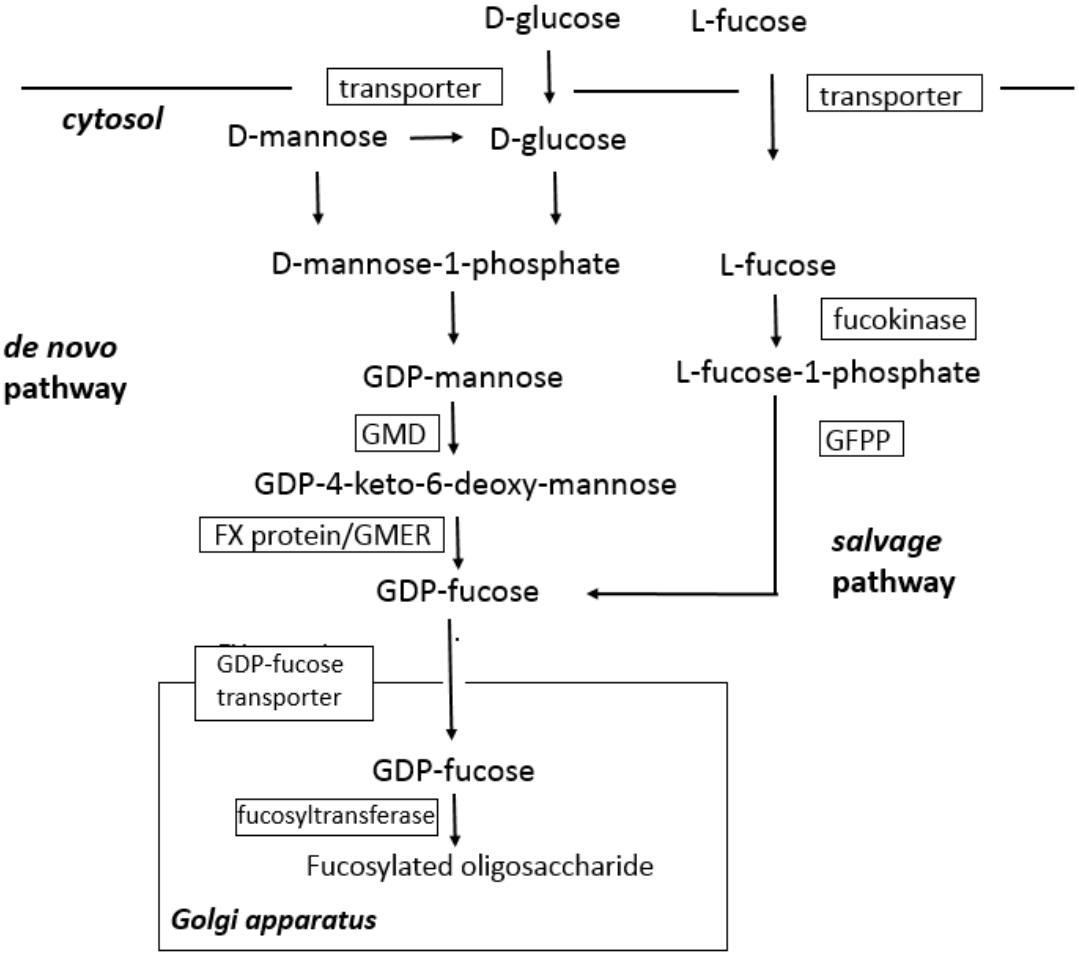

Figure 1-5. Schematic of GlycoDelete strategy, modified from Meuris et al. [165].

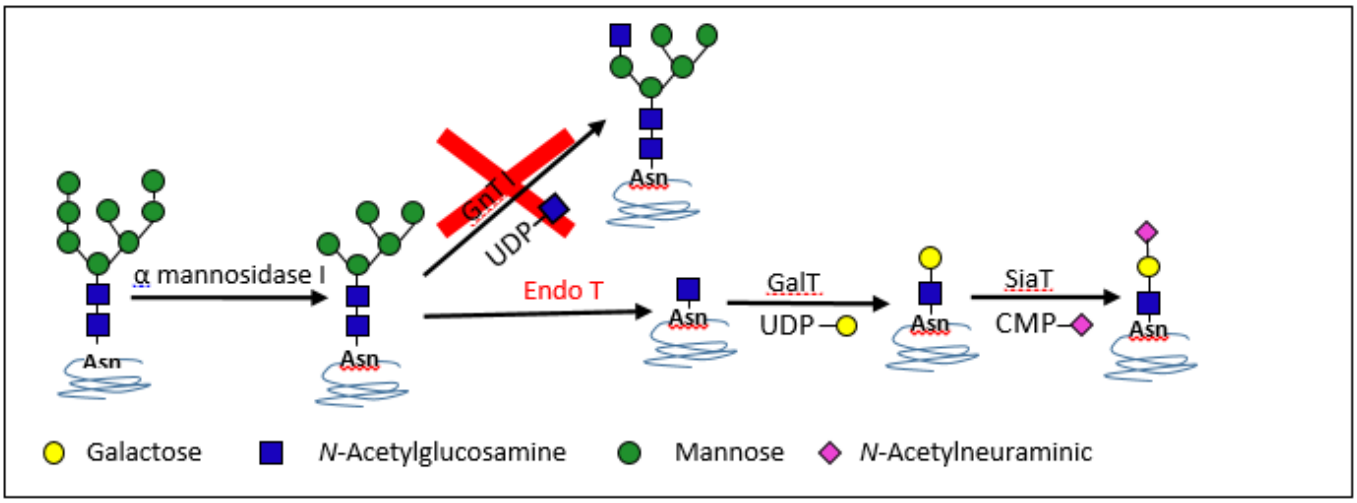

Table 1-1. Summary of Glyco-engineering strategies in CHO cells

	Enzyme name	Enzyme function	Increase biotherapeutic properties	Target Protein	reference
ST6GAL1	α2,6-sialyltransferase 1	Capping Gal residues with α2,6 sialic acid	Increase terminal sialylation to further extend protein half-life	t-PA EPO IFN-ɤ IgG	[43] [44] [96, 168-170] [96, 168]
ST3GAL4	α2,3-sialyltransferase 4	Capping Gal residues with α2,3 sialic acid	Increase terminal sialylation to further extend protein half-life	EPO	[45, 48]
β1,4GALT1	β1,4-galactosyltransferase 1	Adding Gal to GlcNac	Increase galactosylation which can indirectly increase sialylation	EPO	[45]
CMP-SAS	CMP-sialic acid synthase	Synthesize the CMP-sialic acid in the nucleus	Overexpress the enzymes in sialylation pathway to further increase sialylation	EPO	[48, 51, 52]
GNE/ MNK	UDP-GlcNAc 2-epimerase/ ManNAc kinase	Epimerization of GlcNAc to MAnNAc/ phosphprylation of ManNAc	Overexpress the enzymes in sialylation pathway to further increase sialylation	EPO	[48]
CMP-SAT	CMP-sialic acid transporter	Transport CMP-SA from Cytosol to Golgi	Overexpress the enzymes in sialylation pathway to further increase sialylation	INF-ɤ EPO	[52] [171]
GnT-IV **GnT-V**	α-1,3-D-mannoside β-1,4-N-acetylglucosaminyltransferase α-1,6-D-mannoside β-1,6-N-acetylglucosaminyltransferase	Adding GlcNac to α1-3 mannose residue Adding GlcNac to α 1-6 mannose residue	Create tri and tetra antennary glycans and allow more complex and sialylated glycan	INF-ɤ EPO	[55] [170] [172]

GnT-I (+)	N-acetylglucosaminyltransferase I	Trasfer UDP-GlcNAc to the terminal α-1,3-linked Mannose	Increase the first reaction of synthesis of complex glycan further increase sialylation	EPO	[173] [57]
Neu 3	Neuraminidase 3 (membrane sialidase)	Release of sialic acid from the Galactose residue	Reduce activity of sialidase further inhibit cleavage of sialylation	INF-ɤ	[174]
Bcl-x_L	An anti-apoptotic member of the Bcl-2 family	Anti-apoptosis protein prevents cell death	Delay the extracellular accumulation of sialidase	Fc-fusion	[67]
30Kc19	Cell-penetrating protein	Anti-apoptosis	Delay the extracellular accumulation of sialidase activity further increase in sialylation	EPO	[69] [175]

Chapter 2 Characterization of intact glycopeptides reveals the impact of culture media on site-specific glycosylation of EPO-Fc fusion protein generated by CHO-GS cells

2.1 Summary

With the increasing demand to provide more detailed quality attributes, more sophisticated glycan analysis tools are highly desirable for biopharmaceutical manufacturing. Here, we performed an intact glycopeptide analysis method to simultaneously analyze the site-specific N- and O-glycan profiles of the recombinant EPO-Fc protein secreted from a CHO-GS stable cell line and compared the effects of two commercial culture media, EX-CELL (EX) and immediate Advantage (IA) media, on the glycosylation profile of the target protein. EPO-Fc, containing the Fc region of IgG1 fused to erythropoietin (EPO), was harvested at Day 5 and 8 of a batch cell culture process followed by purification and N- and O-glycopeptide profiling. A mixed anion exchange (MAX) chromatographic column was implemented to capture and enrich N-linked glycopeptides. Using intact glycopeptide characterization, the EPO-Fc was observed to maintain their individual EPO and Fc N-glycan characteristics in which the EPO region presented bi-, tri- and tetra-branched N-glycan structures, while the Fc N-glycan displayed mostly bi-antennary glycans. EPO-Fc protein generated in EX medium produced more complex tetra-antennary N-glycans at each of the 3 EPO N-sites while IA medium resulted in a greater fraction of bi- and tri-antennary N-glycans at these same sites. Interestingly, the sialylation content decreased from sites 1 to 4 in both media while the fucosylation progressively increased with a maximum at the final IgG Fc site. Moreover, we observed that low amounts of Neu5Gc were detected and the content increased at the later sampling time in both EX and IA media. For O-glycopeptides, both media produced predominantly three structures, N1F1F0SOG0, N1H1F0S1G0, and N1H1F0S2G0, with

lesser amounts of other structures. This intact glycopeptide method can decipher site-specific glycosylation profile and provide a more detailed characterization of N- and O-glycans present for enhanced understanding of the key product quality attributes such as media on recombinant proteins of biotechnology interest.

2.2 Introduction

The glycan profile of therapeutic proteins expressed in Chinese hamster ovary (CHO) cells is a critical quality attribute (CQA) in biopharmaceutical manufacturing because more than half of the biotherapeutic drugs on the market are glycoproteins and the majority are secreted from CHO cells [176]. As a result, CHO cells are currently the most prevalent platform for biotherapeutic production and monitoring and control of their glycan patterns is an important objective of the biotechnology industry since the glycosylation patterns on therapeutic proteins can sometimes affect their bioactivity, immunogenicity, drug efficiency, and clinical safety [18]. For example, the removal of core fucosylation can significantly improve the antibody-dependent cell-mediated cytotoxicity (ADCC) and increase antibody binding efficiency to the FcγRIIIa receptor [114] and its binding to natural killer (NK) cells [177]. Elimination of terminal galactose on IgG1 reduces its binding to C1q complex and impairs complement-dependent cytotoxicity (CDC) activity [151, 178, 179]. Terminal sialylation on glycoproteins such as erythropoietin (EPO) is important for circulatory half-life in blood [48, 180]. The existence of N-glycolylneuraminic acid (Neu5Gc) in the final drug product represents a potential immunogenic chemical because human cells do not typically generate Neu5Gc due to a genetic mutation of the CMP-Neu5Ac hydroxylase (CMAH) gene [181, 182]. Therefore, the detailed characterization and control of the glycosylation profile of therapeutic proteins is pivotal to ensure the efficacy and safety of final drug products.

According to recent regulatory documents (Fournier 2015), not only the glycan

composition, including mannosylation, galactosylation, fucosylation and sialylation, but also the glycan branch distribution and even the glycosylation site information can be useful and should be well characterized if possible. Indeed, the control and monitoring of the glycan profile of therapeutic drugs to ensure lot-to-lot consistency and accuracy is a continual challenge for manufacturers. Given the non-template driven nature of post-translational glycosylation processes, various parameters intracellularly and extracellularly can affect the final glycoforms on glycoproteins in mammalian cells. The glycosylation process initiates in the lumen of the endoplasmic reticulum (ER) followed by elongation and completion in the Golgi apparatus [13, 183]. As an enzyme-directed, site-specific process, the activity and availability of the relevant glycosyltransferases and the metabolite fluxes through nucleotide sugar synthesis and transportation pathways are critical to the final glycan profile of recombinant proteins [184]. Numerous process effects, such as the composition and nutrients in the culture media, harvest time, culture temperature, pH, CO_2 and dissolved oxygen (DO) level can also affect the final glycoforms of therapeutic proteins [18]. Among all the variations, the culture media composition dictates the nutrients incorporated, which can directly affect the final glycan profile of recombinant proteins. For example, the feeding of uridine, manganese chloride, and galactose in the culture media can improve antibody galactosylation better than individual additions, and the extent of antibody galactosylation can be adjusted by changing their concentrations in the culture media [185, 186]. Supplementation with 20-40 mM *N*-acetylmannosamine (ManNAc), an intermediate precursor in the sialyation pathway, can also increase the protein sialylation about 10-20% [50]. Thus, the variety of glycosyltransferase types and contents, nutrient feedings, and possess parameters can lead to considerable diversity in the glycosylation of recombinant IgG and other therapeutic glycoprotein products. The glycans generated can further pose a daunting challenge for analytics

processing [187].

Advanced analytical techniques based on mass spectrometry have revolutionized the identification and characterization of glycans [188, 189]. Current approaches for glycan analysis typically include the release of carbohydrates from glycoproteins (deglycosylation), either by enzymatic or chemical reactions [189]. For N-glycans, PNGase F, which reacts between the innermost GlcNAc and asparagine residues, is currently the most effective enzyme to cleave most N-glycans. For O-glycans, so far no single enzyme was found to be able to remove all the types of O-glycans, but O-Glycosidase can specifically remove Core 1 and Core 3 O-glycans [190]. Chemical reaction-beta elimination- is still the prevalent method for O-glycan release, which may pose low efficiency and high detection noise drawbacks [191]. Derivatization with a fluorescent tag, such as 2-aminobenzamide (2-AB) and 2-aminobenzoic acid (2-AA) through reductive amination or glycan permethylation are effective approaches to increase the detection sensitivity and gain glycan structural information [189, 192]. However, a major challenge for released glycan analysis is that it cannot provide site-specific glycan information, and often requires multiple sample preparation steps, which may be time-consuming.

A complementary approach for glycan analysis is intact glycopeptide characterization. With glycans remaining attached to the protein sites, this strategy can elucidate the glycopeptide amino acid sequence, the glycosylation site information, and the glycan composition simultaneously [193] [194]. Due to the inherent complexities of intact glycopeptides, this analytical method faces several complications: 1. The glycopeptides can be suppressed by non-glycopeptides in the mass spectrometry because of their low ionization efficiency [195]. Therefore, a glycopeptide enrichment step may help to enhance the mass spectrometry performance. 2. The commonly used collision-induced dissociation (CID) fragmentation method was reported to have

difficulty in generating a diverse collection of peptide backbone fragments, which can make peptide sequence identification problematic [195]. As an alternative approach, higher-energy C-trap dissociation (HCD) fragmentation, often equipped with Orbitrap detection, represents a potentially powerful tool for generating high resolution MS/MS spectra. HCD can provide superior performance in representing low m/z glycan oxonium ions, which normally contain signal ions for glycopeptides [195]. By supporting multiple cleavage events, HCD fragmentation can provide a wealth of peptide identifications [195] [196] [197].

Therefore, in this work, we applied an intact glycopeptide method to determine the site-specific glycosylation profiles for both the N- and O-glycans of a recombinant fusion protein EPO-Fc produced by CHO cells. Containing the well-studied Fc region of IgG1 fused to EPO, this fusion protein was stably expressed in a commercial CHO-GS cell line in order to test the intact glycopeptide analysis method. Furthermore, the impact of adding an anion-exchange chromatographic column to capture N-glycopeptides and the enhancement of the N-glycopeptide abundance was compared with performance without the step. In order to examine the role that culture media plays on glycopeptides and glycan structures generated, we evaluated two different media: EX-CELL (EX) medium and immediate Advantage (IA) medium from Millipore-Sigma and compared the effects of media difference on the EPO-Fc N- and O-glycan profiles using this intact glycopeptide method as illustrated in Figure 2-1 and the workflow in Supplemental Figure S2-1. In particular, we were able to distinguish the differences in the glycan structures at each site as well as the levels of sialylation and fucosylation present at each site, including the three EPO and one Fc N-glycan sites. The glycopeptide analytical method was also used to identify the predominant O-glycans in the different media as well. These findings demonstrate the potential of intact glycopeptide analysis to provide a robust and detailed profiling of both N- and O-glycans

at specific sites, which will allow biotechnologists to better understand and control the glycan compositions emerging from CHO cells and other production hosts in the coming decades.

2.3 Materials and Methods

2.3.1 Cell culture

The recombinant EPO-Fc expressing CHO-GS cell line was graciously provided by Millipore-Sigma as part of the AMBIC intact glycopeptide project. This cell line was cultured in both EX-CELL® CD CHO Fusion medium (Millipore-Sigma, Catalog No. 14365C), and immediate ADVANTAGE medium (Millipore-Sigma, Catalog No. 87093C) individually. These two media were abbreviated as EX and IA media respectively in this work. EX and IA media are commercial proprietary media graciously provided by Millipore-Sigma. EX is a first-generation chemically defined cell culture medium. IA is a second-generation chemically defined medium with a more restricted raw material content focusing on cell growth and productivity. IA contains a streamlined composition so that customers can tailor the formulation later with various raw materials for increasing glycosylation complexity as desired. Cell culture was performed in a humidified 37 °C incubator with 5% CO_2 and 130 rpm shaking speed. Cells were subcultured every 3-4 days at seeding density of 0.5 $\times 10^6$ cells/ml media in 125 ml shake flasks with 30 ml media.

To monitor cell growth rates, recombinant EPO-Fc cells were seeded at 0.3×10^6 cells/ml in 30ml culture EX and IA media separately. Three biological repeats were performed. Cell density was measured every 24 h using a hemocytometer, and viability was determined by distinguishing live cells from dead cells using trypan blue staining (Thermo Fisher Scientific). During the cell growth study, cell supernatants were collected every 24 h and subject to metabolite analysis and EPO-Fc characterization using immunoblotting and Coomassie blue staining as described below. Metabolites (glucose and lactate) were measured by using an YSI 2700 D dual channel select biochemistry analyzer (YSI Life Sciences).

2.3.2 Immunoblots and Coomassie blue staining

Equal volumes (40 µl) of daily supernatants from EX medium-cultured and IA medium-cultured EPO-Fc cells in the growth study were denatured and reduced with 4x sample buffer by boiling at 95 °C for 5 mins. The 4x sample buffer was made of 90% 4x Laemmli Sample Buffer (Bio-Rad, Hercules, CA) and 10% 2-Mercaptoethanol (Millipore-Sigma). After cooling, supernatant samples were fractionated on 10% SDS-PAGE, followed by transfer to a PVDF membrane (Bio-Rad, Hercules, CA). Rabbit anti-human EPO (Abcam, Cambridge, MA) was used as the primary antibody in immunoblots. Horseradish peroxidase (HRP)-linked anti-rabbit IgG was used as secondary antibody for EPO detection (Cell Signaling Technology, Danvers, MA), as previously described [198]. Horseradish peroxidase (HRP)-linked anti-human IgG from Abcam (Cambridge, MA) was used to detect Fc protein expression. The HRP signal was detected using Immun-Star Western Chemiluminescent Kit (Bio-Rad, Hercules, CA) with imaging performed on a Molecular Imager® ChemiDoc™ XRS (Bio-Rad, Hercules, CA) with Quantity One Software (Bio-Rad, Hercules, CA). For Coomassie blue staining, the purified EPO-Fc protein was subjected to SDS-PAGE and followed by staining in Coomassie Blue solution (0.1% Coomassie Blue R250 (ThermoFisher Scientific), 10% acetic acid, 50% methanol and 40% H2O) overnight and destaining in destaining solution (10% acetic acid, 50% methanol and 40% H2O) for 6 hours, replacing the solution every two hours.

2.3.3 EPO-Fc protein purification

The culture supernatant containing recombinant EPO-Fc protein was first filtered through a 0.22-µm-pore-size membrane, and then mixed with Protein A agarose bead slurry (Vector Lab) and incubated at room temperature for 3 hours on a rotator. Then the supernatant was loaded onto a column to retain the agarose beads. After three washes with PBS buffer, the bound EPO-Fc was

eluted with 0.1 M glycine, pH 2.7. The pH of eluate was neutralized by adding 1 M Tris-HCl, pH 9.0. The EPO-Fc eluate was subsequently dialyzed against PBS buffer using Amicon ultra-flow filter with molecular weight cut-off (MWCO) 10 kDa (Millipore). The final protein concentration was measured by bicinchoninic acid (BCA) assay (Thermo Fisher Scientific). The purified EPO-Fc protein purity was assessed by 10% SDS-PAGE followed by Coomassie blue staining.

2.3.4 Enzymatic digestion of purified EPO-Fc protein

2 mg of purified EPO-Fc protein from EX medium and IA medium respectively was denatured in 8.0 M urea/1.0 M ammonium bicarbonate buffer, and reduced in 10 mM 1,4-dithiothreitol (DTT) at 37 °C for 1.0 h. Proteins were alkylated in 10 mM iodoacetamide at room temperature for 30 min in the dark. Samples were diluted 5-fold with nuclease-free water to decrease the concentration of urea. Endoproteinase GluC (New England BioLabs) for N-glycopeptide or trypsin (New England BioLabs) for O-glycopetide (protein:enzyme = 50:1, w/w) were separately added to each sample to digest proteins overnight with shaking at 37 °C. We chose Endoproteinase GluC and trypsin for N- and O-glycopeptide analysis respectively because: 1. GluC can divide EPO-Fc protein into individual glycopeptides with only one glycan site remaining on each glycopeptide, while trypsin cannot separate the first two N-glycosites of EPO-Fc; 2. The O-glycopeptide after GluC digestion was too large to be ionized for routine MS detection while trypsin digestion can generate O-glycopeptide of EPO-Fc with appropriate length for MS detection. After digestion, samples were centrifuged at 13000 x g for 15 mins to remove precipitates, followed by desalting on a C18 cartridge (Waters, Milford, MA) according to the manufacturer's instructions. The peptide samples were dried in a Speed-Vac and stored at -80°C prior to LC−MS/MS analysis.

2.3.5 MAX column for N-glycopeptide enrichment

Oasis MAX is an anion-exchange and reversed-phase polymer column (Waters Company). The protocol for using MAX column for N-glycopeptide enrichment was developed previously by Yang et al.[199]. Briefly, after C18 desalting, peptides were eluted in 60% acetonitrile (ACN), 0.1% trifluoroacetic acid (TFA). Then the binding solution was adjusted to 95% ACN, 1% TFA for N-glycopeptide enrichment using Oasis MAX 1 cc vacuum cartridge (Waters, Milford, MA). Before loading samples, MAX columns were first equilibrated in 1 mL of ACN for three times, then 1ml 100 mM triethylammonium acetate for three times, 1ml water for three times, and finally 1 ml 95% ACN, 1% TFA for three times. Next, the peptide samples in 95% ACN, 1% TFA solution were loaded and washed by 1 mL of 95% ACN, 1% TFA for three times. Finally, bound glycopeptides were eluted in 400 μL of 50% ACN, 0.1% TFA. Concentration of the eluted peptides were determined using Nanodrop spectrophotometer to measure 280 nm absorbance for tryptophan and tyrosine. The peptide samples were dried in Speed-Vac and stored at -80°C prior to LC−MS/MS analysis. The component percentage shown in this work is based on volume ratio (v/v) unless otherwise specified.

2.3.6 Nano LC−MS/MS Analysis.

The dried peptide sample was re-suspended in 3% ACN and 0.1% formic acid (FA). The samples were analyzed on a Q-Extractive mass spectrometer (Thermo Fisher Scientific, Bremen, Germany). The Nano LC-MS/MS parameters were described previously in Yang et al. [200]. First, samples were separated by a Dionex Ultimate 3000 RSLC nano system (Thermo Scientific) with a PepMap RSLC C18 column (75 μm × 50 cm, 2 μm, Thermo Scientific) protected by an Acclaim PepMapC18 column (100 μm × 2 cm, 5 μm, Thermo Scientific). For intact glycopeptides, the mobile phase consisted of 0.1% FA and 3% ACN in water (A) and 0.1% FA, 90% ACN in water (B) using a gradient elution of 0-2% B, 1 min; 2-8% B, 9 min; 8-31%B, 80 min, 31-38% B, 20

min; 38-95% B, 5 min; 95% B, 10 min; 95-2% B, 4 min [200]. The flow rate was kept at 0.3 µl/min. Data-dependent higher-energy collisional dissociation (HCD) MS/MS fragmentation was performed on the 12 most abundant ions. The spray voltage was set to 1.5 kV. Spectra MS1(AGC (Automatic Gain Control) target 3x 10^6 and maximum injection time 60 ms) were collected from 400-2000 m/z at a resolution of 70,000 followed by data-dependent HCD MS/MS (at a resolution of 35,000, NCE (Normalized Collision Energy) 32%, intensity threshold of $4.2x10^4$, AGC target $2x10^5$ and maximum injection time 120 ms) of the 12 most abundant ions using an isolation window of 1.4m/z [200]. Charge state screening was enabled to reject singly charged ions and ions with more than eight charges. A dynamic exclusion time of 30 sec was used to discriminate against previously selected ions. For tryptic peptides, 110 m/z was set as the fixed first mass in MS/MS fragmentation to include all oxonium ions of glycopeptides [200].

2.3.7 Data Analysis

For intact glycopeptide identification, the MS data were searched using an in-house glycopeptide analysis software, GPQuest 3.0, based on GPQuest (Toghi Eshghi et al. 2015). Acquired MS/MS spectra were searched against the RefSeq *Cricetulus griseus* protein database downloaded from the NCBI website with last update June 01, 2016, which contained 46,402 proteins. The human erythropoietin fasta protein sequence and human IgG1 Fc region sequence were also added to the protein database. Database search parameters were set as follows: a maximum of two missed cleavage sites permitted from GluC or trypsin digestion, 10 ppm precursor mass tolerance, 0.06 Da fragment mass tolerance, carbamidomethylation (C, +57.0215 Da) as a fixed modification, and oxidization (M, +15.9949 Da) and deamidation (N, +0.98 Da) as dynamic modifications. Spectral counting was used to quantify the peptides identified from LC-MS/MS data. The parameters for mass tolerance of MS1 and MS2 were 10 ppm and 20 ppm,

respectively. The spectra containing an oxonium ion m/z 204.09 were chosen for further searching. Results were filtered based on the following criteria: (1) false discovery rate (FDR) less than 1%, (2) ≥ 3 glycopeptide spectra matches (PSMs) for each peptide were required, (3) all the PSMs should be annotated by at least one N-linked glycans. All the annotated intact glycopeptides were presented in Supplemental Figures S2-2.

2.4 Results

2.4.1 Comparison of EX-CELL and imMEDIAte Advantage media on EPO-Fc CHO cell growth and protein production

First, EPO-Fc expressing cell growth profiles cultured in EX-CELL (EX) medium and immediate Advantage (IA) medium were obtained for three biological repeats. As shown in Figure 2-2A, EPO-Fc cells in IA medium exhibited an extended exponential growth phase (Day 2 –Day 6) compared to that in EX medium (Day 2-Day 5) and as a result reached a higher cell density than those in EX-CELL medium. On Day 6, EPO-Fc cells in IA medium reached a maximum cell density around 13 million/ml on Day 7 while EX medium reached a maximum cell density of about 8.4 million/ml at Day 6. Furthermore, the viability in EX medium started to drop and declined gradually from Day 6 while the viability in IA medium started to drop on Day 8 but quickly declined to 0 by Day 9. In addition, as a complement to the growth and viability studies, we conducted metabolite analysis of lactate accumulation and glucose consumption (Figure 2-2C and 2D) to gain further insight into the relative impact of EX and IA media on CHO cell metabolism. As shown in Figure 2-2D, IA medium had higher glucose level (5800mg/L) than that (5400 mg/L) in EX medium at Day 0. Cells in EX medium also exhibited a relatively slower glucose consumption and lactate accumulation rates compared to those in IA medium. By Day 8, EPO-Fc cells in IA medium had completely consumed all the glucose and taken up most of the

lactate, which correlated with the drop of cell number and viability observed at Day 9 in IA medium. At Day 9, small amounts of glucose and lactate remained in EX medium, which is also consistent with the more gradual decline in cell density and viability.

Next, the abundance and quality of EPO-Fc protein secreted into EX and IA culture media was evaluated. Briefly, equal amounts of supernatant were harvested every day of the growth study and subjected to SDS-PAGE followed by Coomassie blue staining. Purified EPO-Fc protein was used as a positive control. As shown in Supplemental Figure S2-3A, EPO-Fc protein was the most abundant protein in the supernatant from both EX and IA media cell culture during the growth cycle. In addition, anti-EPO and anti-IgG immunoblots were applied on the daily supernatant samples from the same EX and IA growth study respectively. In Supplemental Figure S2-3B, the intensity of EPO and IgG signal in their respective immunoblots increased gradually with increasing time in culture in both EX and IA media. However, we observed some degradation of the protein for the anti-IgG immunoblot from Day 6 to Day 8 in the IA medium cell culture but not in EX medium and no obvious degradation of EPO-Fc protein for the anti-EPO immunoblot results in both EX and IA media (Supplemental Figure S2-3B). Therefore, some degradation of recombinant EPO-Fc protein during the later days for batch cell growth in IA basal medium may be attributed to the changed concentration of secreted proteases and reductases in IA medium or an increase of truncated or missed glycosylation on EPO-Fc protein. Alternatively, recombinant EPO-Fc protein maintained its integrity in the EX medium. This difference may have been due, in part, to the composition differences of the two media which can affect the cell state and secretory processes. In particular, the IA medium was designed with a streamlined composition which may have affected secretion of certain components at later days for this simple batch cell culture process.

2.4.2 N-glycopeptide enrichment for improving intact glycopeptide MS identification

Prior to the study of media influence on the glycan profile of EPO-Fc protein using intact glycopeptide analysis, in order to improve the EPO-Fc glycopeptide abundance for better MS capture and characterization, chromatographic columns can be applied to concentrate the glycopeptide quantities from digested EPO-Fc peptides. Due to the hydrophilic features of glycans or glycopeptides, strong anion-exchange columns such as the MAX column can be used for highly sensitive and selective extraction of acidic compounds, such as N-glycopeptides [201]. In this work, we adopted the MAX column for EPO-Fc N-glycopeptide enrichment and conducted a comparison on the N-glycopeptide analysis for IA Day 6 culture supernatant with and without MAX column enrichment as shown in Figure 2-3A workflow. Briefly, conditioned media from Day 6 EPO-Fc cell culture in IA medium was harvested and subjected to protein A purification to obtain EPO-Fc protein. Then purified EPO-Fc protein from three biological repeats was digested using GluC endoproteinase individually followed by C18 column desalting of the digested peptides. Subsequently, some desalted peptides were subjected to the MAX column for N-glycopeptide enrichment. Finally, equal amounts (0.4 μg) of peptides from before and after MAX enrichment were subjected to LC-MS/MS analysis.

The characterization of N-glycopeptide mass spectrometric performance is tabulated in Table 2-1. On average, more glycopeptides and glycan types were detected using MAX column enrichment (51.67 ±1.25 PSM and 24 ± 0.81 glycan types detected before MAX enrichment; 85.33 ±4.78 PSM and 31 ± 0.81 glycan types detected after MAX enrichment). Importantly, the representative oxonium ion (m/z=204.09) signal intensity was increased nearly 10-fold using MAX column to enrich the N-glycopeptides. Next, a fucosylation and sialylation comparison was performed as shown in Figure 2-3B. While the fucosylation content of EPO-FC protein (76%) was

slightly higher than the sample without MAX column enrichment (72%), there was no significant fucosylation level difference between MAX column sample and the control sample (Figure 2-3B). Moreover, the sialylation content of the EPO-Fc protein also displayed similar content with or without MAX enrichment (Figure 2-3B). We also explored the N-glycan branch distribution of EPO-Fc protein with and without MAX enrichment. The MAX column enrichment increased the tri- and tetra-antennary content of EPO-Fc protein slightly while decreasing the bi- antennary content, but this result is not significantly different for the three biological repeats. The high-mannose type glycans present similar abundance with or without MAX column enrichment. Furthermore, with more N-glycopeptides and N-glycan types detected after MAX column enrichment, we acquired more consistent results among three biologic repeats compared to the control unenriched counterparts, which identified fewer N-glycopeptides and glycan types. Collectively, these results indicated that MAX column can efficiently enrich N-glycopeptides leading to a more in-depth profiling analysis of the glycans presenting on EPO-Fc glycoprotein.

2.4.3 Comparison of media influence on EPO-Fc N-glycans using intact N-glycopeptide characterization

After evaluating the performance of MAX column for N-glycopeptide enrichment, we next studied the EPO-Fc glycan profile in EX and IA media using the intact glycopeptide characterization method. The workflow is displayed in Supplemental Figure S2-1. Briefly, conditioned media from Day 5 (see Figure 2-2 growth phase) and Day 8 (see Figure 2- 2 stationary phase) in both EX and IA media cell culture were collected and recombinant EPO-Fc protein was obtained and purified from the culture broth. Next, equal amounts of EPO-Fc protein were subjected to GluC endoproteinase digestion followed by C18 column desalting and MAX column enrichment for N-glycopeptide preparation. Finally equal amounts (0.8 μg) of MAX-enriched

peptides were subjected to nano LC-MS/MS analysis.

First, we assessed the size difference of purified EPO-Fc protein from EX and IA media culture. Equal amounts of the purified EPO-Fc protein from both Day 5 and Day 8 EX and IA media cell cultures were loaded onto a SDS-PAGE gel followed by Coomassie blue staining. The result shown in Figure 2-4A indicates that EX medium generated a more homogenous and slightly larger EPO molecule during both the growth and stationary phases compared to their corresponding counterparts from IA medium cell culture. In order to further explore the effect of media on EPO-Fc protein glycan characteristics, for EPO-Fc N-glycopeptide analysis, the distribution of glycan antennary was studied and is displayed at each of the 4 N-glycan sites in Figure 2-4B. There were more combined bi-/ tri-antennary glycans present in IA medium than EX medium both in the growth phase and stationary phase at the first 3 N-glycan sites. In contrast, the EX medium tended to include a larger fraction of tetra-antennary structures at both Day 5 and Day 8. As expected, at the 4th N-glycan site, both Day 5 and Day 8 samples in both EX and IA media present solely bi-antennary structures, consistent with previous studies noting that the N-glycans on the antibody Fc region is predominantly a bi-antennary structure [202]. Alternatively, the prevalent N-glycan types on recombinant EPO protein expressed in CHO cells are often tri- and tetra-branched structures [7, 48, 172]. Therefore, as a fusion protein, EPO-Fc maintained their individual EPO and Fc N-glycan characteristics, which may be attributed to their structural inherence. The N-glycopeptide analysis was in keeping with Coomassie blue gel result with the shown in Figure 2-4A. The EX media generated larger molecules including a large fraction of tetra-antennary glycans in Figure 2-4B, consistent with the more uniform and slightly larger protein band observed for the Coomassie gel result. Alternatively, the IA medium generated a more diverse collection of bi- and tri-antennary branched glycans which is in accordance with broader

EPO-Fc band observed for the IA-derived samples on the Coomassie blue gel.

We further evaluated the sialylation content (Neu5Ac and Neu5Gc) of N-glycans on the EPO-Fc protein. The total Neu5Ac sialylation site occupancy of Day 5 and Day 8 samples in both EX and IA media cell culture is shown in Figure 2-5A. In all tested samples, the Neu5Ac content in growth phase was similar to that in stationary phase for EX medium, while the Neu5Ac level decreased with cell culture time in IA medium. Site-specific analysis of Neu5Ac content on the four N-glycan sites (first 3 of EPO N-glycan sites, the 4th of Fc N-glycan site) is shown in Figure 2-5B. The Neu5Ac sialylation content decreased gradually from the 1st to the 4th N-glycan sites, which is consistent with our analysis of wild-type EPO protein glycans from CHO cell cultures [7]. In the current study, the 4th N-glycan site was fully unsialylated (Figure 2-5B). Similar to the total Neu5Ac sialylation trend in Figure 2-5A, the Neu5Ac sialylation level in the growth phase was consistent with that in stationary phase at the first three N-sites for EX culture, while the Neu5Ac sialylation level decreased along with cell culture time in IA medium for the first three N-sites. Further details about the sialic acid content at the specific sites is summarized in Supplemental Figure S2-4. This analysis revealed that the most widely observed N-glycans include only one sialic acid (S1) for all tested samples at the first three N-glycan sites. N-glycans with two or three sialic acids (S2 and S3) represented a smaller fraction of the N-glycans at each site while N-glycans with four sialic acids (S4) were rare and only traceably detected at the first N-site on the Day 5 EX cultured and the 2nd N-site on the Day 8 IA cultured EPO-Fc samples. Therefore, EX medium can maintain the EPO-Fc protein Neu5Ac sialylation content along with cell culture time while sialylation content decreased slightly with culture duration for the IA medium. On the other hand, the total and site-specific Neu5Gc sialylation analysis is presented in Figure 2-5C and 2-5D. The Neu5Gc sialylation analysis, shown in Figure 2-5C, revealed that low but detectable

amounts of Neu5Gc were detected in all tested samples with Day 8 cultured EPO-Fc protein exhibiting more Neu5Gc content than Day 5 culture samples in both EX and IA media. For site-specific Neu5Gc analysis (Figure 2-5D), Neu5Gc content was highest at the 1st N-glycan site during stationary phase in both media. At 2nd N-site, Neu5Gc was only detected at the stationary phase in IA medium. The 3rd N-glycan site also contained detectable Neu5Gc content with very low levels as the 2nd site and none detected at the 4th site.

The total and site-specific fucosylation analysis is shown in Figure 2-6A and 2-6B, respectively. EPO-Fc from the IA cultured medium had a slightly higher fucosylation content than EX cultured samples during both growth and stationary phases (Figure 2-6A). For the site-specific analysis (Figure 2-6B), interestingly, in contrast to the sialylation analysis, the 1st N-glycan site had the lowest fucosylation occupancy compared to the other N-glycan sites. Furthermore, the 4th N-glycan site was fully fucosylated in all tested samples, and the fucosylation content also remained relatively similar over time at the 2nd, 3rd and 4th N-glycan site for both EX and IA media. The culture media difference in fucosylation content mainly affected the 1st N-glycan site, in which the IA medium exhibited a higher fucosylation level compared to its counterparts in EX medium at same time points.

2.4.4 Comparison of different media impact on EPO-Fc O-glycan profile using intact O-glycopeptide characterization

Finally, we studied the O-glycan profile of EPO-Fc protein cultured in both EX and IA media. The workflow of O-glycopeptide analysis is also illustrated in Supplemental Figure S2-1. After EPO-Fc protein purification, trypsin digestion and C18 desalting, equal amounts (0.8 μg) of two biological O-glycopeptide repeats were subjected to nano LC-MS/MS analysis. The identified O-glycan are summarized in Table 2-2. In all tested samples, GalNAc-Gal, GalNAc-Gal-SA and

GalNAc-Gal-SA_2 (N1F1F0SOG0, N1H1F0S1G0 and N1H1F0S2G0) represented the three major types of O-glycans identified on EPO-Fc protein. Moreover, more O-glycan types were identified in the EX medium in both the growth (7 types) and stationary phases (6 types) compared to the types observed at their corresponding time points in IA medium (5 types and 4 types for growth and stationary phases, respectively), indicating that EX medium results in a more diverse O-glycan profile on EPO-Fc protein than IA medium.

2.5 Discussion

Intact glycopeptide profiling characterizing the site-specific glycans has emerged as an alternative and complementary glycan analysis tool in recent years. Its application includes biomarker discovery, disease diagnosis and biopharmaceutical product quality control [203] [204] [205] [206]. Here we adopted this glycoproteomic method for evaluating the effects of different media compositions on the glycan profile of a recombinant protein, EPO-Fc, secreted from CHO cells. Compared to the traditional released glycan analysis method, this approach can elucidate the glycopeptide sequence, glycan site information, and the glycan structural composition simultaneously [193]. Moreover, this approach requires a less extensive sample preparation process with a turnover time for results in less than 2 days. In this work, we applied two different media, EX-CELL (EX) medium and immediate Advantage (IA) medium from Millipore-Sigma, and compared the effects of the media on the EPO-Fc N- and O-glycan profiles using this intact glycopeptide method. For N-glycosylation, the sialylation content decreased for the 1st through 4th N-glycan sites. Even as a fusion protein, EPO-Fc maintained the N-glycan characteristics that would be expected for the individual EPO (Sites 1 to 3) and Fc (4th site) elements. EPO N-glycans presented bi-, tri- and tetra-branched glycan structures with various sialylation and fucosylation levels at each sites, while the Fc N-glycan displayed mostly fully fucosylated, unsialylated bi-

antennary N-glycans. For the O-glycans, there was a prominence of 3 main glycotypes (N1F1F0SOG0, N1H1F0S1G0 and N1H1F0S2G0) for both media compositions.

For glycopeptide sample preparation, an enrichment step can serve to increase the abundance of glycopeptides among all the digested peptides. For N-glycans, we evaluated the MAX column for N-glycopeptide enrichment and the result shows that more N-glycopeptides and more consistent N-glycan types were detected after MAX column enrichment. For O-glycans, a HyperSep retain AX (RAX) (Thermo Fisher Scientific) column enrichment method was tested [199] but not implemented due to low capture efficiency. There are two possible reasons for this phenomenon: 1. The O-glycan on EPO-Fc protein has generally low occupancy and less diversity [207]. Indeed, using β-elimination method to release O-glycan, we only obtained three types (N1H0F0S0G0, F0N1H1S0G0 and N1H1F0S1G0) of O-glycan on EPO-Fc protein (data not shown), which is consistent with previous studies (Lauber et al. 2015). 2. RAX affinity may have binding bias, which is specific to a certain type of glycan structures and may be inefficient for enriching O-glycan-rare samples [195].

We tested two different commercial culture media, EX and IA media from Millipore-Sigma, and their influence on the complexity of glycan profiles of recombinant EPO-Fc protein secreted from a CHO-GS cell line. Coomassie blue profiling (Figure 2-4A) indicated that the N-glycans produced by cells cultured in the EX medium varied more in size and produced a broader distribution of EPO-Fc protein than that in the IA medium. Furthermore, the detailed glycopeptide antennary analysis (Figure 2-4B) based on glycopeptide spectra match (PSM) revealed a similar wider distribution of glycan types in the IA medium. While the EX medium tended to produce predominantly tetra-antennary N-glycans on the 1st, 2nd, and 3rd sites, CHO cells in IA cell culture produced more bi and tri-antennary structures in addition to the tetra-antennary features at those

same three sites. We also summarized the total N-glycan types identified on the 4 N-sites of EPO-Fc protein, which also revealed that more tetra-branched and fewer tri- and bi-branched glycan types were detected at both Day 5 and Day 8 in EX culture medium than those obtained in IA culture medium (Supplemental Figure S2-5). Interestingly, O-glycopeptide analysis revealed that both media produced highest relative amount of structures containing GalNAc-Gal, GalNAc-Gal-SA and GalNAc-Gal-SA_2 (N1H1F0S0G0, N1H1F0S1G0, N1H1F0S2G0) but the other structures varied somewhat in the two media compositions. Collectively, our results indicate that IA medium produced more diverse N-glycopeptide profile while the EPO-Fc from EX medium tended to contain more tetra-antennary N-glycans. Previous studies by commercial vendors has indicated that the two media will produce different growth and glycan profiles for recombinant proteins generated from CHO cells, and CHO cells grown in the IA medium may produce a less complex glycosylation product than that in EX medium (personal conversation with Dr. Frank Swartzwelder from Millipore-Sigma). Moreover, it is also worthwhile to note that the cell growth is enhanced in IA medium culture with higher cell densities, which may lead to less complete glycan modifications perhaps due to differing allocation of resources or protein transport rates through the Golgi apparatus.

While Neu5Ac is the predominant sialylation type for recombinant glycoproteins in CHO cells, we still detected low amounts of Neu5Gc in all tested samples (Figure 2-5). Neu5Gc, as a side-product in CHO cell culture, should be limited in the final drug product if possible. Interestingly, from our intact glycopeptide analysis, the Neu5Gc amount increased significantly at later times (Day 8) compared with that in the earlier growth phase (Day 5) in both EX and IA media for EPO-Fc cell culture (Figure 2-5C). After CMP-Neu5Ac is synthesized and released from nucleus into the cytosol, CMP-Neu5Ac can be converted into CMP-Neu5Gc with the assistance of CMAH

enzyme [208]. Then both CMP-Neu5Ac and CMP-Neu5Gc in the cytosol will be transported to the Golgi by the same transporter SLC35A1 and involved in the protein glycosylation process [208]. The activity and availability of CMAH enzyme directly affect the incorporation of Neu5Gc into glycoproteins [209]. We propose that the prolonged cell culture time may serve to change CMAH and NADH (a cofactor for CMAH) levels in CHO cells and as a result, the distribution of Neu5Ac and Neu5Gc metabolites intracellularly, which further impacts the Neu5Gc content on glycoproteins.

2.6 Conclusion

In conclusion, we have demonstrated a rapid glycopeptide analysis method can reveal site-specific glycan information on recombinant EPO-Fc protein secreted from CHO cells in different media compositions. Retaining glycans on the peptides enables users to simultaneously elucidate the glycan structure on the specific glycosylation sites and provide insights about how proteins are modified at different points along the polypeptide chain under different culture conditions. Using this intact glycopeptide characterization method, EX medium was revealed to produce a more complex tetra-antennary N-glycan profile than IA medium for EPO-Fc cell cultures. For N-glycosylation analysis, the sialylation content decreased with increasing N-glycan sites of EPO-Fc, which is opposite to the trend of fucosylation content at these same 4 N-glycan sites and consistent with the known profiles of the individual structural regions of the composite protein. EPO N-glycans from EPO-Fc protein presented bi-, tri- and tetra-branched glycans structures with various sialylation and fucosylation levels at each sites, while Fc N-glycan displayed mostly fully fucosylated, unsialylated bi-antennary glycans. O-glycan profiles indicated a predominance of the 3 major structures in both the EX and IA media and lesser amounts of other glycans. In total, intact glycopeptide characterization may become increasingly important as an analytical tool for

biopharmaceutical manufacturing by producing protein therapeutics with well-defined physical properties.

Contributions from collaborators:

Dr. Ganglong Yang and Weiming Yang in Dr. Hui Zhang's lab assisted with experiment design and data analysis generated from LC-MS/MS glycopeptide data.

This research was supported by Advanced Mammalian Biomanufacturing Innovation Center (AMBIC), which is an Industry–University Cooperative Research Center Program under U.S. National Science Foundation (grant no. 1624684) and the National Science Foundation (grant no. CBET-1512265). I would like to acknowledge the support and contributions of Dr. Frank Swartzwelder and other AMBIC mentors as part of this effort. One of the industrial members of AMBIC is Millipore-Sigma, which provided media that was used in this study.

Figures and Tables

Figure 2-1. Illustration of intact glycopeptide characterization method applied in this work.

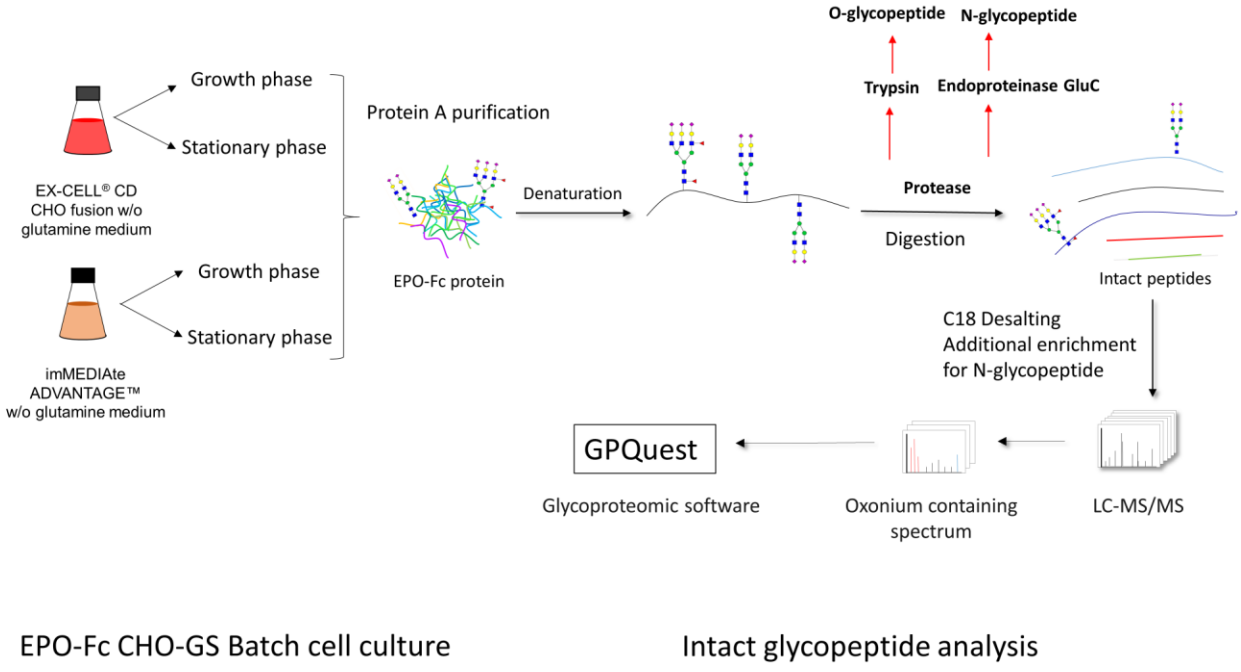

Figure 2-2. Growth study of EPO-Fc CHO-GS cells in EX-CELL (EX) and imMEDIAte ADVANTAGE (IA) media (left and right panels, respectively). (2-2A) The viable cell density (VCD) of EPO-Fc cells; (2-2B) The viability of EPO-Fc cells; (2-2C) The lactate level in the culture media (2-2D) The glucose level in the culture media. Please note that the EPO-Fc cell density declined on Day 8 in EX-CELL medium cell culture but the viability remained more than 90%, so we still recognized Day 8 as the stationary phase in the cell growth cycle.

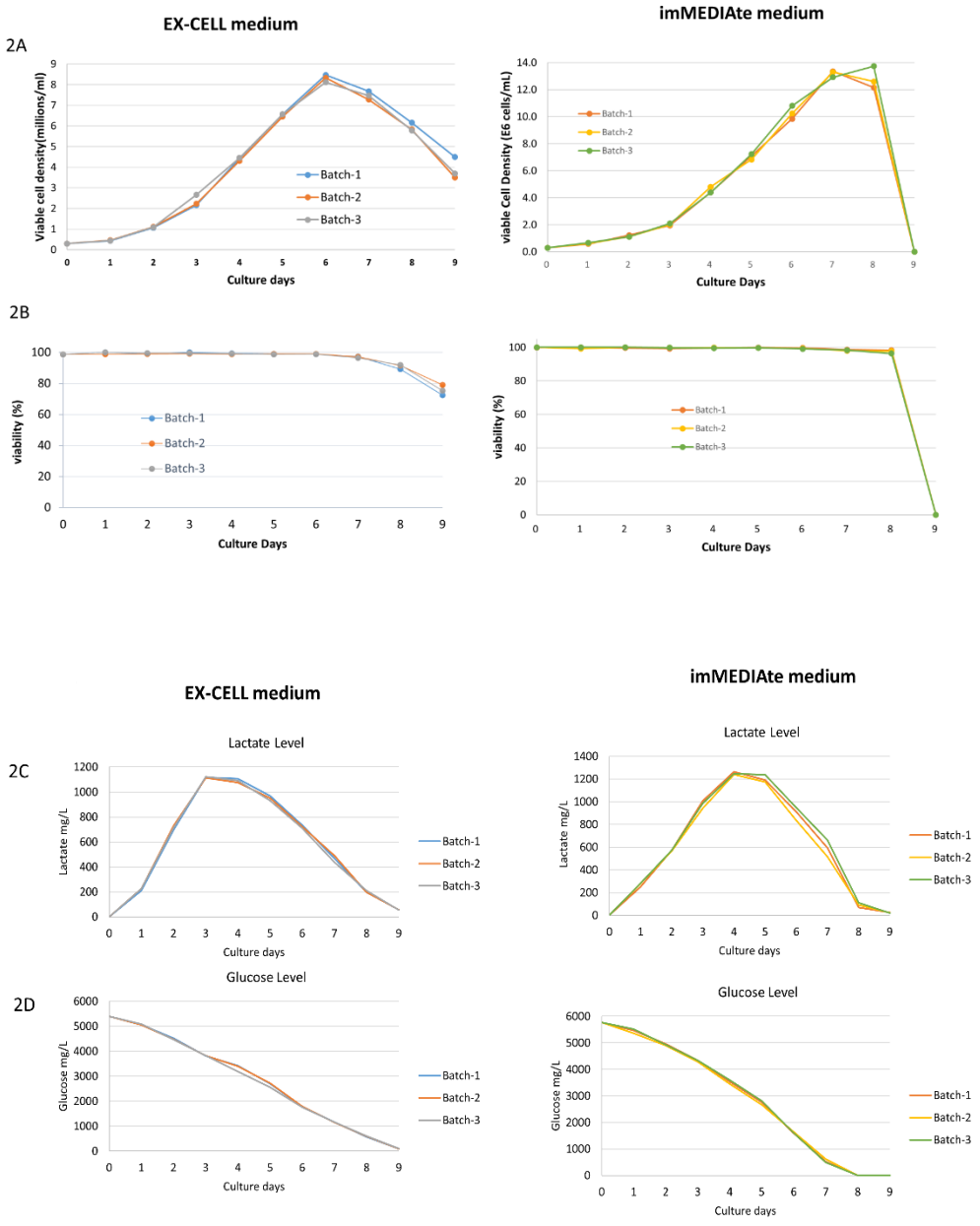

Figure 2-3 The application of MAX column for N-glycopeptide enrichment. (3A) the workflow of MAX column comparison study, (3B) The EPO-Fc fucosylation and sialylation content before and after MAX column enrichment, (3C) The EPO-Fc N-glycan branch distribution before and after MAX enrichment. The p-values for high-mannose, bi-, tri and tetra-antennary glycan types before and after MAX column enrichment is 0.5, 0.12, 0.35, and 0.32 respectively.

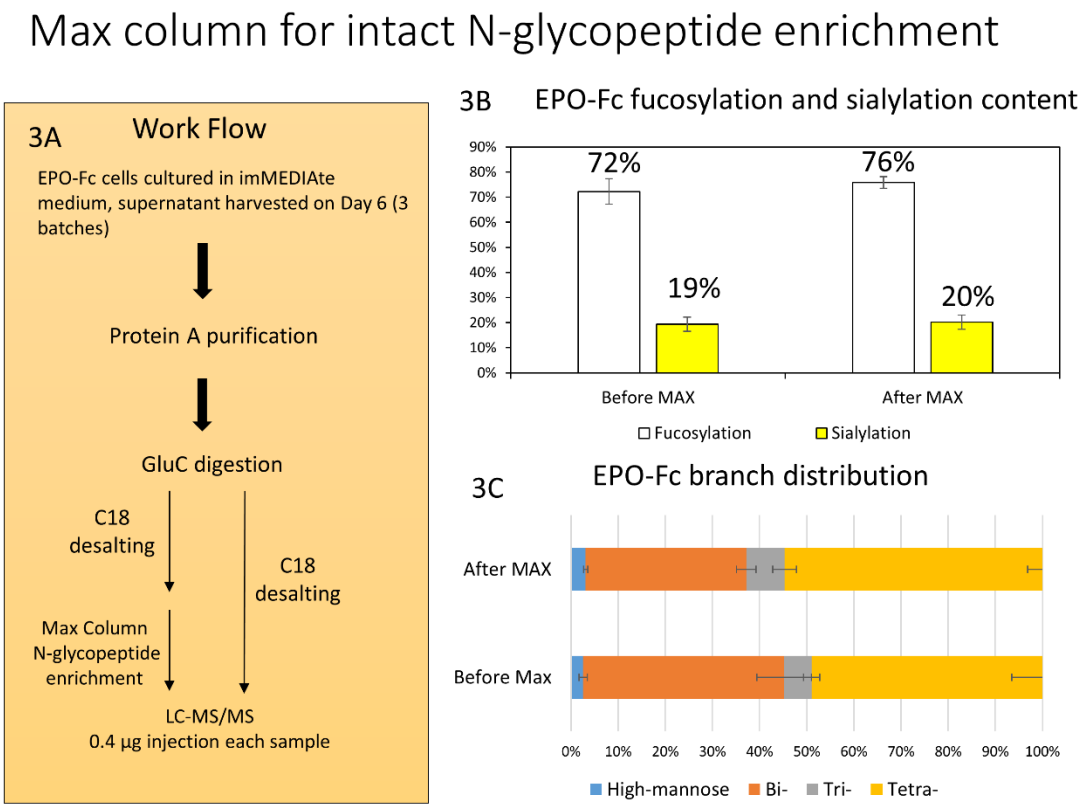

Figure 2-4.(2-4A) Coomassie blue staining result of purified EPO-Fc protein from both exponential and stationary phases in EX and IA media culture respectively. Equal amount of purified EPO-Fc protein were loaded. (2-4B)The site-specific N-glycan antennary analysis of EPO-Fc protein. CHO-GS EPO-Fc expressing cells were cultured in EX and IA media individually and harvested at both exponential and stationary phases.

2-4A

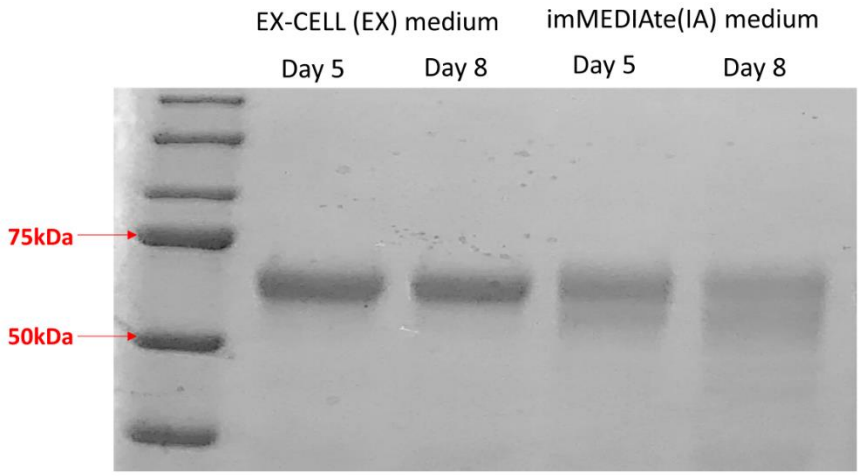

2-4B

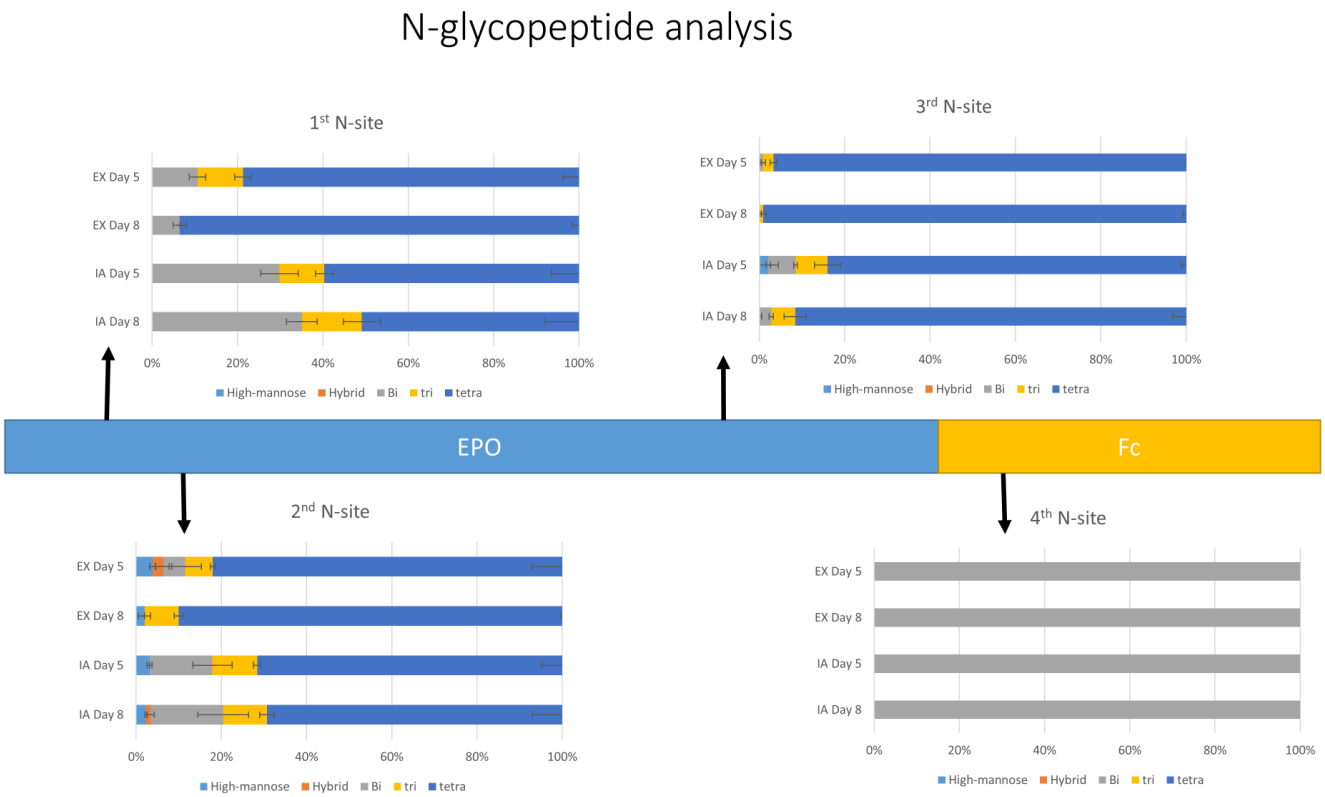

Figure 2-5. The N-glycan sialylation analysis of EPO-Fc protein. (2-5A) and (2-5C) The overall Neu5Ac and Neu5Gc content with 4 N-sites summed up together. (2-5B) and (2-5D) The site-specific Neu5Gc and Neu5Ac content.

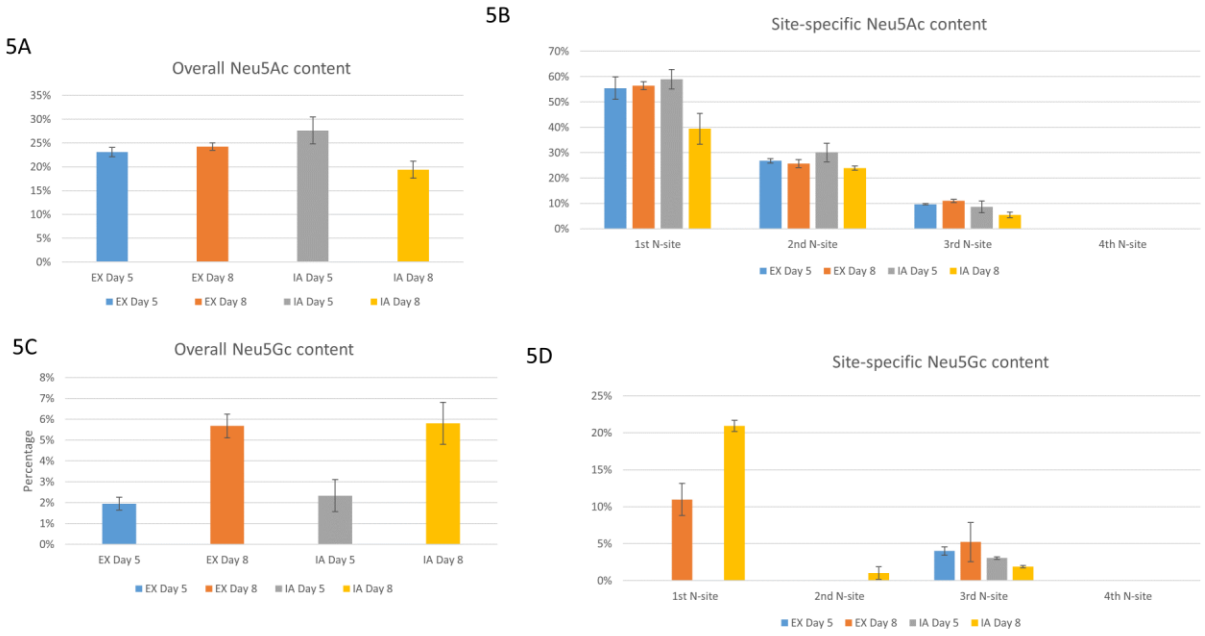

Figure 2-6. The N-glycan fucosylation analysis of EPO-Fc protein. (2-6A) the overall fucosylation content of EPO-Fc protein with 4 N-sites summed up together. (2-6B) the site-specific fucosylation content of EPO-Fc protein.

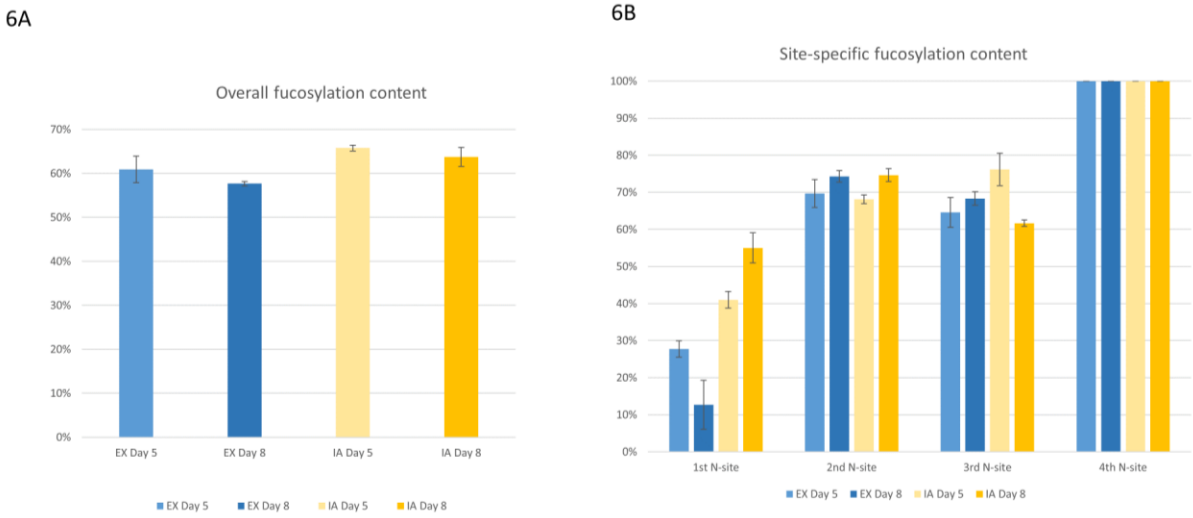

Table 2-1. The comparison of MS characterization of EPO-Fc protein with and without MAX column enrichment.

Control	Batch-1	Batch-2	Batch-3	Average	Standard deviation
Total glycopeptide (PSM)	50	53	52	51.67	1.247219
Glycan types	23	25	24	24	0.816497
Oxonium ion (m/z=204.09) intensity (glycan signal ion)	3.99E6	3.42E6	3.63E6		
Max column	**Batch-1**	**Batch-2**	**Batch-3**	**Average**	**Standard deviation**
Total glycopeptide (PSM)	92	83	81	85.33	4.784233
Glycan types	32	31	30	31	0.816497
Oxonium ion (m/z=204.09) intensity (glycan signal ion)	2.48E7	1.31E7	1.17E7		

Table 2-2, The O-glycan analysis of EPO-Fc protein using O-glycopeptide characterization method.

	O-glycan types	EX-Day5	EX-Day8	IA-Day5	IA-Day8
	N1H0F0S0G0	0%	7%	0%	0%
	N1H1F0S0G0	20%	25%	21%	24%
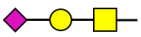	N1H1F0S1G0	46%	50%	57%	48%
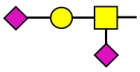	N1H1F0S2G0	26%	10%	15%	26%
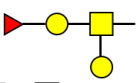	N1H2F1S0G0	2%	0%	2%	0%
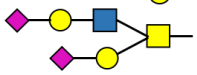	N2H2F0S2G0	2%	0%	0%	0%
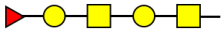	N2H2F1S0G0	2%	5%	4%	2%
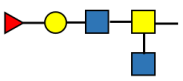	N3H1F1S0G0	2%	2%	0%	0%

Supplemental Figure S2-1. The workflow of experiments in this work.

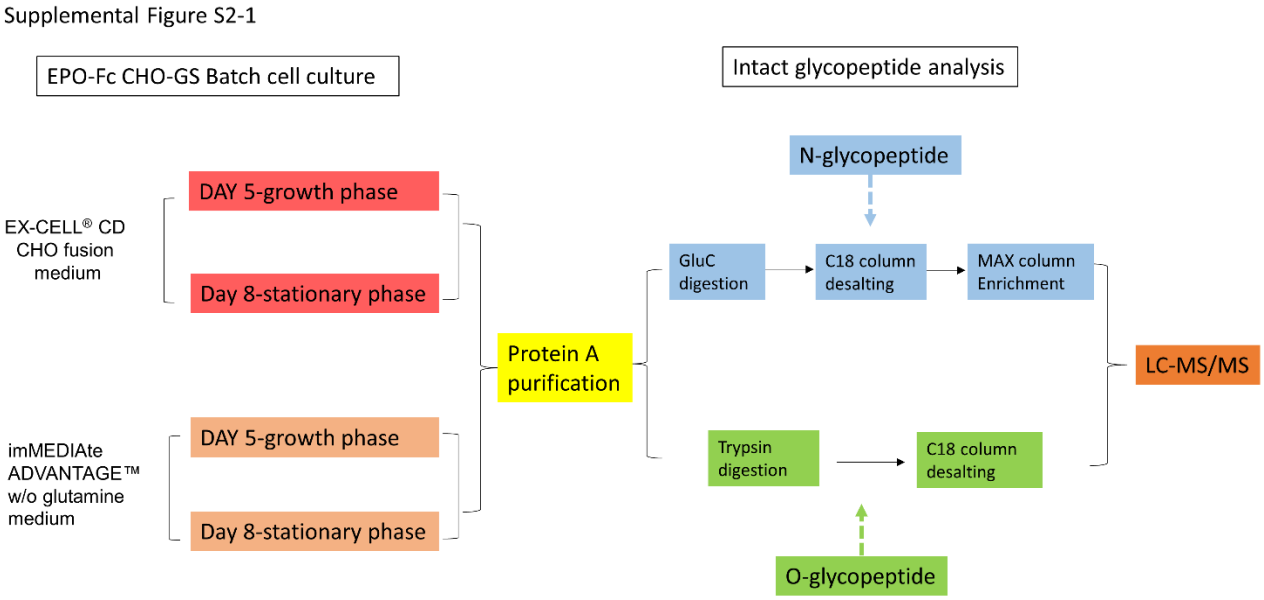

Supplemental Figure S2-2. Representative MS/MS spectra of the identified N- and O-glycopetides in EPO-Fc protein. For example, in Figure S2-2A, Spectral title: AKEAENITTGCAE + N4H5F3S0G0/3. Glycopeptide sequence: AKEAENITTGCAE; N-glycan: N4H5F3S0G0 (N: HexNAc, H: Hex, F: Fuc, S: Neu5Ac, G: Neu5Gc); Charge: 3. The same labeling works for For (S2-2B)-(S2-2E). Upper figure: highlight only oxonium ions in yellow; Lower figure: after removing oxonium ions, highlghts b-, y-, peptide- and peptide-glyan(Y1) fragment ions.

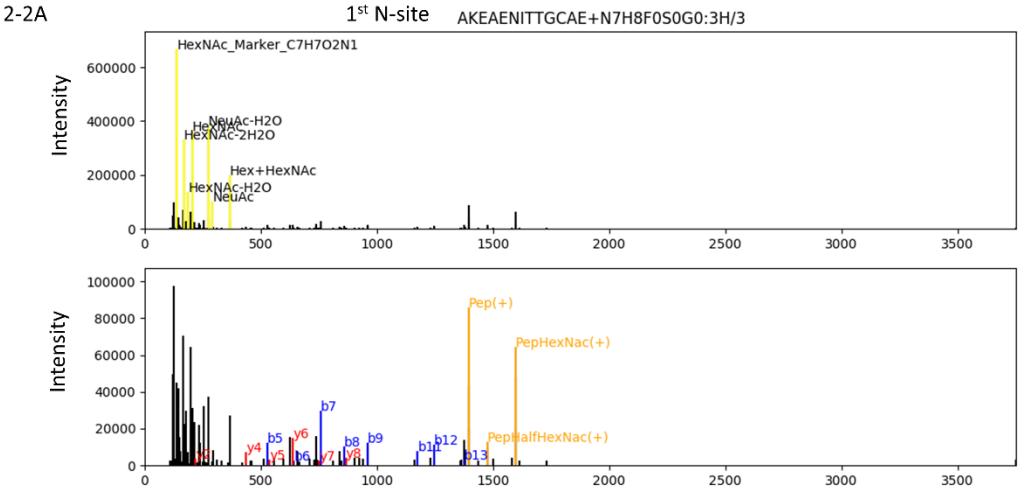

2-2B

2nd N-site HCSLNENITVPDTKVNFYAWKRME+N5H6F1S2G0:5H/5

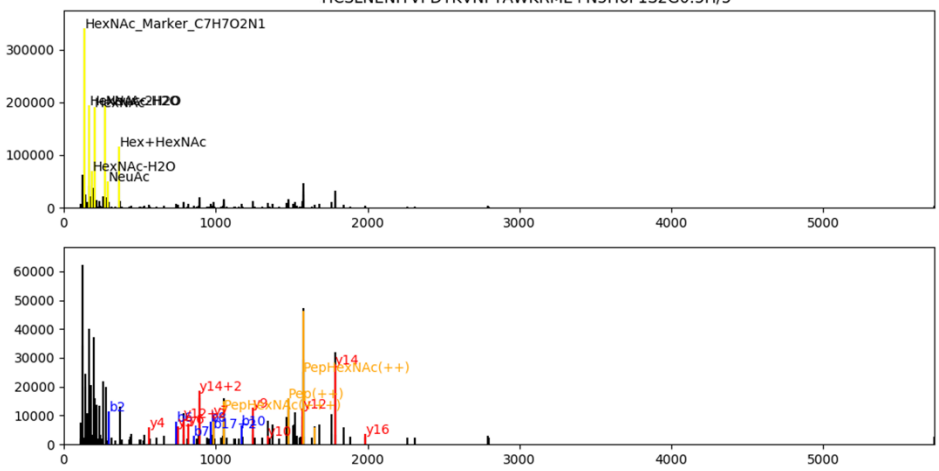

2-2C

3rd N-site AVLRGQALLVNSSQPWEPLQLHVDKAVSGLRSLTTLLRALGAQKE+N8H8F0S0G0:7H/7

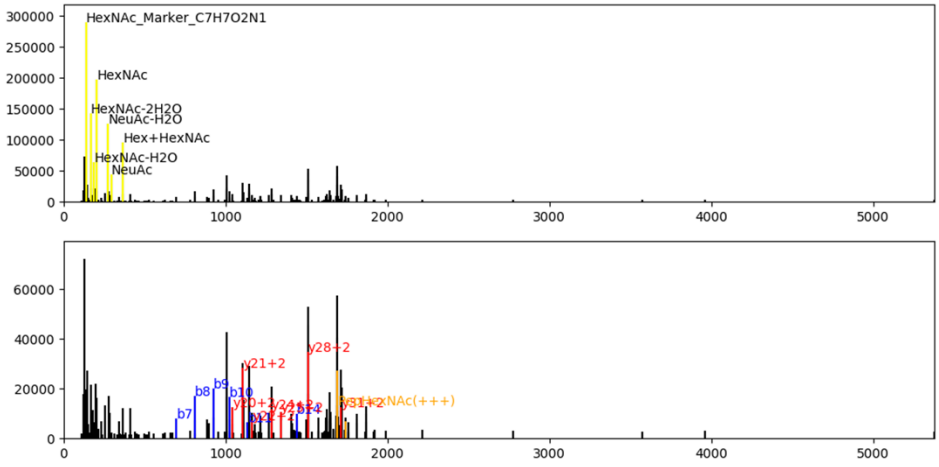

2-2D

4th N-site QYNSTYRVVSVLTVLHQDWLNGKE+N4H3F1S0G0:4H/4

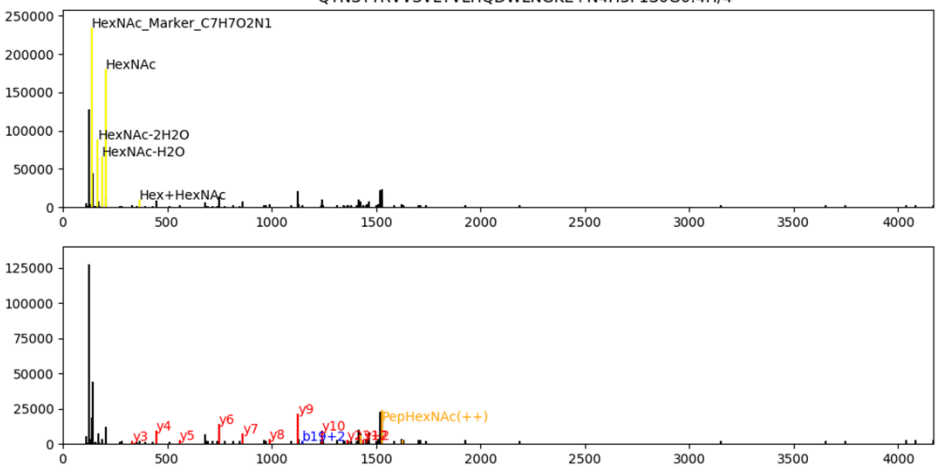

2-2E

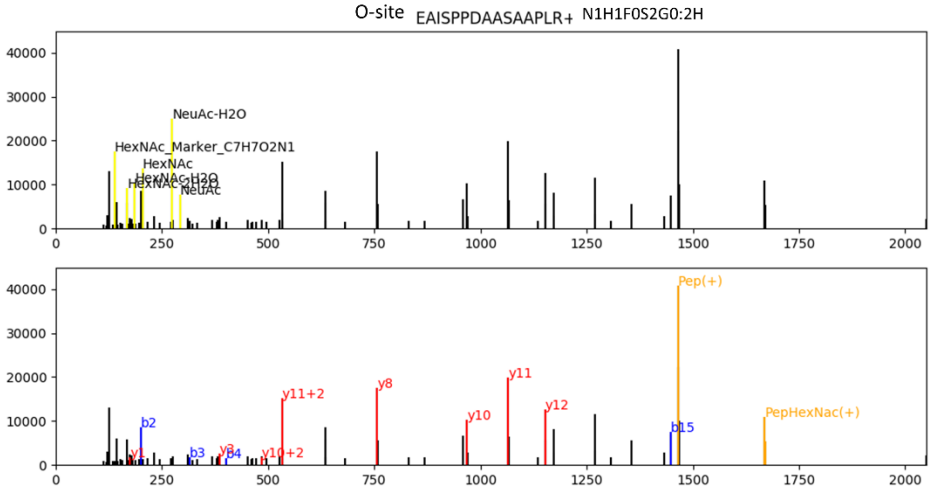
O-site EAISPPDAASAAPLR+ N1H1F0S2G0:2H
NeuAc-H2O
HexNAc_Marker_C7H7O2N1
HexNAc
HexNAc-H2O
NeuAc
Pep(+)
y11+2
y8
y11
y10
y12
b2
b15
PepHexNac(+)
y1
b3
y3
b4
y10+2

2-2F

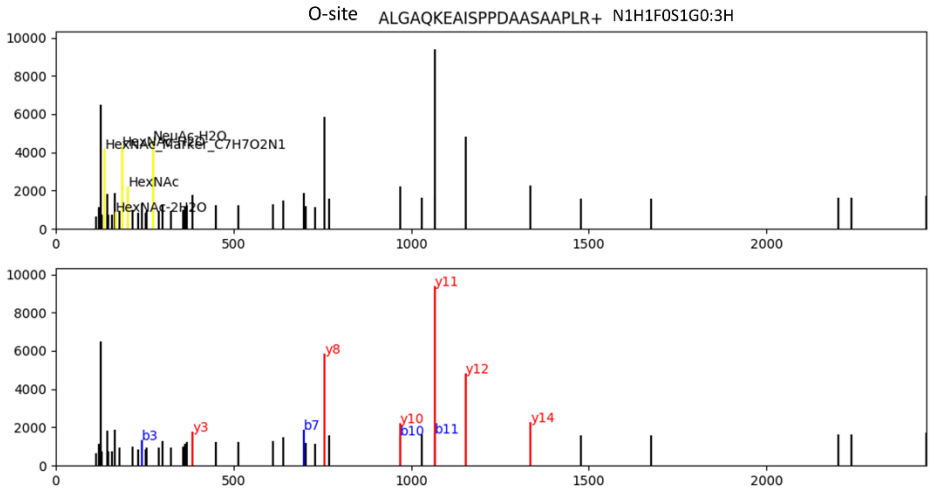
O-site ALGAQKEAISPPDAASAAPLR+ N1H1F0S1G0:3H
NeuAc-H2O
HexNAc_Marker_C7H7O2N1
HexNAc
HexNAc-2H2O
y11
y8
y12
y14
b3
y3
b7
y10
b10
b11

Supplemental Figure S2-3. (S2-3A) The abundance of EPO-Fc protein in the supernatant per day in the growth study. 40ul supernatant sample was loaded each well. 2ug purified EPO-Fc protein from EX-CELL medium on Day 6 cell culture were collected and used as positive control. (S2-3B) Anti-EPO and Anti-IgG immunoblots for detection of EPO-Fc protein in the daily supernatant in the EX-CELL and imMEDIAte media growth studies individually. 15ul supernatant was loaded each well. 500 ng purified EPO-Fc protein from EX-CELL medium on Day 6 cell culture were collected and used as positive control.

2-3A

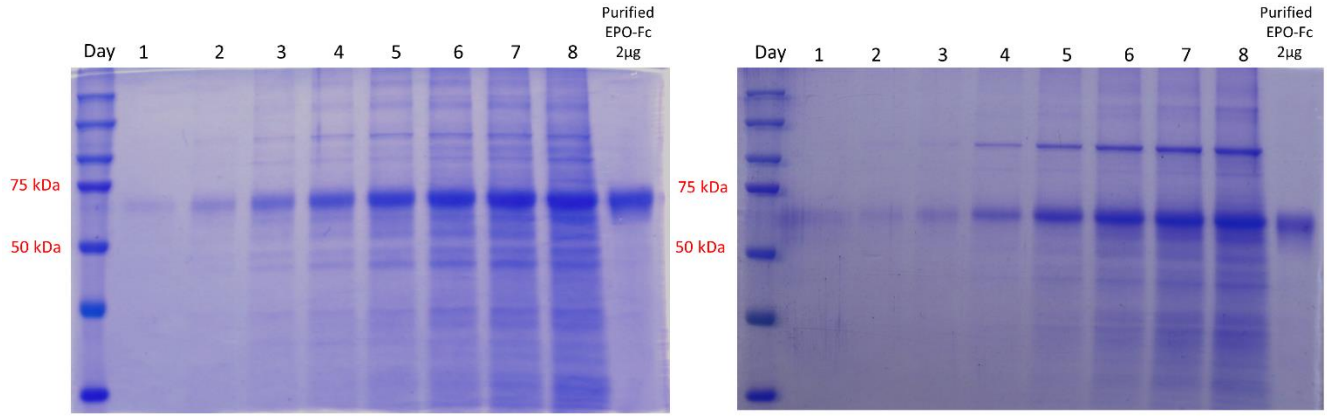

EX-CELL medium **imMEDIAte medium**

2-3B

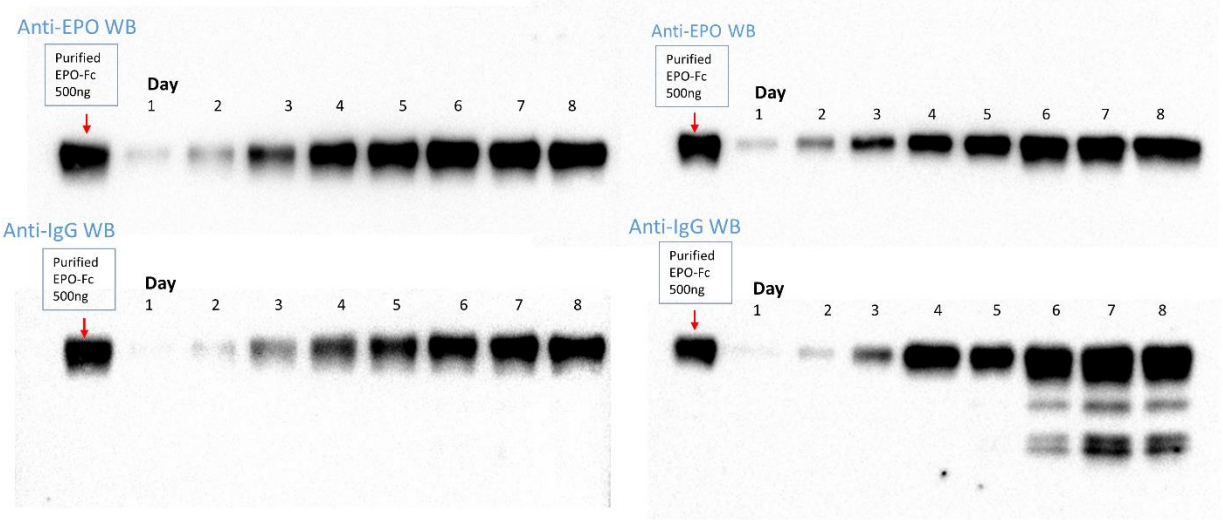

EX-CELL medium **imMEDIAte medium**

Supplemental Figure S2-4, The site-specific Neu5Ac sialylation distribution of EPO-Fc protein. S1: glycans with one sialic acid, S2: glycans with two sialic acids, S3: glycans with three sialic acids, S4: glycans with 4 sialic acids. NITT, NIST and NSS are the amino acids at 1st, 2nd, and 3rd N-glycan sites. At the 4th N-glycan site (Fc N-site), no sialylation has been detected.

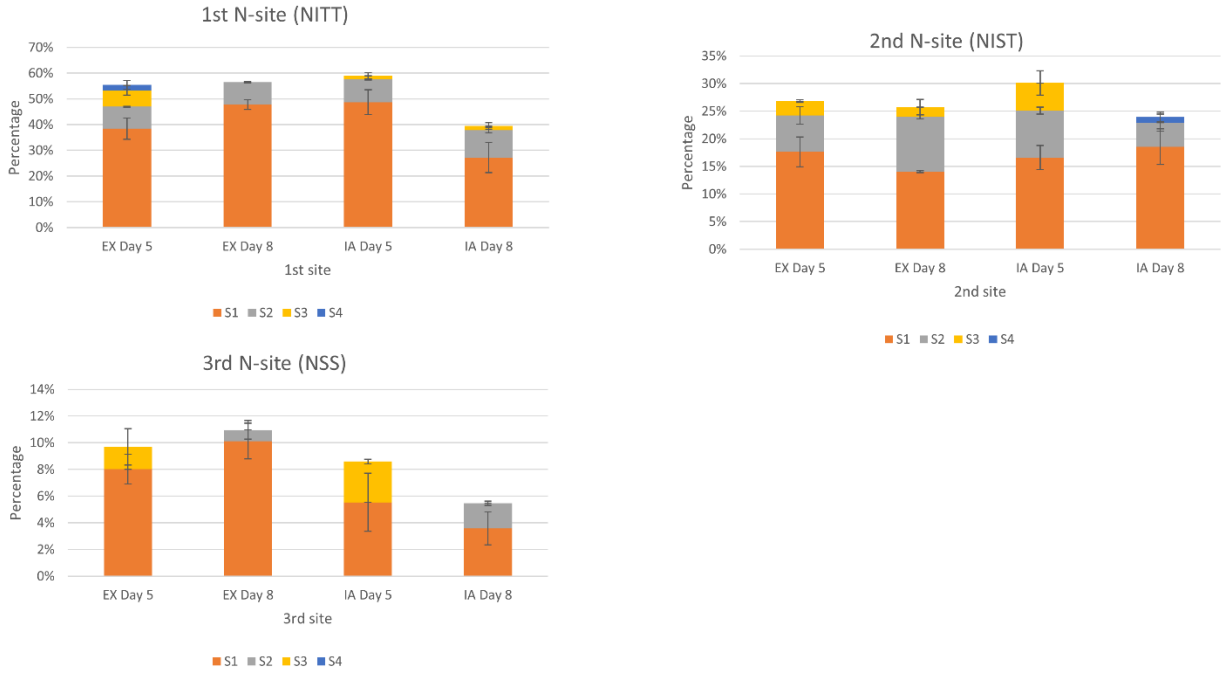

Supplemental Figure S2-5. The N-glycan types analysis of EPO-Fc protein using intact glycopeptide characterization. (S2-5A). The number of N-glycan types identified from each sample. The total glycan types were summarized from two biological runs. (S2-5B) The branch

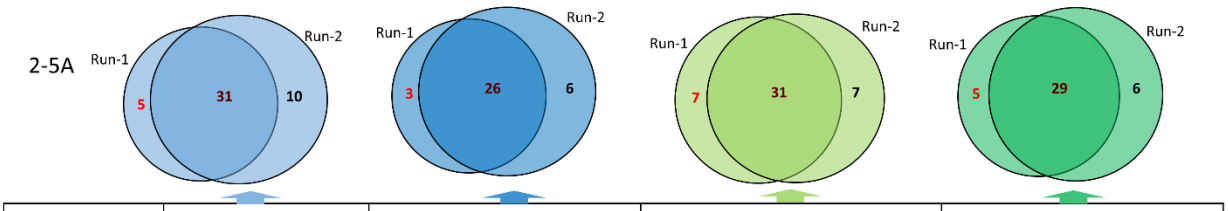

	EX medium Day 5	EX medium Day 5	IA medium Day 5	IA medium Day 8
Total glycan types	46	35	45	40

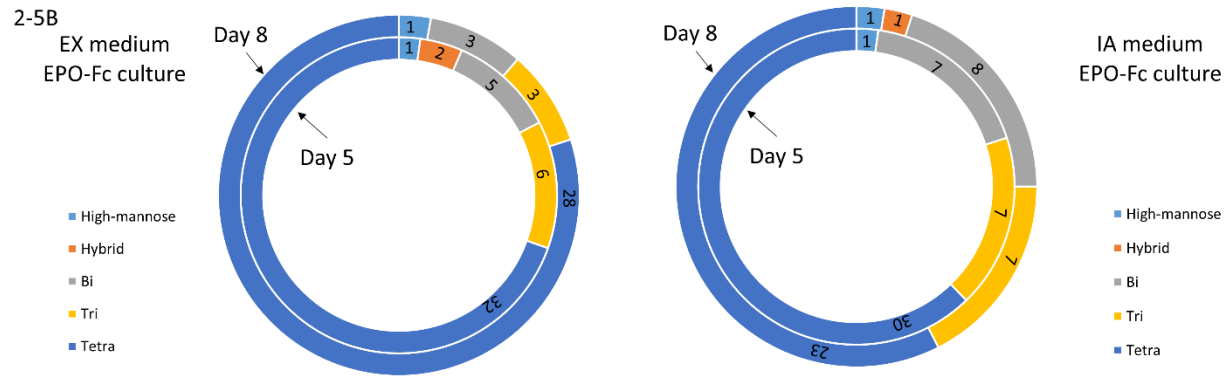

distribution of glycan types of EPO-Fc protein cultured in EX and IA media harvested at growth (Day 5) and stationary (Day 8) phases.

Chapter 3 Comprehensive exploration of the effect of 1,3,4-O-Bu_3ManNAc as a novel sugar supplement on the quality and production of recombinant proteins

3.1 Summary

A desirable feature of many therapeutic glycoprotein production processes is to maximize the final sialic acid content. In the first part of this chapter, the effect of applying a novel chemical analog of the sialic acid precursor N-acetylmannosamine (ManNAc) on the sialic acid content of cellular proteins and a model recombinant glycoprotein, erythropoietin (EPO), was investigated in CHO-K1 cells. By introducing the 1,3,4-O-Bu_3ManNAc analog at 200-300 μM into cell culture media, the intracellular sialic acid content of EPO-expressing cells increased ~8 fold over untreated controls while the level of cellular sialylated glycoconjugates increased significantly as well. Moreover, addition of 200-300 μM 1,3,4-O-Bu_3ManNAc resulted in >40% increase in final sialic acid content of recombinant EPO, while feeding of ManNAc at almost 100 times higher concentration of 20mM concentration produced a less profound change in EPO sialylation. In the second part of this chapter, we also examined an alternative chemical additive, 1,3,4-*O*-Bu_3ManNAc, for its effect on recombinant protein production in CHO. Supplementation with 1,3,4-*O*-Bu_3ManNAc for two stable CHO cell lines, expressing human erythropoietin or IgG, enhanced protein expression for both products with negligible impact on cell growth, viability, glucose utilization, and lactate accumulation. In contrast, the chemical additive sodium butyrate (NaBu) has been applied in cell culture media as a direct and convenient method to increase the protein expression in Chinese hamster ovary (CHO) and other mammalian cells. Sodium butyrate treatment resulted in a ~20 % decrease in maximal viable cell density and ~30 %

decrease in cell viability at the end of cell cultures compared to untreated or 1,3,4-*O*-Bu_3ManNAc treated CHO cell lines for both products. While NaBu treatment enhanced product yields more than the 1,3,4-*O*-Bu_3ManNAc treatment, the NaBu treated cells also exhibited higher levels of caspase 3 positive cells using microscopy analysis. Furthermore, the mRNA levels of 4 cell apoptosis genes (Cul2, BAK, BAX and BCL2L11) was up-regulated more in sodium butyrate treated wild-type, erythropoietin or IgG expressing CHO-K1 cell lines while most of the mRNA levels of apoptosis genes in 1,3,4-*O*-Bu_3ManNAc treated cell lines remained equal or increased only slightly compared to the levels in untreated CHO cell lines. In the last part of this chapter, we compared NaBu and 1,3,4-*O*-Bu_3ManNAc on their effects on the glycan quality of recombinant proteins. The beneficial impact of 1,3,4-O-Bu_3ManNAc on EPO glycan quality, while evident in wild-type CHO cells, was particularly pronounced in glycoengineered CHO cells with stable H Supplementation of 1,3,4-O-Bu_3ManNAc achieved approximately 30% sialylation enhancement on EPO protein in wild-type CHO cells. Overexpression of GnTIV/GnTV/ST6 in CHO cells increased EPO sialylation about 40%. Combining 1,3,4-O-Bu_3ManNAc treatment in glyocengineered CHO cells promoted EPO sialylation about 75% relative to EPO from wild-type CHO cells. Moreover, a detailed mass spectrometric ESI-LC-MS/MS characterization of glycans at each of the three N-glycosylation sites of EPO showed that the 1st N-site was highly sialylated and either the negative impact of NaBu or the beneficial effect 1,3,4-O-Bu_3ManNAc treatments mainly affects the 2nd and 3rd N-glycan sites of EPO protein. In summary, these results indicate inclusion of butyrate-derivatized side chains on ManNAc likely improves the capacity of cells to uptake the analog and incorporate exogenous ManNAc into recombinant glycoproteins such as EPO. This study establishes 1,3,4-O-Bu_3ManNAc as a novel chemical supplement to improve glycoprotein quality and sialylation

levels at concentrations orders of magnitude lower than alternative approaches. These findings also demonstrate that 1,3,4-*O*-Bu_3ManNAc has fewer negative effect on cell cytotoxicity and apoptosis, perhaps as a result of a more deliberate uptake and release of the butyrate compounds, while simultaneously increasing the expression of multiple recombinant proteins and improving the glycosylation characteristics when applied at comparable molarity levels to NaBu. Thus, 1,3,4-*O*-Bu_3ManNAc represents a highly promising media additive alternative in cell culture for improving protein yields without sacrificing cell mass and product quality in future bioproduction processes. Moreover, 1,3,4-O-Bu_3ManNAc can compensate for the negative effect of NaBu on EPO glycan quality while simultaneously enhancing recombinant protein yields. In this way, a platform that integrates glycoengineering with metabolic supplementation can result in synergistic improvements in both production and glycosylation in CHO cells.

3.2 Introduction

Protein glycosylation is a critical quality attribute in biopharmaceutical manufacturing. The glycosylation patterns of recombinant proteins directly affect these drugs' clinical efficacy and safety by modulating their stability, biological activity, circulatory half-life, and pharmacokinetics (PK) [210] [211]. Numerous strategies have been investigated to control the glycan profiles of recombinant proteins including glycoengineering on the glycosylation pathways and metabolite supplementation to the culture media. Glycoengineering involves the modulation of glycogene expression in CHO cells, which includes overexpression of sialyltransferases to enhance terminal sialylation and N-acetylglucosaminyltransferases to improve branching [43, 52] [212]. Chemical supplementation of the culture media provides a convenient way to tailor the glycosylation profiles of recombinant proteins. For example, the addition of 20 to 40 mM N-acetylmannosamine (ManNAc) to culture medium improved

sialylation of recombinant interferon-□ and EPO produced in CHO cells by ~20% [50]. A desirable feature of many therapeutic glycoprotein production processes is to maximize the final sialic acid content. One way to improve sialylation is feeding to the media of nucleotide sugar precursors such as the widely utilized substrate, N-acetylmannosamine (ManNAc), an intermediate metabolite along the sialic acid pathway as shown in Figure 3-1 [213, 214]. Our group as well as other groups detected no significant difference on protein expression level between ManNAc treated and non-treated cells [50].

Another major goal of the biomanufacturing industry is to improve the productivity of mammalian cell cultures, especially Chinese hamster ovary (CHO) cells. To meet this goal, multiple strategies have been implemented to increase therapeutic protein production in CHO cells, including host cell engineering [215, 216], expression vector engineering [217], and culture medium optimization[218-221]. One approach is addition of small chemical molecules including glycerol [222], DMSO [223, 224] and sodium butyrate [225, 226]. Among these strategies, chemical supplementation, sometimes using sodium butyrate (NaBu)- a known yield enhancer, has been considered as a most convenient way to increase protein production. Sodium butyrate, a short chain fatty acid, was originally identified as a product of anaerobic bacterial fermentation. The impact and molecular mechanisms of sodium butyrate on recombinant protein expression have been evaluated in several studies [227, 228]. Sodium butyrate regulates gene expression by inhibiting cell proliferation in cell cultures. As a result of sodium butyrate treatment, the expression of several genes involved in the cell cycle is changed, which inhibits or halts cell growth [227, 228]. Inhibition of histone deacetylase (HDAC) is another of the consequences of sodium butyrate activation of gene expression in cell culture. Due to the resulting hyperacetylated histones, the relaxed chromatin complexes are more readily

accessed by regulatory factors and thus can be more efficiently transcribed [229]. Because of its positive effects on protein expression in mammalian cell culture, sodium butyrate has been extensively used to achieve the high-level production of several recombinant therapeutic proteins in CHO cells such as antibodies and other pharmaceutical proteins (erythropoietin, factor VIII, α-interferon, interleukin-2, and human follicle stimulating hormone) [225, 230-234]. However, the beneficial effects of sodium butyrate on protein expression comes with some potentially compromising side-effects, one of which is the induction of apoptosis. In addition, the presence of sodium butyrate can have additional potentially problematic effects, either directly or indirectly due to its cytotoxicity, on glycosylation processing and especially sialylation [226, 235, 236]. More recently, we developed and applied butyrated alternatives to ManNAc, including 1,3,4-O-Bu_3ManNAc, as a "high-flux" precursor for increasing sialic acid production at much lower concentrations compared to natural ManNAc [5, 237]. Given the expression-enhancing effect of sodium butyrate on proteins, including butyrate "delivered" through ester-conjugation to ManNAc [238], we wanted to examine if 1,3,4-O-Bu_3ManNAc exhibited any effects on recombinant protein production and cell growth in Chinese hamster ovary (CHO) cells as well.

On the other side, considering the unsatisfactory impact of NaBu on the glycosylation quality of recombinant proteins, especially with respect to sialylation, we propose supplying butyrate to cells using the analog 1,3,4-O-Bu_3ManNAc, which is composed of a core ManNAc moiety linked to three butyrate groups (Figure 3-1B). 1,3,4-O-Bu_3ManNAc has several key features that make it attractive for cell culture supplementation. First, the regioisomeric placement of the three butyrate groups at the 1, 3, and 4 positions of the core monosaccharide avoids cytotoxicity associated with fully acylated hexosamines [239] [240] [241]. After efficiently entering cells, a

process assisted by the lipophilic butyrate groups that facilitate diffusion of the hydrophilic core monosaccharide through the plasma membrane, 1,3,4-O-Bu_3ManNAc is disassembled into three equivalents of butyrate and one equivalent of ManNAc by non-specific esterase activity [242] [243]. 1,3,4-O-Bu_3ManNAc has been reported to increase the sialylation of endogenous proteins in different cell types including Jurkat (lymphoma) cells, human breast cancer cells, SW1990 pancreatic cancer cells, and CHO-K1 cells [244] [245]. These previous studies focused on characterizing sialylation. Alternatively, given the wide use of NaBu as a supplement in mammalian cell culture, the comparison of 1,3,4-O-Bu_3ManNAc and NaBu on recombinant protein production and quality would be of interest to biotechnologists.

In the past, glycoengineering strategies and chemical supplementations typically have been pursued independently to tailor the glycan profiles of recombinant proteins, leaving the combined benefits of these two approaches largely untested. In this study we fill this void by combining metabolic supplementation with glycoengineering in CHO cells, as illustrated in Figure 3-1C. The glycoengineered CHO cell line was developed by overexpression of human β-1,4-N-acetylglucosaminyltransferase (GnTIV), human β-1,6-N- acetylglucosaminyltransferase (GnTV) and human α-2,6-sialyltransferase (ST6) in wild-type EPO-expressing CHO cells [246]. In comparison with EPO from wild-type CHO cells (wt-EPO), the EPO from glycoengineered CHO cells (which we refer to as "glycoengineered-EPO") has higher levels of sialylation and increased display of highly branched (tri- and tetra-antennaries) N-glycans. Recombinant EPO combined with these CHO systems provides an ideal test platform to compare the influence of NaBu and 1,3,4-O-Bu_3ManNAc on the glycan quality of recombinant proteins. In tandem, given the abundance and importance of EPO N-glycan, we employed intact glycopeptide analysis using mass spectrometry (MS) to decipher the site-specific N-glycan microheterogeneity of wt-

EPO and glycoengineered-EPO proteins treated with 1,3,4-O-Bu_3ManNAc or NaBu at equivalent butyrate concentrations.

3.3 Materials and Methods

3.3.1 Cell lines and cultures

Wild-type CHO-K1 cells were purchased from Sigma-Aldrich (European Collection of Cell Culture, ECACC). The CHO-K1 with human erythropoietin (EPO) expressing cell line was established previously as described in Yin et al [5]. The establishment of recombinant wild-type human EPO and recombinant glycoengineered human EPO cell lines was previously described in Yin et al [246]. Briefly, human EPO cDNA was fused with a 6x His tag at its C terminus and codon-optimized for expression in CHO cells. Wild-type and glycoengineered CHO lines that expressed human EPO were cultured in conditions widely used for CHO-K1 cell culture, except that Zeocin (300 □g/ml) was added to the wild-type cell cultures to maintain EPO gene expression and Zeocin (300 □g/ml), hygromycin (200 □g/ml), and blasticidin (8.0 □g/ml) were added to the glycoengineered-EPO cell cultures to maintain expression of the recombinant glycogenes (i.e., GnTIV, GnTV, and ST6, respectively) [246]. Plasmids contained grass pollen Phlp7 IgG1 sequences were from Dr. Beavil's lab and obtained from Addgene [247]. Then the IgG1 sequences were subcloned into a mammalian expression vector pBudCE4.1 (Thermo Fisher Scientific). Ham's F12-K medium (Thermo Fisher Scientific) supplemented with 10 % (v/v) fetal bovine serum (FBS, Gibco) was used for CHO cell growth in a humidified atmosphere containing 5% CO2 at 37 ℃. Zeocin (300 μg/ml) was added to both EPO and IgG expressing cell line individually to maintain stable expression.

Human EPO and IgG-expressing cell lines were seeded at the cell density 0.2×106 cells/ml to determine the cell growth curve and metabolite changes. Samples were collected every 12 h. Cell

number was counted using a hemocytometer and metabolites measure using a YSI 2700 D dual-channel select biochemistry analyzer (YSI Life Sciences). Viable cells were distinguished from dead cells using trypan blue (Thermo Fisher Scientific) stain.

3.3.2 Treatment of cultures with Bu_3ManNAc and ManNAc

Sodium butyrate (≥ 98.5 purity GC) was purchased from Sigma-Aldrich. 1,3,4-O-Bu_3ManNAc was synthesized as previously described [240]. NaBu was dissolved in sterile water and 1,3,4-O-Bu_3ManNAc was dissolved in ethanol. Appropriate amounts of NaBu solution and 1,3,4-O-Bu_3ManNAc solution were added in F-12K media with 10% FBS individually to achieve the final concentrations of 1.0 mM NaBu or 0.333 mM 1,3,4-O-Bu_3ManNAc in the culture media (these concentrations were selected to provide the same molar equivalents of butyrate and were used throughout this study based on previous optimization). In certain experiments, recombinant EPO cells were seeded and cultured in F12-K media with chemical supplements for two-day incubation. The cells then were collected and counted for intracellular sialic acid analysis. In alternate experiments, after the two-day incubation (as described) culture media was changed to serum-reduced Opti-MEM media (Thermo Fisher Scientific) with chemical supplements maintained correspondingly and the cells were incubated for an additional two days. Then culture supernatant was collected and subjected to EPO protein purification and the following analysis described below. In other experiments, CHO-K1 cells were seeded at 1×106 cells per dish in 10cm dishes in 10 ml Ham's F-12K media untreated or treated with 20mM ManNAc or various concentrations of Bu_3ManNAc (50μM, 100 μM, 150 μM, 200 μM, 250 μM, 300 μM, 350 μM). Cells were collected at confluency above 90% after 3 days. Similarly, a CHO-EPO cell line was grown in 10ml Ham's F-12K media followed by Opti-MEM (ThermoFisher) supplemented with 20mM ManNAc or Bu_3ManNAc (200 and 300 μM Bu_3ManNAc) after 3 days

in culture. Supernatants were collected after 48-hour incubation with or without treatment and then subjected to EPO purification.

3.3.3 Quantitative real-time PCR

Wild-type CHO-K1, IgG- and EPO-expressing cell lines were treated with NaBu (1 mM) or 1,3,4-O-Bu_3ManNAc (0.33 mM). The three untreated cell lines together with the treated cells were then separately harvested and homogenized using TRIzol reagent (Thermo Fisher Scientific) containing polyacryl-carrier (Molecular Research Center). RNA was extracted by phase separation and precipitated by addition of isopropanol, followed by reverse-transcription by the SuperScript III First-Strand Synthesis System (Thermo Fisher Scientific). Quantitative RT-PCR was performed with Absolute Blue SYBR Low ROX Master Mix (Thermo Fisher Scientific) in an Applied Biosystems 7500 Real-Time PCR system. Actin was used as an internal control using 2-ΔΔCt calculation. Primers for quantitative real-time PCR (qRT-PCR) were designed according to the CHO genome sequences as follows: Bcl2L11(5'-TGACACGGCGTGGTCAAGAG -3' and 5'- TCCGGAGTTGTCACTGGGC -3'), BAX (5′-AGGCCCTGTGTACCAAAGTGC -3′ and 5′- TCAGCCCATGTTCTTCCAGATCGT -3′), BAK (5'- TTTGACCGGCTTCCTGGGC -3' and 5'- AGAATCTGTGTACCACGTACTGGCC -3'), Cul2(5'- TCCAAGCTGCTATCGTCCGC -3' and 5'- ACCCACATCAGAGACGGTGTCA -3') and CHO Actin(5'- TGACCGGATGCAGAAGGAGATCA -3' and 5'-AGAAGCATTTGCGGTGGACGA TG -3').

3.3.4 Immunohistochemistry

Wild-type CHO-K1 cells were grown on glass cover slips coated with 0.1% gelatin, NaBu (1 mM) and 1,3,4-O-Bu3ManNAc (0.33 mM) treated cells were cultured for 6 days prior to immunohistochemistry. For fluorescent staining, cells were fixed for 10 min at room temperature

in 4% paraformaldehyde in PBS and incubated with Caspase-3 antibody (Cell Signaling, 1:800 dilution) followed by fluorescein isothiocyanate-conjugated donkey anti-Rabbit IgG (Thermo Fisher Scientific, 1: 400 dilution). Mounting medium with DAPI (Vector Laboratories) was added before fluorescence microscopic imaging to determine the cell nucleus.

3.3.5 EPO protein purification

The culture supernatant containing recombinant EPO protein was first filtered through a 0.22-□m-pore-size membrane to remove cell debris, and then loaded onto an affinity column packed with Ni-NTA agarose (Qiagen). After several washes of 20 mM imidazole in PBS buffer, the bound EPO was eluted with PBS buffer supplemented with 250 mM imidazole, and the EPO eluate was subsequently dialyzed against PBS buffer. The final protein concentration was measured by bicinchoninic acid (BCA) assay (Thermo Fisher Scientific). The purified EPO protein purity was assessed by 10% SDS-PAGE followed by Coomassie blue staining.

3.3.6 Immunoblots and lectin blots

For immumoblots, chemically-treated cells were lysed using RIPA buffer (Thermo Fisher Scientific) following protocols supplied by the manufacturer. After measuring protein concentrations in cell lysates, equivalent amounts from each sample were fractionated on 10% SDS-PAGE, followed by transfer to a PVDF membrane (Bio-Rad, Hercules, CA). Primary antibodies detecting GnTIV protein expression (rabbit anti-Mgat 4), and β-galactoside α-2,3-sialyltransferase 4 (ST3Gal4) protein expression (rabbit anti-ST4Gal4) were obtained from Abcam (Cambridge, MA), and β-Galactosamide α-2,6-sialyltranferase 1 (ST6) protein expression (mouse anti-ST6) was purchased from Sigma (St. Louis, MO). Horseradish peroxidase (HRP)-linked anti-mouse IgG or anti-rabbit IgG was used as secondary antibodies individually (Cell Signaling Technology, Danvers, MA), as we previously described [246]. IgG

expression was detected using horseradish peroxidase-linked goat anti-human IgG antibody (Abcam). HRP signal from the antibodies was detected by adding an enhanced chemiluminescent (ECL) substrate (Millipore).

For lectin blots, purified EPO proteins were quantified by BCA assay (Thermo Fisher Scientific) and fractioned on 10% SDS-PAGE, followed by transfer to a PVDF membrane (Bio-Rad, Hercules, CA). Membranes were blocked by Carbo-free blocking solution (Vector Labs, Burlingame, CA) and then incubated with biotinylated Sambucus nigra Lectin (SNA), or Maackia amurensis Lectin II (MAL II) individually and then continuously incubated in horseradish peroxidase-avidin (Av-HRP) (Vector Labs, Burlingame, CA), as previously described [246]. The HRP signal from either the bound antibodies or conjugated lectins was detected using Immun-Star Western Chemiluminescent Kit (Bio-Rad, Hercules, CA) on the Molecular Imager® ChemiDoc™ XRS (Bio-Rad, Hercules, CA) with Quantity One Software (Bio-Rad, Hercules, CA).

3.3.7 Anti-EPO enzyme-linked immunosorbent assay (ELISA)

To monitor EPO production, EPO present in the supernatants obtained on a daily basis from the growth study were measured by enzyme-linked immunosorbent assay (ELISA). Briefly, 5.0 □l supernatants from each sample were loaded in a 96-well plate to test biological triplicates. Subsequently, samples were coated with carbonate/bicarbonate buffer overnight at 4 °C, followed with 5% BSA blocking solution, chicken anti-EPO antibody (Thermo Fisher Scientific) and goat anti-chicken IgY antibody linked with HRP (Abcam, Cambridge, MA) were used as capture and detection antibodies, respectively. 3,3',5,5'-Tetramethylbenzidine (TMB, 100 □l, Thermo Fisher Scientific) was added as a chromogenic substrate for HRP into each well and the plate was incubated at room temperature for 5 min followed by the addition of H2SO4

solution (2.0 M) to stop the reaction. Absorbance OD values at 450 nm were then measured immediately.

3.3.8 Intracellular free sialic acid assay

Intracellular sialic acid content was quantified by using the periodate resorcinol method developed by Jourdian et al [248]. In brief, cell pellets consisting of 2 x 106 cells from each sample were resuspended in 300 □l PBS, followed with freeze/thaw cycle three times for cell lysis. The cell lysate was oxidized with 5 µl of 0.4 M periodate acid and kept on ice for 10 min. Then 500 µl resorcinol mixture was added to each sample and heated at 100 °C for 10 min. After the sample cooling, 500 µl of tert-butyl alcohol was added and the samples were vortexed and centrifuged to precipitate cell debris. The supernatants were transferred immediately to a 96-well plate and the absorbance was measured at 630 nm. Sialic acid concentrations were calculated by comparison with a standard curve.

3.3.9 Quantitative determination of EPO sialic acid content

The sialic acid content of purified recombinant EPO was quantified by the fluorescence-labeling method as developed by Hara et al. [249]. Briefly, sialic acid was hydrolyzed in 25-mM sulfuric acid for 1 h at 80 °C and derivatized with 1,2-diamino-4,5-methylenedioxybenzene, dihydrochloride (DMB, Dojindo, Rockville, MD) for 2.5 h at 60 °C. Next, DMB-labeled sialic acids were separated on a Poroshell120-EC-C18 (150MM, 2.7 □m) reverse-phase column (Aglient, Santa Clara, CA) and detected by a fluorescence detector (G1316A, Agilent) with the excitation and emission wavelength at 367 nm and 445 nm.

3.3.10 Intact glycopeptide LC-MS/MS analysis

Equal amounts of purified recombinant EPO obtained from wild-type or glycoengineered CHO lines treated with 0.33 mM 1,3,4-O-Bu_3ManNAc or 1.0 mM NaBu was denatured using 8.0 M urea/1.0 M ammonium bicarbonate buffer, reduced with 10 mM tris (2-chloroethyl) phosphate at 37 °C for 1.0 h and alkylated with 15 mM iodoacetamide at room temperature in the dark for 30 min [250]. The protein sample then was diluted 5-fold with nuclease-free water and digested with endoproteinase GluC (New England BioLabs) (protein:enzyme = 50:1, w/w) overnight with shaking at 37 °C. Sample was centrifuged at 13000 x g for 10 min to remove precipitates and desalted with C18 SPE column (Waters, Milford, MA) as described in Jia et al [250]. The EPO-derived glycopeptides were further enriched by anion-exchange, reversed-phase Oasis MAX column (Waters, Milford, MA) as described in Yang et al [251]. Subsequently, samples were dried in speed-vac and 1 □g each sample was subjected to LC-MS/MS analysis. The LC conditions and MS parameters were described in Jia et al [250]. For EPO intact glycopeptide identification, the MS data were analyzed by an in-house software called GPQuest 3.0 with manual inspection[252]. Data analysis criteria were described in Jia et al [250].

3.4. Results

3.4.1 Compare the effects of 1,3,4-O-Bu_3ManNAc and ManNAc on recombinant protein sialylation

In order to evaluate the effect of Bu_3ManNAc on CHOK1 cells, total cell lysates from treated and untreated cells were subjected to HPLC quantification for evaluation of sialic acid content on glycoproteins and glycolipids (Figure 3-2A). Treatment with 100 μM Bu_3ManNAc increased the bound sialic acid by ~20 fold compared to untreated cells. Furthermore, the sialic acid content increased following addition of higher concentrations, reaching a level 60 fold higher than the untreated cells for 350 μM Bu_3ManNAc. Compared with 20mM ManNAc treatment, 200 μM of

Bu_3ManNAc served to increase the lysate sialic acid content to a similar level at 100 fold less concentration. Moreover, sialic acid content was ~35% and ~56% higher for 300 μM and 350 μM Bu_3ManNAc relative to the 20 mM ManNAc treatment.

To assess the effect of Bu_3ManNAc feeding on intracellular glycoproteins, CHO-K1 cell cultures were introduced with increasing concentrations of Bu_3ManNAc (from 0 to 350 μM)[253]. After a 96-hour incubation, CHO-K1 cells were lysed and subjected to lectin blot using Maackia amurensis lectin II (MAL II), which specifically binds to α2,3 sialylation linkages. As shown in Figure 3-2B, the lectin binding to the oligosaccharide of total glycoproteins increased significantly with Bu_3ManNAc treatment compared to the untreated negative control (0 μM Bu_3ManNAc). Interestingly, MAL II binding efficiency was highest at Bu_3ManNAc concentration between 100 and 350 μM. More importantly, the MAL II binding levels from cell cultures treated with higher concentrations of Bu_3ManNAc (>= 150 μM) exhibited stronger binding signals than that for supplementation with 20mM ManNAc. Combining the results of the lectin blot analysis and HPLC quantification indicates that Bu_3ManNAc addition can enhance sialylation levels in CHO cells with feeding concentrations of Bu_3ManNAc approximately 100 fold lower than that of ManNAc.

Since the total cell lysate contains numerous glycoproteins, subsequent analysis was undertaken to investigate further the role of Bu_3ManNAc on the intracellular sialic acid levels and sialylation of a CHO-K1 expressing a recombinant glycoprotein, erythropoietin (EPO). We first investigated the effect of Bu_3ManNAc feeding on the total intracellular sialic acid content of the EPO-expressing cell line with or without Bu_3ManNAc supplement. As shown in Figure 3-3A, feeding of 200 or 300 μM Bu_3ManNAc resulted in a greater than 8-fold increase in total intracellular sialic acid which exceeded the increase obtained by addition of 20 mM ManNAc.

200-300 μM Bu_3ManNAc feeding can achieve comparable and even higher intracellular sialic acid level than ManNAc feeding at nearly two order of magnitude lower concentration for the analog. Thus, Bu_3ManNAc treatment is more efficient in its conversion into sialic acid in the intracellular pool than supplementation with ManNAc.

Moreover, recombinant EPO was purified from a stable EPO-expressing CHO cell line treated with 0 μM, 200 μM, and 300 μM Bu_3ManNAc as well as 20 mM ManNAc. As is shown in Figure 3-3B, the sialic acid content of EPO from cells following addition of 20mM ManNAc increased ~20%, while the sialylation level increased even more with the treatment of 200 μM or 300 μM Bu_3ManNAc (~40%), compared to the untreated cells. This result suggests that Bu_3ManNAc supplementation can clearly increase the sialic acid content of specific recombinant glycoproteins and the enhancement is consistent with the improvement in total intracellular sialic acid content detected in the cell lysates treated with Bu_3ManNAc.

3.4.2 Butyrated ManNAc analog improves protein expression in Chinese hamster ovary cells

1. Effect of 1,3,4-O-Bu_3ManNAc on recombinant protein production in CHO cells

This novel sugar analog-1,3,4-O-Bu_3ManNAc is composed of a core ManNAc moiety with three ester-linked butyrate groups (Figure 3-1A). Given the expression-enhancing effect of sodium butyrate on proteins, we reasoned that 1,3,4-O-Bu_3ManNAc may also have the potential to affect recombinant protein expression. To examine the impact of this novel analog on recombinant protein production, two stable CHO cell lines, one expressing human EPO and the other producing human IgG, were treated with 0, 100, 200, and 300 μM 1,3,4-O-Bu_3ManNAc followed by collection of the cell culture supernatants for immunoblot analysis. As we expected, expression levels of both EPO and IgG increased progressively with 1,3,4-O-Bu_3ManNAc treatment compared to the corresponding untreated cells (Figure 3-4) with addition of 300 μM

1,3,4-O-Bu_3ManNAc showing the highest expression level of EPO and IgG.

To further assess the effects of 1,3,4-O-Bu_3ManNAc on protein productivity, EPO and IgG cell culture supernatant from unmodified medium and medium supplied with a series of 1,3,4-O-Bu_3ManNAc concentrations (100, 200, 300 μM) were harvested and subjected to Ni-NTA (EPO) or protein A (IgG) purifications followed by SDS-PAGE analysis. As shown in Figure 3-5A, the IgG purified from 1,3,4-O-Bu_3ManNAc treatment exhibited increased productivity with increasing concentrations of the additive compared to the purified IgG from untreated cells. Both in reducing conditions (separate heavy chain and light chain) and non-reducing conditions (full-size antibody), the protein profile of purified IgG displayed a similar pattern of increased productivity for 1,3,4-O-Bu_3ManNAc treated cells with the highest antibody levels produced in cells treated wtih 300 μM of 1,3,4-O-Bu_3ManNAc. For purified EPO, the protein productivity was augmented in higher concentrations (200 and 300 uM) of analog as well (Figure 3-5B). Due to band spreading as a result of glycosylation, the purified EPOs at different 1,3,4-O-Bu_3ManNAc medium levels were treated with the glycosidase PNGase F, which also exhibited higher levels of deglycosylated EPO for the treated samples versus the untreated control.

2. Effects of 1,3,4-O-Bu_3ManNAc on cell growth and metabolism

We further investigated the cell culture growth and metabolic changes in the presence or absence of this novel analog. Cell lines stably expressing IgG (Figure 3-6A and 3-6B) and EPO (Figure 3-6C and 3-6D) were cultured in the media with or without addition of 0.33 mM 1,3,4-O-Bu_3ManNAc and 1mM NaBu respectively and analyzed for cell numbers and viability on a daily basis. Untreated cells entered an exponential growth phase that persisted for 3 days and then the viable cell numbers declined. With the addition of 1,3,4-O-Bu_3ManNAc, both the EPO and IgG expressing cell lines exhibited similar growth patterns and daily viability as the untreated control.

Moreover, the non-treated and 1,3,4-O-Bu_3ManNAc treated cells were able to reach a similar maximum cell density (~3×10^6 mL-1) for both the EPO and IgG expressing cell lines in batch cell culture (Figure 3-6). Another set of cells were treated with 1mM NaBu. For both the EPO and the IgG production cell lines, the NaBu treated cells followed a similar initial growth trajectory as the 1,3,4-O-Bu_3ManNAc treated and untreated control cells. However, the maximum cell densities following NaBu treatment were reduced relative to these other cell lines for both IgG and EPO expressing CHO lines and this culture also exhibited lower viable cell densities during the stationary and death phases relative to the other two cultures. A similar pattern was detected in the viabilities in which the cell cultures treated with NaBu showed progressively lower percent viabilities after 4 and 5 days in culture.

Concentrations of glucose and lactate in the cell culture medium were also monitored throughout the cell culture time course. As shown in Figure 3-6E and 3-6G, the concentration of glucose dropped dramatically in the exponential phase while the concentration of lactate increased over time (Figure 3-6F and 3-6H). In all experiments, there was a negligible effect of the presence of 1,3,4-O-Bu_3ManNAc additives on the overall glucose consumption and lactate accumulation for both the EPO and IgG cell cultures. The glucose levels in the NaBu-treated cells declined at a slightly slower rate for the IgG expressing cell lines. Furthermore, lactate increased more slowly in NaBu treated cells by day 2 and maintained a lower overall level in the cultures up until day 5 of the cultures. Thus, the combined results exhibited that addition of 1,3,4-O-Bu_3ManNAc did not appear to change the overall growth rates, cell viability as well as metabolite consumption and accumulation compared to the untreated cells in both EPO and IgG expressing cell lines. Alternatively, the addition of NaBu had a discernibly negative impact on final cell densities and viabilities in the stationary and growth phases of both CHO cell cultures. The influence of NaBu

was also reflected in lower lactate accumulation levels for the CHO cultures treated with NaBu during the growth and stationary phases.

Recombinant protein accumulation during cell growth

Next, the expression levels were determined over the cell culture process for cells treated with 1,3,4-O-Bu_3ManNAc. Total accumulation levels of EPO and IgG were evaluated daily from conditioned medium of expressing CHO cell lines in the presence or absence of 300 μM 1,3,4-O-Bu_3ManNAc in order to monitor the protein profile over the culture period and define the time for product harvest. As is shown in Figure 3-7, EPO and IgG accumulation levels were at a very low concentration in lag phase and early exponential phases for the untreated (NC) cells, but increased in the late exponential phase and stationary phase to a maximum on the final day at 5 post-inoculation. The product accumulation of EPO in 300 μM 1,3,4-O-Bu_3ManNAc exhibited a more rapid accumulation pattern with times compared to the untreated cells. By day 3, the EPO levels were substantially elevated in the untreated cells and this increase sustained through the duration of the batch process. The IgG production profiles are also elevated in the IgG producing cell line by day 4 and reached a higher final titer at day 5 compared to the untreated cells.

Recombinant protein accumulation during cell growth

Sodium butyrate is widely used as a commercial media supplement to increase protein productivity. The presence of butyrate groups on 1,3,4-O-Bu_3ManNAc may serve a role analogous to NaBu in cell cultures (Figure 3-1). Therefore, another experiment was undertaken to compare the impact of NaBu and 1,3,4-O-Bu_3ManNAc on CHO cell cultures. As shown in Figure 3-8, EPO expression levels were gradually enhanced along with increasing 1,3,4-O-Bu_3ManNAc concentrations from 0.1, 0.2, 0.33 until 0.5 mM. Because 1,3,4-O-Bu_3ManNAc can generate 3 equivalents of butyrate, NaBu was added at 3-fold higher concentrations (0.3, 0.6, 1

and 1.5 mM) than the corresponding 1,3,4-O-Bu_3ManNAc concentrations. The supplementation of NaBu exhibited higher relative EPO expression levels for same molar amount of butyrate compared to the 1,3,4-O-Bu_3ManNAc treatment.

Next, the effect of 1,3,4-O-Bu_3ManNAc and NaBu on cumulative EPO protein production from day 1 to day 5 over the batch cell culture process was examined for comparative levels of molar butyrate, 0.33 mM of 1,3,4-O-Bu_3ManNAc and 1mM NaBu, added at the beginning for EPO expressing cell lines followed by immunoblot analysis. The increase in EPO expression for the 0.33 mM 1,3,4-O-Bu_3ManNAc treated cells was once again observed in mid to late growth stage (day 3 to day 5) as observed previously (Figure 3-7). One mM NaBu treatment of the cells revealed a similar pattern of expanded EPO expression during the exponential phase with a slight increase in protein production compared to 0.33mM 1,3,4-O-Bu_3ManNAc treatment (Figure 3-8B) The viable cell density (VCD) and cell viability were examined as well to assess the cell cytotoxicity of 1,3,4-O-Bu_3ManNAc and NaBu treatments as shown in Figure 3-6. As noted previously, cell culture with 1,3,4-O-Bu_3ManNAc added contained more viable cells and maintained higher cell viability than NaBu at the end of exponential and during the stationary and death phases.

Further, quantitative EPO production analysis was investigated. Briefly, along with the growth study equal amounts of supernatant were collected twice a day and the relative EPO production in the supernatant was measured by enzyme-linked immunosorbent assay (ELISA) with anti-EPO antibody. As shown in Figure 3-9E, the relative production of recombinant EPO over the time period demonstrated increased for both 1,3,4-O-Bu_3ManNAc and NaBu supplement compared to cells not subject to chemical supplementation. Based on the equivalent butyrate concentrations used, 1,3,4-O-Bu_3ManNAc showed a ~ 27% improvement above

untreated cells while NaBu increased recombinant EPO expression by ~ 71% relative to the untreated producer CHO cells.

5. Comparison of 1,3,4-O-Bu_3ManNAc to NaBu on cell apoptosis

A major concern for NaBu applications in mammalian cell culture is its effect on cell viability as well as cell apoptosis [254, 255]. To examine -the effects of these additives on apoptotic cell death, CHO-K1 cells were treated with 1 mM NaBu or 0.33 mM 1,3,4-O-Bu_3ManNAc or left untreated, then fixed and stained with anti-Caspse3 antibody. Caspse 3 protein is an important indicator for cell apoptosis and remarkably active in cell death phase [256]. Stained cells were then incubated by DAPI (4',6-diamidino-2-phenylindole) for showing the nuclei areas and observed under a florescent microscope. The population of anti-caspase3 stained cells numbered as apoptotic cells was observed to increase following the addition of 1 mM NaBu, as compared to the untreated control (Figure 3-9A and 3-9B). Alternatively, no statistical variation (n=10) was observed between 0.33 mM 1,3,4-O-Bu_3ManNAc treated cells and untreated cells in the percentage of apoptotic cells in the population under the fluorescence microscope.

In order to investigate further the activation of cell apoptosis, quantative RT-PCR was used to determine mRNA expression of 4 apoptotic marker genes (Cul2, BAK, BAX and BCL2L11) at day 3 in wild-type and IgG or EPO expressing CHO cell lines left untreated or treated with 1 mM NaBu or 0.33 mM 1,3,4-O-Bu_3ManNAc. The addition of 1,3,4-O-Bu_3ManNAc exhibited comparable and slightly elevated levels (1 to 1.5 fold) of mRNA expression of pro-apoptotic marker genes when compared to untreated cells for wild-type and IgG or EPO expressing CHO cell lines. Alternatively, the addition of 1 mM NaBu resulted in the highest relative expression levels of all pro-apoptotic genes across all the three cell cultures when compared to both untreated cultures and those treated with 0.33 mM 1,3,4-O-Bu_3ManNAc. In particular, NaBu

addition up-regulated BCL2L11 1.7-2.5 fold, BAK 1.2-3.2 fold, BAX 1.1-2 fold and Cul2 1.5-1.8 fold for each of these three different cell lines. Collectively, the combined results of Figure 3-9 and 3-10 showed that both 1,3,4-O-Bu_3ManNAc and NaBu are able to significantly increase the recombinant protein productivity in CHO cells. Although NaBu displays a higher enhancement of protein expression, 1,3,4-O-Bu_3ManNAc showed less cell cytotoxicity and apoptosis induction in CHO cell culture at equivalent butyrate levels.

3.4.3 Combining Butyrated ManNAc with Glycoengineered CHO Cells Improves EPO Glycan Quality

1. Intracellular sialic acid levels increased in 1,3,4-O-Bu_3ManNAc-treated recombinant EPO-expressing CHO cells

We next investigated the impact of the two chemical supplements on intracellular sialic acid content. Wild-type and glycoengineered EPO stably expressing CHO cells (wt-EPO and glycoengineered-EPO) were cultured in F12K media supplemented with 1,3,4-O-Bu_3ManNAc or NaBu using equivalent butyrate concentrations. The CHO-K1 cells were also cultured as a control. After a 2-day incubation, 2 million cells were collected from each culture and subjected to the periodate/resorcinol assay to detect intracellular sialic acid content [248]. As shown in Figure 3-11, 1,3,4-O-Bu_3ManNAc treatment substantially increased the intracellular sialic acid concentrations in both the wild-type and glycoengineered EPO-expressing CHO cell lines (by ~ 7.2- to 8.0-fold in the wild-type and glycoengineered CHO cells, respectively) compared to untreated controls. Sodium butyrate treatment did not measurably change intracellular sialic acid levels compared to untreated controls in either the wild-type or glycoengineered EPO cells. Together, these comparisons confirmed that ManNAc (a key metabolic precursor of sialic acid biosynthesis in mammalian cells) generated from 1,3,4-O-Bu_3ManNAc is efficiently converted

into the sialic acid biosynthesis pathway and enhance intracellular pools of this sugar.

2. Combining chemical supplementation and glycoengineering strategies altered recombinant EPO sialylation

Next, we assessed the effect of 1,3,4-O-Bu_3ManNAc and NaBu addition on the sialylation content of recombinant EPO. The EPO protein was purified from both wild-type and glycoengineered EPO-expressing CHO lines that had been treated with 1,3,4-O-Bu_3ManNAc, NaBu, or left untreated. In order to analyze the alterations on sialic acid linkage specificity, equal amounts of purified EPO were subject to lectin blot analysis using Maackia amurensis lectin II (MAL II) that recognizes α-2,3-linked sialic acid or Sambucus nigra lectin (SNA) that preferentially binds to α-2,6-linked sialoglycoconjugates (Figure 3-12A). The lectin blots revealed that EPO from 1,3,4-O-Bu_3ManNAc treated wild-type CHO cells showed stronger MALII binding compared to EPO produced in comparable cells that were either untreated or supplemented with NaBu. Similarly, EPO produced by the glycoengineered CHO cells supplemented with 1,3,4-O-Bu_3ManNAc displayed stronger binding for MALII and higher binding to SNA compared to NaBu treated or untreated control samples. In contrast, NaBu treated EPO produced in the glycoengineerined cells showed weaker binding of both MALII and SNA compared to untreated controls. These results indicated that 1,3,4-O-Bu_3ManNAc not only increased EPO production (as shown above in Figure 3-4 and 3-5) but measurably enhanced α-2,3-sialylation for EPO from wild-type CHO cells and both α-2,3- and α-2,6-sialylation for EPO from the glycoengineered cells. Sodium butyrate treatment (at 1.0 mM), slightly decreased sialylation of recombinant EPO, especially from glycoengineered cell line in accordance with the literature indicating that NaBu treatment can lower glycan quality[257] [258].

Thus, in order to further investigate the combinatorial effect of chemical supplement with glycoengineering strategies on EPO sialylation, the influence of equivalent levels of butyrate delivered via NaBu or 1,3,4-O-Bu_3ManNAc on sialic acid levels of recombinant EPO produced in the wild-type and glycoengineered CHO cells was performed . Sialic acids on EPO in each sample were derivatized with 1,2-diamino-4,5-methylenedioxybenzene dihydrochloride (DMB) and quantified by HPLC using fluorescence detection (Figure 3-12B). In the absence of chemical supplementation, overexpression of GnTIV, GnTV, and ST6 in the glycoengineered CHO cells increased EPO (glycoengineered-EPO) sialylation by 42%. In chemically-supplemented cells, 1,3,4-O-Bu_3ManNAc enhanced EPO sialylation by 29% in the wild-type CHO cells and by approximately 32% in the cells compared to the respective untreated controls; in contrast, treatment with NaBu reduced sialyation by between 6% and 14%. When the benefits of 1,3,4-O-Bu_3ManNAc supplementation and glycoengineering were combined by comparing EPO produced in untreated wild-type CHO cells (633 ng/ml sialic acid) with EPO produced in 1,3,4-O-Bu_3ManNAc supplemented glycoengineered cells (1,114 ng/ml), a dramatic 75% enhancement in sialic acid content was observed. In summary, lectin blots and HPLC quantification demonstrate that 1,3,4-O-Bu_3ManNAc supplementation enhanced sialylation of recombinant EPO consistent with the increased intracellular sialic acid content in the respective cells (Figure 3-11) and furthermore that combining glycogene overexpression with our metabolite supplementation method increased these levels even more.

3. N-Glycan profiles of wild-type and glycoengineered EPO determined by intact glycopeptide LC-MS/MS analysis

To elucidate N-glycan profiles from EPO produced in wild-type and glycoengineered EPO-

expressing CHO cells treated with 1,3,4-O-Bu$_3$ManNAc or NaBu, we performed intact glycopeptide analysis using nano LC-MS/MS. The unique fragmentation signatures obtained from the MS/MS spectra of intact EPO glycopeptides analyzed by high energy C-trap disassociation (HCD) fragmentation, including oxonium ions (m/z 138, 163, 204, 274 , 292, and 366), peptide fragmentation ions (b- and y-ions), and peptide and peptide+HexNAc fragment ions, were integrated to identify the glycopeptides. Representative EPO glycopeptide MS/MS spectra at each EPO N-glycan site are provided in the Supplemental Results, Figure S3-1. The number of peptide spectral matches (PSM) was used to calculate the overall abundance of different glycoforms or at specific glycosylation sites with two biological repeats.

The EPO glycoforms were first analyzed and organized by antennary distribution (Supplemental Results, Figure S3-2). The antennary distribution of wt-EPO and glycoengineered-EPO glycans showed that overexpressing GnTIV/GnTV genes in glycoengineered CHO cells significantly increased the tetra-antennary structures and simultaneously reduced the tri- and bi-antennary content on the glycoprofile of recombinant EPO. However, treatments with 1 mM NaBu resulted in fewer tetra-antennary structures and an increased fraction of tri-antennary glycans on EPO from glycoengineered CHO cells. Indeed, 3mM NaBu has previously been shown to lower the EPO branch complexity in unmodified CHO cells [259]. Alternatively, 0.333 mM treatment with 1,3,4-O-Bu$_3$ManNAc resulted in an increase in the tetra-antennary and fewer tri-antennary structures on EPO from both wild-type and CHO cells. Treatment with 1 mM NaBu and 0.333 mM 1,3,4-O-Bu$_3$ManNAc did not alter the abundance of oligomannose, mono- and bi-antennary glycans distribution in wild-type and glycoengineered CHO cells.

Next, we explored the impact of NaBu and 1,3,4-O-Bu$_3$ManNAc on the sialylation of EPO from wild-type and glycoengineered CHO cells. The overall ($\frac{\sum sialylated\ glycopeptide\ PSM}{\sum total\ glycopeptide\ PSM}$) and site-

specific sialylation occupancy ($\frac{\sum sialylated\ glycopeptide\ PSM\ at\ specific\ site}{\sum total\ glycopeptide\ PSM\ at\ specific\ site}$) are shown in Figure 3-13A and 3-13B. The sialylation occupancy is defined by the percentage of sialylated glycopeptides detected at a specific site as showed in the raw MS data in the Supplemental Results. With this method we achieved exquisite resolution of the glycan profile at each of the three N-glycan sites of EPO. We first compared EPO produced in wild-type and glycoengineered cells not subject to chemical supplementation. In this case (the first column in Figure 3-13A) we observed that the first N-glycan site (-N51ITT-) of EPO had highest sialylation occupancies of ~ 85% and 77% in EPO from their corresponding two cell lines. A feature of the glycoengineered CHO-derived EPO glycosylation profile was approximately equivalent sialylation at each of the three sites (77, 73, and 76% for sites 1, 2, and 3, respectively) compared to the gradually lower occupancy at three N-sites in wt-EPO. We next compared sialylation occupancy after supplementation with NaBu and found that there was negligible impact to the 1st and 3rd (-N110SSQ) N-glycan sites for wild-type EPO compared with the untreated controls (shown in Figure 3-13A). Supplementation of the glycoengineered cells that produce glycoengineered EPO with NaBu, however, caused measurably decreased sialylation at each site (from 77% to 68% at the 1st N-glycan site, from 73% to 52% at the 2nd, and from 76% to 51% at the 3rd). By comparison, 1,3,4-O-Bu_3ManNAc (Figure 3-13A) increased sialylation occupancy at the 2nd (-N65ITV-) and 3rd N-glcyan sites on both wt-EPO and glycoengineered-EPO compared to untreated controls. These analyses of site-specific sialylation occupancy indicate that the 1st N-glycan site was already highly sialylated under “wild type” conditions, perhaps because in the glycosylaiton process, the first N-site on the nascent EPO peptide is the first one to be glycosylated in Golgi or perhaps the first N-glycan site has less structural hindrance than the other two sites to interact with glycosyltransferases.

Glycosylation difference at different sites have been observed previously by Liu et al., who were looking at Influenza A virus hemagglutinin and the first two N-sites were fully glycosylated while the rest N-sites were not completely glycosylated [260].The study of secretory immunoglobulin A from human colostrum also revealed that for secretory component (SC), the first two N-sites have higher glycosylation and sialylation occupancy than other N-sites and the second N-site has higher glycosylation and sialylation than other N-sites for IgA1/IgA2 perhaps due to structural hindrance to interact with available glycosyltransferases [261].The positive impact of 1,3,4-O-Bu_3ManNAc supplementation primarily contributes to enhanced sialyation of the 2nd and 3rd N-glycan sites of recombinant EPO. Importantly, 1,3,4-O-Bu_3ManNAc supplementation either avoids, or reverses, the deleterious impact of butyrate on glycan quality when this chemical agent is delivered and complexed with ManNAc as opposed to NaBu. Lastly, the overall impact of chemical supplementation on EPO sialylation occupancy with 1 to 4 sialic acids (S1 to S4) is shown in Figure 3-13B where the net effect is summed across all three sites; this combined data shows that NaBu decreases sialylation occupancy in both the wild-type and especially in the glycoengineered CHO lines compared to untreated controls while 1,3,4-O-Bu_3ManNAc increases overall occupancy. In Figure 3-13B, we also classified the glycan structures based on the number of sialic acids found on each of these EPO samples based on the MS analysis. NaBu treatment reduced the proportion of N-glycans with 2, 3, or 4 sialic acids while increasing the fraction of N-glycans with 0 or 1 copies of this sugar for wt- and glycoengineered CHO derived EPOs. By contrast, treatment with 1,3,4-O-Bu_3ManNAc increased the proportion of S2 to S4 sialylated glycans while decreasing the percentage of unsialylated glycans (S0) for both wt-EPO and glycoengineered EPO samples.

3.5 Discussion

Previously Gu et al reported that feeding of ManNAc to CHO cells can improve the interferon-γ sialylation [50]. Furthermore, the study also determined that 20mM was the best concentration to supplement ManNAc in CHO cells because lower levels like 0.2 mM or 2 mM were insufficient while no further improvement in sialylation was achieved when adding more than 40mM ManNAc [50]. Our lectin blot and sialic acid content analysis revealed that the novel Bu_3ManNAc analog can greatly increase total protein sialylation in CHO cells at much lower concentrations compared to ManNAc.

Unlike subsequent sialylation pathway metabolites, ManNAc is able to permeate across the cell membrane, albeit inefficiently [253]. High exogenous addition of ManNAc is required primarily due to the lack of plasma membrane transporters for this monosaccharide. To circumvent the low metabolic uptake of natural ManNAc, acetylated monosaccharides (and disaccharides) were observed to increase cellular uptake efficiency by up to three orders of magnitude [232, 262]. A problem with completely acetylated monosaccharides, however, is that modification of the C6-OH groups results in unacceptable levels of off-target effects such as increased toxicity. Our group has overcome challenges with lipophilicity and toxicity by substituting acetate with the longer chain SCFA (short chain fatty acid) n-butyrate, rendering tri-substituted monosaccharides fully membrane permeable and leaving the C6-OH group unmodified. Specifically, 1,3,4-O-Bu_3ManNAc represents a novel “high-flux” precursor for increasing sialic acid production in mammalian cells at low concentrations compared to natural ManNAc with negligible cytotoxicity[240]. Once inside a cell, non-specific esterases rapidly remove the butyrate groups regenerating natural ManNAc, which enters the sialic acid biosynthetic pathway [242].

Improving recombinant protein production in mammalian cell culture is a major objective of

biopharmaceutical manufacturing. Viable strategies including cell line selection, cell engineering, vector design, medium optimization, and feeding strategies have been employed to maximize the productivity of therapeutic proteins [217, 219, 263]. One strategy used in the biopharmaceutical industry is the addition of chemical compounds to the culture medium in order to improve recombinant protein production using the CHO platform. Chemical modifications of media are convenient and easily implemented. Indeed, additions to the media represent a modification that can be incorporated readily at a later stage in product development or when updating a current production process.

NaBu is one of the most widely used additives in mammalian cell culture to improve the productivity of recombinant proteins. Unfortunately, these enhancements in product yields often come at the expense of product quality. Indeed, while the addition of NaBu provides a number of advantages in terms of yield improvements, its inclusion can be problematic in terms of product quality and cell viability resulting from the effect of this additive on cellular physiology.

In this study, we have characterized the impact of a potentially useful chemical additive, 1,3,4-O-Bu_3ManNAc, on the expression of recombinant proteins in CHO cells. In comparison to the extensively used additive-NaBu, 1,3,4-O-Bu_3ManNAc exhibited several advantages, including decreased cell cytotoxicity, lowered apoptosis and reduced expression of pro-apoptotic genes combined with superior sialylation. Its application may be beneficial as a media supplement and replacement for NaBu both for improved protein yields and enhanced glycosylation with a lower or negligible impact on growth.

N-Acetylmannosamine (ManNAc) is an intermediate in the sialic acid synthesis pathway. Given that ManNAc exhibits low metabolic efficiency and cellular uptake in previous studies, 1,3,4-O-Bu_3ManNAc was designed initially as a substitute for ManNAc. Chemical modifications were

made to this known glycosylation supplement including extending the fatty acid chain length (acetate to n-butyrate) to increase lipophilicity and membrane permeability while leaving the C6-OH group unmodified to negate the toxicity found in fully conjugated hexosamine analogs [237]. The resulting chemical analog, 1,3,4-O-Bu_3ManNAc represents a "high-flux" alternative for incorporating the ManNAc precursor into the cells in order to increase the cellular production of sialic acid used in the sialylation of glycoproteins. Indeed, sialic acid levels in cells incubated with 1,3,4-O-Bu_3ManNAc increased ~2500-fold compared to cells incubated with natural ManNAc [237, 240]. Moreover, application of 1,3,4-O-Bu_3ManNAc in CHO cells and other cell lines improved sialylation of cellular glycoproteins and a recombinant glycoprotein, EPO, at concentrations as much as 100 fold lower compared to natural ManNAc [5].

While this chemical analog has been utilized previously only in the context of enhancing intracellular sialic acid and protein sialylation [5, 240], the current study was initiated to evaluate its capacity to increase recombinant protein production for multiple target proteins. Stable EPO and human IgG-expressing CHO cell lines were selected to investigate the influence of 1,3,4-O-Bu_3ManNAc supplement on recombinant protein expression in CHO cell culture. Increasing the concentration of 1,3,4-O-Bu_3ManNAc supplemented in the cell culture media led to the enhancement of production for two therapeutic protein (EPO and IgG) targets. This capacity to improve production of the two varied proteins suggests that 1,3,4-O-Bu_3ManNAc can be generally applicable for other expressed proteins and potentially in different cell lines. Indeed, HEK 293 cells, treated with 1,3,4-O-Bu_3ManNAc have also shown improved expression of membrane proteins relative to untreated cells (data not shown). Thus, treatment with 1,3,4-O-Bu_3ManNAc appears to be generally applicable for improving recombinant protein production across multiple mammalian cell types and for various therapeutic protein targets. Since the

organic component, ManNAc, has been shown not to alter protein production in CHO cell cultures [50], the yield enhancing activity of 1,3,4-O-Bu_3ManNAc was most probably contributed by the butyrate groups. Indeed, butyrate is known to act as a histone deacetylase inhibitor, and facilitate "opening" the chromatin area for enhanced accessibility to transcription factors [264], The widely-used butyrate chemical-NaBu and this new chemical analog, 1,3,4-O-Bu_3ManNAc, both greatly increased protein production in EPO expressing cells at same concentration of butyrate. While NaBu was more effective than 1,3,4-O-Bu_3ManNAc in enhancing EPO production (Figure 3-9), this chemical is also known for its negative effects on cell growth and activation of cell death. Thus, the impact of 1,3,4-O-Bu_3ManNAc on cell growth and apoptosis in CHO cell culture was an equally important consideration to be examined. As shown in Figure 3-9, both EPO and IgG expressing cell lines with 1,3,4-O-Bu_3ManNAc treatment displayed similar growth profiles as the corresponding untreated controls respectively. 1,3,4-O-Bu_3ManNAc-treated cells were able to reach an equivalent maximum cell density as the untreated control, while no significant differences in cell viability or changes in glucose consumption and lactate production were observed between control cells and cells with 1,3,4-O-Bu_3ManNAc treatment. Alternatively, NaBu-treated cells exhibited a decrease of ~20% in viable cell density as well as >30% decrease in viability compared to control cell lines and 1,3,4-O-Bu_3ManNAc-treated cells.

To address this phenomenon further, we examined the expression of several cell apoptosis genes at the mRNA level for 1,3,4-O-Bu_3ManNAc- and NaBu-treated cells at equivalent butyrate concentration (1mM) and compared these levels to untreated control cells. The two compounds exhibited varying impacts on wild-type CHO, EPO or IgG expressing cell lines. In particular, the mRNA level of 4 cellular apoptosis genes (Bcl2L11, BAK, BAX and Cul2) was substantially up-

regulated (1.2 to >3 fold) with NaBu addition compared to untreated cells in all three CHO cell lines. In contrast, most of the mRNA levels of apoptotic marker genes in 1,3,4-O-Bu_3ManNAc treated cell lines were equal or only slightly increased compared to the levels in untreated cells, with the two exceptions of BAK, which was increased ~2 fold in the IgG expressing cell line, and BAX, up-regulated ~1.5 fold in CHO-K1. These findings indicate that addition of 1,3,4-O-Bu_3ManNAc provides a much milder apoptotic signaling compared to NaBu in CHO cell culture. It is interesting to note that 1,3,4-O-Bu_3ManNAc and NaBu display a varied influence on cell apoptosis and cytotoxicity despite both of them containing the same levels of the active butyrate groups. One possible explanation is that NaBu diffuses into the cytosol more rapidly and is utilized almost immediately. Alternatively, 1,3,4-O-Bu_3ManNAc is larger and likely exhibits a slower and more gradual permeability through the cell membrane (although much superior to natural ManNAc). Moreover, an ester enzyme is required to release the butyrate group from 1,3,4-O-Bu_3ManNAc which may yield a slower-releasing dosage of the butyrate into the cellular cytosol over time.

In this study, we combined 1,3,4-O-Bu_3ManNAc supplementation with glycoengineering in CHO cells in order to construct an integrated production platform which provides synergies for improving quality and simultaneously increasing yields. Applying CHO cells previously engineered to express GnTIV/GnTV was observed to increase the tri- and tetra-antennary structures (Supplemental Figure S3-2), which increases the sialic acid binding sites[246]. In conjunction, overexpressing ST6 can increase α-2,6-sialyltransferase expression in CHO, which facilitates the transfer of sialic acid from the CMP-sialic acid donors to these specific acceptors [265]. Indeed, the combined overexpression of GnTIV/GnTV/ST6 increased sialylation of glycoengineered-EPO about 42% compared to wt-EPO (Figure 3-12B). Alternatively, feeding

1,3,4-O-Bu_3ManNAc significantly increased the intracellular sialic acids which in turned improved sialic acid content on wt-EPO by 29% and by 32% for the glycoengineered-EPO. Furthermore, 1,3,4-O-Bu_3ManNAc as a high-flux precursor is capable of augmenting recombinant protein sialylation at culture concentrations 100-fold lower than natural ManNAc feeding [5]. Furthermore, combining analog sugar feeding of 1,3,4-O-Bu_3ManNAc with glycoengineering of CHO cells (overexpressing GnTIV/GnTV/ST6) achieved the highest sialylation levels, fully 75% higher compared to the wt-EPO control without chemical treatment. These results suggest that both glycosyltransferases activity and sialic acid substrate availability are limiting the sialylation content for recombinant proteins produced in CHO cells. Meanwhile, the impact of 1,3,4-O-Bu_3ManNAc was compared with NaBu for their impact on production and glycan quality of EPO proteins expressed from CHO cells. We observed that under equivalent butyrate concentrations, 1,3,4-O-Bu_3ManNAc and NaBu both increased the EPO expression in CHO cells, but NaBu exhibited a higher yield enhancement than 1,3,4-O-Bu_3ManNAc treatment. In addition, the NaBu treatment negatively affected GnTIV and ST6 expressions while 1,3,4-O-Bu_3ManNAc showed much less impact on expression of GnTIV and ST6 in CHO cell lines (Supplemental Figure S3-34). Moreover, as demonstrated in Figure 3-9, 1 mM NaBu resulted in a 33% decrease in maximal viable cell density and ~30 % decrease in cell viability while 0.333 mM 1,3,4-O-Bu_3ManNAc had a negligible impact on CHO cell growth and viability as compared to the untreated control. A recent report from our group also showed that the mRNA levels of 4 cell apoptosis genes (Cul2, BAK, BAX and BCL2L11) were up-regulated in sodium butyrate treated CHO cells while most of the mRNA levels of apoptosis genes in 1,3,4-O-Bu_3ManNAc treated cells remained constant or increased only slightly compared to untreated CHO cells [266]. These findings suggests that NaBu can induce CHO cell cytotoxicity

and apoptosis while 1,3,4-O-Bu_3ManNAc has a limited or negligible impact on CHO cell cytotoxicity and apoptosis. The reduction in some glycotransferase expression in NaBu treated cells may be linked to the activation of cell apoptosis, which has led to the degradation of glycosylation in the Golgi [267]. Indeed, the mechanism by which NaBu impairs glycosylation may be through multiple mechanisms including activation of cell death pathways and regulation of gene expression. Moreover, proteomics and transcriptomics studies have revealed that sodium butyrate can affect gene expression in CHO cells in both directions (up-regulation and down-regulation), and some genes showed an opposite trend at the transcriptional and translational levels [268] [269]. A comprehensive investigation of NaBu and 1,3,4-O-Bu_3ManNAc on N-glycosylation at both transcriptional and translational levels is warranted to further elucidate the various mechanisms by which NaBu and 1,3,4-O-Bu_3ManNAc impact protein glycosylation in CHO.

A critical finding in this study was that the delivery of butyrate via 1,3,4-O-Bu_3ManNAc rather than by using its sodium salt (NaBu) circumvented diminishing glycan quality, in particular the reduction of sialylation. Indeed, the negative effect of NaBu on protein glycosylation was more evident on heavily glycosylated and sialylated EPO from the glycoengineered CHO than wt-EPO. The HPLC sialic acid quantification (Figure 3-12B) revealed that NaBu decreased the sialic acid content on wt-EPO about 6% and on the glycoengineered EPO about 14%, while 1,3,4-O-Bu_3ManNAc increased the sialic acid content on wt-EPO about 29% and on the glycoengineered EPO about 32% . Detailed intact glycopeptide analysis revealed that NaBu reduced the sialylation occupancy on all 3 N-glycan sites on glycoengineered EPO while 1,3,4-O-Bu_3ManNAc significantly increased sialylation occupancy of both wt-EPO and glycoengineered EPO on both the 2nd and 3rd N-glycan sites. These analyses of site-specific

sialylation occupancy indicate that while the 1st N-glycan site was already highly sialylated under “wild type” conditions, the positive impact of either glycotransferase overexpression or 1,3,4-O-Bu_3ManNAc supplementation primarily contributes to enhanced sialyation of the 2nd and 3rd N-glycan sites of recombinant EPO. Previous reports [270] also demonstrated that NaBu diminished the sialylation content on recombinant proteins from CHO cells and to a lesser extent, the antennary complexity of glycans [270]. These alterations of glycosylation due to NaBu are potentially attributed to two factors: 1. NaBu induces a faster protein biosynthesis rate in cells and this may exceed glycosylation processing at high flux rates through Golgi and 2. NaBu addition triggers cell apoptosis, which can increase ER stress [271] [272] and initiate the degradation of glycosylation and other processing enzymes in Golgi [267]. In contrast, at the same butyrate conditions, 1,3,4-O-Bu_3ManNAc may not impact the glycosylation activity in Golgi as severely as NaBu treatment. Most importantly, 1,3,4-O-Bu_3ManNAc can increase the availability of substrates in order to maintain or increase sialylation levels in CHO cells.

3.5. Conclusion

The current study has expanded the potential applicability of this analog by demonstrating its capacity to improve sialylation of cellular glycoproteins in CHO-K1 cells, and, more importantly, the sialic acid content of a recombinant glycoprotein, EPO, secreted from CHO cells. Furthermore, Bu_3ManNAc is a more effective chemical additive to improve sialylation than widely-used ManNAc with comparable and even superior improvement at concentrations as much as 100 fold lower. Furthermore, the reduced cytotoxicity compared to other chemical analogs suggest this chemical additive may be a valuable supplement for enhancing the glycosylation and sialylation profiles of recombinant proteins produced from CHO and other

mammalian production hosts in the coming decades.

In summary, we present 1,3,4-O-Bu_3ManNAc as a new chemical supplement for enhancing production for a diverse collection of recombinant proteins in cell cultures. Furthermore, our data indicate that 1,3,4-O-Bu_3ManNAc addition has a negligible impact on cell growth, cytotoxicity, apoptosis and metabolite utilization while simultaneously enhancing the sialylation properties of target secreted glycoproteins. All of these properties are valuable attributes for its use as a cell culture additive in CHO cells and other mammalian production hosts. In this way, 1,3,4-O-Bu_3ManNAc can represent a useful replacement to NaBu in future biotechnology efforts to improve protein yields without sacrificing undue negative impacts on the cell growth, viability, apoptosis, and glycosylation. Its capacity to be added as a direct supplement to culture media should allow it to be incorporated readily into current bioproceses as well as those under development.

In conclusion, in this work, we compared two butyrate-based chemical supplementation strategies (NaBu and 1,3,4-O-Bu_3ManNAc) by evaluating their impact on protein production and glycan quality of recombinant EPO expressed from wild-type and glycoengineered CHO cells. 1,3,4-O-Bu_3ManNAc promoted recombinant protein production while increasing sialylation. NaBu, although achieving a higher protein yield than 1,3,4-O-Bu_3ManNAc treatment, induced cell cytotoxicity and resulted in deteriorated EPO glycan sialylation. These findings position 1,3,4-O-Bu_3ManNAc as an attractive chemical supplement for recombinant protein production in biotherapeutics manufacturing. Furthermore, by combining metabolite supplementation with glycoengineering strategies, enhanced glycan quality, and especially sialylation profiles, can be achieved with their potential positive impacts on functional in vivo activity for target glycoproteins [273].

Contributions from collaborators:

Dr. Rahul Bhattacharya and Dr. Kevin J Yarema provided the sugar analogs and assisted with experimental design.

Figures and Tables

Figure 3-1. (3-1A) Structures of 1,3,4-O-Bu$_3$ManNAc, NaBu and ManNAc, (3-1B) The simplified glycosylation pathway in mammalian cells with 1,3,4-O-Bu$_3$ManNAc feeding.

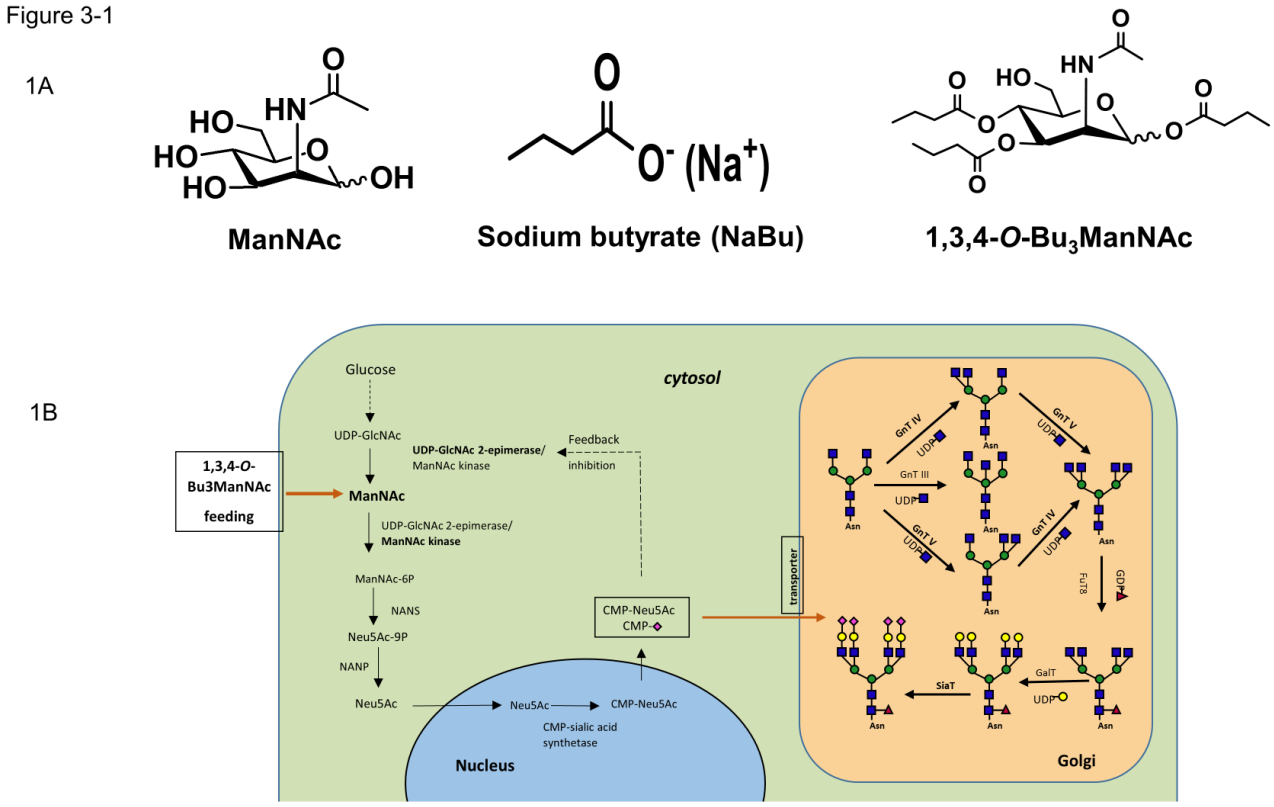

Figure 3-2. Effect of 20 mM ManNAc and increasing Bu_3ManNAc levels on the sialic acid content of the total protein. (3-2A) HPLC quantification of sialic acid content for total proteins from wild type CHO-K1 treated with ManNAc and various Bu_3ManNAc concentrations. (3-2B) MAL lectin blot of total glycoproteins from wild type CHO-K1 cells with ManNAc and increasing Bu_3ManNAc levels.

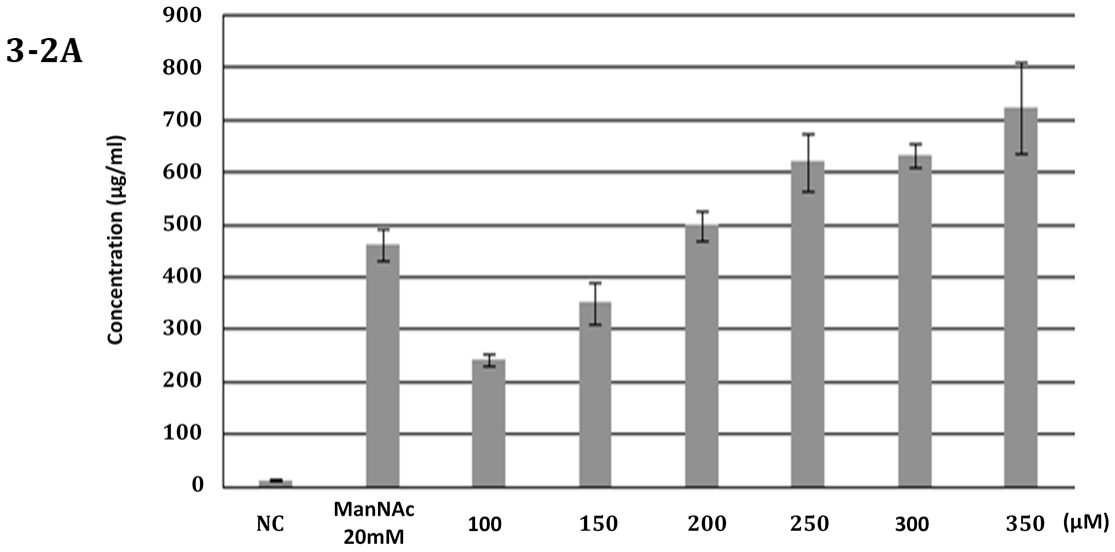

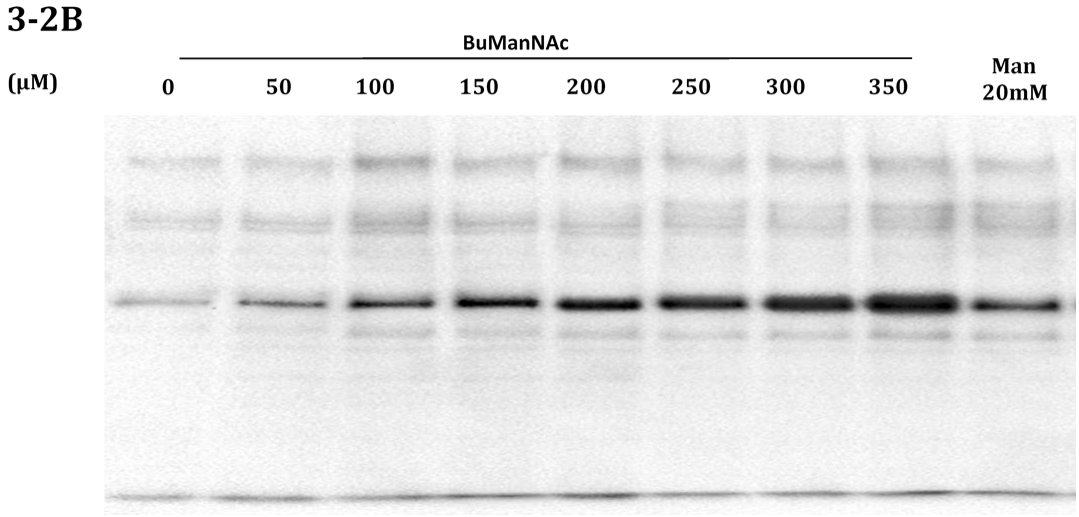

Figure 3-3. (3-3A) Intracellular sialic acid content in untreated parental wild type CHO-K1, NC (negative control, EPO-expressing cell line growing in regular F-12K media), EPO cell line treated with 20mM ManNAc, with 200 and 300 μM Bu_3ManNAc. (3-3B) Sialic acid content on recombinant EPO from CHO-K1 in the presence and absence of supplements: NC (negative control, EPO-expressing CHO-K1 cell line growing in regular untreated F-12K media), EPO-expressing cell line fed with 20mM ManNAc, 200μM, and 300 μM Bu_3ManNAc.

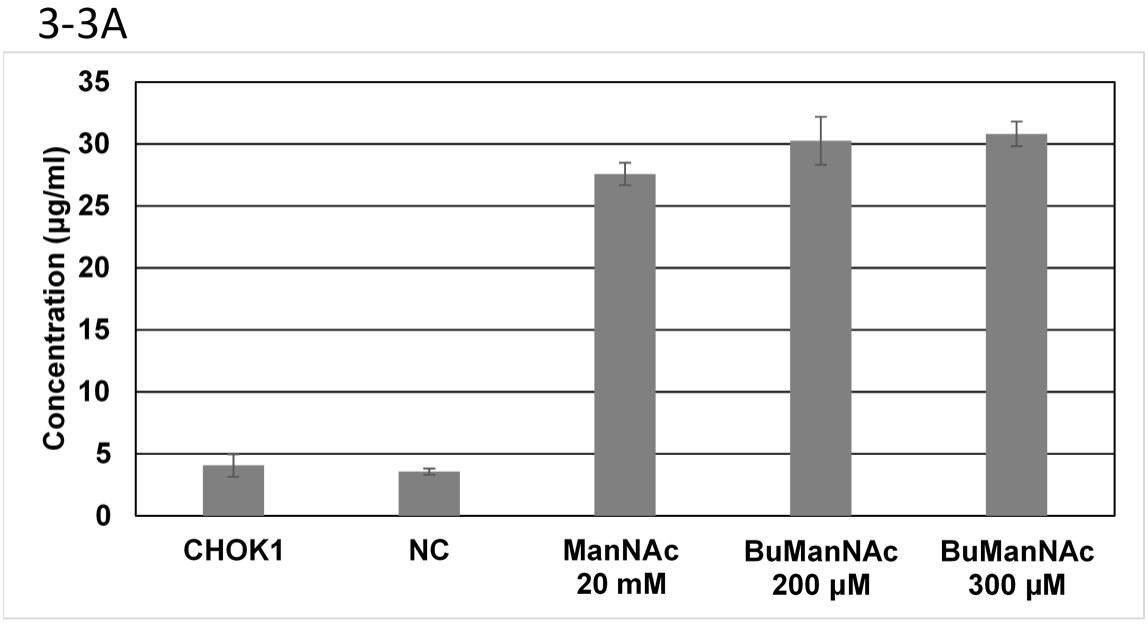

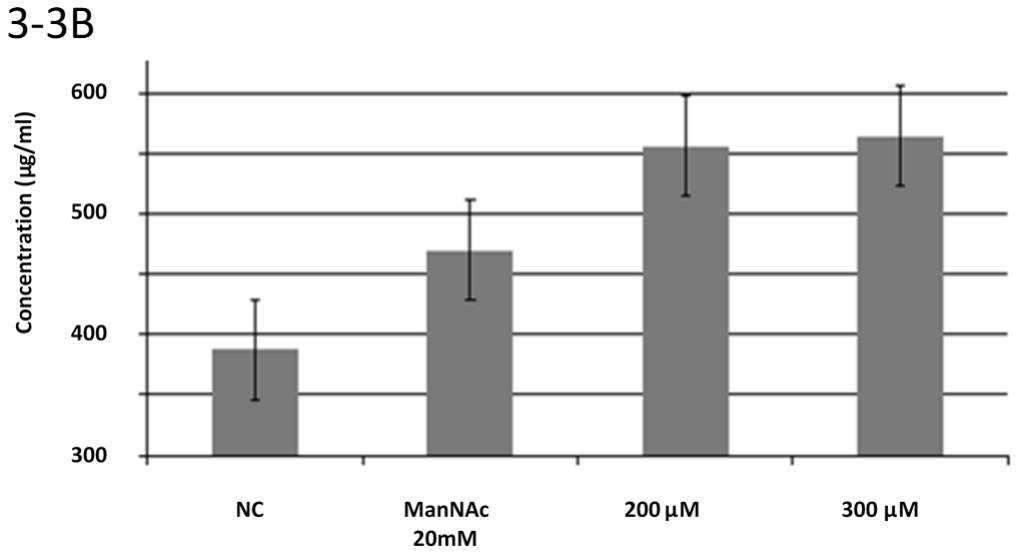

Figure 3-4. Immunoblot of protein expression in EPO- or IgG-expressing cell lines with increasing concentrations of 1,3,4-O-Bu_3ManNAc treatment. EPO- and IgG-expressing cell lines were treated with 100, 200, 300 μM 1,3,4-O-Bu_3ManNAc along with untreated cells as a control. Twenty microliters of supernatant from each sample were loaded into an SDS-PAGE and then anti-EPO or anti-IgG antibodies were employed to detect the expression of EPO and IgG separately.

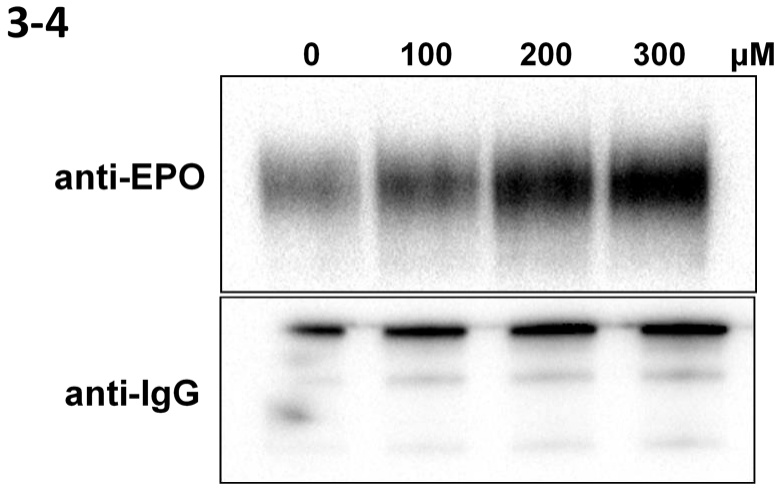

Figure 3-5. Western blot of IgG and EPO purified from expressing CHO cell lines treated with increasing levels of 1,3,4-O-Bu_3ManNAc. EPO- and IgG-expressing cell lines were treated with 100, 200, or 300 μM of 1,3,4-O-Bu_3ManNAc with untreated cells used as the control. Supernatant (2ml) from each EPO or IgG sample were collected and subjected to protein purification. EPO proteins were purified using Ni-NTA resin because of the fused his-tag on the C-terminus, and IgGs were separated using a protein A resin. (A) Purified IgGs were treated with DTT in the loading buffer for SDS-PAGE as the reducing condition and compared to samples without DTT (non-reducing) addition; (B) Purified EPOs were subjected nto SDS-PAGE with or without PNGase F treatment.

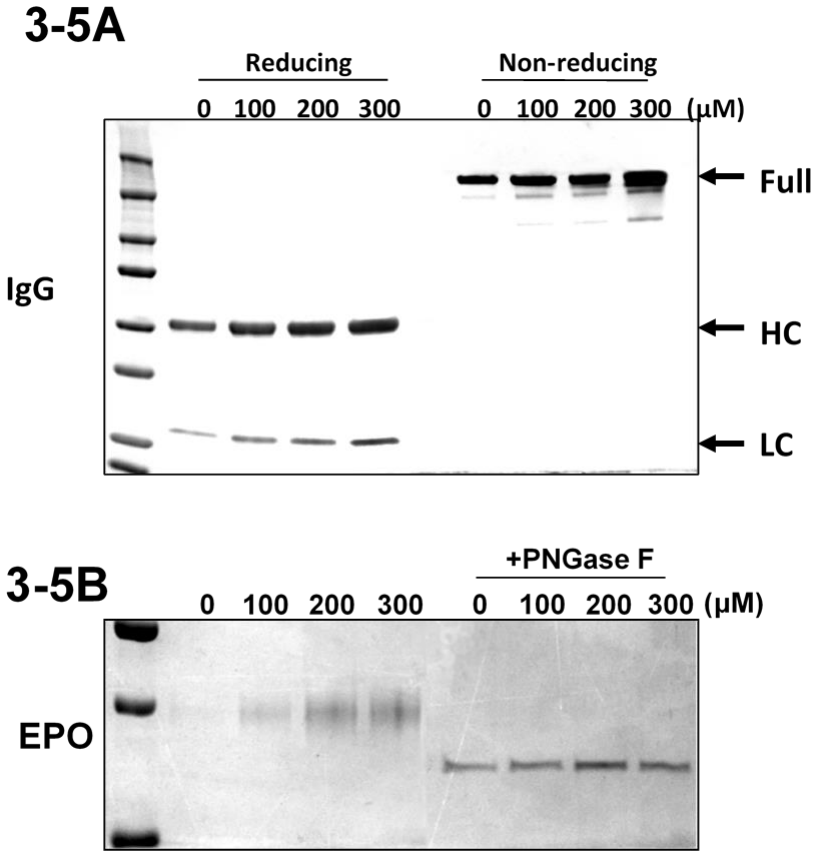

Figure 3-6. Cell growth and metabolite changes in EPO- and IgG-expressing stable CHO cell lines from untreated controls and cells exposed to 1,3,4-O-Bu_3ManNAc (0.33 mM) or NaBu (1 mM). (A) Viable cell densities (VCD) for IgG-expressing lines; (B) Cell viabilities for IgG-expressing cell lines; (C) Viable cell densities for EPO-expressing cell lines; (D) Cell viabilities for EPO-expressing cell lines; (E) Glucose levels for IgG-expressing cell lines; (F) Lactate levels for IgG-expressing cell lines; (G) Glucose levels for EPO-expressing cell lines; (H) Lactate levels for EPO-expressing cell lines.

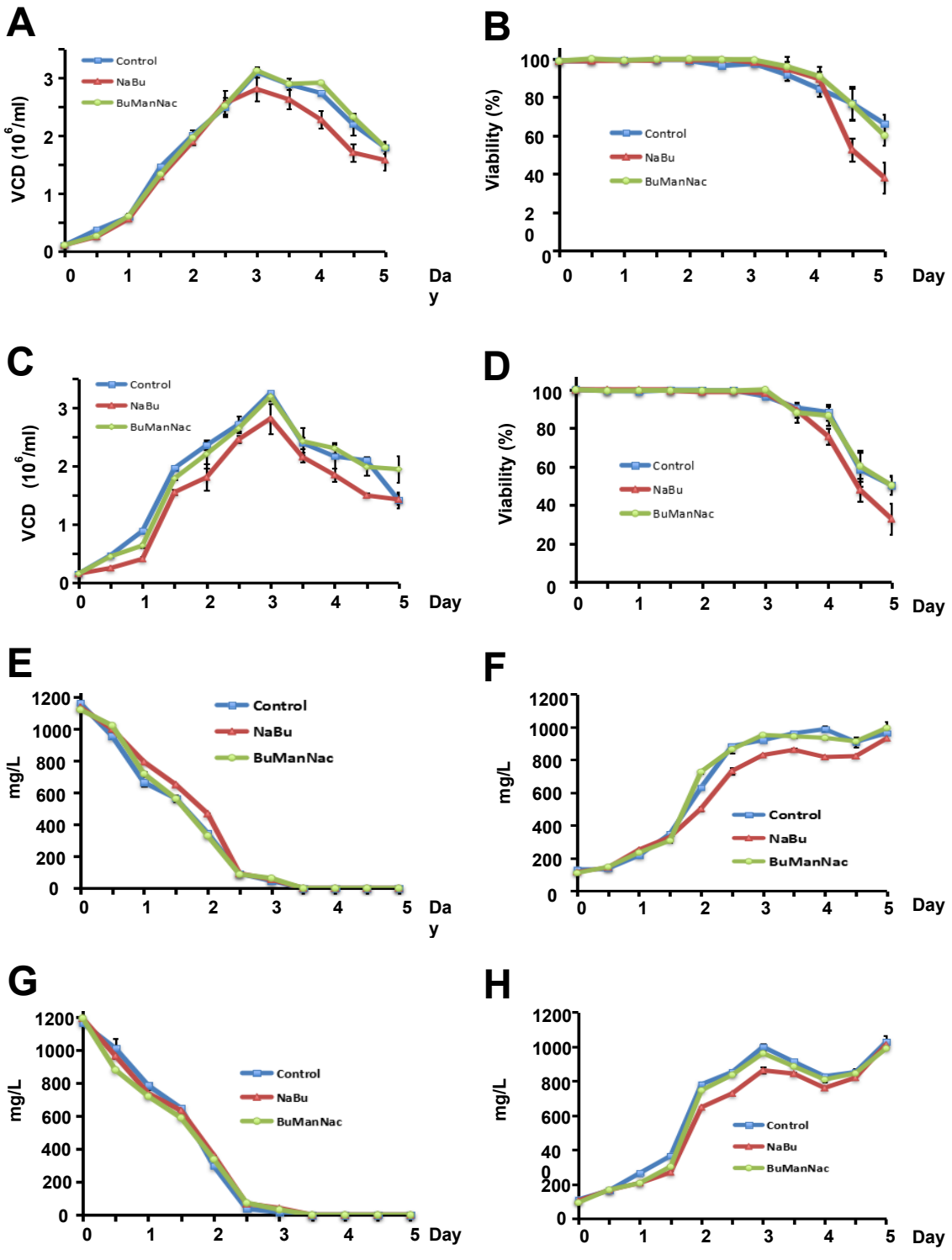

Figure 3-7. The effect of 1,3,4-O-Bu_3ManNAc addition on recombinant protein accumulation with days. Daily aliquots (20 µl) of conditioned media from EPO- and IgG-expressing CHO cell lines were collected in the presence or absence of 300 µM 1,3,4-O-Bu_3ManNAc addition, and subjected to anti-EPO and anti-IgG immunoblot analysis individually in order to monitor the recombinant protein accumulation profile over the 5-day duration of the culture.

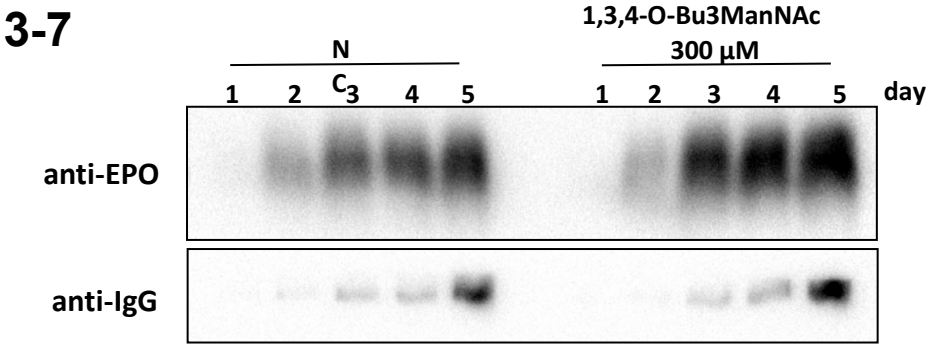

Figure 3-8. Comparison of the effects of 1,3,4-O-Bu_3ManNAc and NaBu on recombinant protein production. (A) The expression level of EPO in the presence of different levels of 1,3,4-O-Bu_3ManNAc and NaBu treatment at equivalent molar butyrate concentration conditions; (B) The accumulation of recombinant EPO from day 1 to day 5 over the batch cell culture process following 0.33 mM of 1,3,4-O-Bu_3ManNAc and 1 mM NaBu addition, which provide comparative levels of molar butyrate. Daily aliquots (20 µl) of conditioned media were used for each sample in immunoblot analysis.

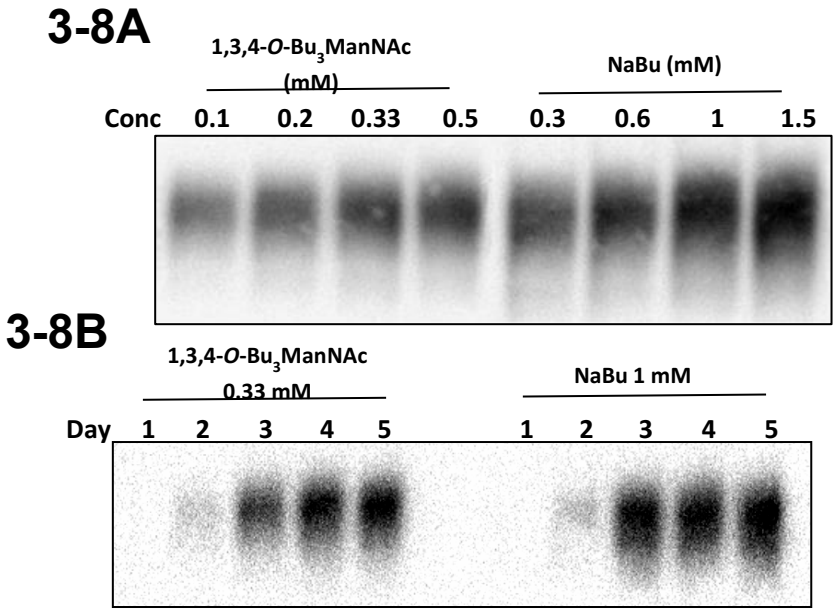

Figure 3-9. Cell growth and EPO productivity in wt-EPO-expressing CHO cell line from untreated controls and 1,3,4-*O*-Bu$_3$ManNAc (0.333 mM) or NaBu (1 mM) treatments. (3-9A) Viable cell densities (VCD) for wt-EPO-expressing line with chemical treatments; (3-9B) Cell viabilities for wt-EPO-expressing line with chemical treatments; (3-9C) Glucose levels for wt-EPO-expressing cell line with chemical treatments; (3-9D) Lactate levels for wt-EPO-expressing cell line with chemical treatments; (3-9E) Relative EPO productivity in the growth cycle in the wt-EPO-expressing line treated with 1,3,4-*O*-Bu$_3$ManNAc (0.333 mM) or NaBu (1 mM) individually.

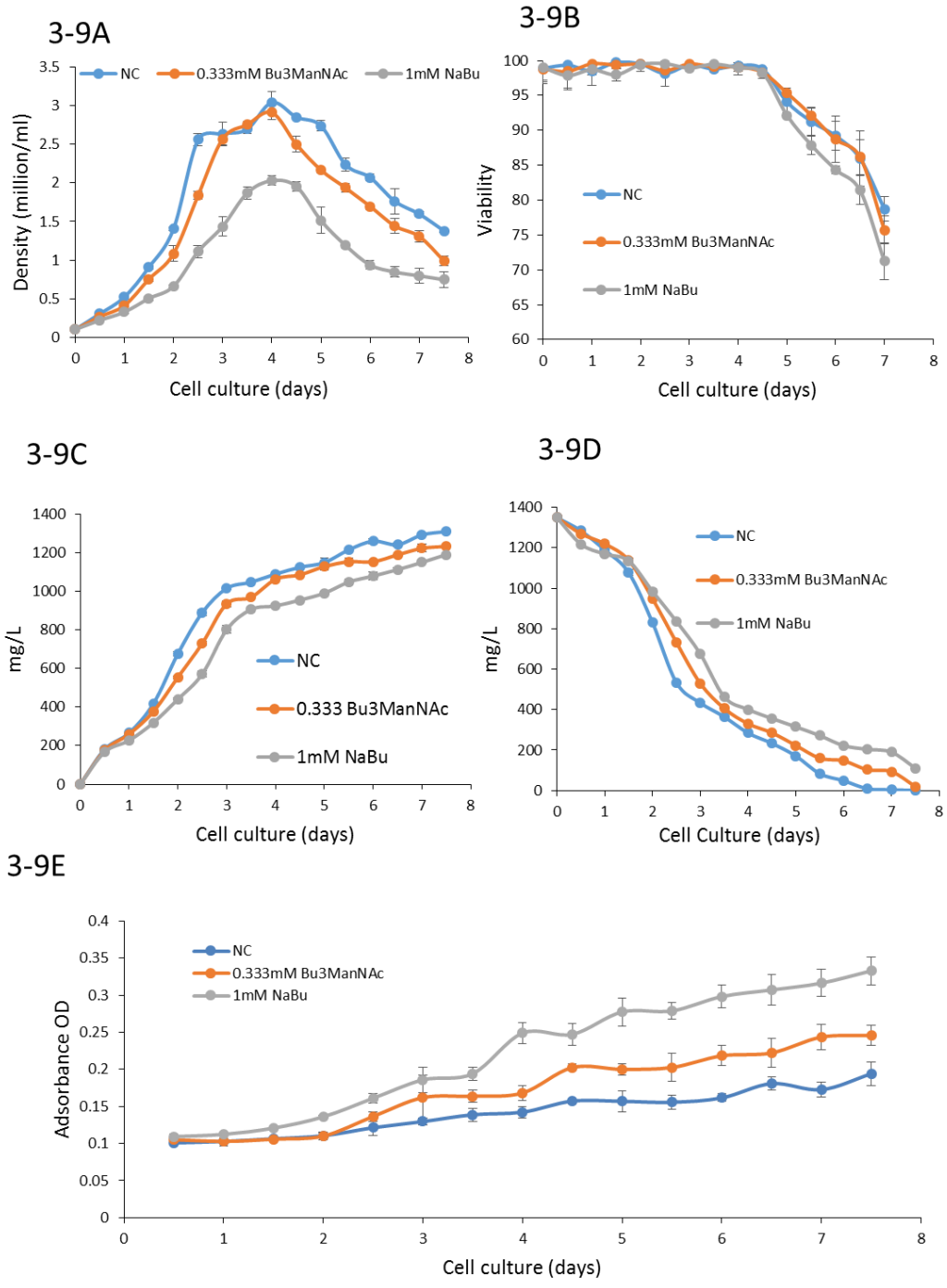

Figure 3-10. Comparison of the impact of 1,3,4-O-Bu_3ManNAc and NaBu on apoptosis and expression of apoptosis-related genes in CHO cells. (A) Microscopic analysis of Caspase 3 protein activity in 1 mM NaBu or 0.33 mM 1,3,4-O-Bu_3ManNAc treated and untreated CHOK1 cells. After fixing and staining with anti-Caspase3 antibody, cells were then incubated with DAPI for showing the nuclei areas and observed under a 20× magnification of a florescence microscope; (B) The mRNA expression of 4 apoptosis marker genes (Cul2, BAK, BAX and BCL2L11) in 1 mM NaBu or 0.33 mM 1,3,4-O-Bu_3ManNAc treated or untreated CHOK1, IgG- and EPO-expressing CHO cell lines.

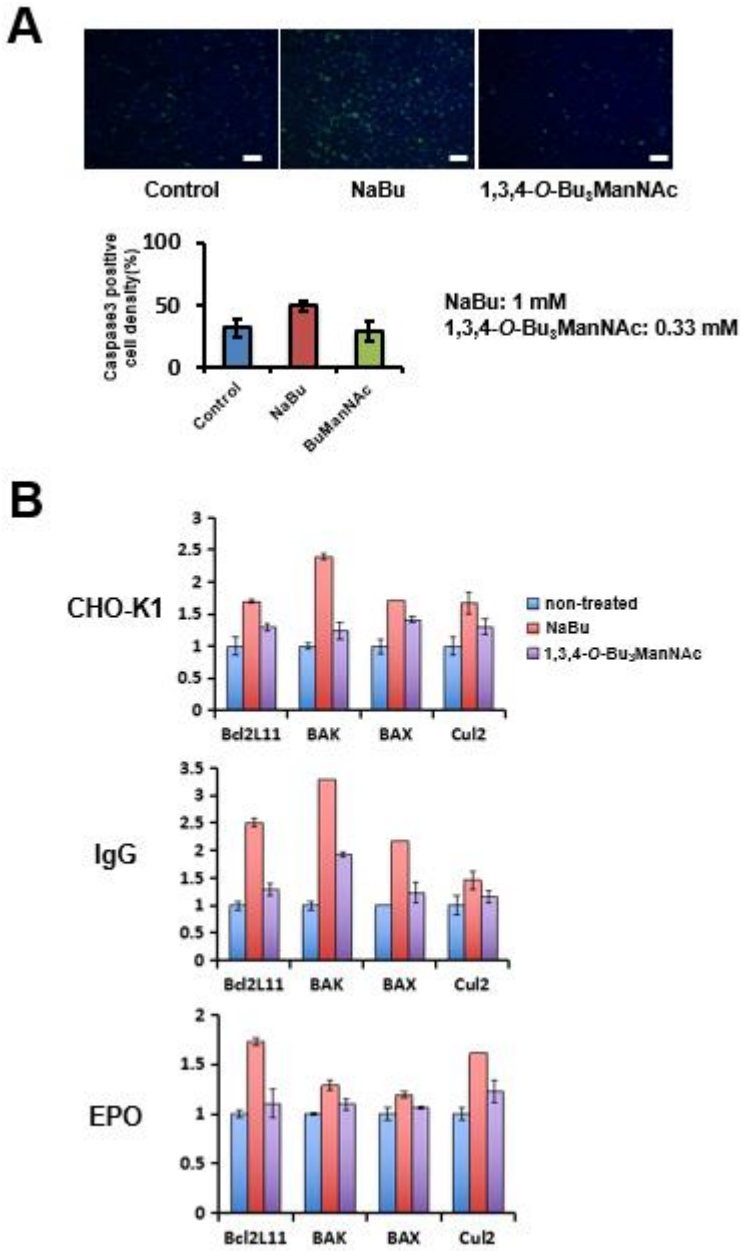

Figure 3-11. Intracellular sialic acid content of EPO expressed in wild-type and glyco-engineered CHO cells supplemented with 1.0 mM NaBu and 0.33 mM 1,3,4-*O*-Bu_3ManNAc (n=3). wt-EPO: EPO expressed in wild-type CHO cells, branch-EPO: EPO expressed in glyco-engineered CHO (overexpression of GNTIV/GNTV/ST6) with higher sialylated and complex glycans. NC: negative control as no-chemical supplemented sample. CHOK1 cells were also analyzed under same condition as control. After two days of incubation with each supplement, 2 x 10^6 cells were collected from each culture batch and subjected to the periodate/resorcinol assay to measure intracellular sialic acid.

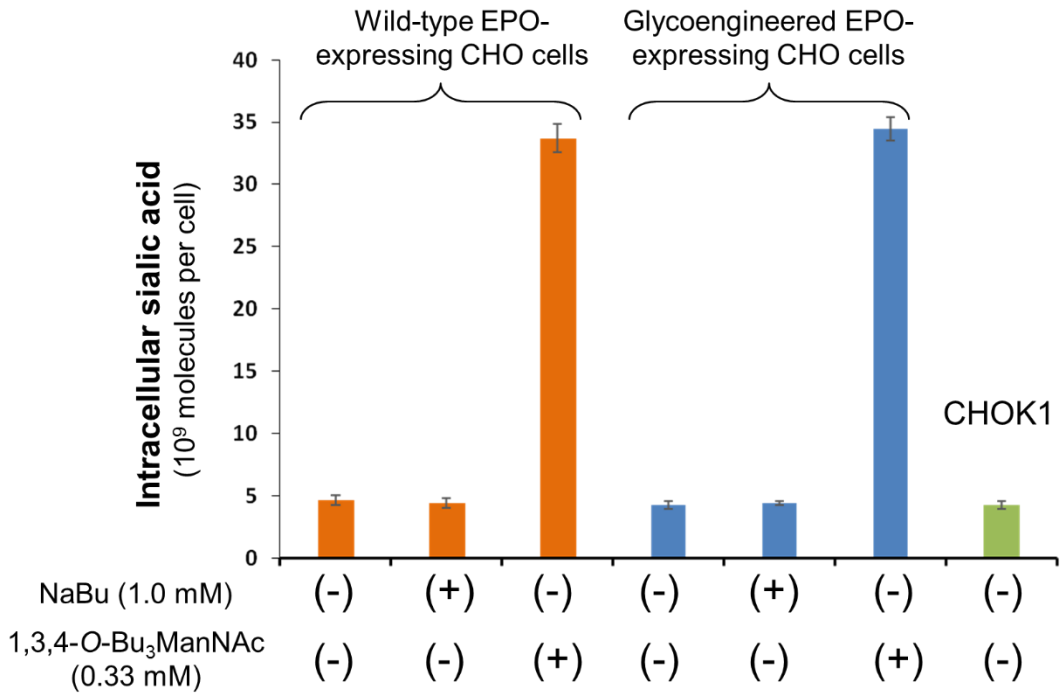

Figure 3-12. Comparison of 1,3,4-*O*-Bu_3ManNAc and NaBu on the sialylation content of recombinant EPOs expressed in wild-type and glyco-engineered CHO cells. (3-11A) Lectin blot analysis of sialylation of EPO from wild-type and glyco-engineered CHO cells treated with 1.0 mM NaBu and 0.333 mM 1,3,4-*O*-Bu_3ManNAc. Purified EPOs from untreated or treated cells were subjected to lectin blot analysis with Maackia amurensis Lectin II (MAL II) for α2,3 sialylation and *Sambucus nigra* Lectin (SNA) for α2,6 sialylation. Coomassie blue staining was used to quantify the purified EPO amount as a loading control. Coomassie blue staining was used to ensure equal amounts of purified EPO proteins loaded in each lane. EPO samples from the lectin blots showed similar molecular size as the purified EPO from Coomassie blue staining result. (3-11B) HPLC quantification of sialic acid content of EPO from wild-type and glyco-engineered CHO cells treated with 1.0 mM NaBu and 0.333 mM 1,3,4-*O*-Bu_3ManNAc. 1.5ug of purified EPO for each sample were labeled by 1,2-diamino-4,5-methylenedioxybenzene dihydrochloride (MDB) and analyzed by HPLC.

3-12A Lectin blot quantification

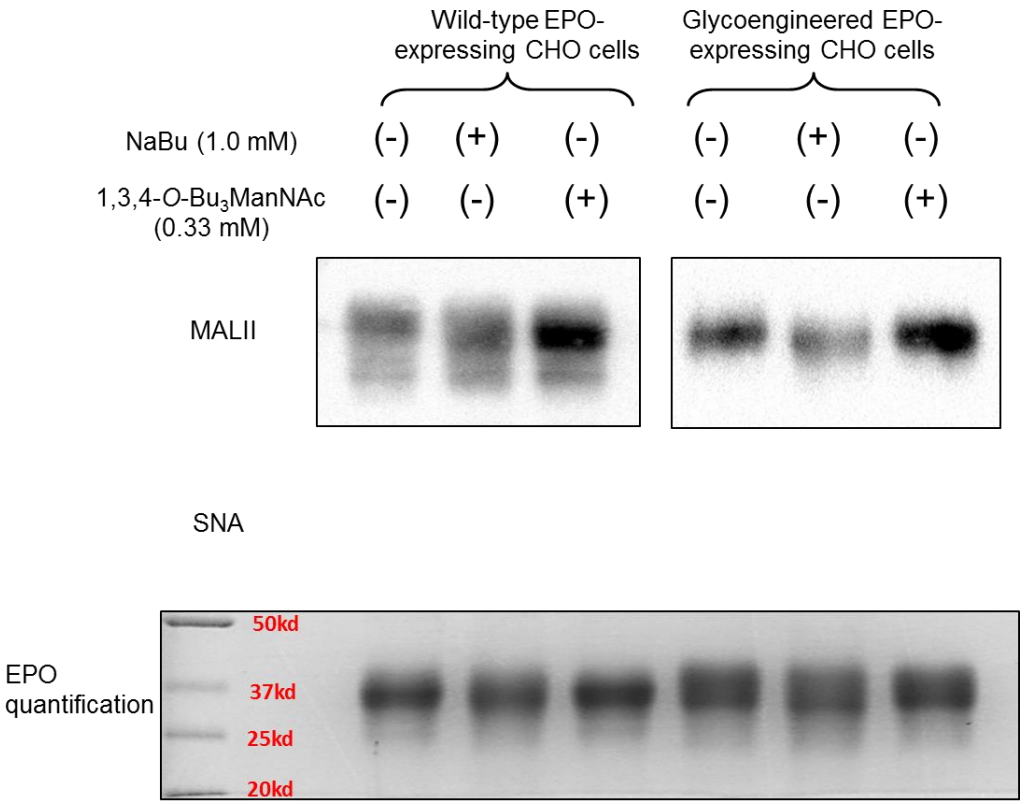

3-12B HPLC (DMB) sialic acid quantification

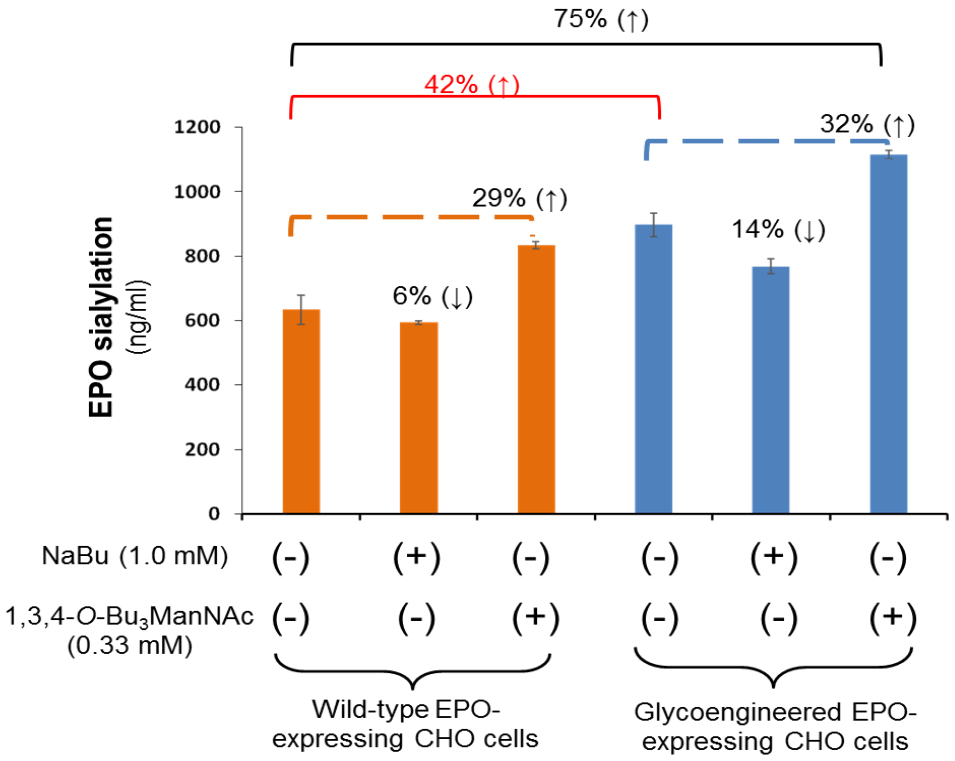

Figure 3-13. Comparison of NaBu and 1,3,4-*O*-Bu_3ManNAc treatments on the overall and site-specific sialylation occupancies of N-glycans on EPO expressed in wild-type and glyco-engineered CHO cells. (3-12A). The sialylation occupancy at each N-glycan site of wt-EPO and branch-EPO treated with NaBu and 1,3,4-*O*-Bu_3ManNAc individually. The site-specific sialylation percentage is calculated by sialylated glycopeptide PSM number in the total identified glycopeptide PSM number at each N-glycan site of EPO. (3-12B). The overall sialylation occupancy (the percentage of total sialylated glycopeptide PSM number in the total identified glycopeptide PSM number). The identified sialylated/ total glycopeptide PSM ratio of each sample was also presented below.

Figure 3-13

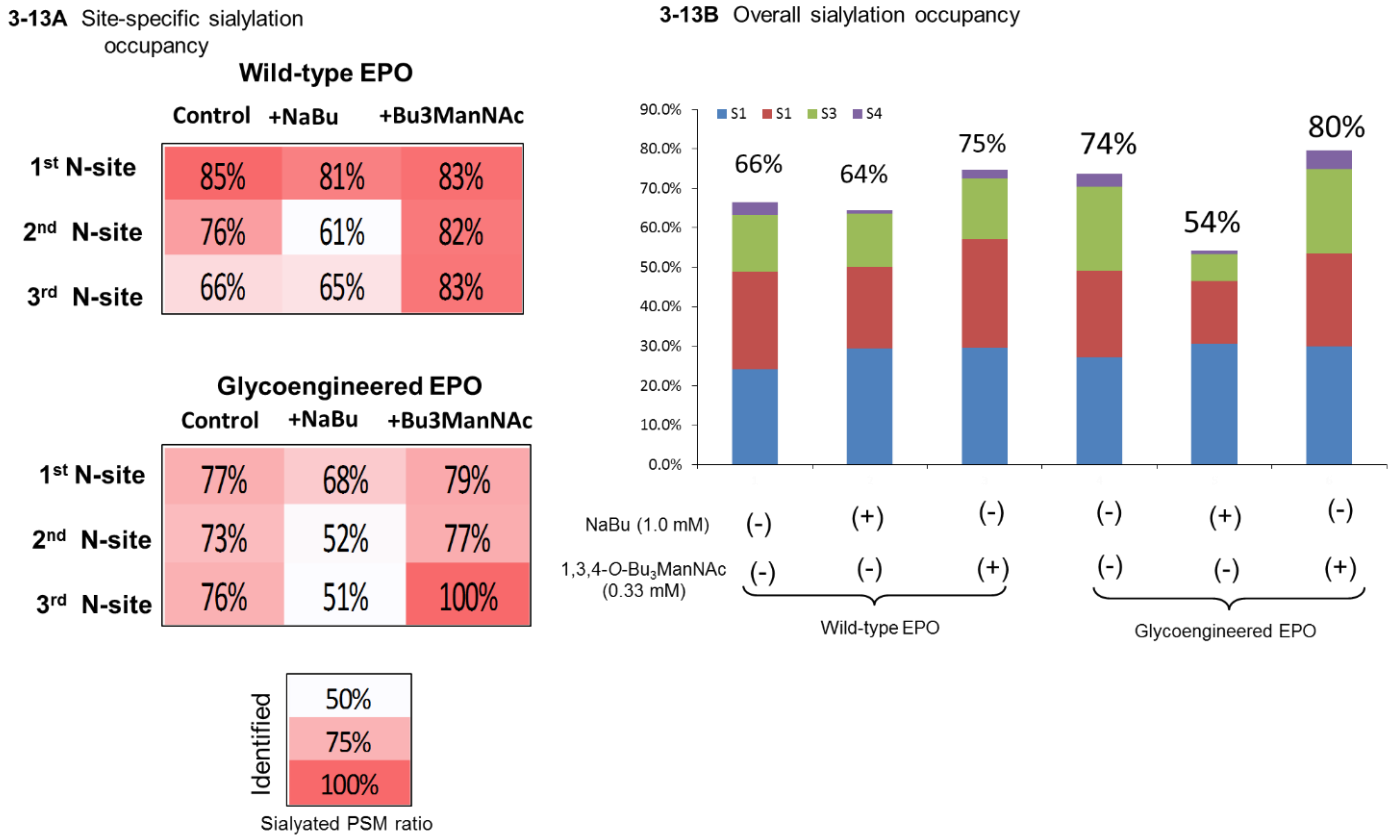

Supplemental Figure S3-1. Representative MS/MS spectra of the 5 identified N-glycopetides in EPO control sample. (S3-1A)Spectral title: AKEAENITTGCAE + N4H5F3S0G0/3. Glycopeptide sequence: AKEAENITTGCAE; N-glycan: N4H5F3S0G0 (N: HexNAc, H: Hex, F: Fuc, S: Neu5Ac, G: Neu5Gc); Charge: 3. The same labeling works for For (S3-1B)-(S3-1E). Upper figure: highlight only oxonium ions in yellow; Lower figure: after removing oxonium ions, highlghts b-, y-, peptide- and peptide-glyan(Y1) fragment ions.

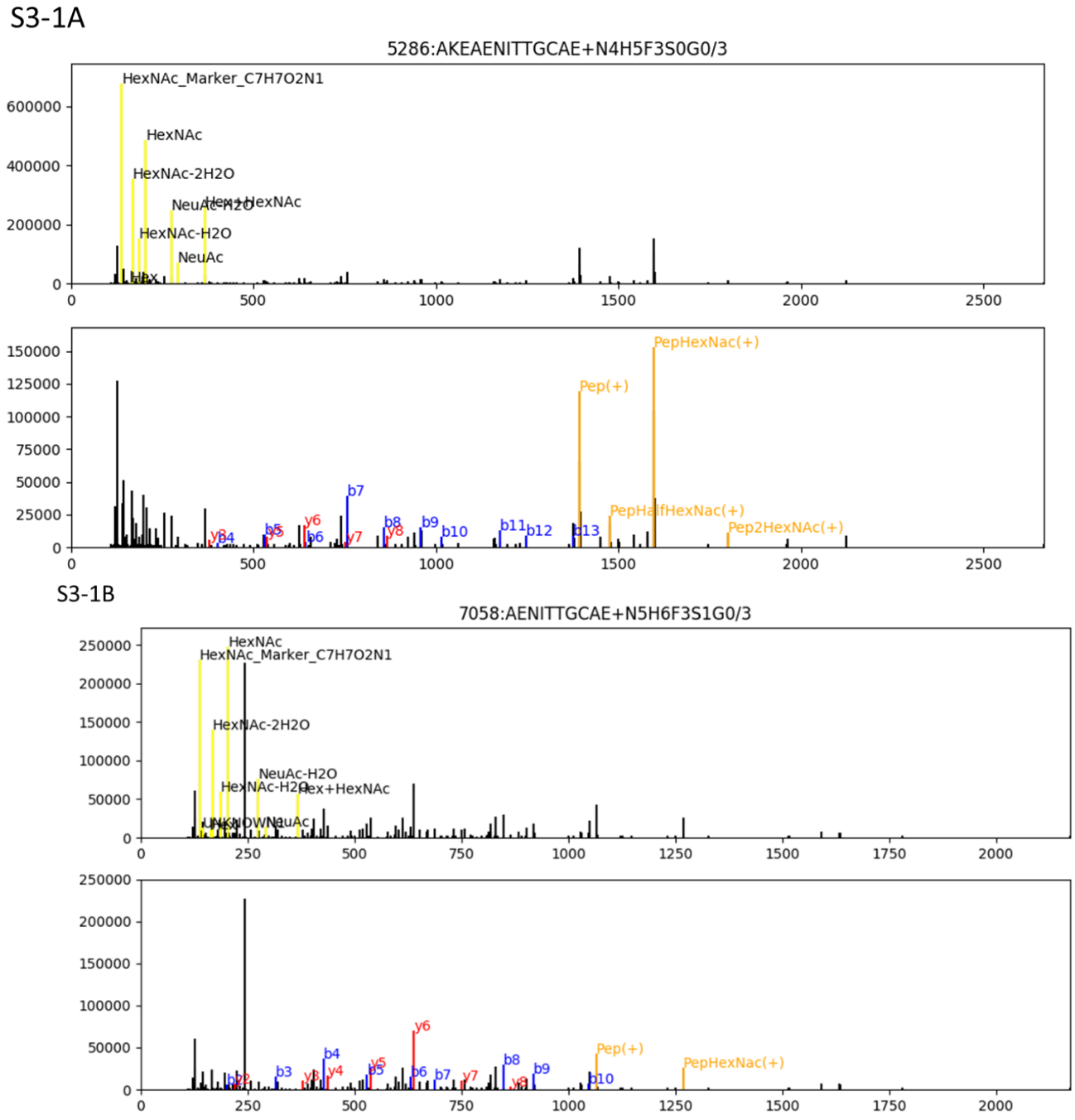

S3-1C

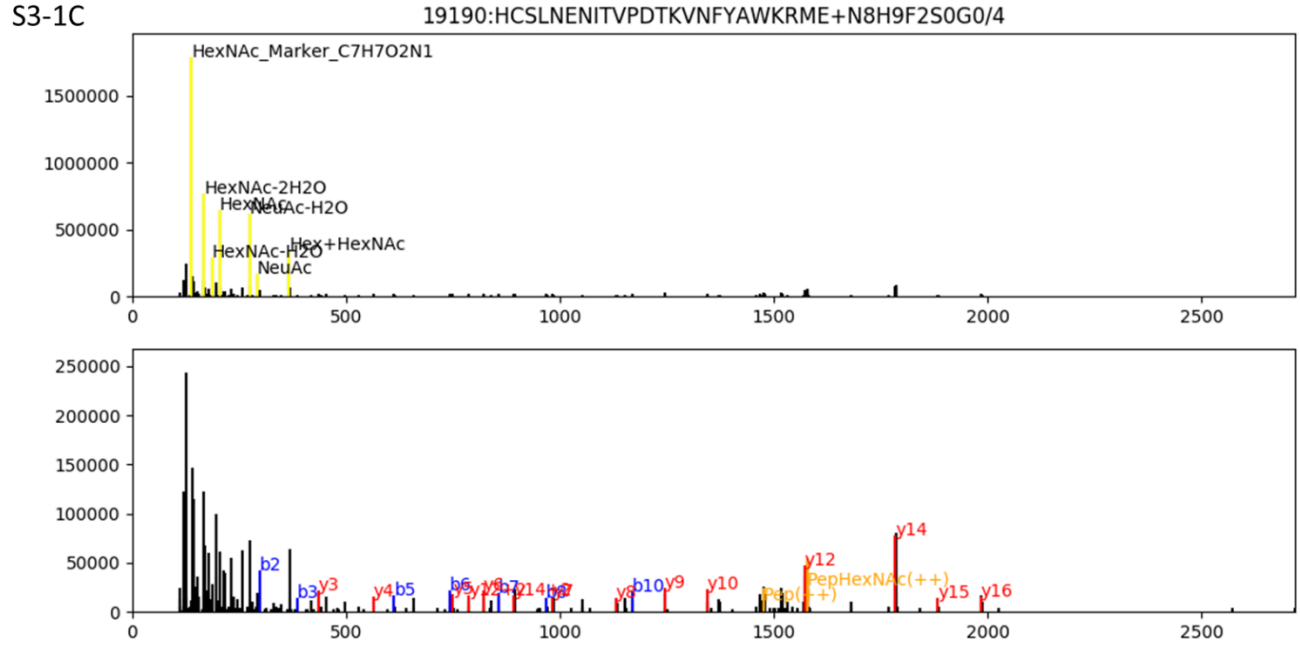
19190:HCSLNENITVPDTKVNFYAWKRME+N8H9F2S0G0/4
HexNAc_Marker_C7H7O2N1
HexNAc-2H2O
HexNAc
NeuAc-H2O
HexNAc-H2O
Hex+HexNAc
NeuAc
b2
b3
y3
y4
b5
b10
y9
y10
y12
PepHexNAc(++)
y14
y15
y16

S3-1D

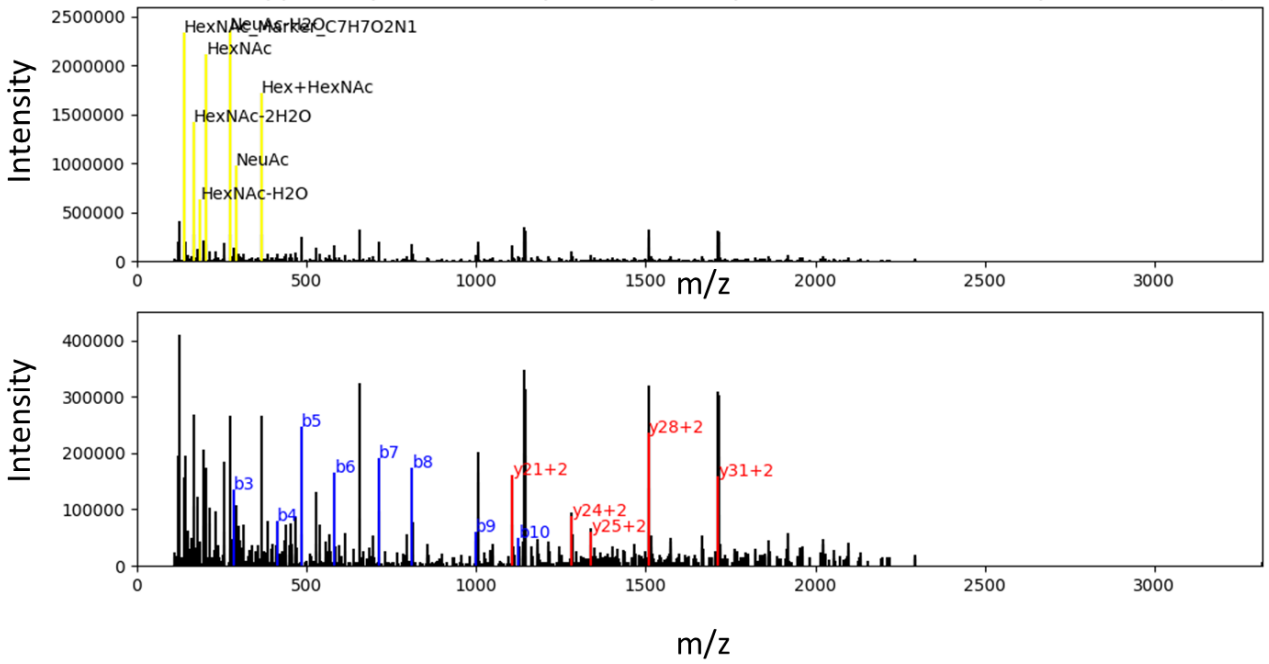
3rd N-site:
VGQQAVEVWQGLALLSEAVLRGQALLVNSSQPWEPLQLHVDKAVSGLRSLTTLLRALGAQKE+N8H9F4S0G0/7
Intensity
HexNAc_Marker_C7H7O2N1
HexNAc
Hex+HexNAc
HexNAc-2H2O
NeuAc
HexNAc-H2O
m/z
b5
b6
b7
b8
b3
b4
b9
b10
y21+2
y24+2
y25+2
y28+2
y31+2

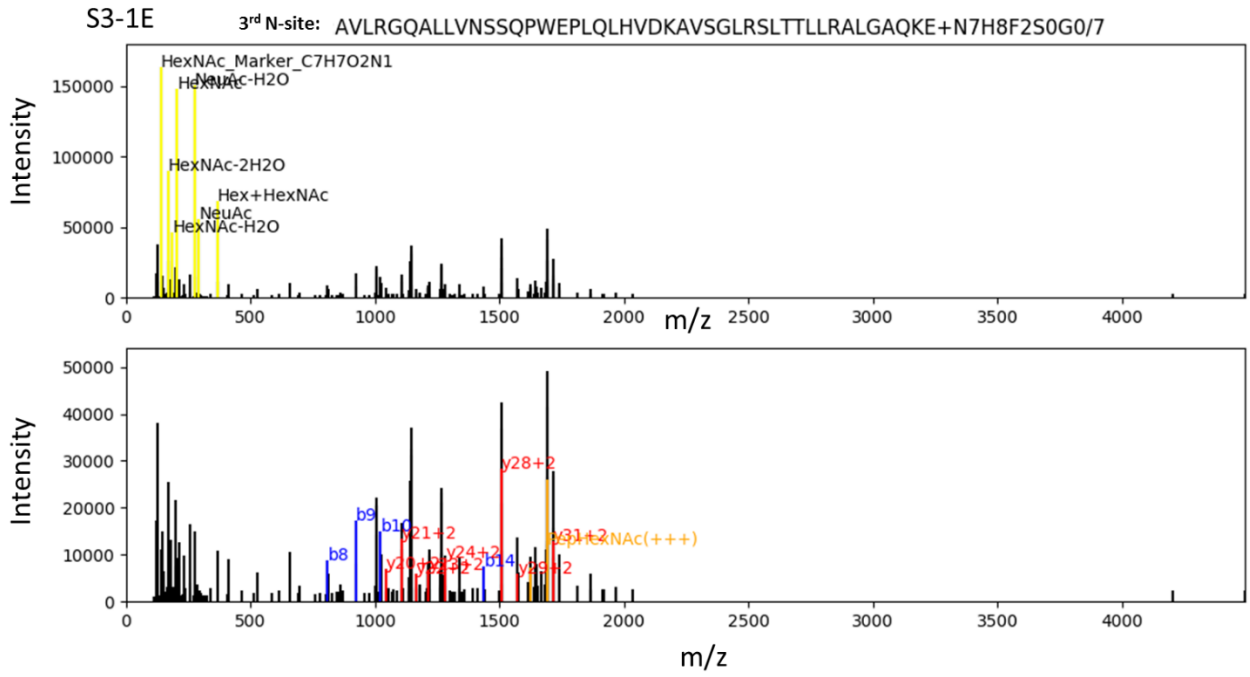

Supplemental Figure S3-2. The N-glycan antennary distribution of EPO expressed in wt-EPO and glycoengineered-EPO cell lines treated with NaBu and 1,3,4-O-Bu_3ManNAc individually.

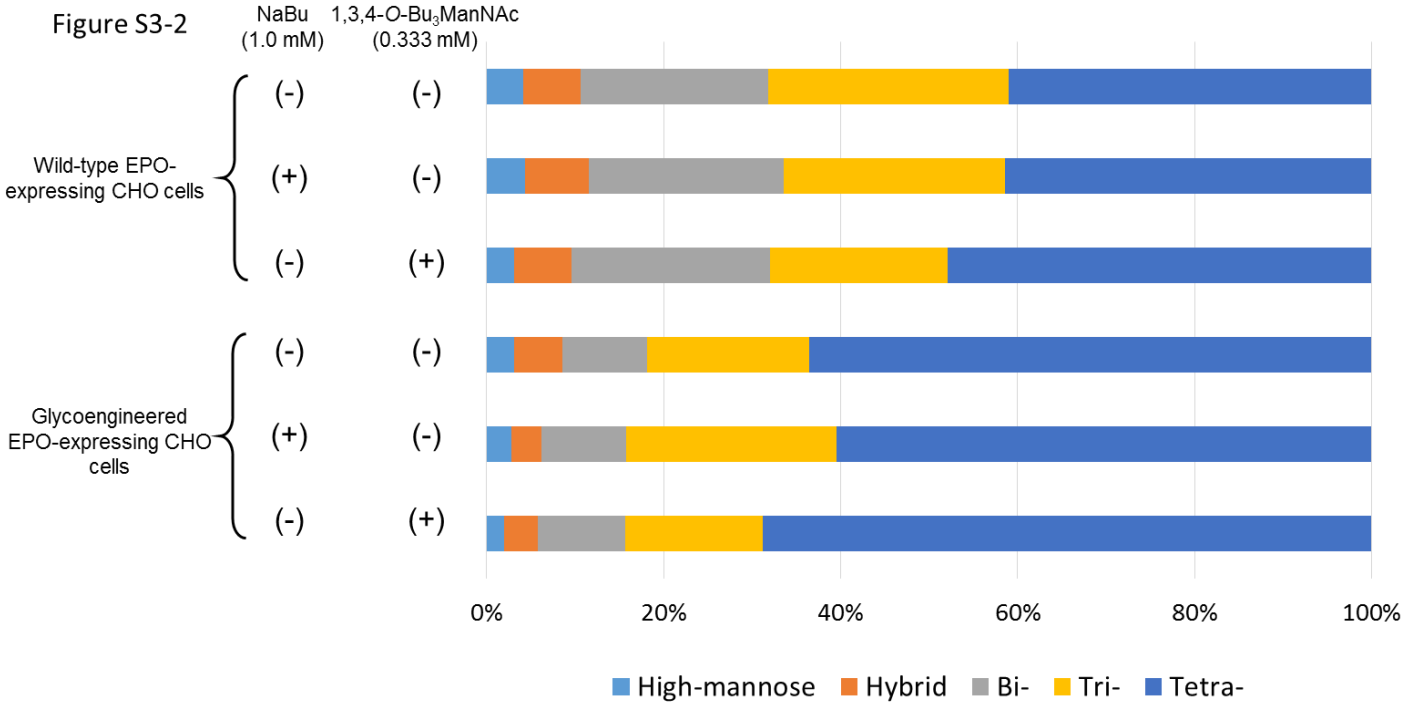

Supplemental Figure S3-3. Comparison of 1,3,4-O-Bu_3ManNAc and NaBu supplementations on some glycotransferases expression in CHO cells. Wild-type EPO- and glyco-engineered EPO-expressing CHO cells treated with 1.0 mM NaBu and 0.333 mM 1,3,4-O-Bu_3ManNAc for 2-day culture. Then, chemically-treated and untreated cells were lysed using RIPA buffer and equivalent cell lysate from each sample was subjected to immunoblot analysis to detect some glycotransferases expressions in cells under chemical treatments (n=3). Actin serves as an internal control. GNTIV: β-1,4-N-acetylglucosaminyltransferase, GNTV: β-1,6-N-acetylglucosaminyltransferase, ST6: α2,6-sialyltransferase 1, ST3: α2,3-sialyltransferase

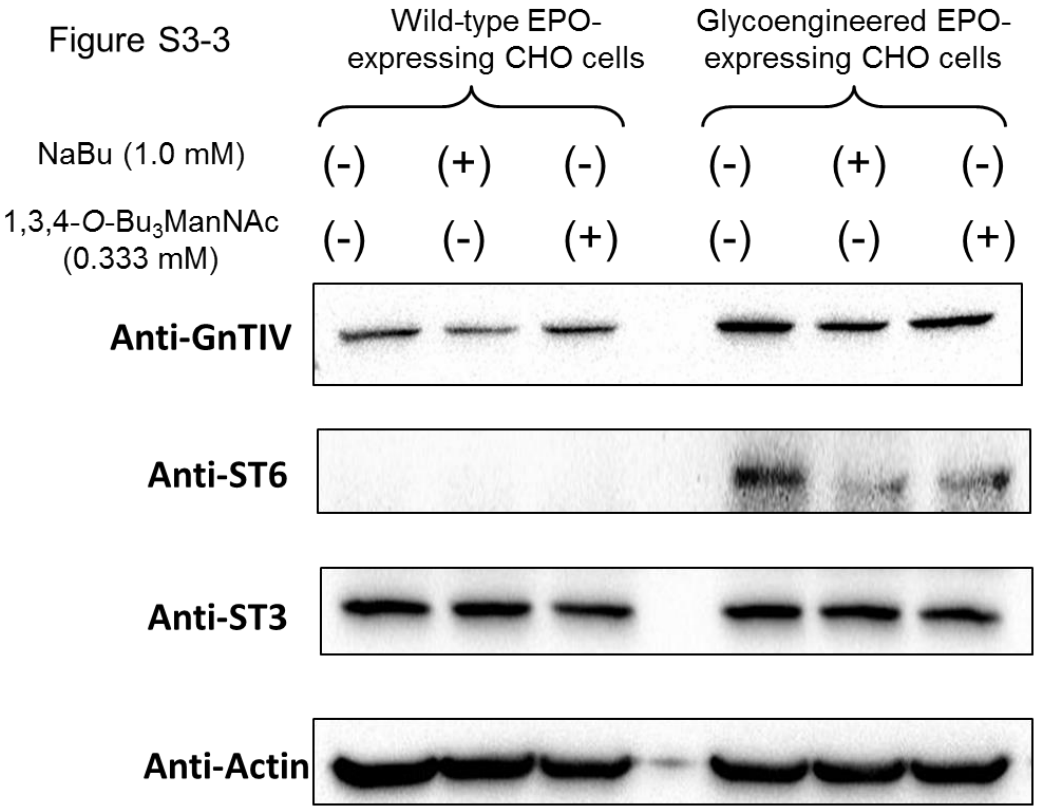

Chapter 4 Exploration of B3GNT2 and B4GALT1 for their functions on N-glycan profile of recombinant EPO in CHO cells

4.1 Summary

β-1,3-N-acetylglucosaminyltransferase 2 (B3GNT2) and β-1,4-galactotransferase 1 (B4GALT1) have been identified as two critical gene for the initiation and elongation of repeated N-acetyllactosamine (poly-LacNAc) units in mammalian cells. Poly-LacNAc serves various cellular functions in differentiation, metastasis, immune response and tumorigenesis Moreover, it also affects recombinant EPO enzymatic activity and circulatory half-life. In this work, we explored the single and dual-incorporation of two LacNAc primary genes-B3GNT2 and B4GALT1 for their roles in the initiation and elongation of LacNAc units in recombinant EPO-expressing CHO cells. However, challenges exited for incorporation of B4GALT1 into B3GNT2-overpressig CHO cells. Furthermore, we also investigated if the capping terminal sialylation impacts the LacNAc elongation or not by eliminating sialylation in CHO cells. To our surprise, the overexpression of B3GNT2 in EPO-expressing CHO cells did not increase the LacNAc content on recombinant EPO protein, but also resulted in nearly 100% elimination of sialylation on recombinant EPO and overall glyco-conjugates in CHO cells.

.

4.2 Introduction

As a common and complex protein post-translational modification, glycosylation has long been known to play major metabolic, structural and physical roles in mammalian cells [274]. Many complex and hybrid N-glycans on glycoproteins and glycolipids have elongated branches, which is composed of repeated N-acetyllactosamine units (LacNAc) and often presented as the poly-LacNAc glycan epitope [275] [276] [277], as shown in Figure 4-1A. The LacNAc glycan is initiated by the addition of a β-linked galactose (Gal) to N-acetylglucosamine (GlcNAc) to generate the ubiquitous building block Galβ1-4GlcNAc. LacNAc can be further extended by the sequential addition of GlcNAc and Gal residues, resulting in tandem repeats of LacNAc (Galβ1–4GlcNAc)n. Poly-LacNAc is identified as a scaffold for other oligosaccharides to display, such as sialyl Lewis X, and also as a binding motif for galectins [276] [278]. In addition, poly-LacNAc also serves various cellular functions in differentiation, metastasis, immune response and tumorigenesis [278]. Moreover, it has also been reported that poly-LacNAc extensions affect recombinant EPO enzymatic activity and circulatory half-life [279] [280].

For LacNAc extension, the polymerization of the alternating GlcNAc and Gal residues is catalyzed by the successive action of two glycotransferases in Golgi--UDP-GlcNAc: βGal β-1,3-N-acetylglucosaminyltransferase and UDP-Gal:βGlcNAc β-1,4-galactosyltransferase, individually [277], as shown in Figure 4-1B. For the β-1,3-N-acetylglucosaminyltransferase family (iGNTs), among 8 homologs, β3Gn-T2 has been reported to be the most effective on an oligosaccharide substrate of polylactosamine structures from *in vitro* enzyme reaction studies [281]. Furthermore, the individual knockout study of B3GNT1/2/8 individually by zinc finger nucleases (ZFNs) revealed that B3GNT2 as the key gene controlling the LacNAc initiation in CHO cells by *Lycopersicon esculentum lectin* (LEL) immunocytology [279]. Thus, β-1,3-N-

acetylglucosaminyltransferase 2 (B3GNT2) has been identified a major poly-lactosamine synthase for the poly-LacNAc initiation and extension in CHO cells. On another hand, for β-1,4-galactotransferase (B4GalT) family, there are two major B4GalTs forms related to LacNAc extension based on sequence similarity-- β-1,4-galactotransferase 1 (B4GALT1) and β-1,4-galactotransferase 2 (B4GALT2). Between these two β-1,4-galactotransferases, B4GALT1 has been widely studied and indicated as the primary β-1,4-galactotransferase for transferring Gal to GlcNAc residue through β-1,4 linkage [276, 279, 282]. The individual B4GalT knockout study by ZFNs demonstrated that knockout of B4GALT1 eliminated immunoreactivity for LacNAc, whereas knockout of B4GALT2 or B4GALT3 or B4GALT4 had no substantial effects [279]. *In vitro* enzyme reaction study also revealed that LacNAc is an acceptor substrate of B4GALT1 [282].

Although ploy-LacNAc is of significance for various cellular functions and the therapeutic recombinant protein properties, limited understanding in the literature for the biosynthesis and influence of poly-LacNAc on N-glycans is available. Interestingly, one recent study reported that the knockdown of B3GNT2 by siRNA slightly increased the sialylation content of recombinant EPO in CHO cells [275]. Typically, the terminal sialylation capping for human glycans is Neu5Ac and the N-glycans on proteins generated from CHO cells are covered with one to four sialic acids per N-glycan often with zero or one at maximum LacNAc elongation group. Therefore, in this study, we examined if capping the glycans with terminal sialylation impacts the LacNAc elongation or not by eliminating sialylation in CHO cells. We also explored the single and dual-incorporation of two LacNAc primary genes-B3GNT2 and B4GALT1 for their roles in the initiation and elongation of LacNAc units in recombinant EPO-expressing CHO cells. Our results showed that the overexpression of B3GNT2 in EPO-expressing CHO cells

surprisingly did not increase the LacNAc content on EPO protein, and further resulted in nearly complete elimination of sialylation on recombinant EPO.

4.3 Materials and Methods

4.3.1 Plasmid construction

The sequence of codon-optimized human EPO was described in Yin et al [246]. pcDNA-EPO plasmid was constructed by inserting the EPO sequence with a 6xhis tag at its C-terminal through the Hind III and Bam HI restriction sites. Human B3GNT2 gene (NCBI Gene ID: 10678) cDNA was codon-optimized and purchased from Biomatik (Wilmington, Delaware) and subcloned into pCHO1.0 vector through Avr II and BstZ17I. Human B4GALT1 gene (NCBI Gene ID: 2683) codon-optimized and purchased from Biomatik (Wilmington, Delaware) and subcloned into pEF6/V5 vector through BamH I and Not I restriction sites. There are two transcripts, which differ only at the 5' end, with approximate lengths of 4.1 kb and 3.9 kb encode the same protein. We used the longer transcript which encodes the type II membrane-bound, trans-Golgi resident protein involved in glyco-conjugate biosynthesis. While the shorter transcript encodes a protein which is cleaved to form the soluble lactose synthase.

For protein expression study, cloned human B3GNT2 and B4GALT1 cDNAs were further introduced into pBudCE4.1 through the Hind III /Bam HI sites under CMV promoter and Not I / Xho I sites under EF1apromoter, respectively. GNT4A cDNA was described previously in Yin et al [246]. Meanwhile, cloned human GNT4A and B4GALT1 cDNAs were further introduced into pBudCE4.1 through the Hind III /Bam HI sites under CMV promoter and Not I / Xho I sites under EF1apromoter simultaneously.

4.3.2 Cell culture and transfection

The generation of wild-type EPO-expressing CHO cells was described in Yin et al [246] and is abbreviated as WTEPO. The generation of sialylation-deficient CHO-K1 cells was described in Chung et al. [283] and is abbreviated as asialylated-CHO cells (dual knockouts of β-galactoside

α-2,3-sialyltransferase 4 (ST3GALT4) and β-galactoside α-2,3-sialyltransferase 6 (ST3GALT6)). We introduced the EPO gene in asial-CHO cells. With limited dilution (LDC), we generated the sialylation-deficient EPO cells and is abbreviated as asialylated-EPO cells. Subsequently, the introduction of B3GNT2, B4GALT1 individually and together in WT-EPO and asialylated-EPO cell lines was performed and abbreviated as WT-EPO-B3GNT2, asialylated-EPO-B3GNT2, WT-EPO-B4GALT1, asialylated-EPO-B4GALT1, WT-EPO-B3GNT2-B4GALT1 and asialylated-EPO-B3GNT2-B4GALT1 cell lines. For transfection, cells were seeded onto a 6-well plate at appropriate densities and transfected 24 h later using lipofectamine 3000(Thermo Fisher Scientific), according to the manufacturer's instructions. After two-day incubation, transfected stable pools were obtained based on drug selection using zeocin (EPO), puromycin (B3GNT2) and blasticidin (B4GALT1). Stable single clones were established by seeding 0.7 cell/well in 96-well plates (Corning,Tewksbury, MA) for limited dilution. All CHO cells were maintained in Ham's F12K media supplied with 10% FBS and 2 mM L-glutamine.

4.3.3 Reverse transcription PCR (RT-PCR) and Quantitative real-time PCR (qRT-PCR)

Wild-type CHO, WT-EPO, asialylated-EPO, WT-EPO-B3GNT2, asialylated-EPO-B3GNT2, WT-EPO-B4GALT1, asialylated-EPO-B4GALT1, WT-EPO-B3GNT-B4GALT1 and asialylated-EPO-B3GNT2-B4GALT1 cell lines were then harvested respectively. 10 million cells from each cell line were subjected to RNA extraction using RNeasy Mini Kit followed by manufacturer's protocol (Qiagen, Gaithersburg, MD). The isolated RNA concentration was determined by Nanodrop 2000. 1 µg of total RNA from each sample was used as the template for RT-PCR to determine the mRNA expression of the corresponding genes. Then the reverse-transcription reaction was performed by phase separation and precipitated by addition of isopropanol, followed by reverse-transcription by the SuperScript III First-Stand Sysnthesis

System (Thermo Fisher Scientific). For RT-PCR, the primer sequences for B3GNT2 were 5'-AGGAGGATCAAGCTGCTG-3' and 5'- TCATCATCAGCACTTCAGG-3'. The primer sequences for B4GALT1 were 5'- ATGAGGCTTCGGGAGC-3' and 5'-CTAGCTCGGTGTCCCG-3'. The primer sequence for internal control gene GAPDH were 5'-ATGGTGAAGGTCGGCG-3' and 5'-TTACTCCTTGGAGGCCATGTA-3'. The PCR products were further analyzed by electrophoresis on a1% agarose gel and visualized by ethidium bromide staining. Quantitative RT-PCR was performed with Absolute Blue SYBR low ROX Master Mix (Thermo Fisher Scientific) in an Applied Biosystems 7500 Real-time PCR system. GAPDH was used as an internal control using Cq value. The primers designed for qRT-PCR were the same as the ones for RT-PCR.

4.4.4 Protein purification

For purification purpose, one the cells became confluent, the media was replaced with Opti-MEM I reduced serum media (Thermo Fisher Scientific) with 2 extra culture days. Then the culture supernatants were filtered through a 0.22-mm-pore-size membrane, then concentrated and dialyzed with PBS by ultra-filtration (AmiconUltra; Millipore). With a 6xHis tag at the C-terminal of recombinant EPO, EPO from the supernatant was purified by Ni-NTA resin (Qiagen). The bound EPO were eluted with PBS supplemented with250mM immidazole, and the fractions were immediately dialyzed with PBS. The concentration of purified EPO was quantified by the bicinchoninic acid (BCA) assay and the purity of purified EPO was evaluated using 10% SDS–PAGE followed by Coomassie blue staining.

4.3.5 HPLC sialic acid quantification

The sialic acid content of purified EPO was quantified by the MDB-labeling method as described previously [249]. Briefly, 2 μg of purified EPO was hydrolyzed in 200 μL of 25 mM sulfuric

acid at 80 °C for an hour and was derivatized with 7 mM of 4,5-methylenedioxy-1,2-phenylenediamine dihydrochloride (DMB) (Dojindo, Kumamoto, Japan) at 60 °C for 2.5 hours. 10 µl of treated samples were injected onto the Agilent 1260 HPLC system with the excitation and emission at 373 and 448 nm wavelengths respectively.

4.3.6 MALDI-TOF N-glycan analysis

We applied the method of glycoprotein immobilization for glycan extraction (GIG) alone with sialic acid protection by p-toluidine [284]. 300 µg of purified EPO were denatured using Glycoprotein denaturing buffer (New England BioLabs, B1704S) and conjugated to AminoLink resin (Thermo Fisher Scientific). To protect the sialic acid groups, N-glycans were incubated with a p-toluidine (Sigma) solution and then washed sequentially with 10% formic acid, 10% acetonitrile, 1 M NaCl and H2O. For N-glycan detachment, 2mL of PNGase F (New England BioLabs, Ipswich, MA) was added to the bead mixture and incubated at 37°C for 2 h. The extracted glycans were subjected to MALDI-TOF glycan analysis. The purified glycan was analyzed by a Bruker AutoFlex MALDI-TOF spectrometer in the positive mode. The MALDI-TOF-MS parameters were set as following: mass range 500~6000 Da, laser 70%, reflective-positive-mode, and 8000 shots per sample, and CID (collision-induced dissociation) MS/MS. We searched glycan composition using database listed in GlycoWorkBench software.

4.4 Results

4.4.1 The incorporation of B3GNT2 and B4GALT1 into EPO-expressing CHO cell lines

In order to examine the single- and dual-incorporations of β-1,3-N-acetylglucosaminyltransferase 2 (B3GNT2) and β-1,4-galactosyltransferase 1 (B4GALT1) genes in wild-type EPO (WT-EPO) and sialyation-deficient EPO (asialylated-EPO) cell lines, stable clones (WT-EPO, asialylated-EPO, WT-EPO-B3GNT2, asialylated-EPO-B3GNT2,WT-EPO-B4GALT1, asialylated-EPO-B4GALT1, WT-EPO-B3GNT2-B4GALT1, asialylated-EPO-B3GNT2-B4GALT1) were generated and these eight stable cell lines along with CHOK1 control cells were subjected to RT-PCR and real-time quantitate PCR analysis for targeted gene expression at transcriptional level (Figure 4-2) and immunoblots using anti-B4GALT1 and anti-B3GNT2 antibodies for protein expression at the translational level (Figure 4-3).

In Figure 4-2A, the RT-PCR analysis revealed that the single-gene incorporation of individual B3GNT2 and B4GALT1 in WT-EPO and sialylation-deficient EPO cell lines (WT-EPO-B3GNT2, asialylated-EPO-FB3GNT2,WT-EPO-B4GALT1, asialylated-EPO-B4GALT1) showed obvious mRNA expression of targeted genes compared to their individual untreated EPO-expressing cell lines (WT-EPO and asialylated-EPO) and CHO-K1 control cells. However, the subsequent stable incorporation of B4GALT1 in B3GNT2-overexpressing cell lines resulted in very weak B4GALT1 mRNA signal, in contrast to the strong B3GNT2 signal in the RT-PCR analysis. This result indicates that the B4GALT1 gene is not expressed at the high transcriptional levels in B3GNT2-overexpressing cells. Glyceraldehyde 3-phosphate dehydrogenase (GAPDH) mRNA expression were also tested in RT-PCR analysis as an internal mRNA loading control. In order to confirm this finding, we also performed real-time quantitative PCR analysis of the single-gene and dual-gene incorporation of B3gnt2 and B4galt1 in WT-EPO and sialylation-deficient EPO cell lines, as displayed in Figure 4-2B. In accordance with the RT-PCR result

(Figure 4-2A), the real-time quantitative PCR analysis showed that the B3GNT2 mRNA level in B3GNT2 overexpressing cells (WT-EPO-B3GNT2, asialylated-EPO-FB3GNT2, WT-EPO-B3GNT2-B4GALT1 and asialylated-EPO-B3GNT2-B4GALT1) was one order of magnitude higher than the control cells (WT-EPO, asialylated-EPO and CHO-K1). The B3GNT2 mRNA content in B4GALT1-overexpressing cells (WT-EPO-B4GALT1 and asialylated-EPO-B4GALT1) showed similar level as the control CHOK1 cells. B4GALT1 mRNA expression in B4GALT1 singe-gene overexpressing cells (WT-EPO-B4GALT1 and asialylated-EPO-B4GALT1) is also higher than the control cells (WT-EPO, asialylated-EPO, WT-EPO-B3GNT2, asialylated-EPO-FB3GNT2 and CHOK1) and B3GNT2-B4GALT1 dual-gene overexpressing cell lines (WT-EPO-B3GNT2-B4GALT1, asialylated-EPO-B3GNT2-B4GALT1). Consistent with the finding in Figure 4-2A, the B4GALT1 content in B3GNT2-B4GALT1 dual-overexpressing cells (WT-EPO-B3GNT2-B4GALT1, asialylated-EPO-B3GNT2-B4GALT1) demonstrated similar B4AGLT1 mRNA content as the untreated and control cells (WT-EPO, asialylated-EPO, WT-EPO-B3GNT2, asialylated-EPO-FB3GNT2 and CHOK1). Both results in Figure 4-2 suggests that there is some inhibition for expressing B4GALT1 gene in B3GNT2-expressing cell lines at the transcriptional level.

Furthermore, immunoblot detection of B3GNT2 and B4GALT1 protein expression was performed and is presented in Figure 4-3. There was obvious B3GNT2 protein expression in B3GALT2-overexpresiing cells (WT-EPO-B3GNT2, asialylated-EPO-FB3GNT2, WT-EPO-B3GNT2-B4GALT1 and asialylated-EPO-B3GNT2-B4GALT1) but B4GNT1 protein only strongly expressed in B4GALT single-gene expressing cell lines (WT-EPO-B4GALT1, asialylated-EPO-B4GALT1). Very weak B4AGLT1 protein signal was detected in B3GNT2-B4GALT1 dual-overexpressing cell line (WT-EPO-B3GNT2-B4GALT1 and asialylated-EPO-

B3GNT2-B4GALT1), indicating that B4GALT1 expression was hampered in B3GNT2 overexpressing cell lines at protein level. The house-keeping gene GAPDH protein was also detected as an internal loading control. Combined the results from Figure 4-2 and Figure 4-3 together, it is reasonable to hypothesize that B3GNT2 inhibits B4GATL1 for gene expression at both transcriptional and translational levels.

4.4.2 The exploration of B4GALT1 and B3GNT2 expression in CHO cells

In order to further explore the relationship between B4GATL1 and B3GNT2, a bi-expression plasmid designed to simultaneously express B3GNT2 (under the EF1a promoter) and B4GALT1 (CMV promoter) was constructed (Pbud-B3GNT2-B4GALT1) along with the B3GNT2 (Pbud-B3GNT2) and B4GALT1 (Pbud-B4GALT1) single-expression using the same vector backbond and same corresponding promotors. Besides, B4GALT1 (CMV promoter) and GNT4A (EF1a promoter) bi-expressing plasmid was also constructed as a control. The illustration of plasmids constructions was presented in Figure 4-4A. Equal amount of each plasmid was transfected in equal amount of CHOK1 cells and the transient transfection result was analyzed via immunoblot two-day post-transfection. As shown in Figure 4-4B, equivalent amount of transfected cell lysate along with untransfected control CHOK1 lysate was loaded. Transfection of Pbud-B3GNT2 and Pbud-B3GNT2-B4GALT1 resulted in B3GNT2 protein expression. Transfection of Pbud-B4GALT1 and Pbud-GNT4A-B4GALT1 resulted in B4GALT1 protein while only trace B4AGLT1 protein expression was detected from Pbud-B3GNT2-B4GALT1 sample. Anti-GNT4A immunoblot only detected GNT4A protein overexpression in Pbud-GNT4A-B4GALT1 transfected cells. The transient transfection result suggests that B3GNT2 inhibits B4GALT1 expression in CHO-K1 cells, while GNT4A and B4GALT1 did not impact each other's expression. Further, amino acid homology analysis revealed that B3GNT2 and B4GALT1

exhibit 24.56% similarity, B3GNT2 and GNT4A contain 46.15% similarity and B4GALT1 and GNT4A have 35.00% similarity through the NCBI Blast protein sequence alignment tool (https://blast.ncbi.nlm.nih.gov).

4.4.3 Characterizing the purified EPO protein from glyco-engineered CHO cell lines

Furthermore, the recombinant EPO from the 8 tested CHO cell lines was purified and equal amounts of purified EPO protein was loaded for SDS-PAGE followed with Coomassie Blue staining (Figure 4-5A). We observed that wild-type EPO from CHO cells had a molecular weight around 37 kilodalton (kDa), which is in accordance with previous publications [7, 172]. The elimination of sialic acid on recombinant EPO (asialylated-EPO) reduced the molecular weight of EPO, which showed a faster migration rate on Figure 4A. Surprisingly, the EPO band from WT-EPO-B3GNT2 as well as asialylated-EPO-B3GNT2 cell lines both presented significantly lower and similar band size (approximately 25 kDa), indicating a faster migration rate compared to wild-type EPO and asialylated-EPO proteins. Moreover, the single introduction of B4GTALT1 in WT-EPO and asialylated-EPO (WT-EPO-B4GALT1 and asialylated-EPO-B4GALT1) cell lines obviously increased the EPO protein size, showing a slower migration rate than other tested samples (Figure 4-5A).

To our surprise, the overexpression of B3GNT2 significantly decreased the molecular weight of recombinant EPO both from wild-type and sialylation-deficient CHO cell lines. To investigate this phenomena, HPLC sialic acid quantification was applied to detect the sialic acid content on each EPO sample. Briefly, sialic acids were released from equal amounts of purified recombinant EPO samples, derivatized with a fluorescence-labeling compound, 1,2-diamino-4,5-methylenedioxybezene dihydrochloride (MDB), and then separated on a reversed-phase C18 column. Interestingly, as shown in Figure 4-5B, recombinant EPO proteins from the B3GNT2-

expressing cell line (WT-EPO-B3GNT2) showed similar levels of sialylation content as EPO from sialylation-deficient cell line (asialylated-EPO). Plus, the sialic acid content of EPO from B3GNT2-expressing sialylation-deficient cell line (asialylated-EPO-B3GNT2) was even lower among all the tested samples. Overexpression of B4GALT1 in WT-EPO cell line increased the sialylation content about 32% compared with wild-type EPO. While overexpression of B4GALT1 in a sialylation-deficient cell line (asialylated-EPO-B4GALT1) did not have an obvious change on the sialylation level compared to the EPO-expressing sialylation-deficient cell line (asialylated-EPO). This HPLC result indicates the change in sialic acid content of total glycans on recombinant EPO, including both N- and O-glycans.

4.4.4 Elucidation of recombinant EPO protein N-glycan profile from glyco-engineered CHO cell lines

Given the changes in protein size and sialylation levels following expression of glycosyltransferases, the next step was to elucidate the specific N-glycan structures attached to recombinant EPO from different cell variants. N-glycan structures were released from purified recombinant EPO derived from PNGase F digestion, and then analyzed on a matrix assisted laser desorption ionization-time of flight mass spectrometry (MALDI-TOF) mass spectrometer. The N-glycan profiles derived from recombinant EPOs produced in wild-type and glycoengineered cell lines are displayed in Figure 4-6. Each peak was labeled with its corresponding predicted structure. The decrease in the larger N-glycans observed in the mass spectra following an increase in transferase modification is qualitatively consistent with the faster migration rates observed on the Commassie blue staining result (Figure 4-5A) for the recombinant EPO from the B3GNT2-containning cell lines.

In order to evaluate the LacNAc changes for individual sugars, the LacNAc analysis was

classified based on the number of GlcNAc-Gal units per N-glycan in each sample, overall LacNAc coverage, and average LacNAc unit per N-glycan (Table 4-1). The removal of sialic acid capping increased the average LacNAc units slightly and coverage on the EPO sample (asialylated-EPO). Furthermore , the overexpression of B4GALT1 in both WT-EPO and asialylated-EPO samples enhanced the average LacNAc units slightly compared to their corresponding control samples, with which asialylated-EPO-B4GALT1 showed more LacNAc units and coverage than WT-EPO-B4AGLT1. This finding is in accordance with our hypothesis that the terminal Neu5Ac suppressed the LacNAc elongation on glycoproteins in CHO cells. In contrast, and also consistent with the coomassie blue and HPLC results, the overexpression of B3GNT2 surprisingly reduced the number of LacNAc units and LacNAc coverage for both wild-type EPO and sialylation-deficient EPO. As the overexpression of B4GALT1 in B3GNT2-expressing cells is very weak, EPO protein from WT-EPO-B3GNT2-B4AGLT1 and asialylated-EPO-B3GNT2-B4GALT1 cell lines displayed a LacNAc profile consistent to the one for their counterparts in WT-EPO-B3GNT2 and asialylated-EPO-B3GNT2 cell lines.

Finally, the sialylated N-glycans on recombinant EPO were classified according to the numbers of terminal sialic acid residues on the observed N-glycan structures for the eight cell lines (Table 4-2). The overexpression of B4GALT1 led to a decrease in the recombinant EPO levels with 2 and 3 sialic acid and an increase in the N-glycans with 0 and 1 sialic acids on wild-type EPO. The dual-knockout of st3gal4 and st3gal6 results in 100% asialylatedylated EPO (asialylated-EPO). Nevertheless, the overexpression of B3GNT2 in both wild-type and sialylation-deficient CHO cell lines led to 99% and 99% asialylatedylated EPO individually. The introduction of B4GALT1 in sialylation-deficient CHO cell line also slowed almost completely asialylatedylated EPO. This result was consistent with the HPLC sialic acid quantification study (Figure 4-5B).

4.5 Discussion

In this study, the impacts of B3GNT2 and B4AGLT1 along with the terminal sialylation in EPO-expressing CHO cells was investigated. The sialic acid is capped at the terminal of N-glycan structure in mammalian cells with LacNAc elongation. We first explored whether the capping terminal sialylation inhibit the LacNAc extension on recombinant glycoprotein or not by knocking out two critical sialyltransferases in CHO cells. The dual-knockout of ST3GALT4 and ST3GALT6 significantly decreased Neu5Ac sialylation content with almost undetectable sialylation level on recombinant EPO proteins from MS N-glycan analysis (Figure 5 and Table 2). Compared to WT-EPO, the removal of sialic acid capping increased the average LacNAc units per N-glycan from 3.54 to 4.02 and coverage from 93.46% to 97.44% on recombinant EPO protein (asialylated-EPO). Also, the overexpression of B4GALT1 in both WT-EPO and asialylated-EPO samples enhanced the LacNAc units slightly compared to their corresponding control samples, with which asialylated-EPO-B4GALT1 showed more LacNAc units and coverage than WT-EPO-B4AGLT1 sample. This results revealed that elimination of terminal sialic acid promoted the LacNAc elongation on N-glycans in CHO cells.

From previous publications, B3GNT2 and B4AGLT1 are identified as two critical genes for the initiation and elongation of LacNAc units in mammalian cells. We explored the individual and dual-incorporation of these two LacNAc primary genes-B3GNT2 and B4GALT1-for their roles on the initiation and elongation of LacNAc units on recombinant EPO protein expressed from CHO cells. To our surprise, unexpected results were revealed with the single gene B3GNT2introduction. The overexpression of B3GNT2 in both WT-EPO and asialylated-EPO cell lines both didn’t increase the LacNAc units on recombinant EPO proteins. Otherwise, it displayed adverse effect on N-glycan profile: 1.The overexpression of B3GNT2 reduced the

average LacNAc number per N-glycan on EPO (Table 1); 2. The sialyation nearly completely disappeared after B3GNT2 incorporation in wild-type EPO cell line (Figure 4B and Figure 5 and Table 2), which is consistent with the smaller EPO size and faster migration rate on Figure 4A. Regarding to asialylated-EPO sample, overexpression of B3GNT2 in wild-type EPO cells showed a similar sialic acid content as the sialylation-deficient EPO protein from both HPLC sialic acid quantification (Figure 4B) and MS N-glycan characterization (Figure 5 and Table2), indicating B3GNT2 overexpression served a sialylation inhibition function, as similar as α2,3 sialyltransferases-knockout did in CHO cells, which is consistent with a previous study that the knockdown of B3GNT2 increased the sialylation on recombinant EPO protein. Meanwhile, the overexpression of B3GNT2 in asialylated-EPO cell line completely achieved sialylation-free EPO proteins. Moreover, we evaluate the effect of B3GNT2 and B4GALT1 overexpression on the sialylation of total glyco-conjugates (glycoproteins and glycolipids) in wild-type and asialylated-CHO cells. Total cell lysates from wild-type and glyco-engineered CHO cells were subjected to HPLC quantification for evaluation of sialic acid content on glycoproteins and glycolipids (Supplemental Figure S4-1). The result revealed that B3GNT2 overexpression reduced the sialylation content at total cell lysate level both in CHOK1 and asialylated-CHO cells, which matches the recombinant EPO protein result in Figure 4-5B.In order to further explain this phenomena, we investigated the expression of sialyltransferases (β-galactoside α-2,3-sialyltransferase 3,4 and 6 ST3GALT3, ST3GALT4 and ST3GALT6)) in wild-type and glyco-engineered CHO cells at transcriptional level, as shown in supplemental Figure S4-1 and S4-2. The RT-PCR and qPCR quantification results demonstrated that no significant difference detected on the mRNA expression of ST3GALT3 enzyme in all tested 8 samples. No great discrimination were observed on ST3GALT4 and ST3GALT6 mRNA expression among cell

lines developed from wild-type CHO (WT-EPO, WT-EPO-B3GNT2 and WT-EPO-B4AGLT1 and CHO cell lines). Similar results also observed among cell lines developed from sialylation-deficient CHO (asialylated-EPO, asialylated-EPO-B3GNT2, asialylated-EPO-B4GALT1 and asialylated-CHO). In accordance with a recent paper from our group {Chung, 2017 #348}, the knockout of SY4GALT1 resulted in the absence of ST4GALT4 mRNA signal on Figure S 4-1 and S4-2. The knockout of ST3GALT6 changed ST4GALT6 mRNA size on Figure S 4-2 and S4-3. Thus, we concluded the overexpression of B3GNT2 did not interfere with the sialyltransferase expression at translational level, although it inhibited the sialylation both on glycoprotein and glycolipids in CHO cells.

Another interesting finding in this project is B4GALT1 cannot be incorporated in B3GNT2-overexpressing CHO cell lines (Figure 4-2 and 4-3). We attempted to introduce human B4GALT1 in both WT-EPO-B3GNT2 and asialylated-EPO-B3GNT2 cell lines twice, but were still unable to generate a dual-overexpression cell line with appropriate B4GALT1 expression compared to their corresponding WT-EPO-B4GALT1 and asialylated-EPO-B4GALT1 control cell lines. For example, the immunoblotting result of WT-B3GNT2-B4GALT1 clone selection was presented in Supplemental Figure S4-4. Therefore, we choose clones with the strongest B4GALT1 expression in B3GNT2-B4GALT2 candidates, although its B4GALT1 expression was dramatically low compared to B4GALT1-expressing CHO cells. As shown in Supplemental Figure S4-4, the B4GALT1 expression in the top WT-EPO-B3GNT2-B4GALT1 clones is relatively very weak compared to the B4GNT1 expression in WT-EPO-B4GALT1 clone. Besides, MALDI-TOF N-glycan elucidation also revealed that the GlcNac/Gal ratio increased nearly one fold for EPOs expressed in B3GNT2-expression CHO and asialylated-CHO cells, while GlcNac/Gal ratio declined a little for EPOs expressed in B4GAT1-expression CHO and

asialylated-CHO cells (Table 4-3). A recent paper {Sumit, 2019 #753} pointed out that the nucleotide sugar donor (NSD) transport protein in Golgi encoded by SLC35A2 serves as a transporter for UDP-Gal, UDP-GalNAc, UDP-GlcNAc {Song, 2013 #754} {Hartley, 2018 #755}. In other words, these three nucleotide sugar substrates competes for each other for transporting into Golgi and further integration on the glycan structure. For LacNAc extension, UDP and UDP are indispensable substrate, even though the levels of average GlcNc per N-glycan on WT-EPO-B3GNT2 and asialylated-EPO-B3GNT2 were similar to the levels on WT-EPO and asial-EPO, the reduction of average Gal per N-glycan definitely hampered the elongation of LacNAc synthesis for WT-EPO-B3GNT2 and asialylated-EPO-B3GNT2. The reduction of LacNAc content on WT-EPO-B3GNT2 and asial-EPO-B3GNT2 was attributed to the lack of galactose on N-glycan.

Contributions from Collaborators:

Dr. Xiaozhi Ren contributed to qPCR experimental design. Dr. Eric Sakowski and Dr. Sarah Preheim at Environmental Engineering department at JHU for providing the qPCR machine.

Figures and Tables

Figure 4-1. (4-1A) The typical complex N-glycan structures with bi-, tri- and tetra-branches found on glycoproteins from mammalian cells. (4-1B.) The synthesis of poly-LacNAc chain in Golgi through the formation of (β1-4Gal-β1-3 GlcNAc)n units.

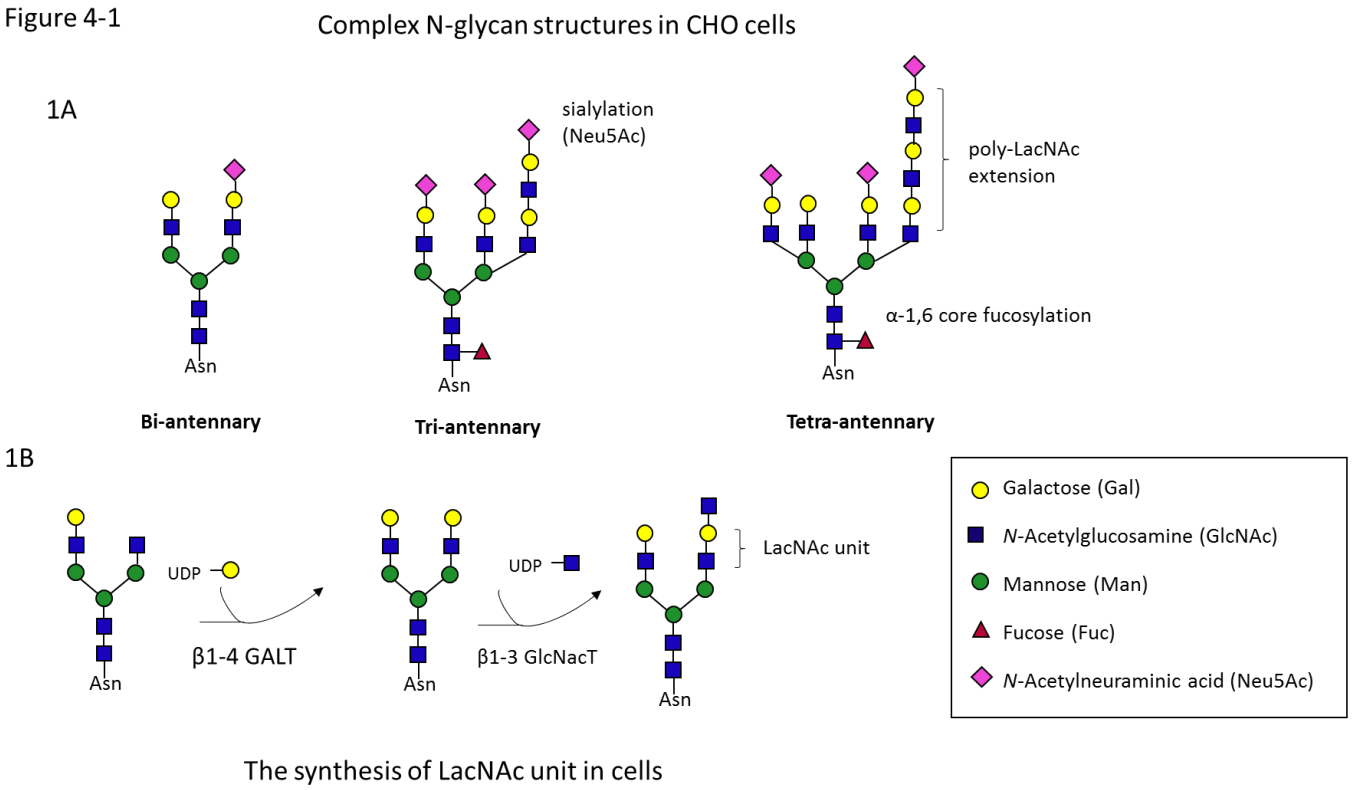

Figure 4-2. RT-PCR (4-2A) and qPCR (4-2B) analysis for B3GNT2 and B4GALT1 expressions in both WT-EPO and asialylated-EPO cell lines.

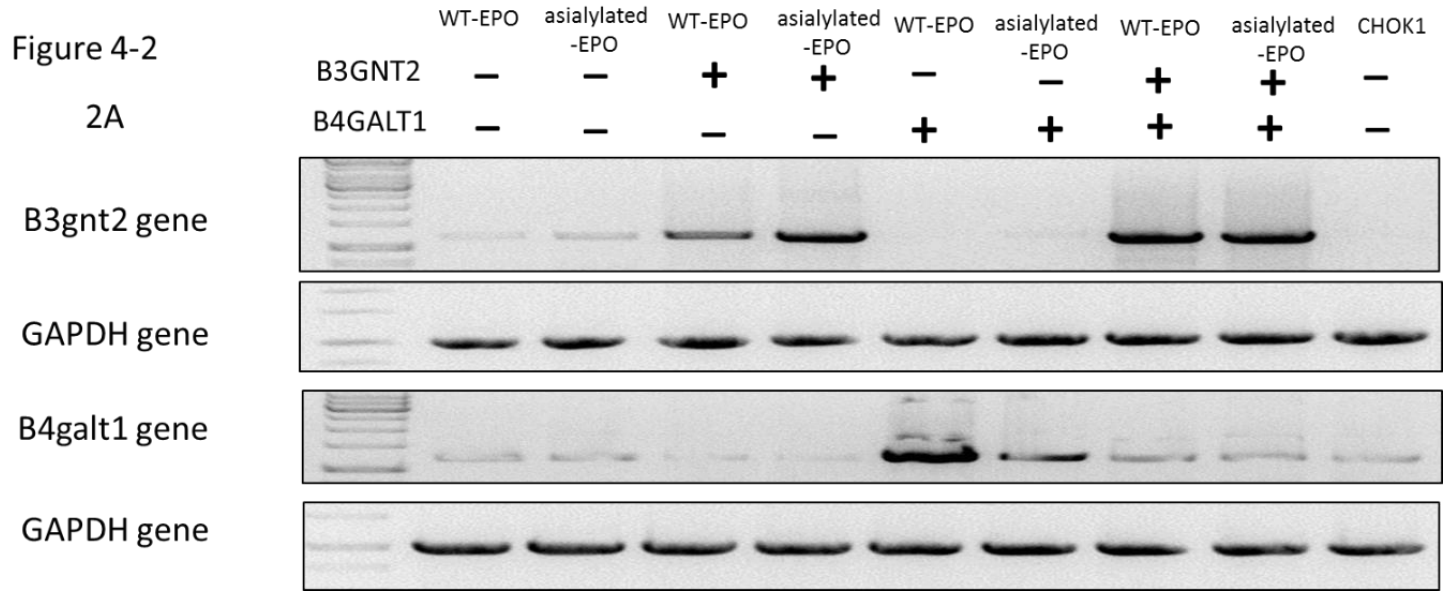

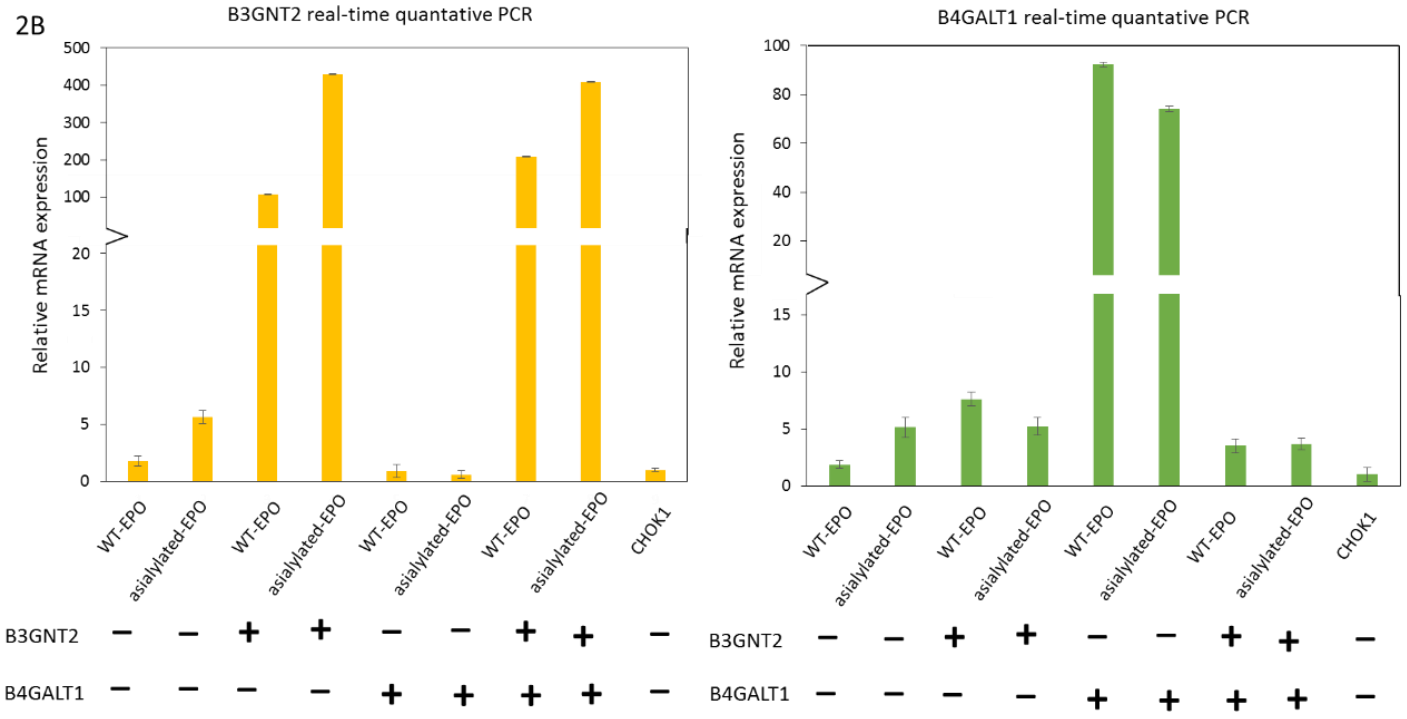

Figure 4-3. Immunoblotting of transfected human glycotransferases in different recombinant EPO-expressing CHO cell lines. GAPDH serves as internal control.

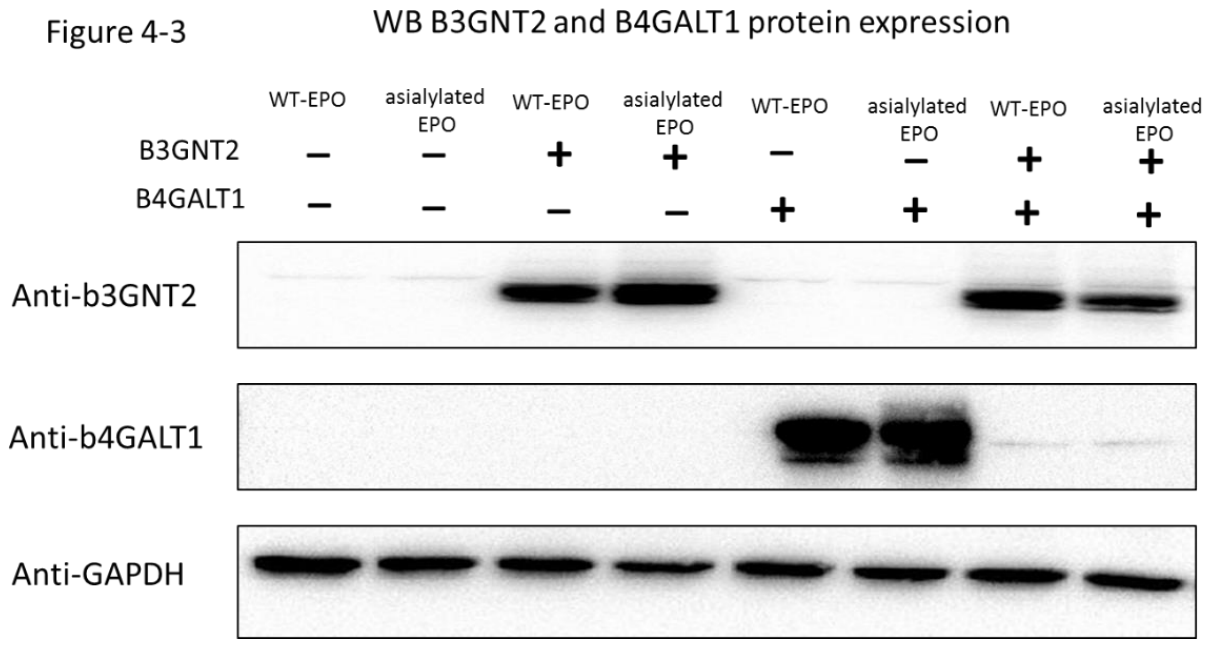

Figure 4-4. The single- and dual-expression of B3GNT2 and B4GALT1 in CHOK1 cells. (4-4A). The single- and bi-expression plasmid constructions. (4-4B).The immunoblotting analysis of B3GNT2 and B4GALT1 expressions in CHO-K1 cells at transient transfection level.

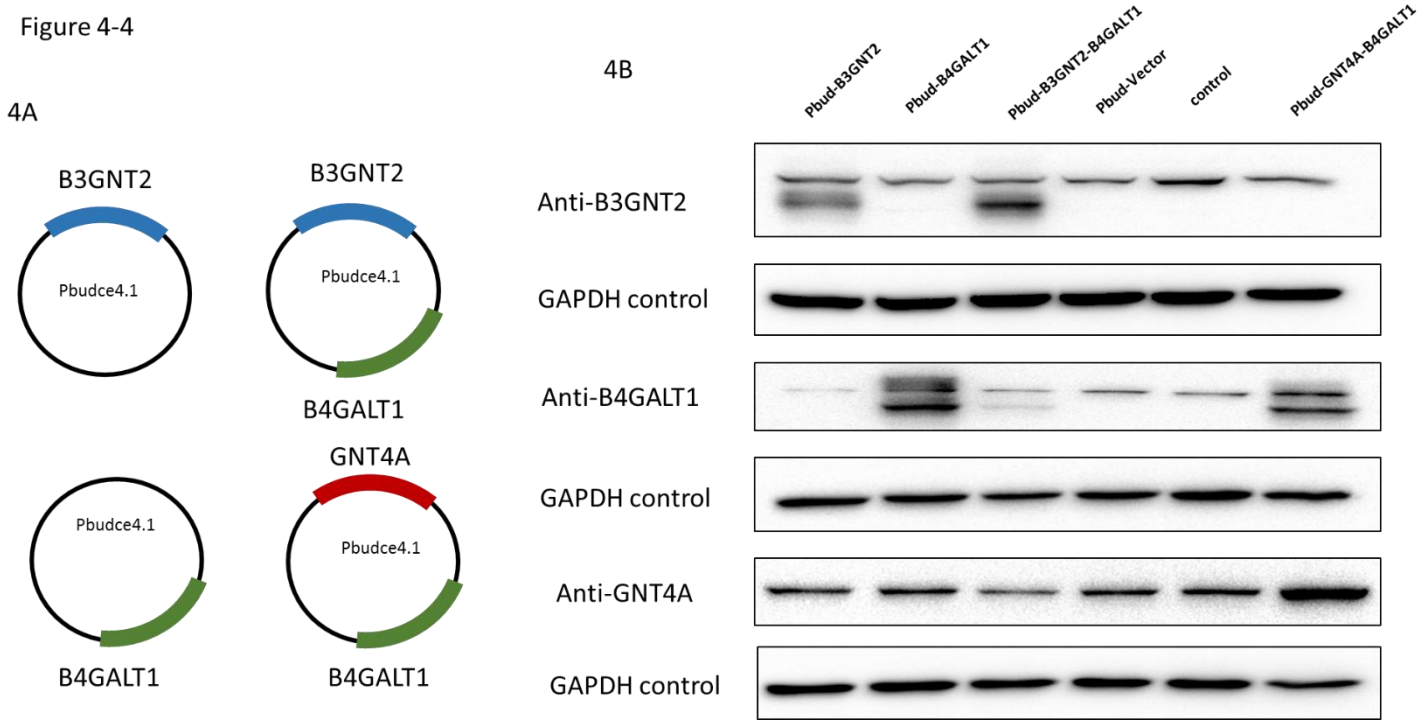

Figure 4-5. (4-5A) Coomassie blue staining of purified recombinant EPO protein from glyco-engineered CHO cell lines. Equal amount of purification protein were loaded. (4-5B) The HPLC sialic acid analysis. Sialic acids were released from equal amount of purified recombinant EPO samples, derivatized with a fluorescence-labeling compound, 1,2-diamino-4,5-methylenedioxybezene dihydrochloride (MDB), and then separated on a reversed-phase C18 column.

Figure 4-5

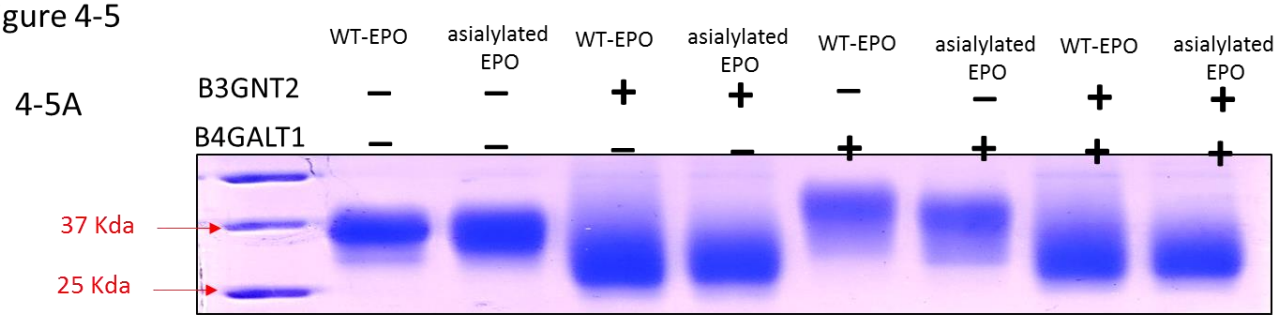

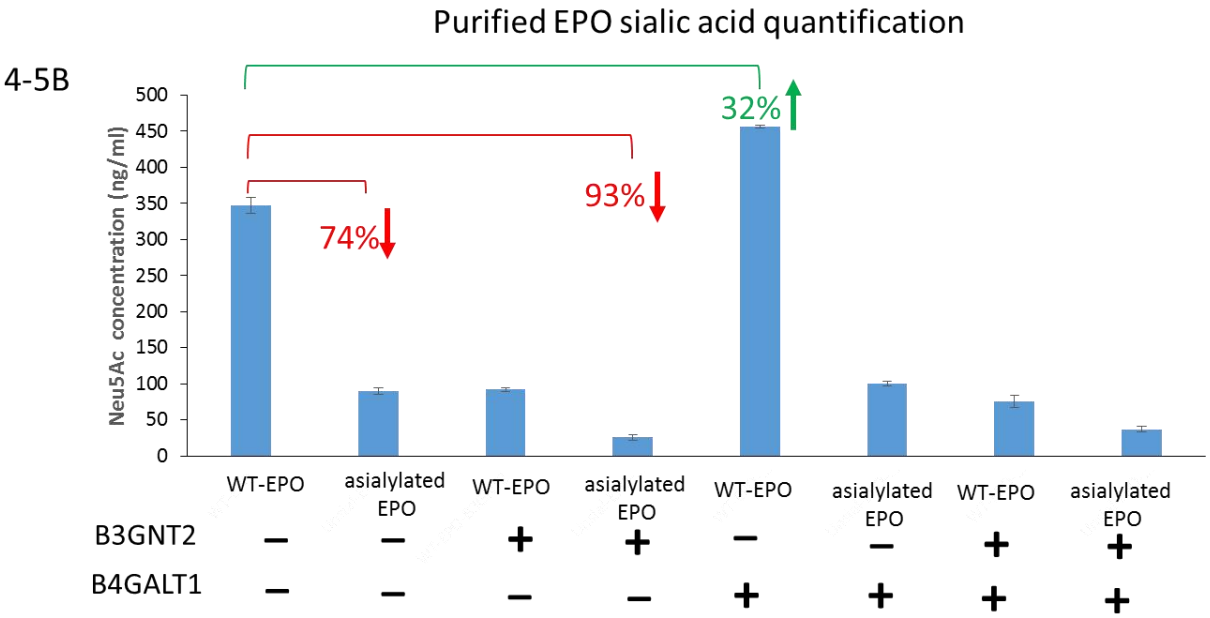

Figure 4-6. N-glycosylation MALDI-MS profiles of different recombinant EPO proteins in this work. Equal amount of EPO protein were analyzed.

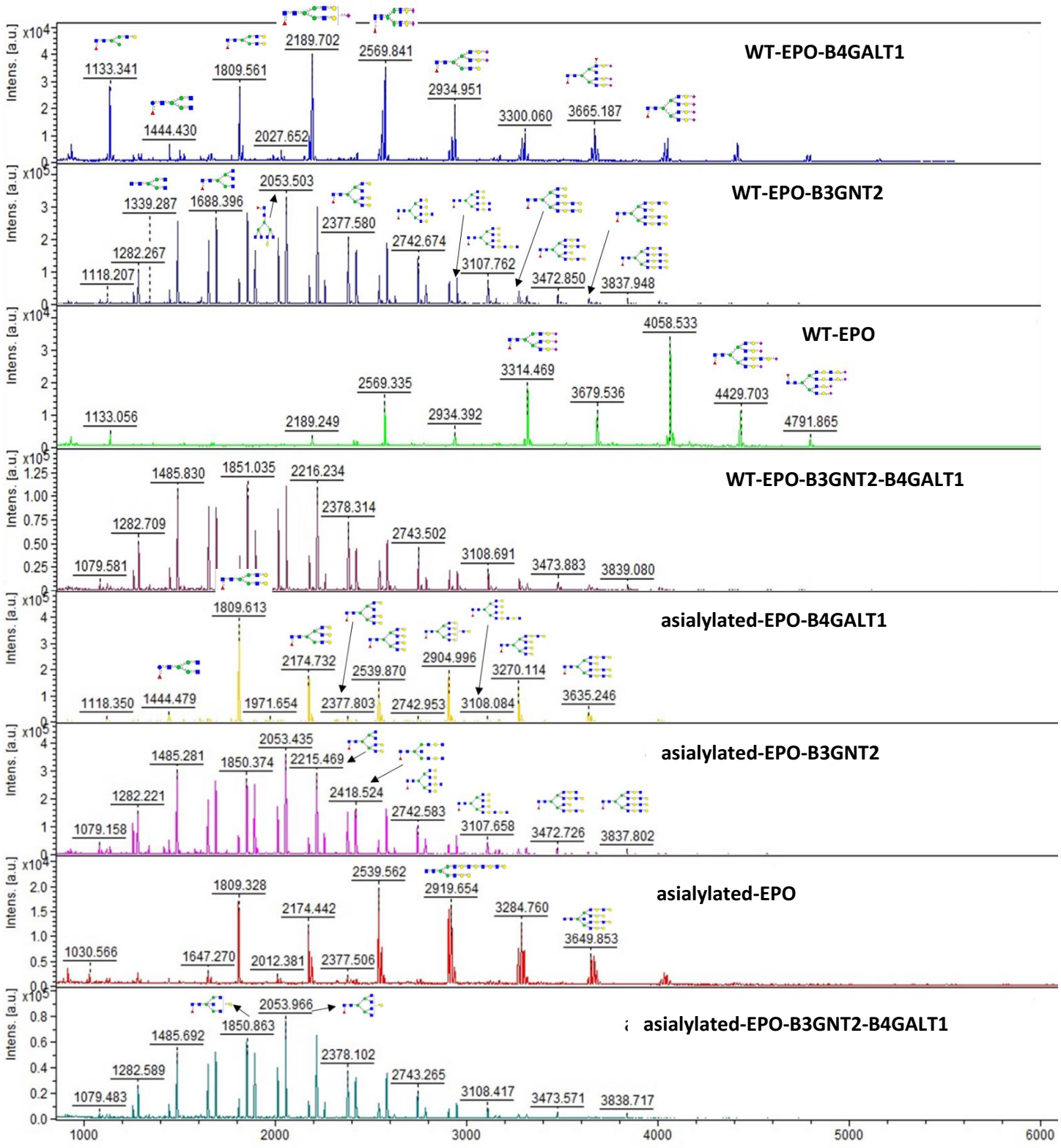

Table 4-1 LacNAc analysis

LacNAc unit number	1	2	3	4	5	6	7	8	9
WT-EPO	5.7%	15.0%	29.9%	16.8%	7.7%	7.4%	3.0%	1.5%	0.0%
STDEV	3.5%	4.2%	3.4%	1.2%	1.6%	1.0%	1.2%	1.4%	
WT-B4GALT1	7.2%	10.9%	34.1%	14.2%	6.7%	12.5%	3.5%	1.4%	0.5%
STDEV	1.0%	2.6%	7.7%	1.8%	1.6%	0.6%	0.8%	0.6%	0.5%
WT-EPO-B3GNT2	28.2%	20.4%	12.0%	7.4%	3.6%	1.8%	0.8%	0.5%	0.2%
STDEV	0.4%	1.1%	1.0%	1.4%	0.8%	0.6%	0.4%	0.3%	0.1%
WT-EPO-B3GNT2-B4GALT1	23.9%	15.1%	12.4%	8.2%	4.2%	2.5%	0.6%	0.4%	0.1%
STDEV	0.8%	1.1%	0.9%	0.1%	0.2%	0.1%	0.2%	0.2%	0.1%
Asialo-EPO	4.7%	14.0%	20.6%	27.9%	15.2%	9.1%	1.3%	0.2%	0.0%
STDEV	0.2%	3.6%	3.8%	2.0%	1.8%	0.1%	0.2%	0.0%	
Asialo-B4GALT1	8.8%	25.2%	16.6%	12.2%	10.9%	10.7%	3.4%	1.4%	0.5%
STDEV	0.5%	1.0%	1.8%	1.0%	1.5%	0.9%	0.2%	0.0%	0.0%
Asialo-EPO-B3GNT2	28.3%	17.6%	9.6%	5.9%	3.3%	1.4%	0.8%	0.3%	0.2%
STDEV	2.4%	1.9%	0.8%	0.1%	1.3%	0.0%	0.2%	0.0%	0.2%
Asialo-EPO-B3GNT2-B4GALT1	27.6%	23.9%	11.6%	5.9%	3.1%	1.6%	0.8%	0.4%	0.1%
STDEV	1.2%	1.0%	0.6%	0.2%	0.3%	0.1%	0.1%	0.1%	0.2%

35%
30%
25%
20%
15%
10%
5%
0%

Table 4-2 Sialic acid analysis

Sialylation (S)	S0	S1	S2	S3	S4
WT-EPO	25.5%	22.9%	29.0%	19.1%	3.4%
WT-B4GALT1	39.5%	28.8%	21.9%	8.1%	1.7%
WT-EPO-B3GNT2	97.1%	2.9%			
WT-EPO-B3GNT2-B4GALT1	93.8%	4.3%	1.7%	0.2%	
Asialo-EPO	80.0%	9.6%	7.1%	3.1%	0.3%
Asialo-B4GALT1	90.2%	6.7%	2.0%	1.1%	
Asialo-EPO-B3GNT2	99.4%	0.3%		0.3%	
Asialo-EPO-B3GNT2-B4GALT1	97.5%	0.7%	1.4%	0.5%	

40%
30%
20%
10%
0%

*S0: no sialic acid per N-glycan, S1: one sialic acid per N-glycan, S2: two sialic acids per N-glycan, S3: three sialic acids per N-glycan, S4: four sialic acids per N-glycan

Table 4-3. The GlcNAc and Galactose analysis

Sample	Average GlcNAc	Average Gal	GlcNAc/Gal ratio
WT-WPO	5.7	3.6	1.6
asialylated-EPO	6.5	4.1	1.6
WT-EPO-B3GNG2	5.9	2.1	2.8
asialylated-EPO-B3GNT2	5.6	1.7	3.3
WT-EPO-B4GALT1	6.1	4.1	1.5
asialylated-EPO-B4GALT1	6.2	4.6	1.3
WT-EPO-B3GNT2-B4GALT1	5.7	2.0	2.9
asialylated-EPO-B3GNT2-B4GALT1	5.7	1.8	3.1

Supplemental Figure 4-1. HPLC sialic acid quantification of overall glyco-conjugates. Total cell lysate were loaded from glyco-engineered and wild-type CHO cells at equal amount level.

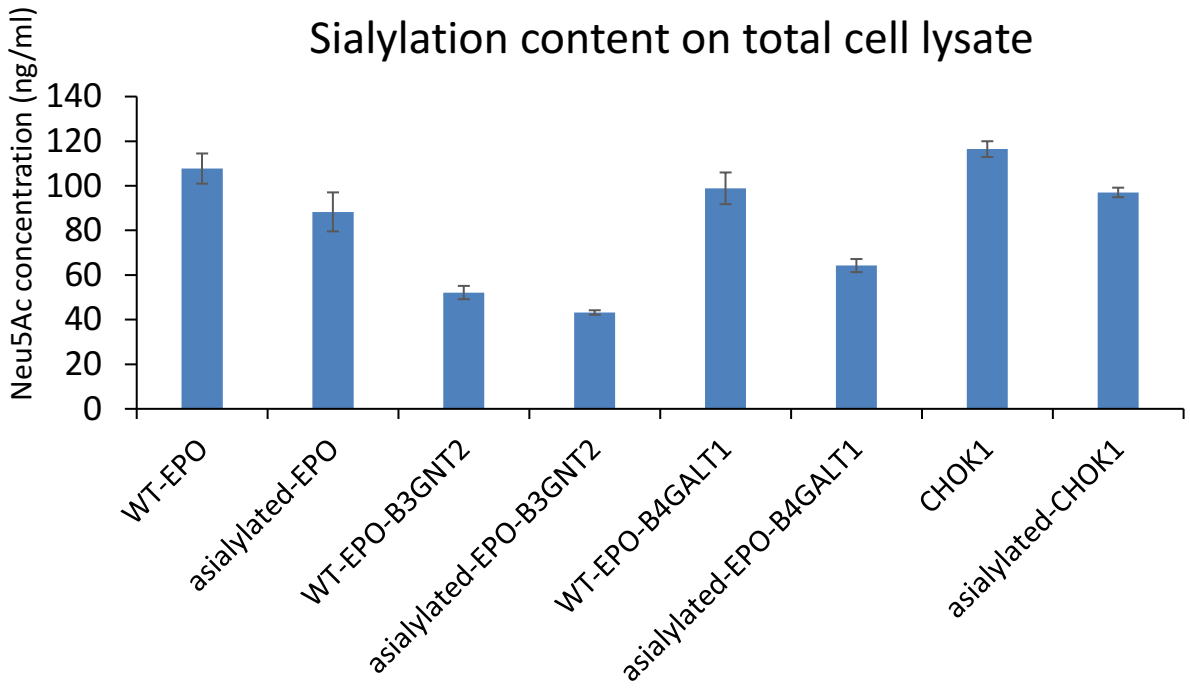

Supplemental Figure 4-2. The expression of sialyltransferases at transcriptional level. (S4-2A). RT-PCR analysis. (S4-2B) qPCR quantification.

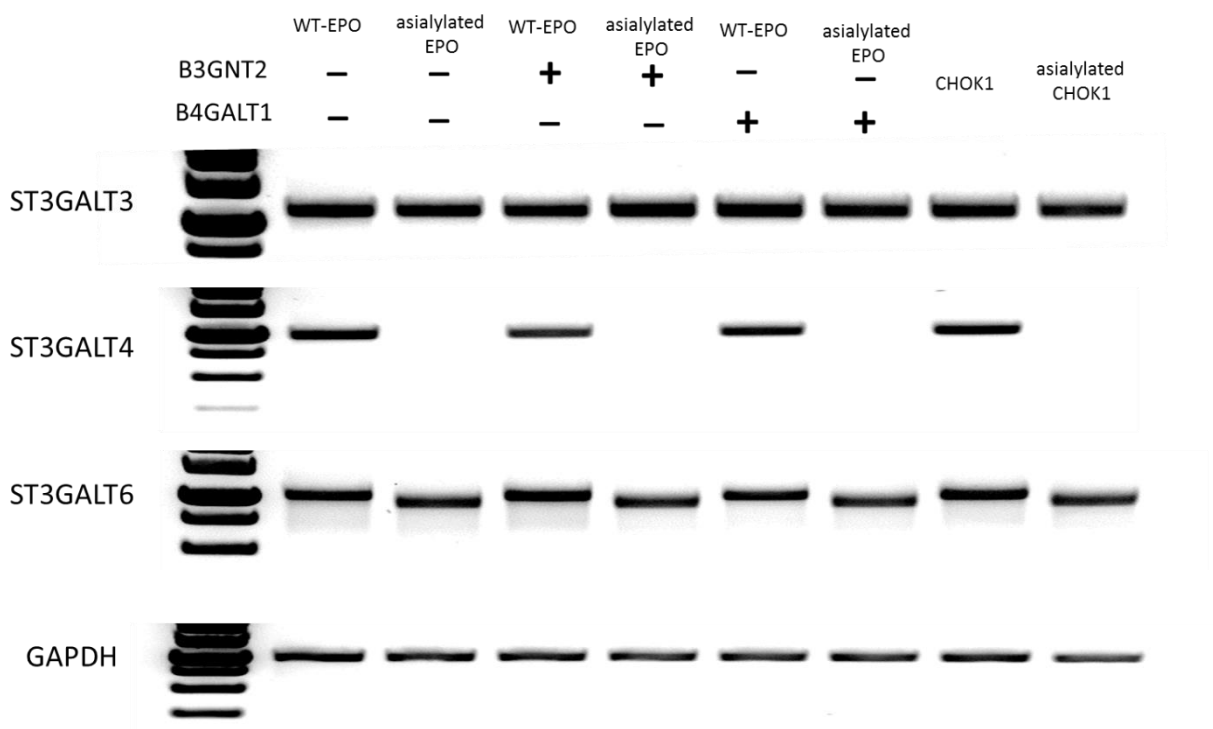

S4-2 B

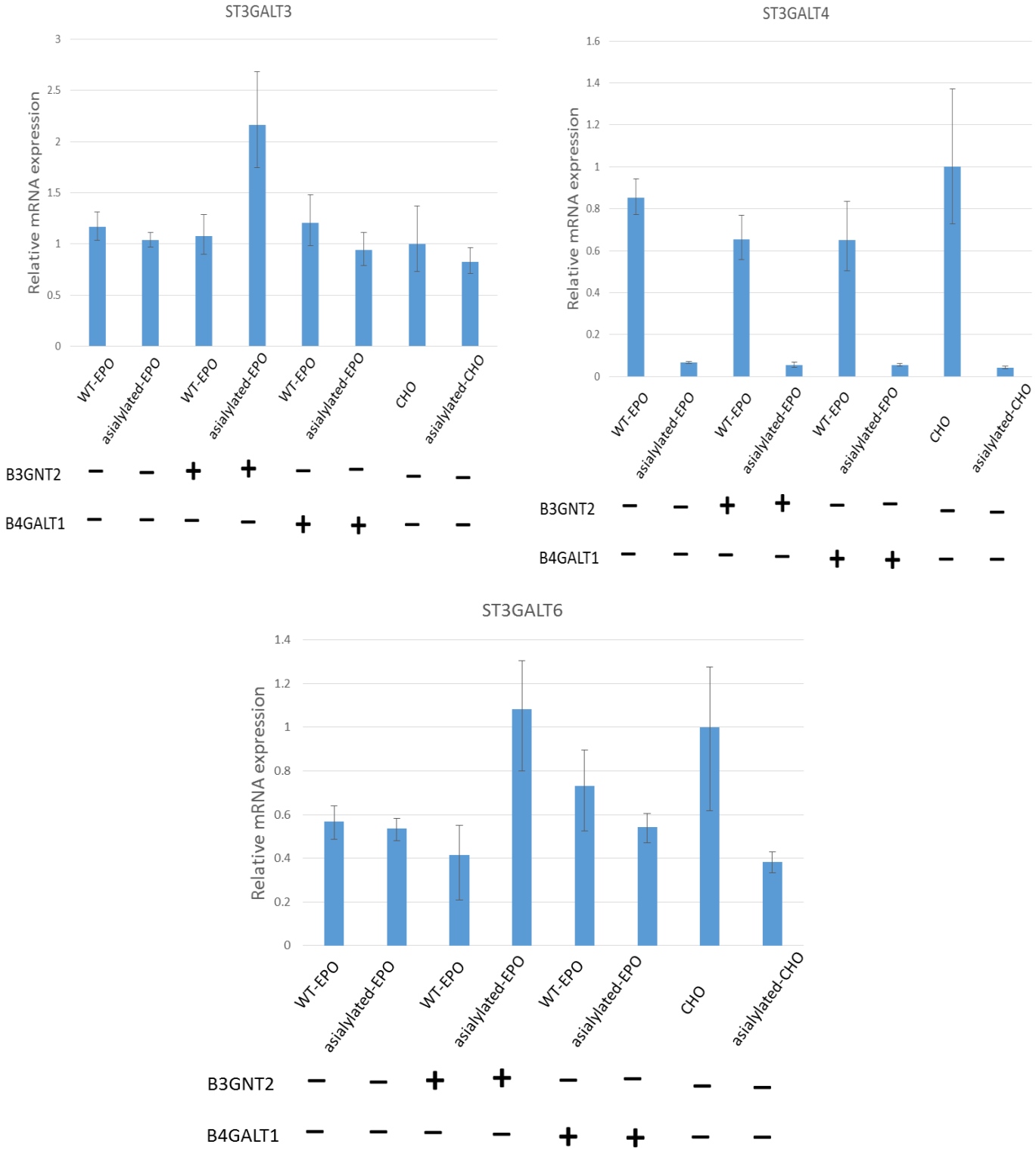
ST3GALT3
Relative mRNA expression
3
2.5
2
1.5
1
0.5
0
WT-EPO
asialylated-EPO
WT-EPO
asialylated-EPO
WT-EPO
asialylated-EPO
CHO
asialylated-CHO
B3GNT2 − − + + − − − −
B4GALT1 − − − − + + − −
ST3GALT4
Relative mRNA expression
1.6
1.4
1.2
1
0.8
0.6
0.4
0.2
0
WT-EPO
asialylated-EPO
WT-EPO
asialylated-EPO
WT-EPO
asialylated-EPO
CHO
asialylated-CHO
B3GNT2 − − + + − − − −
B4GALT1 − − − − + + − −
ST3GALT6
Relative mRNA expression
1.4
1.2
1
0.8
0.6
0.4
0.2
0
WT-EPO
asialylated-EPO
WT-EPO
asialylated-EPO
WT-EPO
asialylated-EPO
CHO
asialylated-CHO
B3GNT2 − − + + − − − −
B4GALT1 − − − − + + − −

Supplemental figure S4-3. The immunoblotting of B3GNT2 and B4GALT1 expression in WT-EPO-B3GNT2-B4GALT1 cell line selection.

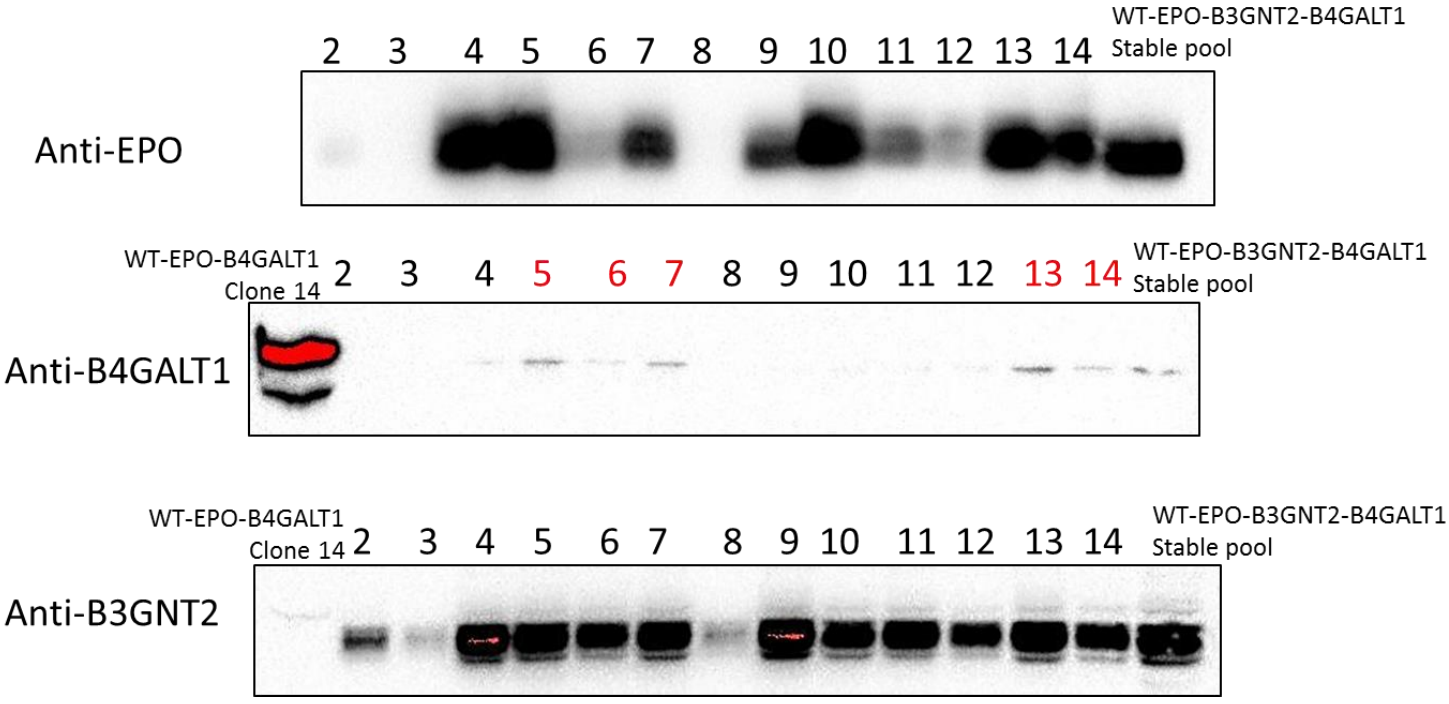

Chapter 5 Application of the CRISPR/Cas9 gene editing method for modulating antibody fucosylation in CHO cells

5.1 Summary

Genetic engineering plays an essential role in the development of cell lines for biopharmaceutical manufacturing. Advanced gene editing tools can improve both the productivity of recombinant cell lines as well as the quality of therapeutic antibodies. Antibody glycosylation is a critical quality attribute for therapeutic biologics because the glycan patterns on the antibody fragment crystallizable (Fc) region can alter its clinical efficacy and safety as a therapeutic drug. As an example, recombinant antibodies derived from Chinese hamster ovary (CHO) cells are generally highly fucosylated; the absence of fucose significantly enhances antibody dependent cell-mediated cytotoxicity (ADCC) against cancer cells. This chapter describes a protocol applying clustered regularly interspaced short palindromic repeats (CRISPR) and CRISPR-associated protein 9 (Cas9) to disrupt the α-1,6-fucosyltranferase (FUT8) gene and subsequently inhibit α-1,6 fucosylation on antibodies expressed in CHO cells.

5.2 Introduction

Targeted gene knockout has been extensively studied and widely used in mammalian cell line development. Traditionally, targeted gene editing is achieved by homologous recombination [285], but due to inherently low recombination rates, homologous recombination can be less efficient and more time-consuming [108]. The emergence of advanced genetic engineering technologies, such as zinc finger nucleases (ZFNs), transcription activator-like effector nucleases

(TALENs), and clustered regularly interspaced short palindromic repeats (CRISPR) with CRISPR-associated protein 9 (Cas9), has dramatically accelerated the gene editing process and significantly improved gene knockout efficiency [286]. These advanced gene editing tools are based on the use of engineered nucleases comprised of programmable and sequence-specific DNA-binding domains fused to a non-specific DNA cleavage module [285]. Specifically, ZFNs and TALENs employ a protein-DNA binding domain fused to a FokI endonuclease and require a pair of ZFNs or TALENs to generate a DNA double-strand break (DSB). More recently, the development of the CRISPR/Cas9 system, utilizing a guided RNA complementary to the target DNA sequence fused to a Cas9 nuclease, exhibits higher target binding specificity than ZFNs or TALENs and only requires RNA-binding to a single strand of DNA in order to generate a nick in the sequence [285]. The evolutionary origin of CRISPR stems from an adaptive immunological response in some bacteria and archaea to protect the host against foreign DNA [285]. Among the three identified CRISPR systems, the Type II CRISPR/Cas9 system of Streptococcus pyogenes (SpCas9) has been studied most extensively (Figure 5-1A). In this system, short segments of foreign DNA (approx. 20 nucleotides) known as “protospacers” are integrated within the bacterial CRISPR genomic loci; individual protospacers are separated by short palindromic repeats [285]. To generate short CRISPR-targeting RNA (crRNA), protospacers are transcribed as pre-crRNA, which anneals to trans-acting crRNA (tracrRNA) via a conserved dinucleotide protospacer adjacent motif (PAM) upstream of the target region [285]. The CRISPR/Cas9 system can thereby direct sequence-specific cleavage to excise foreign DNA by Cas9 proteins. By re-designing the crRNA sequence, CRISPR can be engineered to target any DNA sequence of interest in the host genome. For the CRISPR/Cas9 gene editing system, there are two prerequisites: the targeted sequence must be unique in the host genome and the target sequence

must be present immediately upstream of a protospacer adjacent motif (PAM).

Monoclonal antibody (mAb) therapeutics comprise a multi-billion dollar market [287]. The wide-ranging applications of mAb biologics not only treat major diseases such as cancer, autoimmune diseases, inflammation and Alzheimer's disease [287], but also provide diverse types of therapies, including radioimmunotherapy [288], antibody-directed enzyme prodrug therapy [289], antibody-drug conjugates [290], immunoliposome therapy [291] and checkpoint inhibitor therapy [292]. Except for neutralization with pathogens, antibodies (especially IgGs) oftentimes execute their functions by phagocytosis of antibody-bound pathogens. In particular, antibody dependent cell-mediated cytotoxicity (ADCC) is triggered when pathogen-bound antibodies interact with Fc receptors of lymphocytes (mainly natural killer cells) [186]. The conserved N-glycan on the IgG Fc domain greatly affects this binding affinity. The core-fucose residue of the heavy chain constant region (CH)-associated N-glycans plays a critical role in regulating antibody effector function in ADCC [105-109, 112, 211, 293]. Compared to the fucosylated antibodies from wild-type CHO cells, defucosylated antibodies exhibited 100-fold higher ADCC in vitro [110, 114] as a result of a subtle conformational change [109, 111, 112]. Inactivation of the α-1,6 fucosyltransferase, encoded by the FUT8 gene in mammals, represents the most efficient single modification to inhibit the addition of fucose to the core of the complex N-glycan [116, 184].

In this chapter, we describe a robust method for generating a single-gene knockout CHO cell line with an engineered glycosylation pathway using the CRISPR/Cas9 system. The biological significance of the FUT8 gene makes it an ideal target for our proof-of-concept study. Importantly, we employed the lectin selection methodology to isolate specific glycan types in antibody-expressing clones, which is a unique step in the knockout cell line development

process. The choice of stable antibody-expressing CHO cells as our parental cells makes our protocol practical and useful for industrial purposes.

5.3. Materials

5.3.1 Reagents and Kits

1. Plasmid Miniprep kit
2. 1.5 mL Eppendorf microcentrifuge tubes
3. 12 × 75 mm tubes with cell strainer cap (FACS tubes)
4. Nuclease-Free Water
5. BbsI restriction enzyme (New England Biolabs)
6. NEBuffer 2.1. (New England Biolabs)
7. QIAquick Gel Extraction Kit (Qiagen)
8. QIAquick PCR Purification Kit (Qiagen)
9. S.O.C. Medium
10. LB Broth (Miller)
11. LB Agar powder (Lennox)
12. NEBuffer 4 (New England Biolabs)
13. T4 DNA ligase buffer
14. Ampicillin
15. T4 DNA ligase
16. Taq DNA polymerase with standard Taq buffer
17. PCR tubes
18. NEB 5-alpha component *E. coli* (New England Biolabs)
19. Opti-MEM™ I Reduced Serum Medium (ThermoFisher Scientific)

20. Lipofectamine™ 3000 Transfection Reagent. (ThermoFisher Scientific)

21. Lens Culinaris Agglutinin (LCA) (Vector Laboratories)

22. Biotinylated Lens Culinaris Agglutinin (LCA) (Vector Laboratories)

23. Fetal Bovine Serum (FBS)

24. L-Glutamine (200 mM)

25. T25 flask

26. T75 flask

27. Dimethyl sulfoxide (DMSO)

28. 6-well cell culture plate

29. 12-well cell culture plate

30. 96-well cell culture plate

31. Ham's F-12K (Kaighn's) Medium (ThermoFisher Scientific)

32. Trypan Blue Solution

33. UltraPure™ Agarose

34. 50× TAE buffer

35. Phusion High-Fidelity DNA Polymerase (New England Biolabs)

36. Cryovial tubes 1.2 ml

37. Surveyor mutation detection kit (Integrated DNA technologies (IDT))

38. Phosphate buffered saline (PBS) solution

39. Ethylenediaminetetraacetic acid (EDTA)

40. HEPES Buffer

41. Zero Blunt™ TOPO™ PCR Cloning Kit (ThermoFisher Scientific)

42. 17 mm × 100 mm round-bottom snap-capped tubes for *E. coli* culture

43. Petri dishes
44. Qiagen DNeasy Blood & Tissue Kit (Qiagen)
45. GeneRuler 1kb DNA ladder (ThermoFisher Scientific)

5.3.2 Formulas

1. CHOK1 cell culture: F12K medium with 10% FBS and 2 mM L-glutamine
2. FACS sorting buffer: 1× PBS with 1 mM EDTA, 25 mM HEPES and 1% FBS
3. 1% agarose gel: 1 g agarose powder in 100 ml 1x TAE buffer, boil the solution to dissolve the agarose
4. 1000× ampicillin stock: 1 g ampicillin powder in 10 ml sterile water
5. LB-agar (ampicillin): 35 g LB agar powder in 1 L deionized water, then autoclave it. After LB-agar solution cools to 50 °C, add ampicillin stock in 1000× dilution ratio.
6. 1× TAE buffer for DNA gel electrophoresis: dilute 50× TAE buffer with deionized water

5.3.3 Equipment

1. Forma™ Series II 3110 Water-Jacketed CO_2 Incubators (ThermoFisher Scientific)
2. Microcentrifuge
3. Laboratory water bath
4. Heat block
5. NanoDrop™ 2000 Spectrophotometer (ThermoFisher Scientific)
6. Fluorescence-activated cell sorter (FACS)
7. Hemocytometer
8. Microscope
9. PCR thermocycler

10. ChemiDoc™ XRS+ System (Bio-rad)
11. Horizontal DNA Electrophoresis System (Bio-rad)
12. Protein blot Electrophoresis System (Bio-rad)
13. Microwave oven

5.4. Methods

5.4.1 Design sgRNAs against targeted gene

The sequence specificity of the CRISPR/Cas9 system is determined by choosing 20 nucleotides (nts) from the target gene to serve as the single guide RNA (sgRNA) sequence [294]. In order to express the small chimeric sgRNA, an RNA pol III promoter, such as U6, is required [295, 296]. Since the U6 promoter initiates transcription at guanine (G), this base must be present in the 5' end of the gene target site. Thus, the 20 nts from target DNA site located immediately at 5' of a protospacer-adjacent motif (PAM, 5'-NGG-3') are in the form of 5'-GNNNNNNNNNNNNNNNNNNN-NGG-3' (N can be A,G, C ,or T) [294, 297].

1. Search your gene of interest using the CHO Cas9 target Finder http://staff.biosustain.dtu.dk/laeb/crispy [129] (see Note 1). Be aware that your gene of interest may have multiple variants in CHO cells. For example, FUT8 gene (Gene ID: 100751648) has two variants in CHO: one variant (protein ID: XP 003501783.1) containing 11 exons as a full-size α-1,6-fucosyltransferase, the other variant (protein ID: XP 007640580.1) containing 9 exons as a truncated α-1,6-fucosyltransferase.
2. A list of target sequences will be presented. We choose the target sequence from Exon 9 because Exon 9 exists in both CHO α-1,6-fucosyltransferase variants and its amino acid sequence covers the active region of the FUT8 enzyme [298, 299] (see Note 2).

3. From the CHO Cas9 target Finder search result, two target sequences in Exon 9, each followed by a PAM sequence (5'-NGG-3') was chosen, as shown in Table 5-1 (see Note 3).
4. Design sgRNA primers

Based on the target sgRNA sequences from Subheading 3.1.3, we designed the sgRNA cloning primers according to the px458 CRISPR protocol from Dr. Feng Zhang's lab at Addgene http://www.addgene.org/crispr/zhang/[129]. The target sequence minus the "5'-NGG-3'" PAM sequence is the varying region that primers overlap with each other, as described in Table 5-1 and illustrated in Figure 5-1C.

5.4.2 Construction of px458 plasmid with designed sgRNAs

5.4.2.1 Preparation of px458 vector

1. The construct plasmid px458 was kindly provided by Dr. Feng Zhang (MIT) [300]. Subclone this plasmid into *E. coli* to make a bacterial glycol stock.
2. Inoculate a small amount of *E. coli* from the frozen bacterial glycol stock in LB medium supplemented with 100 μg/ml ampicillin.
3. Culture overnight at 37°C with shaking at 250 rpm.
4. Extract plasmid DNA from *E. coli* culture using a plasmid purification kit (depending on the culture volume to choose mini-, midi- or maxi- plasmid purification kit and follow the manufacturer's protocol). Elute the empty px458 plasmid in nuclease-free water (NFW) and measure the DNA concentration using the Nanodrop 2000 (see Note 4)

5.4.2.2 Digestion of px458 plasmid

1. Based on the px458 empty plasmid concentration, digest an appropriate amount of px458 plasmid with Bbsl enzyme and 1× NEBuffer 2.1 digestion buffer as shown in Table 5-2.
2. Analyze digested product by DNA electrophoresis on 1% agarose gel and check the size and linearization of px458 plasmid.
3. Cut the DNA band (containing linearized px458 plasmid) with appropriate size (~9.3 kb) to remove primer dimers and isolate the linearized px458 plasmid by using a gel extraction kit following the manufacturer's protocol.
4. Elute the linearized px458 plasmid in nuclease-free water (NFW).
5. Measure the DNA concentration using a Nanodrop 2000.

5.4.2.3 Anneal sgRNA primers for the sgRNA construct (see Note 5)

1. The primers are synthesized by a custom primer service and dissolved in NFW to a concentration of 100 μM.
2. Mix the sense and anti-sense primers (100 μM) with following components in a tube as shown in Table 5-3.
3. Boil the primer mixture at 95°C for 5 min using a heating block or thermocycler and allow the oligo duplex to slowly cool to room temperature. Freshly annealed oligo duplex is recommended for the sgRNA plasmid construction.

5.4.2.4 The sgRNA plasmid construction (ligation)

Mix components in a tube according to Table 5-4. If not immediately used, store at -20°C.

5.4.2.5 Transformation of sgRNA plasmid in *E.coli*

1. Take the DH5-alpha component *E. coli* vials out from -80°C freezer and thaw them on ice.
2. After *E. coli* thaws, add 1-3 μl ligation product into one vial of competent cells.

3. Mix gently by flicking the bottom of the tube with your finger twice.
4. Prepare another vial of competent cells without adding ligation product as a negative control.
5. Incubate the competent *E. coli* cells on ice for 30 min
6. Heat shock the vial in a 42 °C water bath for 30 sec
7. Place the vial in ice for 5 min.
8. Add 950 µl room temperature SOC medium to each vial and incubate in a shaker at 250 rpm at 37°C for 1 h.
9. Centrifuge at 5000 *g* for 5 min and remove the supernatant.
10. Add 150 µl fresh SOC media to each vial, pipette up and down to resuspend the *E. coli* pellet.
11. Spread two densities (high and low) of transformed *E. coli* onto 10 cm LB agar plates containing 100 µg/ml ampicillin.
12. Incubate the agar plates overnight at 37 °C. Very few colonies should be expected on the negative control agar plate.

5.4.2.6 Analyze transformation colony

1. Pick a few colonies using a pipette tip and individually transfer to 4 ml LB medium supplemented with 100 µg/ml ampicillin in an *E. coli* culture snap-capped tube.
2. Place tubes in shaking incubator at 250 rpm at 37°C overnight
3. Purify the sgRNA plasmid using a plasmid purification kit following the manufacturer's protocol and measure the DNA concentration using the Nanodrop 2000.
4. Sequence the constructed plasmid using Sanger sequencing.

5. After confirming the sequence of the constructed sgRNA plasmid, store sgRNA plasmid at -20°C for further transfection (see Note 6).

5.4.3 Transfection of sgRNA plasmids into an IgG expressing CHO cell line

5.4.3.1 Day 0: seed cells for transfection

1. Use healthy IgG expressing CHO cell line (viability >97%) at early passage, for higher transfection efficiency. The IgG expressing CHO cell line was previously described [301].
2. Count cells using a cell counter or hemocytometer.
3. Plate cells at a density 7×10^5 cells per well in a 6-well plate, add culture medium to 2 ml per well. At least two wells are needed: one well for transfection and another well for control.
4. Incubate cell cultures at 37°C in a humidified incubator with 5% CO_2 for 24 h.

5.4.3.2 Day 1: transfection with lipofectamine 3000

1. Check cell confluency. Cells should be 80-90% confluent at the time of transfection. Replace the old culture medium with 2 ml reduced serum Opti-MEM medium in each well.
2. Use lipofectamine 3000 for transfection following the manufacturer's protocol. Warm lipofectamine 3000 reagent to room temperature and thaw sgRNA plasmids from -20°C freezer. Flick the tube a couple times and quick spin before using.
3. Place two sterile tubes, each containing 125 µl of Opti-MEM medium, and label them Tube 1 and Tube 2
4. Lipofectamine 3000/Opti-MEM mixture: Add 5 µl Lipofectamine 3000 reagent into Tube 1

5. Diluted DNA mixture: Add 2.5 μg sgRNA plasmids (sgRNA1 plasmid: sgRNA2 plasmid=1:1 (w/w)) into Tube 2. And then add 5 μl P3000 reagent. Gently pipet up and down to mix them well.
6. Add Lipofectamine 3000/Opti-MEM mixture to the plasmid-P3000 reagent mixture.
7. Incubate for 20 min at room temperature
8. Add the transfection mixture into a well in the 6-well plate.
9. Gently shake the 6-well plate to evenly distribute the transfection mixture.
10. Incubate cells for 2 days at 37°C in 5% CO_2 with humidity.

5.4.4 LCA lectin selection of the transfected cells

1. Two days post-transfection, the supernatant from transfected cells is collected and subjected to LCA lectin blot analysis to detect fucosylation of the recombinant antibody. An example of LCA lectin result is shown in Figure 5-3A.
2. For transfected cells, selection of FUT8 knockout cells was performed by supplementing the culture medium with 50 μg/ml *lens culinaris agglutinin* (LCA). The transfected pool in one well of 6-well plate was passed into a T25 flask with F12K culture medium containing 50 μg/ml unconjugated LCA for a week to select the transfected cells with reduced fucosylation. The same amount of untransfected parental cells supplemented with equal concentrations of LCA is also performed as a negative control (see Note 7).

5.4.5 (Optional) Fluorescence activated cell sorting to enrich for sgRNA plasmid expression (see Note 8)

1. Prior to LCA selection, the transfected pool is seeded at 1×10^6 cells per 100 mm culture dish for overnight incubation.

2. When the confluency is above 90%, cells are collected by trypsinization and centrifuged at 500 × g for 15 min to obtain a cell pellet.
3. Wash the cells twice using sterile PBS and resuspend the cell pellet in sorting buffer using a 12 × 75 mm tube with cell strainer cap.
4. Cells are then subjected to FACS.
5. Cells expressing GFP within the top 5% intensity of signal are sorted and collected in culture medium.
6. Sorted cells are transferred to a 50 ml tube with culture medium up to 40 ml.
7. Centrifuge 2100 × *g* for 5 min and remove sorting buffer and culture medium.
8. Resuspend cells in a T75 flask with 50 μg/ml LCA for selection.
9. Incubate the sorted cells for 3 days at 37°C in 5% CO_2 with humidity.
10. When the sorted cells grow, this indicates a successful sorting process. Passage the cells and allow them to grow to >80% confluency for the following analysis or cryopreservation.

5.4.6 Surveyor mutation assay to check the knockout efficiency

The Surveyor enzyme can cleave the mismatch in the DNA duplex where a mutated sequence is hybridized with the wild-type sequence. The PCR product after cleavage will produce bands of different size that are separable on an agarose gel (see Note 9).

1. After 2-3 passages, harvest 1×10^6 cells from the LCA selected stable pool.
2. Centrifuge at 1000 × *g* and remove the supernatant.
3. Extract the genomic DNA from the cell pellet using DNeasy blood & Tissue kit following the manufacturer's protocol. Also extract the genomic DNA from untransfected parental cells for use as a negative control.

4. Design sequencing forward and reverse primers: Design your primers using ApE software (http://biologylabs.utah.edu/jorgensen/wayned/ape/) or NCBI primer-BLAST (http://www.ncbi.nlm.nih.gov/tools/primer-blast/). Please see Note 10 for primer design instructions. The sequencing primers can be used for Surveyor mutation detection as described here or for Sanger sequencing as described in Subheading 3.8.
5. Mix the following components (Table 5-5) in a 1.5 ml Eppendorf tube (master mix) and add 25 μl from the master mix to each PCR tube. Prepare 4 tubes for the knockout sample and 4 tubes for the control sample.

6. Place the PCR tubes in a thermocycler, and run the program outlined in Table 5-6 (see Note 11):

7. After PCR amplification, pool 4 PCR repeats together and take 5 μl of the PCR product from knockout and control samples and run them individually on 1% agarose gel. There should be only one clear band from your control sample (if not, redo your PCR or troubleshoot your primer design).

8. Check the PCR product on the gel, if not much primer dimer is present, the PCR product can be purified by a PCR purification kit following the manufacturer's protocol; if primer dimers are abundant, the PCR product has to be processed through a gel extraction step to remove primer dimers before proceeding to the next step.

9. Combine purified knockout PCR product with control wild-type PCR product in a new PCR tube as shown in Table 5-7.

10. Place the combined PCR mixture in a thermocycler and run the DNA hybridization protocol as shown in Table 5-8. When the PCR amplification is done, put the sample on ice immediately.

11. Mix the components for the following two reactions as outlined in Table 5-9.

12. Incubate the PCR tubes for 60 min at 42 °C.

13. Then add 1.3 µl Stop solution to each PCR tube to terminate the surveyor endonuclease reaction. Put the samples on ice.

14. Load the products on a 2% agarose gel and run for 30 min. Your results should be similar to what is shown in Figure. 5-3B.

5.4.7 Limited dilution cloning (clone isolation) (see Note 12)

1. Trypsinize the cells from the stable knockout pool and count the cell density.
2. Perform a 1:10 serial dilution with fresh medium to a final concentration of ~ 1,000 viable cells/ml.
3. Transfer 160 µl of 1,000 cell/ml solution to 39.8 ml fresh medium to bring the concentration to about 4 cell/ml. Low LCA lectin concentration (10-20 ug/ml) in the medium is preferred in this step.
4. Add 200 µl of the 4 cells/mL solution into each well of the 96-well plate, allowing each well to be seeded at an average density of 0.8 cells/well.
5. Leave the cells undisturbed in an incubator until Day 7 or 8, then start to check cell growth to identify single colonies in the 96-well plates. Wells with more than one colony should not be marked.
6. After 11 or 12 days, check the growth of single-cell clones daily.
7. Before the cultures become over-confluent, trypsinize the clonal cells from each well and expand them to 12-well plates individually.

5.4.8 Clonal cell line selection

After the isolated clones grow, make three repeats of each. One culture serves a maintenance

purpose. One culture is subjected to screen the clonal cells for FUT8 knockout efficiency by using surveyor mutation detection assay (Figure 5-4A) and Sanger sequencing (Figure 5-4B). The other culture is subjected to LCA lectin blot and western blot analysis against α1,6 fucosylation and antibody titer analysis.

5.4.8.1 Sanger sequencing to analyze gene mutation

1. After the clones in 6-well plate become confluent, the genomic DNA from each clone is extracted using a Qiagen DNeasy Blood & Tissue Kit DNA extraction kit following the manufacturer's protocol.
2. Measure the extracted genomic DNA concentration and use the designed sequencing primers in Subheading 3.6 to perform the PCR amplification and PCR product purification.
3. Check the PCR product quality by DNA gel electrophoresis and measure the purified PCR product concentration using a Nanodrop.
4. Perform a Surveyor mutation analysis to detect FUT8-knockout efficiency in each clone.
5. The mutant clones from the analysis are chosen and processed as in the next step.
6. For sequencing the mutated region in each clone, TOPO cloning of the PCR product is performed following the manufacturer's protocol. Alternative methods are also provided in Note 13.
7. The TOPO plasmids constructed with the mutated region from each clone are purified and mixed with the forward and reverse sequencing primers as in Subheading 3.6, individually based on the Sanger sequencing service company's instructions.
8. Analyze Sanger sequencing results using ApE software.

5.4.8.2 LCA lectin blot to check FUT8 knockout efficiency

A LCA lectin blot against potential FUT8 knockout clone cell lysates can also be used to verify the FUT8 knockout efficiency (Please see Figure 5-5 for an example of LCA lectin blot result).

5.4.8.3 Antibody titer analysis

The antibody productivity in each clone is analyzed by enzyme-linked immunosorbent assay (ELISA) or high-performance liquid chromatography (HPLC).

5.5. Notes

Note 1. Other CRISPR sgRNA design software are also available [302], such as CRISPR MultiTargeter (http://www.multicrispr.net/), E-CRISP (http://www.e-crisp.org/E-CRISP/) and CRISPRseek (http://bioconductor.org/packages/release/bioc/html/CRISPRseek.html). We chose CRISPY because this Cas9 target finding software is built on the CHO-K1 genome.

Note 2. For improving gene disruption efficiency, we chose two sgRNAs targeting two close sites in one exon in the targeted gene (as shown in Figure 5-1B). The exon or exons covering the activity domain of the targeted protein are recommended. This protocol is also applicable for one target site using one sgRNA.

Note 3. sgRNA selection criteria are as follows:

a. If the targeted protein's activity domain has been defined, design the sgRNA within the activity domain coding sequence. For example, Exon 9 covers the active site of both variants of FUT8 in CHO cells. If the targeted protein's activity domain has not yet been determined,

it is preferable to design multiple sgRNAs targeting different exons and test the sgRNA knockout efficacy of each one.

b. The sgRNA should be unique in the CHO genome with minimum off-target effects. Given that Cas9 digests between 3 and 4 nts upstream of the PAM sequence of the targeted knockout sequence [297], it is important to make sure the first 10 nts in the selected sgRNA has no off-target activity. Many sgRNA software programs also predict the off-target activity for each sgRNA. Alternatively, you can manually align your sgRNA sequence with the CHO genome using NCBI BLAST (https://blast.ncbi.nlm.nih.gov/Blast.cgi). No or low off-target activity is an important consideration for sgRNA selection.

Note 4. It is recommended to check the px458 vector sequence before BbsI digestion, especially the BbsI digestion region for sgRNA insertion.

Note 5. It is not necessary to phosphorylate the oligo duplex. The oligo duplex without phosphorylation can also work well.

Note 6. For transfection purposes, it is suggested to use sterile NFW to elute the sgRNA plasmid.

Note 7. LCA is a plant lectin which preferentially binds to the α-linked mannose of N-glycans. LCA can cause cytotoxicity in cells expressing core-fucosylated proteins [108].

Note 8. The px458 plasmid contains the GFP marker, which can be used for cell analysis by FACS to enrich for cells with a high plasmid expression level. Given that the CRISPR system is efficient and LCA selection alone is enough to generate FUT8-/- cells, we provide the FACS protocol here as a supplement. FACS should be performed prior to LCA lectin blot selection because after LCA selection, transient px458 plasmid expression may be terminated.

Note 9. Other enzymes can also detect mismatched DNA sequences, such as T7 endonuclease. For an example of a detailed mutation assay methodology, please refer to the Surveyor mutation detection protocol from Integrated DNA Technologies (IDT).

Note 10. Generally, a PCR product between 600-1000 bp is a suitable length for PCR amplification. This product should span the knockout binding site in your targeted gene. Primers should be placed ≥ 50 bp outside the region of interest and have 18-25 bp in length with a GC content around 45-60%.

Note 11. The annealing temperature is dependent on the length and GC content of your primers.

Note 12. For a more detailed CHO limited dilution protocol, please refer to the Freedom™ CHO-S™ protocol. As an alternative to the limited dilution protocol, single cell sorters can also be applied to perform clone isolation.

Note 13. The uracil-specific excision reagent (*USER*) cloning method can also be used as a cloning tool to check for mutated sequences [303].

Figures and Tables

Figure 5-1. (5-1A) Schematic of CRISPR/Cas9-mediated gene mutation. (5-1B) The illustration of sgRNA binding sites in the FUT8 gene. (5-1C) The workflow of px458 plasmid construction.

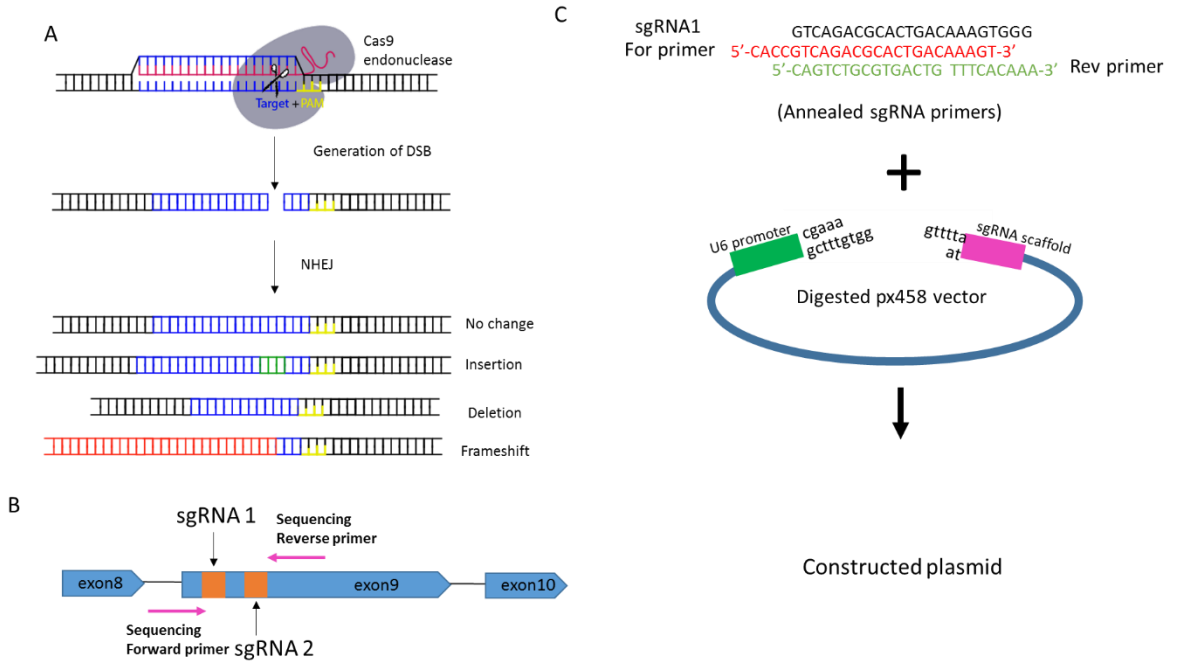

Figure 5-2. Workflow of the knockout cell line generation and analysis using the CRISPR/Cas9 method described in this protocol.

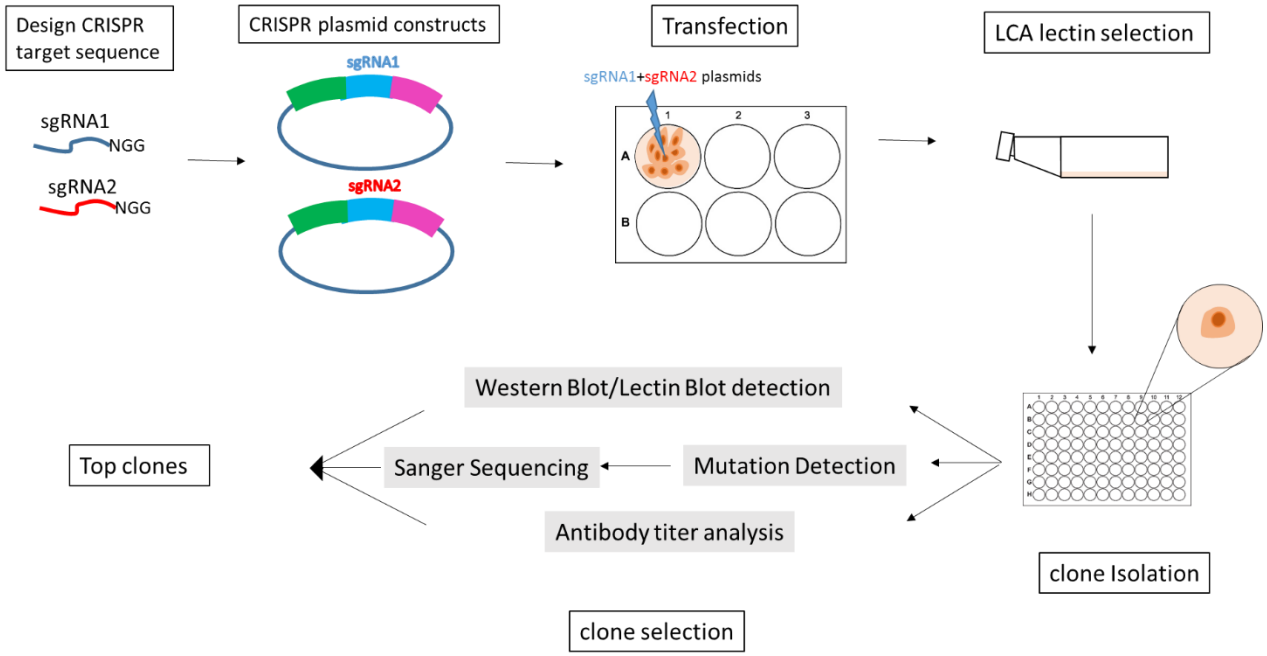

Figure 5-3. (5-3A) LCA lectin blot analysis of α-1,6 fucosylation level on antibody secreted from FUT8-KO stable pools. (5-3B) The mutation detection assay of FUT8 exon 9 knockout efficiency in stable pools. In the mutation detection analysis, equal amounts of knockout stable pool DNA and wild-type DNA were mixed together to serve as mutant/WT cross hybridization (Lane 2 and 3). At the same time, equal amounts of wild-type DNA was also prepared to serve as the self- hybridization control (Lane 1). After annealing, equal amounts of self-hybridization and cross hybridization mixtures were treated with Surveyor Nuclease individually and analyzed by gel electrophoresis. The mutant/WT cross hybridization results in mismatched heteroduplexes. Surveryor Nuclease can digest the mismatched DNA and produce cleavage products as shown as an uncut wild-type fragment and multiple cleavage fragments in the cross hybridization mixtures (lanes 2 and 3). While no mismatch results from the wild-type self-hybridization as the Surveryor Nuclease does not cleave this homoduplex (lane 1).

Figure 5-3A. LCA lectin blot

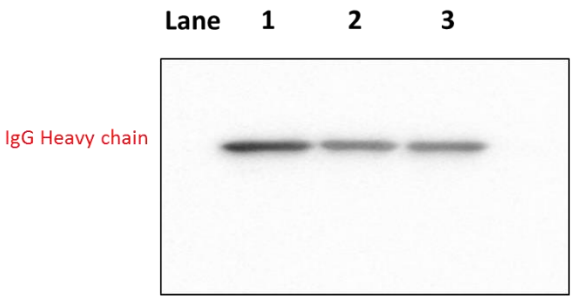

Figure 5-3B. FUT8 Knockout mutation detection

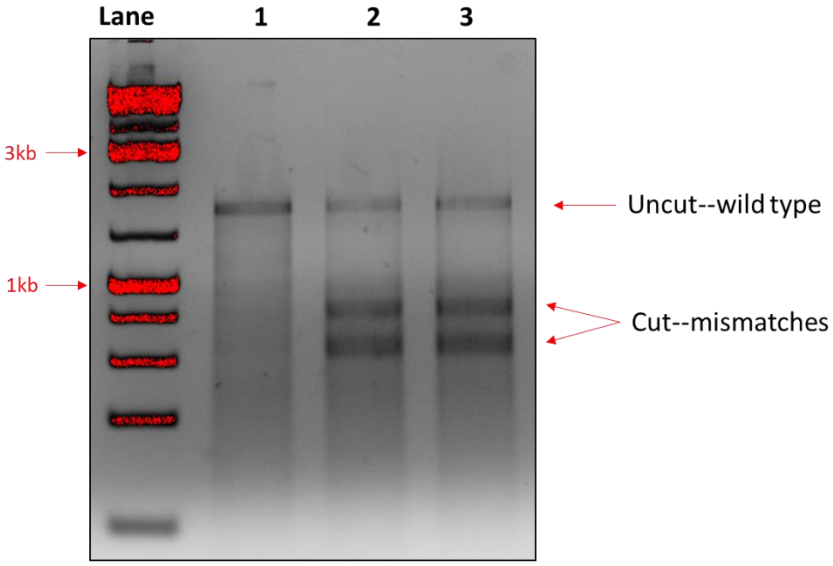

Lane 1: Parental IgG expressing cell line
Lane 2: FUT8-KO IgG expressing stable pool 1
Lane 3: FUT8-KO IgG expressing stable pool 2

Figure 5-4. (5-4A) Mutation detection analysis of knockout efficiency in FUT8-knockout clones. (5-4B) The DNA sequences of selected FUT8-knockout cell clones.

Figure 5-4A Mutation detection analysis of knockout efficiency in FUT8-Knockout clones

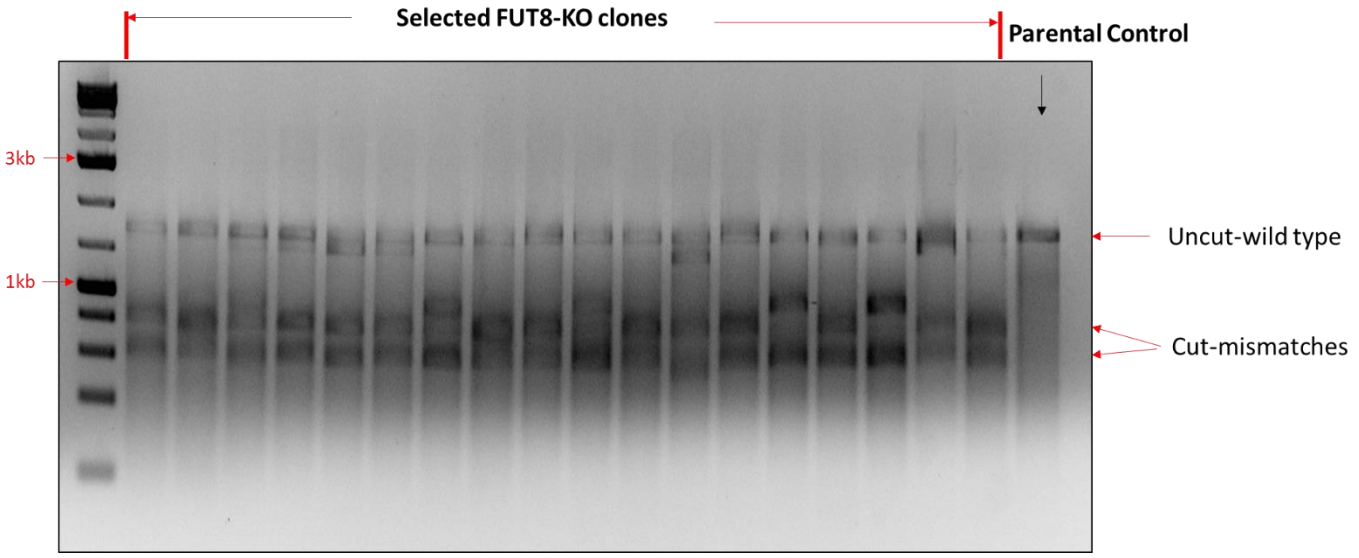

Figure 5-4B. The mutation sequences of selected FUT8-knockout cell clones

Clone 13-3: Insertion

Wild-type: GTCAGACGCACTGACAAAGTGGGAACAGAAGCAGCCTTCCATCCCATTGAGGAATACATGGTACACGTTGAAGAACATTTTCAGCTTCTCGAACGCAGAATGAAAGTGGATAAAAAAAGAGTGTATCTGG

Mutant: GTCAGACGCACTGACAAAGTGGGAACAGAAGCAGCCTTCCATCCCATTGAAGGAATACATGGTACACGTTGAAGAACATTTTCAGCTTCTCGAACGCAGAATGAAAGTGGATAAAAAAAGAGTGTTATCTGG

Clone 4-1: Deletion

Wild-type: GTCAGACGCACTGACAAAGTGGGAACAGAAGCAGCCTTCCATCCCATTGAGGAATACATGGTACACGTTGAAGAACATTTTCAGCTTCTCGAACGCAGAATGAAAGTGGATAAAAAAAGAGTGTATCTGG

Mutant: GTCAGACGCACTGACAAAGTGGGAACAGAAGCAGCCTTCCATCCCAT----------GGTACACGTTGAAGAACATTTTCAGCTTCTCGAACGCAGAATGAAAGTGGATAAAAAAAGAGTGTATCTGG

Clone 24-2: Deletion

Wild-type: GTCAGACGCACTGACAAAGTGGGAACAGAAGCAGCCTTCCATCCCATTGAGGAATACATGGTACACGTTGAAGAACATTTTCAGCTTCTCGAACGCAGAATGAAAGTGGATAAAAAAAGAGTGTATCTGG

Mutant: GTCAGACGCACTGACAAAGTGGGAACAGAAGCAGCCTTCCATCCCATTGA----------ATCTGG

Clone 19-1: Insertion + deletion

Wild-type: GTCAGACGCACTGACAAAGTGGGAACAGAAGCAGCCTTCCATCCCATTGAGGAATACATGGTACACGTTGAAGAACATTTTCAGCTTCTCGAACGCAGAATGAAAGTGGATAAAAAAAGAGTGTATCTGG

Mutant: GTCAGACGCACTGACAAAGTGGGAACAGAAGCAGCCTTCCATCCCATTGAAGGAATACATGGTACACGTTGAAGAACATTTTCAGCTTCT----------

Figure 5-5. LCA lectin blot of CHO cell lysates.

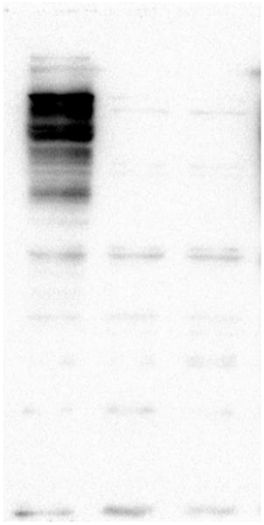

1. FUT8 (+/+) CHO parental cells
2. FUT8 (-/-) CHO cells-clone 1
3. FUT8 (-/-) CHO cells-clone 2

Table 5-1. sgRNAs and their primer sequences.

guided RNA sequence	Primers for cloning into Px458 (5' to 3')		
sgRNA 1	GTCAGACGCACTGACAAAGTGGG	Forward	CACCGTCAGACGCACTGACAAAGT
		Reverse	AAACACTTTGTCAGTGCGTCTGAC
sgRNA 2	GGATAAAAAAAGAGTGTATCTGG	Forward	CACCGGATAAAAAAAGAGTGTATC
		Reverse	AAACGATACACTCTTTTTTTATCC

Table 5-2. px458 digestion reaction.

Component		**Volume**
BbsI enzyme		3 µl
px458 plasmid		3 µg
1× NEBuffer 2.1		5 µl
Total Reaction Volume		50 µl
	Reaction conditions	
Incubation Time		2 h
Incubation Temperature		37 ºC

Table 5-3. reagents for sgRNA construct.

Component	Volume
10× NEBuffer 4	10 µl
sgRNA forward primer (100 µM)	10 µl
sgRNA reverse primer (100 µM)	10 µl
NFW	70 µl
Total	100 µl

Table 5-4. Reagents for sgRNA plasmid ligation.

COMPONENT	**ligation (20 µl reaction)**
T4 DNA Ligase Buffer (10×)	2 µl
px458 linearized plasmid DNA	100 ng
Annealed sgRNA insert DNA	1 µl of oligo duplex from Step 3.2.3 (1:20 dilution)
T4 DNA ligase	1 µl
NFW	to 20 µl
Reaction Conditions	
Incubation Time	2 h
Incubation Temperature	Room Temperature

Table 5-5. Reagents for FUT8 sequencing PCR reaction.

Component	FUT8-KO (4.5 reactions)	Control (4.5 reactions)
5× HF buffer	5×4.5=22.5µl	5×4.5=22.5µl
NFW	15.9×4.5=71.55µl	15.9×4.5=71.55µl
10 mM dNTPs	0.6×4.5=2.7µl	0.6×4.5=2.7µl
10 µM Forward Primer	1.25×4.5=5.625µl	1.25×4.5=5.625µl
10 µM Reverse Primer	1.25×4.5=5.625µl	1.25×4.5=5.625µl
Genomic DNA (from Step 5.4.6.3)	FUT8-KO genomic DNA 100 ng	Control genomic DNA 100 ng
Phusion Polymerase	0.3×4.5=1.35 µl	0.3×4.5=1.35 µl
Total reaction volume	25×4.5= 112.5µl	25×4.5=112.5µl

Table 5-6. PCR program to amplify FUT8 knockout sequence.

Step		mperature	Time
Initial denaturation		98°C	3 min
0 cycles	Denaturation	98°C	10 sec
	Annealing	62°C	20 sec
	Extension	72°C	22 sec
Final extension		72°C	7 min
Hold		4°C	∞

Table 5-7. Reagents for DNA hybridization.

Component	Volume
Knockout PCR	400 ng
Control wild-type PCR	400 ng
10× Taq buffer	2 µl
NFW	Up to 20 µl
Total	20 µl

Table 5-8. PCR program for DNA hybridization.

95°C	10 min
95°C -85°C	-2.0°C /sec
85°C	1 min
85-75°C	-0.3°C /sec
75°C	1 min
75-65°C	-0.3°C /sec
65°C	1 min
65-55°C	-0.3°C /sec
55°C	1 min
55-45°C	-0.3°C /sec
45°C	1 min
45-35°C	-0.3°C /sec
35°C	1 min
35-25°C	-0.3°C /sec
25°C	1 min
4°C	Hold ∞

Table 5-9. Reagents for surveyor enzyme mutation detection.

Component	ontrol WT PCR product	-WT hybridized PCR mixture
ized DNA sample	10 µl	10 µl
gCl_2 solution	1 µl	1 µl
Enhancer S	1 µl	1 µl
Nuclease S	1 µl	1 µl
Total	13 ul	13 µl

Chapter 6 Conclusions and future work

6.1 Final Thoughts

The goal of this dissertation was to apply multiple glycoengineering strategies to tailor the glycan profile on recombinant proteins in CHO cells and to develop an advanced glycoprofile analysis method.

The development of a rapid glycopeptide analysis method can reveal site-specific glycan information on recombinant EPO-Fc protein secreted from CHO cells in different media compositions. Retaining glycans on the peptides enables users to simultaneously elucidate the glycan structure on the specific glycosylation sites and provide insights about how proteins are modified at different points along the polypeptide chain under different culture conditions. As a complementary approach to the conventional released glycan analysis method, this rapid and easy glycoproteomic method-intact glycopeptide analysis can decipher site-specific glycan information on therapeutic proteins, which is highly beneficial for biopharmaceutical manufacturing. Intact glycopeptide characterization may become increasingly important as an analytical tool for producing protein therapeutics with well-defined physical properties.

With the assistance of genetic, protein and metabolic engineering, glycoengineering on glycosylation process can delicately manipulate the glycan profile in mammalian cells. However, given the non-template driven nature of glycosylation, the regulation of one glycotransferase expression can unexpectedly affect other glycotansferase expression in Golgi. Plus, the nucleotide sugar substrate content is also determinant to the final glycan profile. That's why the culture media composition is of significant importance for the biopharmaceutical manufacturing. Therefore,a comprehensive and sophisticated design of glyco-engineering approaches

containing genetic, protein and metabolic engineering is highly recommended to achieve well-defined and precisely-controlled glycan profile in mammalian cells.

6.2 Future Work

A comparison of intact glycopeptide analysis with the conventional released glycan analysis to reveal the discrimination between these two methods will be performed on EPO-Fc protein cultured in the same media and same cell culture condition. Further optimization is needed for these two methods to improve the detection sensitivity and accuracy for glycan characterization for providing better-defined therapeutic proteins.

B3GNT2 is a critical gene for LacNAc extension in mammalian cells. Previous work and my current work both demonstrated that the overexpression and inhibition of B3GN2 gene expression both adversely impact the LacNAc unit initiation and extension on recombinant proteins in CHO cells. Nevertheless, although causing similar results, these two approaches are attributed to different machines. The knockdown of B3GNT2 resulted in the reduction GlcNAc content on N-glycan profile, while the overexpression of B3GNT2 resulted the reduction of Gal content on N-glycan profile . Given that LacNAc unit is composed of GlcNAc and Gal. The missing or reduction of either component will result in the decline of LacNAc units on N-glycans. For generating long LacNAc extensions, the overexpression of B4GALT1 in B3GNT2-expressing cells is necessary, by optimizing the expression system, such as testing different promoters. Another approach is to increase neclueotide sugar transporter expression on the membrane of Golgi, which can bring more UDP-galactose and UDP-GlcANc substrates for LacNAc extension.

The overexpression of B3GNT2 somehow resulted in the inhibition of sialylation of glycoproteins and glycolipids in CHO cells, indicating its suppressing effect on the sialylation

process in Golgi. Nevertheless, the sialyltransferase expressions at transcriptional level has unaffected. Next step, the detection of CMP-sialic acid substrate is highly recommended to bring more insights to explain this phenomenon.

References

1. Wang, Q., et al., *Antibody Glycoengineering Strategies in Mammalian Cells.* Biotechnol Bioeng, 2018.
2. Wang, Q. and M.J. Betenbaugh, *Metabolic engineering of CHO cells to prepare glycoproteins.* Emerging Topics in Life Sciences, 2018.
3. Wang, Q., et al., *Strategies for Engineering Protein N-Glycosylation Pathways in Mammalian Cells*, in *Glyco-Engineering: Methods and Protocols*, A. Castilho, Editor. 2015, Springer New York: New York, NY. p. 287-305.
4. Wang, Q., et al., *Glycoengineering of CHO Cells to Improve Product Quality*, in *Heterologous Protein Production in CHO Cells: Methods and Protocols*, P. Meleady, Editor. 2017, Springer New York: New York, NY. p. 25-44.
5. Yin, B., et al., *A novel sugar analog enhances sialic acid production and biotherapeutic sialylation in CHO cells.* Biotechnol Bioeng, 2017. **114**(8): p. 1899-1902.
6. Yin, B., et al., *A novel sugar analog enhances sialic acid production and biotherapeutic sialylation in CHO cells.* Biotechnology and Bioengineering, 2017. **114**(8): p. 1899-1902.
7. Wang, Q., et al., *Combining Butyrated ManNAc with Glycoengineered CHO Cells Improves EPO Glycan Quality and Production.* Biotechnology Journal. **0**(0): p. 1800186.
8. Walsh, G. and R. Jefferis, *Post-translational modifications in the context of therapeutic proteins.* Nat Biotechnol, 2006. **24**(10): p. 1241-52.
9. Palomares, L.A., S. Estrada-Mondaca, and O.T. Ramirez, *Production of recombinant proteins: challenges and solutions.* Methods Mol Biol, 2004. **267**: p. 15-52.
10. Gavel, Y. and G. Vonheijne, *Sequence Differences between Glycosylated and Nonglycosylated Asn-X-Thr Ser Acceptor Sites - Implications for Protein Engineering.* Protein Engineering, 1990. **3**(5): p. 433-442.
11. An, H.J., et al., *Determination of N-glycosylation sites and site heterogeneity in glycoproteins.* Anal Chem, 2003. **75**(20): p. 5628-37.
12. Stavenhagen, K., et al., *Quantitative mapping of glycoprotein micro-heterogeneity and macro-heterogeneity: an evaluation of mass spectrometry signal strengths using synthetic peptides and glycopeptides.* J Mass Spectrom, 2013. **48**(6): p. i.
13. Varki, A. and R. Schauer, *Sialic Acids*, in *Essentials of Glycobiology*, A. Varki, et al., Editors. 2009: Cold Spring Harbor (NY).
14. Aebi, M., *N-linked protein glycosylation in the ER.* Biochim Biophys Acta, 2013. **1833**(11): p. 2430-7.
15. Aebi, M., et al., *N-glycan structures: recognition and processing in the ER.* Trends Biochem Sci, 2010. **35**(2): p. 74-82.
16. Butler, M. and A. Meneses-Acosta, *Recent advances in technology supporting biopharmaceutical production from mammalian cells.* Applied Microbiology and Biotechnology, 2012. **96**(4): p. 885-894.
17. Ghaderi, D., et al., *Production platforms for biotherapeutic glycoproteins. Occurrence, impact, and challenges of non-human sialylation.* Biotechnol Genet Eng Rev, 2012. **28**: p. 147-75.
18. Hossler, P., S.F. Khattak, and Z.J. Li, *Optimal and consistent protein glycosylation in mammalian cell culture.* Glycobiology, 2009. **19**(9): p. 936-49.
19. Swiech, K., V. Picanco-Castro, and D.T. Covas, *Human cells: new platform for recombinant therapeutic protein production.* Protein Expr Purif, 2012. **84**(1): p. 147-53.

20. Padler-Karavani, V. and A. Varki, *Potential impact of the non-human sialic acid N-glycolylneuraminic acid on transplant rejection risk.* Xenotransplantation, 2011. **18**(1): p. 1-5.
21. Bosques, C.J., et al., *Chinese hamster ovary cells can produce galactose-alpha-1, 3-galactose antigens on proteins (vol 28, pg 1153, 2010).* Nature Biotechnology, 2011. **29**(5): p. 459-459.
22. Muchmore, E.A., et al., *Biosynthesis of N-glycolyneuraminic acid. The primary site of hydroxylation of N-acetylneuraminic acid is the cytosolic sugar nucleotide pool.* J Biol Chem, 1989. **264**(34): p. 20216-23.
23. Chung, C.H., et al., *Cetuximab-induced anaphylaxis and IgE specific for galactose-alpha-1,3-galactose.* N Engl J Med, 2008. **358**(11): p. 1109-17.
24. Butler, M. and M. Spearman, *The choice of mammalian cell host and possibilities for glycosylation engineering.* Curr Opin Biotechnol, 2014. **30**: p. 107-12.
25. Croset, A., et al., *Differences in the glycosylation of recombinant proteins expressed in HEK and CHO cells.* J Biotechnol, 2012. **161**(3): p. 336-48.
26. Zhao, Y., et al., *Branched N-glycans regulate the biological functions of integrins and cadherins.* FEBS J, 2008. **275**(9): p. 1939-48.
27. Raju, T.S. and R.E. Jordan, *Galactosylation variations in marketed therapeutic antibodies.* MAbs, 2012. **4**(3): p. 385-91.
28. Niwa, R. and M. Satoh, *The Current Status and Prospects of Antibody Engineering for Therapeutic Use: Focus on Glycoengineering Technology.* Journal of Pharmaceutical Sciences, 2015. **104**(3): p. 930-941.
29. Spearman, M. and M. Butler, *Glycosylation in Cell Culture.* Animal Cell Culture, 2015. **9**: p. 237-258.
30. Sareneva, T., et al., *N-Glycosylation of Human Interferon-Gamma - Glycans at Asn-25 Are Critical for Protease Resistance.* Biochemical Journal, 1995. **308**: p. 9-14.
31. Wright, A. and S.L. Morrison, *Effect of glycosylation on antibody function: implications for genetic engineering.* Trends Biotechnol, 1997. **15**(1): p. 26-32.
32. Sola, R.J. and K. Griebenow, *Glycosylation of therapeutic proteins: an effective strategy to optimize efficacy.* BioDrugs, 2010. **24**(1): p. 9-21.
33. Angata, T. and A. Varki, *Chemical diversity in the sialic acids and related alpha-keto acids: an evolutionary perspective.* Chem Rev, 2002. **102**(2): p. 439-69.
34. Harduin-Lepers, A., et al., *The human sialyltransferase family.* Biochimie, 2001. **83**(8): p. 727-37.
35. Wang, Q., et al., *Strategies for Engineering Protein N-Glycosylation Pathways in Mammalian Cells.* Methods Mol Biol, 2015. **1321**: p. 287-305.
36. Ashwell, G. and J. Harford, *Carbohydrate-specific receptors of the liver.* Annu Rev Biochem, 1982. **51**: p. 531-54.
37. Cole, E.S., et al., *Invivo Clearance of Tissue Plasminogen-Activator - the Complex Role of Sites of Glycosylation and Level of Sialylation.* Fibrinolysis, 1993. **7**(1): p. 15-22.
38. !!! INVALID CITATION !!! [13].
39. Schauer, R., *Sialic acids: fascinating sugars in higher animals and man.* Zoology (Jena), 2004. **107**(1): p. 49-64.
40. Chung, C.Y., et al., *Assessment of the coordinated role of ST3GAL3, ST3GAL4 and ST3GAL6 on the alpha 2,3 sialylation linkage of mammalian glycoproteins.* Biochemical and Biophysical Research Communications, 2015. **463**(3): p. 211-215.

41. Hamamoto, T. and S. Tsuji, *ST6Gal-I*, in *Handbook of Glycosyltransferases and Related Genes*, N. Taniguchi, et al., Editors. 2002, Springer Japan. p. 295-300.
42. Lee, E.U., J. Roth, and J.C. Paulson, *Alteration of terminal glycosylation sequences on N-linked oligosaccharides of Chinese hamster ovary cells by expression of beta-galactoside alpha 2,6-sialyltransferase.* J Biol Chem, 1989. **264**(23): p. 13848-55.
43. Minch, S.L., P.T. Kallio, and J.E. Bailey, *Tissue plasminogen activator coexpressed in Chinese hamster ovary cells with alpha(2,6)-sialyltransferase contains NeuAc alpha(2,6)Gal beta(1,4)Glc-N-AcR linkages.* Biotechnol Prog, 1995. **11**(3): p. 348-51.
44. Schlenke, P., et al., *Expression of human α2, 6-Sialyltransferase in BHK-21A cells increases the sialylation of coexpressed human erythropoietin: NeuAc-transfer onto GalNAc(βl-4)GlcNAc-R motives*, in *Animal Cell Technology*, M.T. Carrondo, B. Griffiths, and J.P. Moreira, Editors. 1997, Springer Netherlands. p. 475-480.
45. Jeong, Y.T., et al., *Enhanced sialylation of recombinant erythropoietin in CHO cells by human glycosyltransferase expression.* J Microbiol Biotechnol, 2008. **18**(12): p. 1945-52.
46. !!! INVALID CITATION !!! [27].
47. Reinke, S.O., et al., *Regulation and pathophysiological implications of UDP-GlcNAc 2-epimerase/ManNAc kinase (GNE) as the key enzyme of sialic acid biosynthesis.* Biol Chem, 2009. **390**(7): p. 591-9.
48. Son, Y.D., et al., *Enhanced sialylation of recombinant human erythropoietin in Chinese hamster ovary cells by combinatorial engineering of selected genes.* Glycobiology, 2011. **21**(8): p. 1019-28.
49. Wong, N.S., et al., *An investigation of intracellular glycosylation activities in CHO cells: effects of nucleotide sugar precursor feeding.* Biotechnol Bioeng, 2010. **107**(2): p. 321-36.
50. Gu, X. and D.I. Wang, *Improvement of interferon-gamma sialylation in Chinese hamster ovary cell culture by feeding of N-acetylmannosamine.* Biotechnol Bioeng, 1998. **58**(6): p. 642-8.
51. Lawrence, S.M., et al., *Cloning and expression of human sialic acid pathway genes to generate CMP-sialic acids in insect cells.* Glycoconj J, 2001. **18**(3): p. 205-13.
52. Jeong, Y.T., et al., *Enhanced sialylation of recombinant erythropoietin in genetically engineered Chinese-hamster ovary cells.* Biotechnol Appl Biochem, 2009. **52**(Pt 4): p. 283-91.
53. Demetriou, M., et al., *Negative regulation of T-cell activation and autoimmunity by Mgat5 N-glycosylation.* Nature, 2001. **409**(6821): p. 733-9.
54. Misaizu, T., et al., *Role of antennary structure of N-linked sugar chains in renal handling of recombinant human erythropoietin.* Blood, 1995. **86**(11): p. 4097-104.
55. Fukuta, K., et al., *Remodeling of sugar chain structures of human interferon-gamma.* Glycobiology, 2000. **10**(4): p. 421-30.
56. Chan, K.F., J.S.Y. Goh, and Z. Song, *Improving sialylation of recombinant biologics for enhanced therapeutic efficacy.* Pharmaceutical Bioprocessing, 2014. **2**(5): p. 363-366.
57. Goh, J.S., et al., *RCA-I-resistant CHO mutant cells have dysfunctional GnT I and expression of normal GnT I in these mutants enhances sialylation of recombinant erythropoietin.* Metab Eng, 2010. **12**(4): p. 360-8.
58. Iskratsch, T., et al., *Specificity analysis of lectins and antibodies using remodeled glycoproteins.* Anal Biochem, 2009. **386**(2): p. 133-46.

59. Ngantung, F.A., et al., *RNA interference of sialidase improves glycoprotein sialic acid content consistency.* Biotechnol Bioeng, 2006. **95**(1): p. 106-19.
60. Burg, M. and J. Muthing, *Characterization of cytosolic sialidase from Chinese hamster ovary cells: part I: cloning and expression of soluble sialidase in Escherichia coli.* Carbohydr Res, 2001. **330**(3): p. 335-46.
61. de Geest, N., et al., *Systemic and neurologic abnormalities distinguish the lysosomal disorders sialidosis and galactosialidosis in mice.* Hum Mol Genet, 2002. **11**(12): p. 1455-64.
62. Gramer, M.J., et al., *Removal of sialic acid from a glycoprotein in CHO cell culture supernatant by action of an extracellular CHO cell sialidase.* Biotechnology (N Y), 1995. **13**(7): p. 692-8.
63. Ferrari, J., et al., *Chinese hamster ovary cells with constitutively expressed sialidase antisense RNA produce recombinant DNase in batch culture with increased sialic acid.* Biotechnol Bioeng, 1998. **60**(5): p. 589-95.
64. Chao, D.T. and S.J. Korsmeyer, *BCL-2 family: regulators of cell death.* Annu Rev Immunol, 1998. **16**: p. 395-419.
65. Reed, J.C., et al., *Structure-function analysis of Bcl-2 family proteins. Regulators of programmed cell death.* Adv Exp Med Biol, 1996. **406**: p. 99-112.
66. Kim, R., *Unknotting the roles of Bcl-2 and Bcl-xL in cell death.* Biochem Biophys Res Commun, 2005. **333**(2): p. 336-43.
67. Lee, J.H., Y.G. Kim, and G.M. Lee, *Effect of Bcl-xL overexpression on sialylation of Fc-fusion protein in recombinant Chinese hamster ovary cell cultures.* Biotechnol Prog, 2015. **31**(4): p. 1133-6.
68. Rhee, W.J., E.H. Lee, and T.H. Park, *Expression of Bombyx mori 30Kc19 Protein in Escherichia coli and Its Anti-Apoptotic Effect in Sf9 Cell.* Biotechnology and Bioprocess Engineering, 2009. **14**(5): p. 645-650.
69. Wang, Z., et al., *Enhancement of recombinant human EPO production and sialylation in chinese hamster ovary cells through Bombyx mori 30Kc19 gene expression.* Biotechnol Bioeng, 2011. **108**(7): p. 1634-42.
70. Reusch, D. and M.L. Tejada, *Fc glycans of therapeutic antibodies as critical quality attributes.* Glycobiology, 2015. **25**(12): p. 1325-34.
71. Nimmerjahn, F., R.M. Anthony, and J.V. Ravetch, *Agalactosylated IgG antibodies depend on cellular Fc receptors for in vivo activity.* Proc Natl Acad Sci U S A, 2007. **104**(20): p. 8433-7.
72. Kaneko, Y., F. Nimmerjahn, and J.V. Ravetch, *Anti-inflammatory activity of immunoglobulin G resulting from Fc sialylation.* Science, 2006. **313**(5787): p. 670-3.
73. Quast, I., et al., *Sialylation of IgG Fc domain impairs complement-dependent cytotoxicity.* The Journal of Clinical Investigation, 2015. **125**(11): p. 4160-4170.
74. Raymond, C., et al., *Production of alpha 2,6-sialylated IgG1 in CHO cells.* Mabs, 2015. **7**(3): p. 571-583.
75. Naso, M.F., et al., *Engineering host cell lines to reduce terminal sialylation of secreted antibodies.* MAbs, 2010. **2**(5): p. 519-27.
76. Scallon, B.J., et al., *Higher levels of sialylated Fc glycans in immunoglobulin G molecules can adversely impact functionality.* Molecular Immunology, 2007. **44**(7): p. 1524-1534.

77. von Gunten, S., et al., *IVIG pluripotency and the concept of Fc-sialylation: challenges to the scientist.* Nat Rev Immunol, 2014. **14**(5): p. 349-349.
78. Dwyer, J.M., *Manipulating the immune system with immune globulin.* N Engl J Med, 1992. **326**(2): p. 107-16.
79. Anthony, R.M., et al., *Recapitulation of IVIG anti-inflammatory activity with a recombinant IgG Fc.* Science, 2008. **320**(5874): p. 373-6.
80. Schwab, I., et al., *IVIg-mediated amelioration of ITP in mice is dependent on sialic acid and SIGNR1.* Eur J Immunol, 2012. **42**(4): p. 826-30.
81. Schwab, I., et al., *Broad requirement for terminal sialic acid residues and FcgammaRIIB for the preventive and therapeutic activity of intravenous immunoglobulins in vivo.* Eur J Immunol, 2014. **44**(5): p. 1444-53.
82. Anthony, R.M. and J.V. Ravetch, *A novel role for the IgG Fc glycan: the anti-inflammatory activity of sialylated IgG Fcs.* J Clin Immunol, 2010. **30 Suppl 1**: p. S9-14.
83. Washburn, N., et al., *Controlled tetra-Fc sialylation of IVIg results in a drug candidate with consistent enhanced anti-inflammatory activity.* Proc Natl Acad Sci U S A, 2015. **112**(11): p. E1297-306.
84. Jefferis, R., *Antibody therapeutics: isotype and glycoform selection.* Expert Opin Biol Ther, 2007. **7**(9): p. 1401-13.
85. Stadlmann, J., M. Pabst, and F. Altmann, *Analytical and Functional Aspects of Antibody Sialylation.* J Clin Immunol, 2010. **30 Suppl 1**: p. S15-9.
86. Kasermann, F., et al., *Analysis and functional consequences of increased Fab-sialylation of intravenous immunoglobulin (IVIG) after lectin fractionation.* PLoS One, 2012. **7**(6): p. e37243.
87. Holland, M., et al., *Differential glycosylation of polyclonal IgG, IgG-Fc and IgG-Fab isolated from the sera of patients with ANCA-associated systemic vasculitis.* Biochim Biophys Acta, 2006. **1760**(4): p. 669-77.
88. Bondt, A., et al., *Immunoglobulin G (IgG) Fab glycosylation analysis using a new mass spectrometric high-throughput profiling method reveals pregnancy-associated changes.* Mol Cell Proteomics, 2014. **13**(11): p. 3029-39.
89. Stadlmann, J., et al., *A close look at human IgG sialylation and subclass distribution after lectin fractionation.* Proteomics, 2009. **9**(17): p. 4143-53.
90. Bohm, S., et al., *The role of sialic acid as a modulator of the anti-inflammatory activity of IgG.* Semin Immunopathol, 2012. **34**(3): p. 443-53.
91. Lund, J., et al., *Multiple interactions of IgG with its core oligosaccharide can modulate recognition by complement and human Fc gamma receptor I and influence the synthesis of its oligosaccharide chains.* J Immunol, 1996. **157**(11): p. 4963-9.
92. Jassal, R., et al., *Sialylation of Human IgG-Fc Carbohydrate by Transfected Rat α2,6-Sialyltransferase.* Biochemical and Biophysical Research Communications, 2001. **286**(2): p. 243-249.
93. Lin, N., et al., *Chinese hamster ovary (CHO) host cell engineering to increase sialylation of recombinant therapeutic proteins by modulating sialyltransferase expression.* Biotechnol Prog, 2015. **31**(2): p. 334-46.
94. Xu, X., et al., *The genomic sequence of the Chinese hamster ovary (CHO)-K1 cell line.* Nat Biotech, 2011. **29**(8): p. 735-741.

95. Onitsuka, M., et al., *Enhancement of sialylation on humanized IgG-like bispecific antibody by overexpression of alpha2,6-sialyltransferase derived from Chinese hamster ovary cells.* Appl Microbiol Biotechnol, 2012. **94**(1): p. 69-80.
96. Jassal, R., et al., *Sialylation of human IgG-Fc carbohydrate by transfected rat alpha2,6-sialyltransferase.* Biochem Biophys Res Commun, 2001. **286**(2): p. 243-9.
97. Chung, C.-y., et al., *Integrated Genome and Protein Editing Swaps α-2,6 Sialylation for α-2,3 Sialic Acid on Recombinant Antibodies from CHO.* Biotechnology Journal, 2017. **12**(2): p. 1600502-n/a.
98. Jefferis, R. and J. Lund, *Glycosylation of antibody molecules: structural and functional significance.* Chem Immunol, 1997. **65**: p. 111-28.
99. Subedi, Ganesh P. and Adam W. Barb, *The Structural Role of Antibody N-Glycosylation in Receptor Interactions.* Structure. **23**(9): p. 1573-1583.
100. Yu, X., et al., *Engineering Hydrophobic Protein–Carbohydrate Interactions to Fine-Tune Monoclonal Antibodies.* Journal of the American Chemical Society, 2013. **135**(26): p. 9723-9732.
101. Mimura, Y., et al., *Enhanced sialylation of a human chimeric IgG1 variant produced in human and rodent cell lines.* J Immunol Methods, 2016. **428**: p. 30-6.
102. Haryadi, R., et al., *CHO-gmt5, a novel CHO glycosylation mutant for producing afucosylated and asialylated recombinant antibodies.* Bioengineered, 2013. **4**(2): p. 90-4.
103. Thomann, M., et al., *In vitro glycoengineering of IgG1 and its effect on Fc receptor binding and ADCC activity.* PLoS One, 2015. **10**(8): p. e0134949.
104. Boyd, P.N., A.C. Lines, and A.K. Patel, *The effect of the removal of sialic acid, galactose and total carbohydrate on the functional activity of Campath-1H.* Mol Immunol, 1995. **32**(17-18): p. 1311-8.
105. Shields, R.L., et al., *Lack of fucose on human IgG1 N-linked oligosaccharide improves binding to human Fcgamma RIII and antibody-dependent cellular toxicity.* J Biol Chem, 2002. **277**(30): p. 26733-40.
106. Shinkawa, T., et al., *The absence of fucose but not the presence of galactose or bisecting N-acetylglucosamine of human IgG1 complex-type oligosaccharides shows the critical role of enhancing antibody-dependent cellular cytotoxicity.* J Biol Chem, 2003. **278**(5): p. 3466-73.
107. Satoh, M., S. Iida, and K. Shitara, *Non-fucosylated therapeutic antibodies as next-generation therapeutic antibodies.* Expert Opin Biol Ther, 2006. **6**(11): p. 1161-73.
108. Yamane-Ohnuki, N., et al., *Establishment of FUT8 knockout Chinese hamster ovary cells: an ideal host cell line for producing completely defucosylated antibodies with enhanced antibody-dependent cellular cytotoxicity.* Biotechnol Bioeng, 2004. **87**(5): p. 614-22.
109. Iida, S., et al., *Nonfucosylated therapeutic IgG1 antibody can evade the inhibitory effect of serum immunoglobulin G on antibody-dependent cellular cytotoxicity through its high binding to FcgammaRIIIa.* Clin Cancer Res, 2006. **12**(9): p. 2879-87.
110. Peipp, M., et al., *Antibody fucosylation differentially impacts cytotoxicity mediated by NK and PMN effector cells.* Blood, 2008. **112**(6): p. 2390-9.
111. Matsumiya, S., et al., *Structural comparison of fucosylated and nonfucosylated Fc fragments of human immunoglobulin G1.* J Mol Biol, 2007. **368**(3): p. 767-79.

112. Kanda, Y., et al., *Comparison of biological activity among nonfucosylated therapeutic IgG1 antibodies with three different N-linked Fc oligosaccharides: the high-mannose, hybrid, and complex types.* Glycobiology, 2007. **17**(1): p. 104-18.
113. Masuda, K., et al., *Enhanced binding affinity for FcgammaRIIIa of fucose-negative antibody is sufficient to induce maximal antibody-dependent cellular cytotoxicity.* Mol Immunol, 2007. **44**(12): p. 3122-31.
114. Yamane-Ohnuki, N. and M. Satoh, *Production of therapeutic antibodies with controlled fucosylation.* mAbs, 2009. **1**(3): p. 230-236.
115. Okazaki, A., et al., *Fucose Depletion from Human IgG1 Oligosaccharide Enhances Binding Enthalpy and Association Rate Between IgG1 and FcγRIIIa.* Journal of Molecular Biology, 2004. **336**(5): p. 1239-1249.
116. Miyoshi, E., et al., *The alpha1-6-fucosyltransferase gene and its biological significance.* Biochim Biophys Acta, 1999. **1473**(1): p. 9-20.
117. Mori, K., et al., *Engineering Chinese hamster ovary cells to maximize effector function of produced antibodies using FUT8 siRNA.* Biotechnol Bioeng, 2004. **88**(7): p. 901-8.
118. Ma, B., J.L. Simala-Grant, and D.E. Taylor, *Fucosylation in prokaryotes and eukaryotes.* Glycobiology, 2006. **16**(12): p. 158r-184r.
119. Mori, K., et al., *Non-fucosylated therapeutic antibodies: the next generation of therapeutic antibodies.* Cytotechnology, 2007. **55**(2-3): p. 109-14.
120. Stanley, P., *Chinese hamster ovary mutants for glycosylation engineering of biopharmaceuticals.* Pharmaceutical Bioprocessing, 2014. **2**(5): p. 359-361.
121. Malphettes, L., et al., *Highly efficient deletion of FUT8 in CHO cell lines using zinc-finger nucleases yields cells that produce completely nonfucosylated antibodies.* Biotechnol Bioeng, 2010. **106**(5): p. 774-83.
122. Cristea, S., et al., *In vivo cleavage of transgene donors promotes nuclease-mediated targeted integration.* Biotechnology and Bioengineering, 2013. **110**(3): p. 871-880.
123. Urnov, F.D., et al., *Genome editing with engineered zinc finger nucleases.* Nat Rev Genet, 2010. **11**(9): p. 636-46.
124. Gaj, T., C.A. Gersbach, and C.F. Barbas, *ZFN, TALEN and CRISPR/Cas-based methods for genome engineering.* Trends in biotechnology, 2013. **31**(7): p. 397-405.
125. Perez, E.E., et al., *Establishment of HIV-1 resistance in CD4+ T cells by genome editing using zinc-finger nucleases.* Nat Biotech, 2008. **26**(7): p. 808-816.
126. Sun, T., et al., *Functional knockout of FUT8 in Chinese hamster ovary cells using CRISPR/Cas9 to produce a defucosylated antibody.* Engineering in Life Sciences, 2015. **15**(6): p. 660-666.
127. Barrangou, R., et al., *CRISPR Provides Acquired Resistance Against Viruses in Prokaryotes.* Science, 2007. **315**(5819): p. 1709-1712.
128. DiCarlo, J.E., et al., *Genome engineering in Saccharomyces cerevisiae using CRISPR-Cas systems.* Nucleic Acids Research, 2013.
129. Ronda, C., et al., *Accelerating genome editing in CHO cells using CRISPR Cas9 and CRISPy, a web-based target finding tool.* Biotechnology and Bioengineering, 2014. **111**(8): p. 1604-1616.
130. Mali, P., et al., *RNA-Guided Human Genome Engineering via Cas9.* Science, 2013. **339**(6121): p. 823-826.
131. Ran, F.A., et al., *Genome engineering using the CRISPR-Cas9 system.* Nat. Protocols, 2013. **8**(11): p. 2281-2308.

132. Grav, L.M., et al., *One-step generation of triple knockout CHO cell lines using CRISPR/Cas9 and fluorescent enrichment.* Biotechnology Journal, 2015. **10**(9): p. 1446-1456.
133. Narasimhan, S., *Control of glycoprotein synthesis. UDP-GlcNAc:glycopeptide beta 4-N-acetylglucosaminyltransferase III, an enzyme in hen oviduct which adds GlcNAc in beta 1-4 linkage to the beta-linked mannose of the trimannosyl core of N-glycosyl oligosaccharides.* J Biol Chem, 1982. **257**(17): p. 10235-42.
134. Umana, P., et al., *Engineered glycoforms of an antineuroblastoma IgG1 with optimized antibody-dependent cellular cytotoxic activity.* Nat Biotechnol, 1999. **17**(2): p. 176-80.
135. Ferrara, C., et al., *Modulation of therapeutic antibody effector functions by glycosylation engineering: influence of Golgi enzyme localization domain and co-expression of heterologous beta1, 4-N-acetylglucosaminyltransferase III and Golgi alpha-mannosidase II.* Biotechnol Bioeng, 2006. **93**(5): p. 851-61.
136. Ferrara, C., et al., *The carbohydrate at FcgammaRIIIa Asn-162. An element required for high affinity binding to non-fucosylated IgG glycoforms.* J Biol Chem, 2006. **281**(8): p. 5032-6.
137. Davies, J., et al., *Expression of GnTIII in a recombinant anti-CD20 CHO production cell line: Expression of antibodies with altered glycoforms leads to an increase in ADCC through higher affinity for FC gamma RIII.* Biotechnol Bioeng, 2001. **74**(4): p. 288-94.
138. Schuster, M., et al., *Improved effector functions of a therapeutic monoclonal Lewis Y-specific antibody by glycoform engineering.* Cancer Res, 2005. **65**(17): p. 7934-41.
139. Becker, D.J. and J.B. Lowe, *Fucose: biosynthesis and biological function in mammals.* Glycobiology, 2003. **13**(7): p. 41R-53R.
140. Omasa, T., et al., *Decrease in antithrombin III fucosylation by expressing GDP-fucose transporter siRNA in Chinese hamster ovary cells.* J Biosci Bioeng, 2008. **106**(2): p. 168-73.
141. Imai-Nishiya, H., et al., *Double knockdown of alpha1,6-fucosyltransferase (FUT8) and GDP-mannose 4,6-dehydratase (GMD) in antibody-producing cells: a new strategy for generating fully non-fucosylated therapeutic antibodies with enhanced ADCC.* BMC Biotechnol, 2007. **7**: p. 84.
142. Kanda, Y., et al., *Establishment of a GDP-mannose 4,6-dehydratase (GMD) knockout host cell line: a new strategy for generating completely non-fucosylated recombinant therapeutics.* J Biotechnol, 2007. **130**(3): p. 300-10.
143. Ripka, J., A. Adamany, and P. Stanley, *Two Chinese hamster ovary glycosylation mutants affected in the conversion of GDP-mannose to GDP-fucose.* Arch Biochem Biophys, 1986. **249**(2): p. 533-45.
144. Kanda, Y., et al., *Comparison of cell lines for stable production of fucose-negative antibodies with enhanced ADCC.* Biotechnol Bioeng, 2006. **94**(4): p. 680-8.
145. Louie, S., et al., *FX knockout CHO hosts can express desired ratios of fucosylated or afucosylated antibodies with high titers and comparable product quality.* Biotechnol Bioeng, 2016.
146. von Horsten, H.H., et al., *Production of non-fucosylated antibodies by co-expression of heterologous GDP-6-deoxy-D-lyxo-4-hexulose reductase.* Glycobiology, 2010. **20**(12): p. 1607-1618.

147. Winterbourne, D.J., C.G. Butchard, and P.W. Kent, *2-Deoxy-2-fluoro-L-fucose and its effect on L-[1-14C]fucose utilization in mammalian cells.* Biochem Biophys Res Commun, 1979. **87**(4): p. 989-92.
148. Kang, S., et al., *Metabolic markers associated with high mannose glycan levels of therapeutic recombinant monoclonal antibodies.* J Biotechnol, 2015. **203**: p. 22-31.
149. Wright, A. and S.L. Morrison, *Effect of altered CH2-associated carbohydrate structure on the functional properties and in vivo fate of chimeric mouse-human immunoglobulin G1.* J Exp Med, 1994. **180**(3): p. 1087-96.
150. Yu, M., et al., *Production, characterization and pharmacokinetic properties of antibodies with N-linked Mannose-5 glycans.* mAbs, 2012. **4**(4): p. 475-487.
151. Reusch, D. and M.L. Tejada, *Fc glycans of therapeutic antibodies as critical quality attributes.* Glycobiology, 2015. **25**(12): p. 1325-1334.
152. Zhong, X., et al., *Engineering novel Lec1 glycosylation mutants in CHO–DUKX cells: Molecular insights and effector modulation of N-acetylglucosaminyltransferase I.* Biotechnology and Bioengineering, 2012. **109**(7): p. 1723-1734.
153. Chen, W. and P. Stanley, *Five Lec1 CHO cell mutants have distinct Mgat1 gene mutations that encode truncated N-acetylglucosaminyltransferase I.* Glycobiology, 2003. **13**(1): p. 43-50.
154. Stanley, P., *N-Acetylglucosaminyltransferase-I*, in *Handbook of Glycosyltransferases and Related Genes*, N. Taniguchi, et al., Editors. 2002, Springer Japan. p. 61-69.
155. Shi, H.H. and C.T. Goudar, *Recent advances in the understanding of biological implications and modulation methodologies of monoclonal antibody N-linked high mannose glycans.* Biotechnology and Bioengineering, 2014. **111**(10): p. 1907-1919.
156. Stanley, P., *Lectin-resistant CHO cells: selection of new mutant phenotypes.* Somatic Cell Genet, 1983. **9**(5): p. 593-608.
157. Stanley, P. and W. Chaney, *Control of carbohydrate processing: the lec1A CHO mutation results in partial loss of N-acetylglucosaminyltransferase I activity.* Mol Cell Biol, 1985. **5**(6): p. 1204-11.
158. Wright, A., et al., *In vivo trafficking and catabolism of IgG1 antibodies with Fc associated carbohydrates of differing structure.* Glycobiology, 2000. **10**(12): p. 1347-55.
159. Longmore, G.D. and H. Schachter, *Product-identification and substrate-specificity studies of the GDP-L-fucose:2-acetamido-2-deoxy-beta-D-glucoside (FUC goes to Asn-linked GlcNAc) 6-alpha-L-fucosyltransferase in a Golgi-rich fraction from porcine liver.* Carbohydr Res, 1982. **100**: p. 365-92.
160. Voynow, J.A., et al., *Purification and characterization of GDP-L-fucose-N-acetyl beta-D-glucosaminide alpha 1----6fucosyltransferase from cultured human skin fibroblasts. Requirement of a specific biantennary oligosaccharide as substrate.* Journal of Biological Chemistry, 1991. **266**(32): p. 21572-21577.
161. Sealover, N.R., et al., *Engineering Chinese hamster ovary (CHO) cells for producing recombinant proteins with simple glycoforms by zinc-finger nuclease (ZFN)-mediated gene knockout of mannosyl (alpha-1,3-)-glycoprotein beta-1,2-N-acetylglucosaminyltransferase (Mgat1).* J Biotechnol, 2013. **167**(1): p. 24-32.
162. Lee, J.S., et al., *Site-specific integration in CHO cells mediated by CRISPR/Cas9 and homology-directed DNA repair pathway.* Sci Rep, 2015. **5**: p. 8572.
163. !!! INVALID CITATION !!! [148].

164. Elliott, S., et al., *Control of rHuEPO biological activity: the role of carbohydrate.* Exp Hematol, 2004. **32**(12): p. 1146-55.
165. Meuris, L., et al., *GlycoDelete engineering of mammalian cells simplifies N-glycosylation of recombinant proteins.* Nat Biotech, 2014. **32**(5): p. 485-489.
166. Lepenies, B. and P.H. Seeberger, *Simply better glycoproteins.* Nat Biotech, 2014. **32**(5): p. 443-445.
167. Yang, Z., et al., *Engineered CHO cells for production of diverse, homogeneous glycoproteins.* Nat Biotech, 2015. **33**(8): p. 842-844.
168. Bragonzi, A., et al., *A new Chinese hamster ovary cell line expressing alpha 2,6-sialyltransferase used as universal host for the production of human-like sialylated recombinant glycoproteins.* Biochimica Et Biophysica Acta-General Subjects, 2000. **1474**(3): p. 273-282.
169. Monaco, L., et al., *Genetic engineering of alpha2,6-sialyltransferase in recombinant CHO cells and its effects on the sialylation of recombinant interferon-gamma.* Cytotechnology, 1996. **22**(1-3): p. 197-203.
170. Fukuta, K., et al., *Genetic engineering of CHO cells producing human interferon-gamma by transfection of sialyltransferases.* Glycoconj J, 2000. **17**(12): p. 895-904.
171. Wong, N.S., M.G. Yap, and D.I. Wang, *Enhancing recombinant glycoprotein sialylation through CMP-sialic acid transporter over expression in Chinese hamster ovary cells.* Biotechnol Bioeng, 2006. **93**(5): p. 1005-16.
172. Yin, B., et al., *Glycoengineering of Chinese hamster ovary cells for enhanced erythropoietin N-glycan branching and sialylation.* Biotechnol Bioeng, 2015. **112**(11): p. 2343-51.
173. Goh, J.S., et al., *Producing recombinant therapeutic glycoproteins with enhanced sialylation using CHO-gmt4 glycosylation mutant cells.* Bioengineered, 2014. **5**(4): p. 269-73.
174. Zhang, M., et al., *Enhancing glycoprotein sialylation by targeted gene silencing in mammalian cells.* Biotechnology and Bioengineering, 2010. **105**(6): p. 1094-1105.
175. Park, J.H., et al., *Enhancement of recombinant human EPO production and glycosylation in serum-free suspension culture of CHO cells through expression and supplementation of 30Kc19.* Appl Microbiol Biotechnol, 2012. **96**(3): p. 671-83.
176. Lalonde, M.-E. and Y. Durocher, *Therapeutic glycoprotein production in mammalian cells.* Journal of Biotechnology, 2017. **251**: p. 128-140.
177. Niwa, R., et al., *Enhanced natural killer cell binding and activation by low-fucose IgG1 antibody results in potent antibody-dependent cellular cytotoxicity induction at lower antigen density.* Clin Cancer Res, 2005. **11**(6): p. 2327-36.
178. Thomann, M., et al., *Fc-galactosylation modulates antibody-dependent cellular cytotoxicity of therapeutic antibodies.* Molecular Immunology, 2016. **73**: p. 69-75.
179. Hodoniczky, J., Y.Z. Zheng, and D.C. James, *Control of Recombinant Monoclonal Antibody Effector Functions by Fc N-Glycan Remodeling in Vitro.* Biotechnology Progress, 2005. **21**(6): p. 1644-1652.
180. Heffner, K.M., et al., *Glycoengineering of Mammalian Expression Systems on a Cellular Level.* Adv Biochem Eng Biotechnol, 2018.
181. Irie, A., et al., *The Molecular Basis for the Absence ofN-Glycolylneuraminic Acid in Humans.* Journal of Biological Chemistry, 1998. **273**(25): p. 15866-15871.

182. Peri, S., et al., *Phylogenetic Distribution of CMP-Neu5Ac Hydroxylase (CMAH), the Enzyme Synthetizing the Proinflammatory Human Xenoantigen Neu5Gc.* Genome Biol Evol, 2018. **10**(1): p. 207-219.
183. Spiro, R.G., *Protein glycosylation: nature, distribution, enzymatic formation, and disease implications of glycopeptide bonds.* Glycobiology, 2002. **12**(4): p. 43R-56R.
184. Chung, C.-Y., et al., *SnapShot: N-Glycosylation Processing Pathways across Kingdoms.* Cell, 2017. **171**(1): p. 258-258.e1.
185. Gramer, M.J., et al., *Modulation of antibody galactosylation through feeding of uridine, manganese chloride, and galactose.* Biotechnol Bioeng, 2011. **108**(7): p. 1591-602.
186. Wang, Q., et al., *Antibody Glycoengineering Strategies in Mammalian Cells.* Biotechnology and Bioengineering: p. n/a-n/a.
187. Zhang, L., S. Luo, and B. Zhang, *Glycan analysis of therapeutic glycoproteins.* mAbs, 2016. **8**(2): p. 205-215.
188. Yang, S., S. Chatterjee, and J. Cipollo, *The Glycoproteomics-MS for Studying Glycosylation in Cardiac Hypertrophy and Heart Failure.* Proteomics Clin Appl, 2018. **12**(5): p. e1700075.
189. Han, L. and C.E. Costello, *Mass spectrometry of glycans.* Biochemistry (Mosc), 2013. **78**(7): p. 710-20.
190. Koutsioulis, D., D. Landry, and E.P. Guthrie, *Novel endo-alpha-N-acetylgalactosaminidases with broader substrate specificity.* Glycobiology, 2008. **18**(10): p. 799-805.
191. Mulagapati, S., V. Koppolu, and T.S. Raju, *Decoding of O-Linked Glycosylation by Mass Spectrometry.* Biochemistry, 2017. **56**(9): p. 1218-1226.
192. Zhang, L., S. Luo, and B. Zhang, *Glycan analysis of therapeutic glycoproteins.* MAbs, 2016. **8**(2): p. 205-15.
193. Mayampurath, A., et al., *Computational Framework for Identification of Intact Glycopeptides in Complex Samples.* Analytical Chemistry, 2014. **86**(1): p. 453-463.
194. Stadlmann, J., et al., *Analysis of immunoglobulin glycosylation by LC-ESI-MS of glycopeptides and oligosaccharides.* PROTEOMICS, 2008. **8**(14): p. 2858-2871.
195. Cao, L., et al., *Intact glycopeptide characterization using mass spectrometry.* Expert Rev Proteomics, 2016. **13**(5): p. 513-22.
196. Frese, C.K., et al., *Improved peptide identification by targeted fragmentation using CID, HCD and ETD on an LTQ-Orbitrap Velos.* J Proteome Res, 2011. **10**(5): p. 2377-88.
197. Jedrychowski, M.P., et al., *Evaluation of HCD- and CID-type fragmentation within their respective detection platforms for murine phosphoproteomics.* Mol Cell Proteomics, 2011. **10**(12): p. M111.009910.
198. Yin, B., et al., *Butyrated ManNAc analog improves protein expression in Chinese hamster ovary cells.* Biotechnology and Bioengineering, 2018. **115**(6): p. 1531-1541.
199. Yang, W., et al., *Comparison of Enrichment Methods for Intact N- and O-Linked Glycopeptides Using Strong Anion Exchange and Hydrophilic Interaction Liquid Chromatography.* Analytical Chemistry, 2017. **89**(21): p. 11193-11197.
200. Yang, G., et al., *Comprehensive Glycoproteomic Analysis of Chinese Hamster Ovary Cells.* Analytical Chemistry, 2018. **90**(24): p. 14294-14302.
201. Hagglund, P., et al., *A new strategy for identification of N-glycosylated proteins and unambiguous assignment of their glycosylation sites using HILIC enrichment and partial deglycosylation.* J Proteome Res, 2004. **3**(3): p. 556-66.

202. Jefferis, R., *Glycosylation as a strategy to improve antibody-based therapeutics.* Nat Rev Drug Discov, 2009. **8**(3): p. 226-234.
203. Narimatsu, H., et al., *Current Technologies for Complex Glycoproteomics and Their Applications to Biology/Disease-Driven Glycoproteomics.* Journal of Proteome Research, 2018.
204. Bora de Oliveira, K., et al., *Site-specific monitoring of N-Glycosylation profiles of a CTLA4-Fc-fusion protein from the secretory pathway to the extracellular environment.* Biotechnology and Bioengineering, 2017. **114**(7): p. 1550-1560.
205. Moh, E.S.X., et al., *Site-Specific N-Glycosylation of Recombinant Pentameric and Hexameric Human IgM.* Journal of The American Society for Mass Spectrometry, 2016. **27**(7): p. 1143-1155.
206. Kolarich, D., et al., *Determination of site-specific glycan heterogeneity on glycoproteins.* Nat Protoc, 2012. **7**(7): p. 1285-98.
207. Tsuda, E., et al., *The role of carbohydrate in recombinant human erythropoietin.* Eur J Biochem, 1990. **188**(2): p. 405-11.
208. Wickramasinghe, S. and J.F. Medrano, *Primer on genes encoding enzymes in sialic acid metabolism in mammals.* Biochimie, 2011. **93**(10): p. 1641-1646.
209. Malykh, Y.N., L. Shaw, and R. Schauer, *The role of CMP-N-acetylneuraminic acid hydroxylase in determining the level of N-glycolylneuraminic acid in porcine tissues.* Glycoconj J, 1998. **15**(9): p. 885-93.
210. Jenkins, N. and E.M.A. Curling, *Glycosylation of recombinant proteins: Problems and prospects.* Enzyme and Microbial Technology, 1994. **16**(5): p. 354-364.
211. Heffner, K.M., et al., *Glycoengineering of Mammalian Expression Systems on a Cellular Level*. Springer Berlin Heidelberg: Berlin, Heidelberg. p. 1-33.
212. Chung, C.Y., et al., *SnapShot: N-Glycosylation Processing Pathways across Kingdoms.* Cell, 2017. **171**(1): p. 258-258.e1.
213. Schachter, H. and L. Roden, *The biosynthesis of animal glycoproteins.* Metabolic conjugation and metabolic hydrolysis, 1973. **3**: p. 1-149.
214. Corfield, A. and R. Schauer, *Current aspects of glycoconjugate biosynthesis.* Biologie Cellulaire, 1979. **36**(3): p. 213-226.
215. Chen, K., et al., *Engineering of a mammalian cell line for reduction of lactate formation and high monoclonal antibody production.* Biotechnol Bioeng, 2001. **72**(1): p. 55-61.
216. Seth, G., et al., *Engineering cells for cell culture bioprocessing--physiological fundamentals.* Adv Biochem Eng Biotechnol, 2006. **101**: p. 119-64.
217. Aldrich, T.L., A. Viaje, and A.E. Morris, *EASE vectors for rapid stable expression of recombinant antibodies.* Biotechnol Prog, 2003. **19**(5): p. 1433-8.
218. Altamirano, C., et al., *Strategies for fed-batch cultivation of t-PA producing CHO cells: substitution of glucose and glutamine and rational design of culture medium.* J Biotechnol, 2004. **110**(2): p. 171-9.
219. Sandadi, S., S. Ensari, and B. Kearns, *Heuristic optimization of antibody production by Chinese hamster ovary cells.* Biotechnol Prog, 2005. **21**(5): p. 1537-42.
220. Xie, L. and D.I.C. Wang, *Fed-batch cultivation of animal cells using different medium design concepts and feeding strategies.* Biotechnology and Bioengineering, 2006. **95**(2): p. 270-284.

221. Xie, L. and D.I.C. Wang, *High cell density and high monoclonal antibody production through medium design and rational control in a bioreactor.* Biotechnology and Bioengineering, 1996. **51**(6): p. 725-729.
222. Rodriguez, J., et al., *Enhanced Production of Monomeric Interferon-β by CHO Cells through the Control of Culture Conditions.* Biotechnology Progress, 2005. **21**(1): p. 22-30.
223. Ling, W.L., et al., *Improvement of monoclonal antibody production in hybridoma cells by dimethyl sulfoxide.* Biotechnol Prog, 2003. **19**(1): p. 158-62.
224. Liu, C.H. and L.H. Chen, *Promotion of recombinant macrophage colony stimulating factor production by dimethyl sulfoxide addition in Chinese hamster ovary cells.* J Biosci Bioeng, 2007. **103**(1): p. 45-9.
225. Mimura, Y., et al., *Butyrate increases production of human chimeric IgG in CHO-K1 cells whilst maintaining function and glycoform profile.* Journal of immunological methods, 2001. **247**(1): p. 205-216.
226. Sung, Y.H., et al., *Effect of sodium butyrate on the production, heterogeneity and biological activity of human thrombopoietin by recombinant Chinese hamster ovary cells.* J Biotechnol, 2004. **112**(3): p. 323-35.
227. Mariani, M.R., et al., *Correlation between butyrate-induced histone hyperacetylation turn-over and c-myc expression.* J Steroid Biochem Mol Biol, 2003. **86**(2): p. 167-71.
228. Kobayashi, H., E.M. Tan, and S.E. Fleming, *Acetylation of histones associated with the p21WAF1/CIP1 gene by butyrate is not sufficient for p21WAF1/CIP1 gene transcription in human colorectal adenocarcinoma cells.* Int J Cancer, 2004. **109**(2): p. 207-13.
229. Vidali, G., et al., *Butyrate suppression of histone deacetylation leads to accumulation of multiacetylated forms of histones H3 and H4 and increased DNase I sensitivity of the associated DNA sequences.* Proc Natl Acad Sci U S A, 1978. **75**(5): p. 2239-43.
230. Dorner, A.J., L.C. Wasley, and R.J. Kaufman, *Increased synthesis of secreted proteins induces expression of glucose-regulated proteins in butyrate-treated Chinese hamster ovary cells.* J Biol Chem, 1989. **264**(34): p. 20602-7.
231. KIM, E., et al., *High-level expression of recombinant human interleukin-2 in Chinese hamster ovary cells using the expression system containing transcription terminator.* Journal of microbiology and biotechnology, 2004. **14**(4): p. 810-815.
232. Kim, E.J., et al., *Characterization of the metabolic flux and apoptotic effects of O-hydroxyl- and N-acyl-modified N-acetylmannosamine analogs in Jurkat cells.* J Biol Chem, 2004. **279**(18): p. 18342-52.
233. Heum, N.K., et al., *Purification and characterization of recombinant human follicle stimulating hormone produced by Chinese hamster ovary cells.* Journal of microbiology and biotechnology, 2005. **15**(2): p. 395-402.
234. Oh, H.K., et al., *Effect of N-Acetylcystein on butyrate-treated Chinese hamster ovary cells to improve the production of recombinant human interferon-beta-1a.* Biotechnol Prog, 2005. **21**(4): p. 1154-64.
235. Santell, L., et al., *Aberrant metabolic sialylation of recombinant proteins expressed in Chinese hamster ovary cells in high productivity cultures.* Biochem Biophys Res Commun, 1999. **258**(1): p. 132-7.
236. Chung, B., et al., *Effect of sodium butyrate on glycosylation of recombinant erythropoietin*, in *Animal Cell Technology: From Target to Market*. 2001, Springer. p. 207-209.

237. Almaraz, R.T., et al., *Metabolic oligosaccharide engineering with N-Acyl functionalized ManNAc analogs: cytotoxicity, metabolic flux, and glycan-display considerations.* Biotechnol Bioeng, 2012. **109**(4): p. 992-1006.
238. Sampathkumar, S.G., et al., *Targeting glycosylation pathways and the cell cycle: sugar-dependent activity of butyrate-carbohydrate cancer prodrugs.* Chem Biol, 2006. **13**(12): p. 1265-75.
239. Kim, E.J., et al., *Characterization of the Metabolic Flux and Apoptotic Effects of O-Hydroxyl- and N-Acyl-modified N-Acetylmannosamine Analogs in Jurkat Cells.* Journal of Biological Chemistry, 2004. **279**(18): p. 18342-18352.
240. Aich, U., et al., *Regioisomeric SCFA attachment to hexosamines separates metabolic flux from cytotoxicity and MUC1 suppression.* ACS Chem Biol, 2008. **3**(4): p. 230-40.
241. Wang, Z., et al., *Hexosamine analogs: from metabolic glycoengineering to drug discovery.* Current Opinion in Chemical Biology, 2009. **13**(5): p. 565-572.
242. Mathew, M.P., et al., *Extracellular and intracellular esterase processing of SCFA-hexosamine analogs: implications for metabolic glycoengineering and drug delivery.* Bioorg Med Chem Lett, 2012. **22**(22): p. 6929-33.
243. Mathew, M.P., et al., *Glycoengineering of Esterase Activity through Metabolic Flux-Based Modulation of Sialic Acid.* Chembiochem, 2017. **18**(13): p. 1204-1215.
244. Tian, Y., et al., *Identification of sialylated glycoproteins from metabolically oligosaccharide engineered pancreatic cells.* Clinical Proteomics, 2015. **12**(1): p. 11.
245. Tian, Y., et al., *Altered Expression of Sialylated Glycoproteins in Breast Cancer Using Hydrazide Chemistry and Mass Spectrometry.* Molecular & Cellular Proteomics : MCP, 2012. **11**(6): p. M111.011403.
246. Yin, B., et al., *Glycoengineering of Chinese hamster ovary cells for enhanced erythropoietin N-glycan branching and sialylation.* Biotechnology and Bioengineering, 2015. **112**(11): p. 2343-2351.
247. Dodev, T.S., et al., *A tool kit for rapid cloning and expression of recombinant antibodies.* Sci Rep, 2014. **4**: p. 5885.
248. Jourdian, G.W., L. Dean, and S. Roseman, *The sialic acids. XI. A periodate-resorcinol method for the quantitative estimation of free sialic acids and their glycosides.* J Biol Chem, 1971. **246**(2): p. 430-5.
249. Hara, S., et al., *Highly sensitive determination of N-acetyl- and N-glycolylneuraminic acids in human serum and urine and rat serum by reversed-phase liquid chromatography with fluorescence detection.* J Chromatogr, 1986. **377**: p. 111-9.
250. Jia, X., et al., *Detection of aggressive prostate cancer associated glycoproteins in urine using glycoproteomics and mass spectrometry.* PROTEOMICS, 2016. **16**(23): p. 2989-2996.
251. Yang, W., et al., *Glycoform Analysis of Recombinant and Human Immunodeficiency Virus Envelope Protein gp120 via Higher Energy Collisional Dissociation and Spectral-Aligning Strategy.* Analytical Chemistry, 2014. **86**(14): p. 6959-6967.
252. Toghi Eshghi, S., et al., *GPQuest: A Spectral Library Matching Algorithm for Site-Specific Assignment of Tandem Mass Spectra to Intact N-glycopeptides.* Analytical Chemistry, 2015. **87**(10): p. 5181-5188.
253. Almaraz, R.T., et al., *Metabolic oligosaccharide engineering with N-Acyl functionalized ManNAc analogs: Cytotoxicity, metabolic flux, and glycan-display considerations.* Biotechnology and Bioengineering, 2012. **109**(4): p. 992-1006.

254. Lee, J.S. and G.M. Lee, *Effect of sodium butyrate on autophagy and apoptosis in Chinese hamster ovary cells.* Biotechnol Prog, 2012. **28**(2): p. 349-57.
255. Wang, Y., et al., *Sodium butyrate-induced apoptosis and ultrastructural changes in MCF-7 breast cancer cells.* Ultrastruct Pathol, 2016. **40**(4): p. 200-4.
256. Porter, A.G. and R.U. Janicke, *Emerging roles of caspase-3 in apoptosis.* Cell Death Differ, 1999. **6**(2): p. 99-104.
257. Hong, J.K., et al., *Effect of sodium butyrate on the assembly, charge variants, and galactosylation of antibody produced in recombinant Chinese hamster ovary cells.* Appl Microbiol Biotechnol, 2014. **98**(12): p. 5417-25.
258. Sung, Y.H., et al., *Effect of sodium butyrate on the production, heterogeneity and biological activity of human thrombopoietin by recombinant Chinese hamster ovary cells.* Journal of Biotechnology, 2004. **112**(3): p. 323-335.
259. Chung, B., et al., *Effect of Sodium Butyrate on Glycosylation of Recombinant Erythropoietin*, in *Animal Cell Technology: From Target to Market: Proceedings of the 17th ESACT Meeting Tylösand, Sweden, June 10–14, 2001*, E. Lindner-Olsson, N. Chatzissavidou, and E. Lüllau, Editors. 2001, Springer Netherlands: Dordrecht. p. 207-209.
260. Liu, Y.-J., et al., *Characterization of Site-Specific Glycosylation in Influenza A Virus Hemagglutinin Produced by Spodoptera frugiperda Insect Cell Line.* Analytical Chemistry, 2017. **89**(20): p. 11036-11043.
261. Huang, J., et al., *Site-Specific Glycosylation of Secretory Immunoglobulin A from Human Colostrum.* Journal of Proteome Research, 2015. **14**(3): p. 1335-1349.
262. Jones, M.B., et al., *Characterization of the cellular uptake and metabolic conversion of acetylated N-acetylmannosamine (ManNAc) analogues to sialic acids.* Biotechnol Bioeng, 2004. **85**(4): p. 394-405.
263. Kim, N.S. and G.M. Lee, *Overexpression of bcl-2 inhibits sodium butyrate-induced apoptosis in Chinese hamster ovary cells resulting in enhanced humanized antibody production.* Biotechnol Bioeng, 2000. **71**(3): p. 184-93.
264. Riggs, M., et al., *n-Butyrate causes histone modification in HeLa and Friend erythroleukaemia cells.* Nature, 1977. **268**(5619): p. 462-464.
265. in *Essentials of Glycobiology*, A. Varki, et al., Editors. 2009, Cold Spring Harbor Laboratory Press: Cold Spring Harbor (NY).
266. Yin, B., et al., *Butyrated ManNAc analog improves protein expression in Chinese hamster ovary cells.* Biotechnol Bioeng, 2018.
267. Rapoport, E. and J. Le Pendu, *Glycosylation alterations of cells in late phase apoptosis from colon carcinomas.* Glycobiology, 1999. **9**(12): p. 1337-1345.
268. Kantardjieff, A., et al., *Transcriptome and proteome analysis of Chinese hamster ovary cells under low temperature and butyrate treatment.* J Biotechnol, 2010. **145**(2): p. 143-59.
269. Yee, J.C., et al., *Genomic and proteomic exploration of CHO and hybridoma cells under sodium butyrate treatment.* Biotechnology and Bioengineering, 2008. **99**(5): p. 1186-1204.
270. Damiani, R., et al., *Enhancement of human thyrotropin synthesis by sodium butyrate addition to serum-free CHO cell culture.* Appl Biochem Biotechnol, 2013. **171**(7): p. 1658-72.

271. Szegezdi, E., et al., *Mediators of endoplasmic reticulum stress-induced apoptosis.* EMBO Rep, 2006. **7**(9): p. 880-5.
272. Tabas, I. and D. Ron, *Integrating the mechanisms of apoptosis induced by endoplasmic reticulum stress.* Nat Cell Biol, 2011. **13**(3): p. 184-90.
273. Hammerling, U., et al., *In vitro bioassay for human erythropoietin based on proliferative stimulation of an erythroid cell line and analysis of carbohydrate-dependent microheterogeneity.* J Pharm Biomed Anal, 1996. **14**(11): p. 1455-69.
274. Varki, A., *Biological roles of glycans.* Glycobiology, 2017. **27**(1): p. 3-49.
275. Lee, C.-G., et al., *Inhibition of poly-LacNAc biosynthesis with release of CMP-Neu5Ac feedback inhibition increases the sialylation of recombinant EPO produced in CHO cells.* Scientific Reports, 2018. **8**(1): p. 7273.
276. Lee, P.L., J.J. Kohler, and S.R. Pfeffer, *Association of beta-1,3-N-acetylglucosaminyltransferase 1 and beta-1,4-galactosyltransferase 1, trans-Golgi enzymes involved in coupled poly-N-acetyllactosamine synthesis.* Glycobiology, 2009. **19**(6): p. 655-64.
277. Albers, S., J. Eichler, and M. Aebi, *Archaea*, in *Essentials of Glycobiology*, rd, et al., Editors. 2015: Cold Spring Harbor (NY). p. 283-292.
278. Kupper, C.E., et al., *Chemo-enzymatic modification of poly-N-acetyllactosamine (LacNAc) oligomers and N,N-diacetyllactosamine (LacDiNAc) based on galactose oxidase treatment.* Beilstein J Org Chem, 2012. **8**: p. 712-25.
279. Yang, Z., et al., *Engineered CHO cells for production of diverse, homogeneous glycoproteins.* Nature Biotechnology, 2015. **33**: p. 842.
280. Fukuda, M., et al., *Survival of recombinant erythropoietin in the circulation: the role of carbohydrates.* Blood, 1989. **73**(1): p. 84-89.
281. Togayachi, A., T. Sato, and H. Narimatsu, *β1,3-glycosyltransferase Gene Family and IGnT Gene Family*, in *Experimental Glycoscience: Glycobiology*, N. Taniguchi, et al., Editors. 2008, Springer Japan: Tokyo. p. 24-29.
282. Elling, L., et al., *UDP-N-Acetyl-α-D-glucosamine as acceptor substrate of β-1,4-galactosyltransferase. Enzymatic synthesis of UDP-N-acetyllactosamine.* Glycoconjugate Journal, 1999. **16**(7): p. 327-336.
283. Chung, C.Y., et al., *Integrated Genome and Protein Editing Swaps alpha-2,6 Sialylation for alpha-2,3 Sialic Acid on Recombinant Antibodies from CHO.* Biotechnol J, 2017. **12**(2).
284. Yang, S., et al., *Simultaneous quantification of N- and O-glycans using a solid-phase method.* Nat Protoc, 2017. **12**(6): p. 1229-1244.
285. Gaj, T., C.A. Gersbach, and C.F. Barbas, 3rd, *ZFN, TALEN, and CRISPR/Cas-based methods for genome engineering.* Trends Biotechnol, 2013. **31**(7): p. 397-405.
286. Liang, Z., et al., *Targeted Mutagenesis in Zea mays Using TALENs and the CRISPR/Cas System.* Journal of Genetics and Genomics, 2014. **41**(2): p. 63-68.
287. Chames, P., et al., *Therapeutic antibodies: successes, limitations and hopes for the future.* British Journal of Pharmacology, 2009. **157**(2): p. 220-233.
288. Larson, S.M., et al., *Radioimmunotherapy of human tumours.* Nature Reviews Cancer, 2015. **15**: p. 347.
289. Bagshawe, K.D., S.K. Sharma, and R.H. Begent, *Antibody-directed enzyme prodrug therapy (ADEPT) for cancer.* Expert Opin Biol Ther, 2004. **4**(11): p. 1777-89.

290. Zolot, R.S., S. Basu, and R.P. Million, *Antibody–drug conjugates.* Nature Reviews Drug Discovery, 2013. **12**: p. 259.
291. Alavizadeh, S.H., F. Soltani, and M. Ramezani, *Recent Advances in Immunoliposome-Based Cancer Therapy.* Current Pharmacology Reports, 2016. **2**(3): p. 129-141.
292. Sharma, P. and J.P. Allison, *The future of immune checkpoint therapy.* Science, 2015. **348**(6230): p. 56-61.
293. Iida, S., et al., *Two mechanisms of the enhanced antibody-dependent cellular cytotoxicity (ADCC) efficacy of non-fucosylated therapeutic antibodies in human blood.* BMC Cancer, 2009. **9**: p. 58.
294. Sander, J.D. and J.K. Joung, *CRISPR-Cas systems for genome editing, regulation and targeting.* Nature biotechnology, 2014. **32**(4): p. 347-355.
295. Mali, P., et al., *RNA-Guided Human Genome Engineering via Cas9.* Science (New York, N.Y.), 2013. **339**(6121): p. 823-826.
296. Jinek, M., et al., *A programmable dual-RNA-guided DNA endonuclease in adaptive bacterial immunity.* Science, 2012. **337**(6096): p. 816-21.
297. Fujihara, Y. and M. Ikawa, *CRISPR/Cas9-based genome editing in mice by single plasmid injection.* Methods Enzymol, 2014. **546**: p. 319-36.
298. Ihara, H., et al., *Crystal structure of mammalian alpha1,6-fucosyltransferase, FUT8.* Glycobiology, 2007. **17**(5): p. 455-66.
299. Chung, C.-y., et al., *Combinatorial genome and protein engineering yields monoclonal antibodies with hypergalactosylation from CHO cells.* Biotechnology and Bioengineering, 2017. **114**(12): p. 2848-2856.
300. Ran, F.A., et al., *Genome engineering using the CRISPR-Cas9 system.* Nat Protoc, 2013. **8**(11): p. 2281-2308.
301. Yin, B., et al., *Butyrated ManNAc analog improves protein expression in Chinese hamster ovary cells.* Biotechnology and Bioengineering: p. n/a-n/a.
302. Zhu, L.J., *Overview of guide RNA design tools for CRISPR-Cas9 genome editing technology.* Frontiers in Biology, 2015. **10**(4): p. 289-296.
303. Nour-Eldin, H.H., F. Geu-Flores, and B.A. Halkier, *USER cloning and USER fusion: the ideal cloning techniques for small and big laboratories.* Methods Mol Biol, 2010. **643**: p. 185-200.

Curriculum Vitae

Qiong Wang

Email: qiongwang314@gmail.com, Phone: 4437107486

Summary

- Biotechnological researcher focusing on the glyco-engineering and glyco-analytics of therapeutic proteins secreted from mammalian cells.
- Mammalian cell culture and cell line development expert
- Mass spectrometry glycan analysis expert

Education

Ph. D. of Chemical Engineering (08/2015-Now, expected to graduate in May 2019)

Department of Chemical and Biomolecular Engineering, Johns Hopkins University (JHU)

Advisor: Dr. Michael Betenbaugh, Department of Chemical Engineering

Dr. Hui Zhang, Department of Pathology

Dr. Kevin J. Yarema, Department of Biomedical Engineering

Master of Science Engineering (08/2013-05/2015)

Department of Chemical and Biomolecular Engineering, Johns Hopkins University (JHU)

Current GPA: 3.88/4 Advisor: Dr. Michael Betenbaugh

Bachelor of Science (09/2009-06/2013)

Department of Chemical Engineering, East China University of Science and Technology (ECUST)

Major: Chemical Engineering; GPA: 3.84/4.0; Rank: 8/145

Minor: English, Bachelor of Arts

Research Experience

Glyco-engineering to optimize the glycan profile of recombinant Erythropoietin (EPO) and antibody

1. Overexpressing branching genes (GNT IV+V) together with a2,6 sialyltransferase (ST6) to generate glyco-modified CHO EPO expressing cell lines using RT-PCR, immunoblot and lectin blot detection. The sialylation of recombinant EPO is detected by HPLC.
2. Using ManNAc analog supplementation to further increase sialic acid content by increasing the sialic acid substrate availability. Explore the effects of this chemical feeding on CHO cell growth by metabolite analyzer, on recombinant protein (EPO and IgG) expression by Immunoblot and Coomassie blue staining and on sialylation content by intracellular sialic acid assay, lectin blot and HPLC.

Explore the functions of glycotransferases through gene knockouts and knockins

1. Systematically knockdown three essential genes for a2,3 sialyltransferase in CHO, silenced these genes with RNAi and monitored the reduction of sialylation level on total protein using ELISA method; applied this gene silencing approach on the expression of recombinant EPO in CHO cells

and analyzed the reduction of sialylation by lectin blot and HPLC.

2. Use CRISPR knockout to disrupt glycotransferases genome, use ELISA and immunoblot to screen monoclones, then use Surveyor assay and Sanger sequencing to analyze genome modification

Develop methods to efficiently express and purify recombinant human butyrylcholinesterase (HuBChE) in mammalian cells

Explore various promoters and codon optimization method to establish CHO BCHE stably expressing cell lines with high enzymatic activity. Use proline-rich sequences through *in vivo* coexpression and *in vitro* assembly to achieve efficient recombinant BCHE tetramerization by native electrophoresis. Purify HuBCHE tetramers through Tangential flow filtration (TFF), Ni-NTA method, ultrafiltration and dialysis.

Publications

Research Articles:

Wang Q, Ganglong Y, Tiexin Wang, Weiming Y, Betenbaugh MJ, Zhang H. Characterization of intact glycopeptides reveals the impact of culture media on site-specific glycosylation of EPO-Fc fusion protein generated by CHO-GS cells. Biotechnology and Bioengineering. 2019

Wang Q, Chung C-Y, Yang W, Yang G, Chough S, Chen Y, Yin B, Bhattacharya R, Hu Y, Saeui CT, Yarema KJ, Betenbaugh MJ, Zhang H. Combining Butyrated ManNAc with Glycoengineered CHO Cells Improves EPO Glycan Quality and Production. Biotechnology journal. 2018

Wang Q, Chung C-Y, Rosenberg JN, Yu G, Betenbaugh MJ. Application of the CRISPR/Cas9 Gene Editing Method for Modulating Antibody Fucosylation in CHO Cells. In: Hacker DL, editor. Recombinant Protein Expression in Mammalian Cells: Methods and Protocols. New York, NY: Springer New York; 2018. p. 237-57.

Wang Q, Chen CH, Chung C-y, Priola J, Chu JH, Tang J, Ulmschneider MB, Betenbaugh MJ. Proline-Rich Chaperones Are Compared Computationally and Experimentally for Their Abilities to Facilitate Recombinant Butyrylcholinesterase Tetramerization in CHO Cells. Biotechnology journal. 2018;13(3):1700479.

Yin B, **Wang Q**, Chung C-Y, Ren X, Bhattacharya R, Yarema KJ, Betenbaugh MJ. Butyrated ManNAc analog improves protein expression in Chinese hamster ovary cells. Biotechnology and Bioengineering. 2018;115(6):1531-41.

Chung C-Y, **Wang Q**, Yang S, Ponce SA, Kirsch BJ, Zhang H, Betenbaugh MJ. Combinatorial genome and protein engineering yields monoclonal antibodies with hypergalactosylation from CHO cells. Biotechnology and Bioengineering. 2017;114(12):2848-56.

Yin B, **Wang Q**, Chung CY, Bhattacharya R, Ren X, Tang J, Yarema KJ, Betenbaugh MJ. A novel sugar analog enhances sialic acid production and biotherapeutic sialylation in CHO cells. Biotechnol Bioeng. 2017;114(8):1899-902. Epub 2017/03/16.

Chung CY, **Wang Q**, Yang S, Yin B, Zhang H, Betenbaugh M. Integrated Genome and Protein Editing Swaps alpha-2,6 Sialylation for alpha-2,3 Sialic Acid on Recombinant Antibodies from CHO. Biotechnology journal. 2017;12(2). Epub 2016/12/13.

Chung CY, Yin B, **Wang Q**, Chuang KY, Chu JH, Betenbaugh MJ. Assessment of the coordinated role of ST3GAL3, ST3GAL4 and ST3GAL6 on the alpha2,3 sialylation linkage of

mammalian glycoproteins. Biochem Biophys Res Commun. 2015;463(3):211-5. Epub 2015/05/23.

Ganglong Yang, Yingwei Hu, Shisheng Sun, Chuanzi Ouyang, Weiming Yang, **Qiong Wang**, Michael Betenbaugh, and Hui Zhang, Comprehensive Glycoproteomic Analysis of Chinese Hamster Ovary Cells, Analytical Chemistry 2018 90 (24), 14294-1430

Reviews:

Wang Q, Chung C-Y, Chough S, Betenbaugh MJ. Antibody glycoengineering strategies in mammalian cells. Biotechnology and Bioengineering. 2018

Wang Q, Betenbaugh MJ. Metabolic engineering of CHO cells to prepare glycoproteins. Emerging Topics in Life Sciences. 2018;2(3):433-42.

Wang Q, Yin B, Chung CY, Betenbaugh MJ. Glycoengineering of CHO Cells to Improve Product Quality. Methods Mol Biol. 2017;1603:25-44. Epub 2017/05/12.

Wang Q, Stuczynski M, Gao Y, Betenbaugh MJ. Strategies for Engineering Protein N-Glycosylation Pathways in Mammalian Cells. Methods Mol Biol. 2015;1321:287-305.

Heffner KM, **Wang Q**, Hizal DB, Can O, Betenbaugh MJ. Glycoengineering of Mammalian Expression Systems on a Cellular Level. Advances in biochemical engineering/biotechnology. 2018

Chung CY, Majewska NI, **Wang Q**, Paul JT, Betenbaugh MJ. SnapShot: N-Glycosylation Processing Pathways across Kingdoms. Cell. 2017;171(1):258-.e1. Epub 2017/09/25.

Presentations

Qiong Wang, Sandra Chough, Michael J. Betenbaugh, and Hui Zhang, "Intact glycopeptide analysis of recombinant protein from CHO cells" in "Cell Culture Engineering XVI", A. Robinson, PhD, Tulane University R. Venkat, PhD, MedImmune E. Schaefer, ScD, J&J Janssen Eds, ECI Symposium Series, (2018)

Qiong Wang. "Glycoengineering in CHO cells for biomanufacturing. Abstract of papers of the American Chemical Society (2016)

Skills

Molecular Biology: Plasmid design and construction, site-specific mutation, CRISPR, ZFN, immunoblot and lectin blot, native electrophoresis, ELISA, RT-PCR, confocal microscopy, FACS and analysis, HPLC, sialic acid analysis, antibody ADCC and CDC assays

Cell culture: adherent and suspension mammalian cell culture (CHO and HEK), human B and T cell culture, cell adaption, cell line development and characterization, Lipofectamine and electroporation transfection

Protein purification: TFF, FPLC, Ni-NTA purification, Protein A purification

Mass spectrometry (MALTI-TOF and LC-MS/MS): Released glycan analysis, Glycan permethylation, Glycan derivative labeling (2AA and 2AB), Intact glycopeptide analysis

Animal Skills: Vein tail injection

Computational skills: MATLAB, Microsoft Office, AutoCAD, ApE, Adobe Illustration and Photoshop,flowJo, ImageJ

Internship Experience

1. Cell line development Co-op at Eli Lilly, Indianapolis, IN (08/2016-02/2017)

Teaching Experience

Mentored high school students, undergraduates, masters and junior Ph.D. students